NEURAL CORRELATES OF UNIMANUAL AND BIMANUAL EYE-HAND COORDINATION ACROSS HEALTHY AND DEMENTIA-RISK POPULATIONS

Alica Rogojin

A dissertation submitted to the Faculty of Graduate Studies in partial fulfillment of the requirements for the degree of

Doctor of Philosophy

Graduate Program in Kinesiology and Health Science

York University
Toronto, Ontario
September, 2022

ABSTRACT

Eye-hand coordination is essential to our functional independence and relies on communication between widespread brain regions for successful unimanual and bimanual motor control. Eye-hand coordination performance has been shown to differ between the sexes, as well as between healthy aging individuals and those with dementia risk. The studies included within this dissertation were designed to characterize the structural and functional neural correlates of skilled movements across various populations in order to gain a better understanding of previously reported behavioural performance differences. The first two studies investigated changes in structural and functional integrity, respectively, of brain networks that may underlie known visuomotor behavioural deficits in older adults with an increased genetic (APOE e4) risk for Alzheimer's disease. Alzheimer's disease is thought to be a disconnection syndrome with characteristic patterns of disruption to structural and functional connectivity in the brain. A visuomotor task requiring the integration of different cognitive and motor domains via communication across multiple brain regions presents one way to test the integrity of these brain networks. The anatomical, diffusion-weighted, and resting state functional connectivity imaging data revealed that in older adult APOE e4 carriers, visuomotor deficits were predicted by i) lower grey matter volume and thickness of medial temporal lobe regions, ii) lower white matter integrity in several major tracts, and iii) decreased functional connectivity within the default mode and dorsal attention networks, in advance of any cognitive deficits. Historically, sex differences in unimanual and bimanual eye-hand coordination have also been observed, and a better understanding of the neural correlates of these differences could inform clinical practices on how to better tailor bimanual movement-based rehabilitation to the individual. The third study investigated the sex differences in functional connectivity of bimanual control, demonstrating connectivity differences between men and women despite equivalent behavioural performance. Taken together, these data provide novel insight into the neural correlates underlying one of our most fundamental human behaviours, eye-hand coordination, and their potential clinical implications.

ACKNOWLEDGEMENTS

I would not be here if not for my incredible mentor, Dr. Lauren Sergio. I am so fortunate to have had such a fulfilling and wonderful graduate school experience, and that is in large part thanks to your guidance, kindness, support, and good humour over the past 6 years. I could not have asked for a better mentor, and I am forever grateful to you. My doctoral projects have been so challenging but also so much fun – and I have come out the other side with pretty brain pictures (and a degree)! Dr. Diana Gorbet, thank you so much for everything. I would still be slogging away with AFQ right now, if not for you! You are everything I hope to emulate in my research career. You have helped me gain so much confidence in my research skills, and if I can reach even a fraction of your levels of awesomeness then I would consider myself incredibly lucky. I would also like to thank my committee members for making my defence such an unexpectedly enjoyable moment, and for your suggestions and kind words.

(Dr.) Alanna and (soon-to-be Dr.) Holly, my partners in crime in the "moty control" lab, I would have mentally crashed and burned without you. I am so thankful for the countless hours of tears and laughter we have shared on this learning journey together, and I cannot wait to see the good things coming our way! George and Shanaa, thank you for the support, very much needed writing accountability sessions, and of course D&D – one of the most unexpectedly awesome things to come out of grad school. To my best friends outside of academia, thank you for lifting me up and reminding me that there's more to life than research.

To my family – Ma, Pa, Yanka, Byl', and Dyl' – words are not enough. You have been my biggest cheerleaders my entire life. Thank you for always believing in me, even when I struggled with it myself. Most importantly, thank you for your unconditional love. It makes me feel like I can accomplish anything. I love you no matter what.

And to Jess, my best friend and partner in life. Thank you for your unwavering love, patience, and support in this last (most difficult) leg of my doctoral journey. I am so excited for where life takes us next.

TABLE OF CONTENTS

LIST OF TABLES

LIST OF FIGURES

ABBREVIATIONS

Alzheimer's disease

AD	Alzheimer's disease
APOE	apolipoprotein E
APP	amyloid protein precursor
AT(N)	Aβ deposition, pathologic tau, and neurodegeneration
Aβ	beta-amyloid
EOAD	early-onset Alzheimer's disease
FH-	no family history of dementia
FH+	positive family history of dementia
LOAD	late-onset Alzheimer's disease
MoCA	Montreal Cognitive Assessment
NIA-AA	National Institute on Aging and the Alzheimer’s Association
PSEN1	presenilin-1
PSEN2	presenilin-2

Brain regions, tracts, and networks

AG	angular gyrus
AIP	anterior intraparietal area
CA1	cornu ammonis-1
CA2/3	cornu ammonis-2/3
CA4	cornu ammonis-4
CMA	cingulate motor area
DAN	dorsal attention network
DG	dentate gyrus
DLPFC	dorsolateral prefrontal cortex
DMN	default mode network
EC	entorhinal cortex
FPN	frontoparietal control network
HATA	hippocampal-amygdala-transition-area
IFOF	inferior fronto-occipital fasciculus
ILF	inferior longitudinal fasciculus
IPL	inferior parietal lobule
IPS	intraparietal sulcus
LIP	lateral intraparietal area
lPFC	lateral prefrontal cortex

LTC	lateral temporal cortex
MFG	middle frontal gyrus
MIP	medial intraparietal area
mPFC	medial prefrontal cortex
MTG	middle temporal gyrus
MTL	medial temporal lobe
pCun/PCC	precuneus/posterior cingulate cortex
PFC	prefrontal cortex
PHC	parahippocampal cortex
PMd	dorsal premotor cortex
PMv	ventral premotor cortex
PO	parietal operculum
PPC	posterior parietal cortex
PreCG	precentral gyrus
RSFC	resting state functional connectivity
S1/M1	primary sensorimotor cortex
SFG	superior frontal gyrus
SLF	superior longitudinal fasciculus
SMA	supplementary motor area
SMG	supramarginal gyrus
SMN	somatomotor network
SPL	superior parietal lobule
STG	superior temporal gyrus
UF	uncinate fasciculus
V1	primary visual cortex
VAN	ventral attention network
VIP	venrtral intraparietal area
VLPFC	ventrolateral prefrontal cortex

Neuroimaging

ACPC	anterior commissure-posterior commissure
AFNI	Analysis of Functional Images software
AFQ	automated fibre quantification
ANATICOR	anatomy-based correlation correction model
AxD	axial diffusivity
BOLD	blood-oxygen-level-dependent
CMRglc	cerebral metabolic rate of glucose

CONN	functional connectivity toolbox
DTI	diffusion tensor imaging
EPI	echo planar imaging
FA	fractional anisotropy
FDG-PET	[18F]-fluorodeoxyglucose positron emission tomography
fMRI	functional magnetic resonance imaging
FOV	field of view
FSL	FMRIB software library
GPIP	group prior individual parcellation
gPPI	generalized psychophysiological interaction
ICV	intracranial volume
MAD	mean absolute deviations
MD	mean diffusivity
MP-RAGE	magnetization-prepared rapid gradient echo
MRI	magnetic resonance imaging
RD	radial diffusivity
ROI	region of interest
TE	echo time
TR	repetition time
VOI	volume of interest

Visuomotor integration

AE	absolute error
CPL	corrective path length
DR	direction reversal
EE score	endpoint error score
FR	feedback reversal condition
MTf	full movement time
PC	plane-change condition
PC+FR	plane-change feedback reversal condition
PL	path length
PLb	ballistic path length
PLf	full path length
PV	peak velocity
RT	reaction time
S	standard condition
VE	variable error

Chapter One

General Introduction

1.1. Research in context

To get to the point where you are reading this sentence, you will have had to interact with objects in your environment to navigate to this page of the dissertation. Perhaps you're reading a physical copy and had to directly reach to pick this book off the shelf and flip to this page. Or maybe you're reading this on your computer and had to use your mouse to navigate a cursor on your screen to bring you here. Hundreds of times per day we find ourselves reaching out with one, or both, hands to interact with the objects around us. The coordination of vision and limb motion for interaction with the external environment requires a complex level of control carried out by a number of interconnected brain regions. Performance of eye-hand coordination tasks has been shown to differ between men and women, as well as between healthy aging and neurodegenerative disease. This dissertation will characterize differences in the neural underpinnings of various skilled movements, both involving unimanual as well as bimanual coordination.

One focus of the research presented here is Alzheimer's disease and its impact on unimanual visually-guided movements. Alzheimer's disease (AD) is the most common cause of dementia (Reitz and Mayeux 2014), and is often associated with decrements in cognitive function (Hebert et al. 2010). Dementia is a major cause of disability and dependency among older people worldwide, and as the disease progresses, individuals need assistance with activities of daily living (World Health Organization 2015). Visuomotor deficits in the AD population have received little study to date. This may be because the most prominent impairments in AD are in the cognitive domain, and have been the primary focus of most assessments and research (Hebert et al. 2010). Recently, it has become evident that complex movements can also be affected by the disease, with studies reporting declines in skilled eye-hand coordination performance in AD patients (Ghilardi et al. 1999; Tippett and Sergio 2006; Tippett et al. 2007). Some of the movements we perform in everyday life involve more direct

"standard" visually-guided arm movements, and typically involve looking towards the intended target of a reach and making an arm movement to the same location, such as reaching out and picking up a cup of tea (Gielen et al. 1984; Wise et al. 1996; Helsen et al. 1998). However, with the advent of tool-use and living in an increasingly technology-driven world, many of the daily activities that we perform routinely require us to spatially dissociate the targets of the gaze and arm movements. These decoupled or "non-standard" visually-guided reaches rely on the integration of skilled movements with aspects of cognition (Johnson et al. 1996); the mapping between the visual stimulus and response in these more complex and cognitively-demanding movements must be learned and calibrated (Wise et al. 1996). An example of this is learning that scrolling "up" on a laptop trackpad will move the page on the screen "down".

Preliminary research in our laboratory suggests that, relative to age-matched individuals without known risk factors for dementia, dementia risk is associated with the deterioration of non-standard visuomotor performance (Hawkins and Sergio 2014; Rogojin et al. 2019). Complex movements requiring non-standard visuomotor integration show deficits in advance of any detectable cognitive decline, as determined using standardized cognitive assessments. Furthermore, previous studies from our lab have demonstrated that even when cognitively healthy men and women show equal non-standard visuomotor task proficiency, the underlying brain activity associated with completing the task differs between the sexes in ways that are likely to be clinically relevant (Grön et al. 2000; Gur et al. 2000; Gorbet and Sergio 2007; Hawkins et al. 2015; Hawkins and Sergio 2016). This dissertation first provides an introduction to AD, looking at the biology, risk factors, and neural correlates of the disease (**section 1.2**). Unimanual visuomotor tasks are then discussed in the context of AD risk (**section 1.3**). These sections will outline how visuomotor tasks may be used to advance our understanding of AD compared to healthy aging.

While many of the movements we make throughout our day involve just one upper limb, most daily movements require a certain degree of coordination between both upper limbs (Kilbreath and Heard 2005; Vega-González and Granat 2005). Even though bimanual movements are more abundant than unimanual movements, they have been studied less extensively (Swinnen and Wenderoth 2004). Historically, the literature has demonstrated sex differences in eye-hand coordination tasks where women typically outperform men in tasks involving fine motor skills and accuracy, while men excel in spatiomotor tasks as well as tasks assessing reaction time and movement speed (Kimura 1993; Fozard et al. 1994; Hall and Kimura 1995). Functional neuroimaging studies have shown sex-differences in brain activity underlying processes required for motor control (Grön et al. 2000; Sadato et al. 2000; Jordan et al. 2002; Weiss et al. 2003; Seurinck et al. 2004), even in the absence of sex-related differences in behavioural performance (Gorbet and Sergio 2007). It has been suggested that performance asymmetries between men and women in eye-hand coordination tasks may arise from sex-specific differences in hemisphere asymmetry and interhemispheric connectivity (Allen et al. 1991; Dubb et al. 2003; Ingalhalikar et al. 2014; Shiino et al. 2017). Yet despite the well-known sex-based differences in hemisphere asymmetry, interhemispheric connectivity, and organization of the motor cortex (Amunts et al. 2000), sex-differences in the functional neural correlates underlying bimanual performance have not been explicitly investigated. The final section of this general introduction switches focus from unimanual to bimanual visually-guided movements (**section 1.4**), presenting current findings from neuroimaging studies investigating bimanual coordination as well as identifying gaps in the literature.

1.2. Overview of Alzheimer's disease

AD is an irreversible neurodegenerative brain disease, and is the most common cause of dementia (Reitz and Mayeux 2014). Dementia is not a single disease; rather, it's an umbrella term that refers to a set of symptoms that arise as a result of damage to brain cells. Dementia is characterized by a decline in cognitive abilities, where symptoms include memory loss, difficulties with decision making, language problems, and behavioural changes (Burns and Iliffe 2009). Damage to nerve cells in the brain may be caused by a number of conditions or diseases, with AD accounting for approximately 60-80% of all dementia cases (Alzheimer's Association 2019). The brain changes seen in AD lead to the eventual disruption of activities in daily living such as bathing and eating, and are ultimately fatal.

The pathophysiological hallmarks of AD include the presence of 1) extracellular amyloid plaques formed by the abnormal accumulation of the beta-amyloid (Aβ) protein, 2) intracellular neurofibrillary tangles composed of hyperphosphorylated tau protein, and 3) neurodegeneration (dos Santos Picanco et al. 2016). Aβ monomers first form low- to mid-range molecular weight oligomers which then gradually deposit as high molecular weight oligomers, fibrils, and senile plaques (Guo et al. 2020). Aggregation of Aβ leads to the activation of pathways that generate reactive oxygen species, mitochondrial dysfunction, hyperphosphorylated tau protein, and neuroinflammation (Canevari et al. 2004; Mattson 2004; Devi et al. 2006). Aβ can damage neurites through these different pathways, and amyloid plaques reduce the number of synapses, all of which may result in neuronal and synaptic dysfunction leading to AD (Chen et al. 2017). Tau protein is a microtubule-associated protein expressed in neurons, and it is involved in the proper functioning of the cytoskeletal network via microtubule assembly (Binder et al. 1995). Microtubules are essential for delivery of presynaptic components to axon terminals and postsynaptic components to dendrites (Vallee 1991); tangles made up of hyperphosphorylated tau protein disrupt this transport system in the brain, leading to synaptic dysfunction (Bloom 2014).

AD is a slowly progressive brain disease that begins decades before symptoms emerge and there is a diagnosis of clinical dementia (Morris 2005). Clinical symptoms of dementia appear only after there has already been significant damage to the brain (Sperling et al. 2011). Preclinical stages of AD are used by the National Institute on Aging and the Alzheimer's Association (NIA-AA) workgroup to encompass individuals who are clinically normal but thought to be on a trajectory towards the symptomatic stages of AD (Sperling et al. 2011). These stages represent a continuum and are based primarily on AD biomarkers assessed directly through cerebrospinal fluid analysis or indirectly via brain imaging. Biomarker measures include Aβ accumulation, cerebrospinal fluid tau levels, and brain atrophy evaluated using volumetric magnetic resonance imaging (MRI). The preclinical stages are applicable to both individuals with genetic risk (such as having the apolipoprotein E (APOE) e4 allele) and age risk; they include those with no or subtle cognitive or behavioural changes who have not yet progressed to the point of clinical impairment diagnosed as mild cognitive impairment or dementia. The focus of this dissertation will be on the preclinical stage, investigating individuals at an increased risk for AD due to genetic factors or dementia family history (discussed in more detail below) and who have no cognitive impairment.

1.2.1. Risk factors for dementia due to Alzheimer's disease

The prevalence and incidence of AD suggest that age is the primary risk factor, where the number of Canadians living with dementia more than doubles every 5 years after the age of 65 (Public Health Agency of Canada 2017). While less than 1% of Canadians between the ages of 65 and 69 have dementia, this number increases to 25% for those aged 85 and over. Although age is the primary risk factor for developing AD, AD is not a normal part of aging. AD can be defined based on age of onset (early-onset or late-onset), as well as on family determinants (familial or sporadic). Early-onset AD (EOAD) has an age of onset before the

age of 65 (Rossor et al. 2010), and accounts for a small percentage of all AD cases (between 1-8%) (Prince et al. 2014; Zhu et al. 2015; Alzheimer's Association 2019; Canadian Institute for Health Information 2019). This is an arbitrary age cutoff that doesn't have any specific biological significance, but rather is indicative of a sociological partition based on employment and retirement age. Late-onset AD (LOAD) has an age of onset after the age of 65 and is the more common form of AD, accounting for approximately 95% of all AD cases (Reitz and Mayeux 2014). See **Table 1** for a summary of these statistics. This dissertation will focus on LOAD; specifically, on the long preclinical phase, lasting approximately 15-20 years before onset of cognitive impairment (Bateman et al. 2012).

Table 1. Summary of Alzheimer's disease statistics.

<table>
<tr><td colspan="4">Alzheimer's disease (AD)
60-80% of all dementia cases[1]
The APOE e4 variant is associated with an increased risk for AD, especially LOAD but also EOAD, where 50-70% of subjects with AD carry at least one e4 allele[2,3]</td></tr>
<tr><td colspan="2">Early-onset AD (EOAD)
1-8% of all AD cases[4,5,6]</td><td colspan="2">Late-onset AD (LOAD)
95% of all AD cases[7]</td></tr>
<tr><td>Familial
60% of EOAD[8]

13% have an autosomal dominant form of inheritance due to mutations in one of three genes:
- APP (10-15%)
- PSEN1 (20-70%)
- PSEN2 (5%)</td><td>Sporadic
40% of EOAD</td><td>Familial
<10% of LOAD

- First-degree relatives of a person with LOAD have a cumulative lifetime risk of approximately 20-25%, whereas the risk in the general population is 10.4%[8]
- APOE e4 is most highly associated with LOAD for individuals with a family history of dementia, and this association is highest for individuals that carry 2 APOE e4 alleles (e4/e4 genotypes), where e4/e4 is found in 1% of normal Caucasian controls but in nearly 19% of familial LOAD populations[8]</td><td>Sporadic
>90% of LOAD[8]

APOE is the only gene that has been consistently associated with sporadic LOAD, where approximately 58% of persons with LOAD have the APOE e4 allele[6]</td></tr>
</table>

1. (Alzheimer's Association 2019); 2. (Kamboh 2004); 3. (Singh et al. 2006); 4. (Canadian Institute for Health Information 2019); 5. (Prince et al. 2014); 6. (Zhu et al. 2015); 7. (Reitz and Mayeux 2014); 8. (Bekris et al. 2010)

Family history risk

After older age, the risk for most AD cases appears to be a complex interplay of multiple susceptibility genes and environmental factors. The exception to this is the familial EOAD case in which there is an autosomal dominant pattern of inheritance due to single-gene disorders (Karch et al. 2014). These individuals have mutations in three genes: Aβ precursor protein (APP), presenilin 1 (PSEN1), and presenilin 2 (PSEN2) (Rogaeva 2002). In contrast, more than 90% of individuals with LOAD appear to have the sporadic form, meaning there is no specific familial link (Dorszewska et al. 2016). Sporadic AD is thought to be determined by a combination of genetics (70%) (Alonso Vilatela et al. 2012) and environmental contributors (30%), such as diet, hormonal factors, and toxicological exposure (Lahiri et al. 2007). LOAD is a complex genetic disorder, with an estimated heritability of 60-80% based on one of the largest twin studies done to date (Gatz et al. 2006). This study found that in twin pairs where both twins had AD, the intrapair difference in age of onset was significantly greater in dizygotic (fraternal) compared to monozygotic (identical) twins. This suggests a genetic component in timing of the disease. Another twin study reported a higher concordance rate (when both twins develop AD) in monozygotic pairs compared to dizygotic pairs, further confirming the contribution of a genetic component (Räihä et al. 1996). Importantly, the onset age differed by as much as 15 years in concordant pairs, reflecting the influence of environmental factors on AD. First-degree relatives of people with LOAD have a greater lifetime risk for developing dementia (approximately 30-40%) (Silverman et al. 1994; Farrer et al. 1995; Lautenschlager et al. 1996) compared to those without first-degree relatives with LOAD (approximately 12%) (Silverman et al. 1994). The number of additional affected family members also appears to increase risk of close relatives; by age 80, children with two affected parents (conjugal AD) have a higher lifetime risk of AD (54%), 1.5 times the risk of children with just one affected parent, and nearly 5 times the risk of children with non-affected parents (Lautenschlager et al.

1996). Age at onset may also be earlier in those with a more extensive family history, beyond just having parents with AD (Jayadev et al. 2008).

The biological mechanisms through which family history of AD confers increased risk for LOAD are not yet known. There is evidence that maternal transmission of LOAD may have a greater impact on offspring than paternal transmission. Maternal transmission of AD is more frequent than paternal transmission (Gómez-Tortosa et al. 2007); a review study found that in AD patients with one affected parent, the ratio of mother:father affected is approximately 3:1 (Mosconi et al. 2010). A consistent feature of AD is a reduction in the cerebral metabolic rate of glucose (CMRglc) measured using [18F]-fluorodeoxyglucose positron emission tomography (FDG-PET) (Mosconi 2005). A study examining clinically normal individuals found that those who had a mother with AD had reduced CMRglc compared with those who had a father with AD and with those who had no parents affected (Mosconi et al. 2007). CMRglc reductions in participants with maternal AD history were found in brain regions that are typically affected in AD patients, including the parieto-temporal, posterior cingulate, precuneus, medial temporal, and prefrontal cortices. These CMRglc reductions due to maternal AD history remained significant after controlling for age, gender, education, and genetic risk (namely involving the APOE gene, discussed in more detail below). Conversely, there were no CMRglc differences between children with a paternal AD family history and the children of parents without AD.

Genetic risk factors

Recently, genome-wide association studies have identified over 20 polymorphisms in or near genes that modify risk for LOAD (Karch and Goate 2015). The effects of each gene on AD risk is small, where they are associated with a 1.1 to 1.2 times increased risk (Rabin et al. 2019). The only widely accepted susceptibility gene that has been consistently linked to both

familial and sporadic LOAD across multiple genetic studies is the APOE gene (Bekris et al. 2010; Karch and Goate 2015). APOE is located on chromosome 19 and encodes three common alleles - e2, e3, e4 (Corder et al. 1993) - with a worldwide frequency of 8.4%, 77.9% and 13.7%, respectively (Farrer et al. 1997). The e4 allele specifically is associated with an increased risk for AD across multiple ethnic groups (Tang et al. 1996; Farrer et al. 1997; Bekris et al. 2010). APOE e4 carrier prevalence in LOAD cases varies across studies due to factors such as country hosting the study and the study design, but mean estimates are approximately between 40-65% in subjects with AD (Rebeck et al. 1993; Crean et al. 2011), compared to 12% in controls (Poirier et al. 1993). A systematic review of 139 publications from January 1, 1985 to May 31, 2010 was done on studies reporting the APOE e4 status of patients diagnosed with AD (Ward et al. 2012). The meta-analysis reported that APOE e4 carrier (defined as having at least one e4 allele) prevalence was 48.7% (95% confidence interval, CI: 46.5-51.0), and a homozygous e4 prevalence of 9.6% (95% CI: 8.4-10.8). Another study looking at APOE genotypes of elderly adults over the age of 85 reported that 4% of healthy controls and 6% of AD patients were homozygous for the e4 allele, compared to 34% of healthy controls and 50% of AD patients who were heterozygous for the e4 allele (Skoog et al. 1998). Homozygous e4 individuals are rare in the population, and many research studies will therefore combine homozygous and heterozygous e4 individuals into one group. For these studies, the definition of an APOE e4 carrier is an individual with at least one e4 allele, which includes both homozygous and heterozygous e4 individuals. Another study reported that the proportion of individuals with AD also increases with the number of e4 alleles from 20% of subjects with no e4 alleles, to 47% of e4 heterozygotes and 91% of e4 homozygotes (Corder et al. 1993). Compared to the other genes identified in genome-wide association studies, the e4 allele confers a much greater risk for developing AD; one e4 allele results in a 3-fold increase of AD risk, while two e4 alleles increase AD risk by 8- to 12-fold (Corder et al. 1993; Farrer et al.

1997). APOE e4 is also associated with a dose-dependent decrease in the age of onset, where each e4 allele reduces the average age of symptom onset by about a decade: mean onset is approximately 84 years in subjects without an e4 allele, 76 years in subjects with one e4 allele, and 68 years in subjects with two e4 alleles (Corder et al. 1993).

In the central nervous system, APOE is mainly synthesized and secreted by astrocytes and microglia (Boyles et al. 1985; Liu et al. 2013), and plays a central role in lipid and cholesterol transport, lipoprotein metabolism, neuroplasticity, and neuroinflammation (Bales et al. 2000; Mahley and Rall 2000; Kim et al. 2009). In most, if not all, proposed AD pathogenic pathways, the APOE e4 allele either reduces protection or increases toxicity compared to the e3 and e2 alleles. A lot of the literature has focused on the isoform-specific effects of APOE on protection against Aβ-induced neurotoxicity (Mahley and Rall 2000; Manelli et al. 2004). The APOE E3 protein binds to Aβ with higher affinity than APOE E4 (LaDu et al. 1994), and APOE E2 protein binding to the Aβ peptide has been shown to be comparable to E3-Aβ complex formation (LaDu et al. 1997). Therefore, the higher affinity binding of APOE E3 and E2 to Aβ may enhance the clearance, and thus prevent accumulation, of the neurotoxic Aβ species in individuals with the e3 allele (LaDu et al. 1997). Indeed, APOE E4 has been shown to form insoluble, high-molecular-weight complexes with the Aβ peptide whereas APOE E3 is less reactive and doesn't form such extensive and dense complexes (Sanan et al. 1994). In a cohort of cognitively normal individuals under the age of 70, biomarkers of brain Aβ accumulation were present at a frequency that corresponded to their APOE genotype, that is e4 > e3 > e2 (Castellano et al. 2011). The same study also looked at a mouse model of Aβ-amyloidosis expressing human APOE isoforms, and found that consistent with their observation in human participants, mice also developed Aβ deposition in an APOE isoform-dependent pattern (E4 > E3 > E2). Furthermore, E4 appears to destabilize microtubule assembly while E3 stabilizes the formation of microtubules (Nathan et al. 1995). Though the

mechanism remains unclear, the binding of APOE E3 and E2 to tau may protect it from hyperphosphorylation, and therefore prevent intracellular deposits of tau in the form of neurofibrillary tangles characteristic of AD (Strittmatter et al. 1994).

Another mechanism by which APOE may affect AD pathology is through modulation of neuroinflammatory responses. In addition to amyloid plaques and neurofibrillary tangles, an activation of inflammatory responses is observed in the brains of AD patients and is thought to contribute to the pathogenesis of AD (Bales et al. 2000). Aβ is a stimulator of glial-mediated neuroinflammatory responses (Guo et al. 2004). Interestingly, Aβ also induces upregulation of APOE expression and release, and these increased levels of APOE may serve as a feedback mechanism to limit Aβ-driven neuroinflammation (LaDu et al. 2000). Isoform-dependent differences in the anti-inflammatory properties of APOE may in part explain the differential risk for AD caused by e2, e3, and e4 alleles. This has been shown *in vivo* with human-APOE knock-in mice, where e4 knock-in mice had a greater pro-inflammatory response compared to e3 knock-in mice (Guo et al. 2004). Having an APOE e4 allele may therefore exacerbate or ineffectively prevent neuroinflammation in AD. Several other mechanisms by which the e4 allele has been shown to contribute to AD risk is through network hyperexcitability, reduced glucose metabolism, decreased vascular health, and mitochondrial dysfunction (Liu et al. 2013). As both i) first-degree relatives of persons with LOAD, and ii) individuals with the APOE e4 allele have a greater risk for developing AD, family history and APOE e4 status are important predictors of AD risk.

1.2.2. Neural correlates of early Alzheimer's disease

Historically, AD has been classified based on appearance of clinical symptoms. As previously mentioned, however, one of the pathophysiological hallmarks of AD is neurodegeneration, beginning decades before any cognitive symptoms arise (Morris 2005). In

2011, the National Institute on Aging and the Alzheimer's Association (NIA-AA) Working Group proposed criteria that incorporate neuroimaging biomarkers for diagnosis of probable AD (Sperling et al. 2011). The NIA-AA research framework has since been updated to group biomarkers into those of Aβ deposition, pathologic tau, and neurodegeneration [AT(N)] (Jack et al. 2018). This dissertation focuses on the neurodegeneration component of the AT(N) framework, and the following section will introduce some MRI biomarkers of preclinical AD, prior to the appearance of cognitive symptoms. **Figure 1** and **Figure 2** provide visual representations of some of the grey and white matter anatomical brain regions, respectively, that will be discussed in the sub-sections below. The prevalent etiological model for AD suggests that brain changes characteristic of AD pathology follow a specific temporal order, and these changes map onto the amnestic cognitive decline phenotype (Braak and Braak 1991a; Braak et al. 2011; Jack et al. 2016; Riedel et al. 2018).

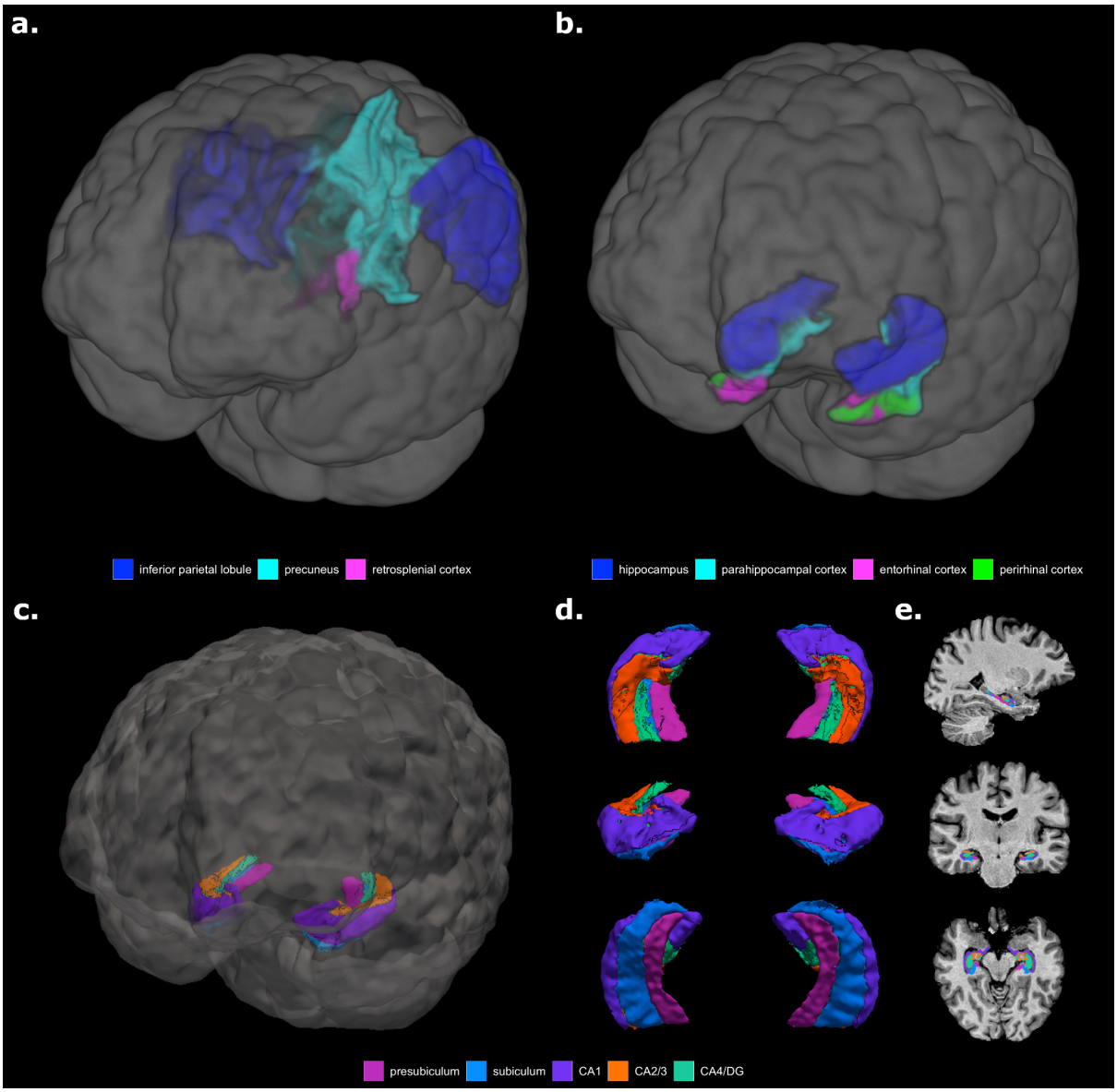

Figure 1. 3D depictions of **a)** areas of the medial temporal lobe, and **b)** areas important for non-standard visuomotor integration. Hippocampal subfields obtained from FreeSurfer segmentation are shown in **c)** a 3D brain, **d)** 3D superior, anterior, and inferior views, and **e)** sagittal, coronal, and axial slices. Figure taken from Rogojin et al. (from **chapter 2**).

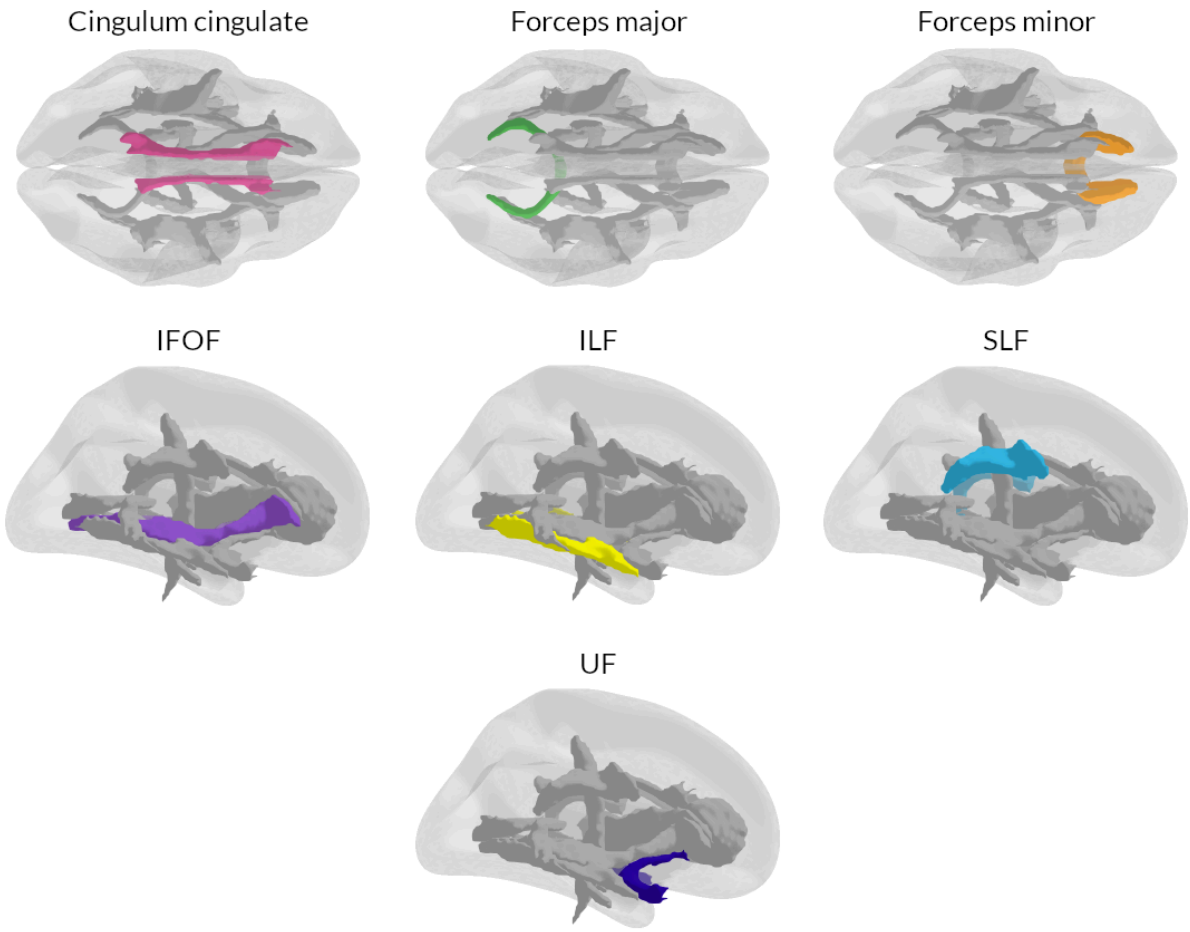

Figure 2. Major white matter tracts affected in the preclinical stage of Alzheimer's disease, some of which are also important for visuomotor control. IFOF, inferior fronto-occipital fasciculus; ILF, inferior longitudinal fasciculus; SLF, superior longitudinal fasciculus; UF, uncinate fasciculus. Brain figures made with "ggseg" R package (Mowinckel and Vidal-Piñeiro 2020).

Anatomical magnetic resonance imaging

Anatomical, or structural, MRI is clinically valid, non-invasive, and sensitive to the changes seen in brain structure starting in early AD (Belleville et al. 2014). Anatomical MRI detects declines in grey matter volume as a measure of atrophy that results from global neuronal loss (Ewers et al. 2011). Normal aging, even without AD pathology, has been shown to lead to declines in grey matter volume. Advanced aging has been found to result in volume loss in areas of the prefrontal cortex, inferior parietal lobule (IPL), and hippocampal formation (Jack et al. 2000; Raz et al. 2005). Hippocampal and entorhinal volume declines with increasing age have also been shown to predict worse performance on memory tasks (Rosen et al. 2003; Rodrigue and Raz 2004). The medial temporal lobe (MTL) includes the hippocampus and the surrounding perirhinal, parahippocampal, and entorhinal cortical regions. Converging evidence from imaging studies has supported the hypothesis that the MTL, working in concert with the prefrontal cortex (Sperling et al. 2001; Sperling et al. 2003), is involved in episodic memory (Eichenbaum et al. 1996; Yonelinas et al. 2001; Zeineh et al. 2003).

Cognitively normal adults with a maternal family history of AD show lower grey matter volumes in AD-vulnerable brain areas, with progressive grey matter atrophy in the parahippocampal gyrus and precuneus (Honea et al. 2011). In the same study, these authors found that APOE e4 carriers had more regional atrophy in the superior frontal and inferior frontal cortices compared to e4 non-carriers. A meta-analysis reported that atrophy in the transentorhinal region, hippocampus, IPL, and precuneus may predict progression from mild cognitive impairment to AD (Schroeter et al. 2009). Cognitively healthy individuals with a family history of LOAD have also shown decreased grey matter in the precuneus, superior frontal, middle frontal, and inferior frontal gyri compared with individuals with no family history (Honea et al. 2010). Furthermore, those with a maternal family history had significantly smaller inferior frontal, middle frontal, precuneus, and lingual gyri compared with subjects

with either a paternal family history or no family history. These findings complement and extend reports of cerebral metabolic differences in individuals with a maternal family history (Mosconi et al. 2007). Many of these areas that show early grey matter atrophy in preclinical AD, including the medial prefrontal cortex, precuneus, IPL, and regions of the MTL, are areas of the default mode network (DMN) discussed below (Parvizi et al. 2006; Sperling et al. 2010; Márquez and Yassa 2019), which is a resting state functional network negatively impacted in preclinical AD.

The hippocampus is one of the earliest brain areas to be affected by AD pathology, with abnormal accumulation of Aβ protein in plaques and hyperphosphorylated tau in neurofibrillary tangles (Braak and Braak 1991a). Several studies have shown that atrophy in areas of the MTL, namely the hippocampus and entorhinal cortex, is a significant predictor of progression from being cognitively healthy to developing mild cognitive impairment, and eventually to AD (Jack et al. 2000; Pennanen et al. 2004; Apostolova et al. 2006; DeCarli et al. 2007; Fleisher et al. 2007; Risacher et al. 2009; Apostolova et al. 2010). Atrophy in the hippocampus has been consistently shown in preclinical AD populations. Family history of AD and APOE e4 status are independently associated with hippocampal, parahippocampal, and entorhinal cortical thinning (Donix, Burggren, Suthana, Siddarth, Ekstrom, Krupa, Jones, Martin-Harris, et al. 2010). Family history specifically was associated with a thinner cortex in the hippocampal cornu ammonis field 1 (CA1) and subiculum. APOE e4 carriers, when compared with non-carriers, showed thinning of the subiculum. In 2-year longitudinal study completed by the same group, cognitively healthy APOE e4 carriers showed significantly greater cortical thinning in the subiculum of the hippocampus, as well as in the entorhinal cortex, compared to non-carriers of the allele (Donix, Burggren, Suthana, Siddarth, Ekstrom, Krupa, Jones, Rao, et al. 2010). Similar results were reported in another longitudinal study of elderly subjects who were cognitively healthy at baseline, some of whom were later diagnosed

with mild cognitive impairment and AD at 3- and 7-years follow-up, respectively (Apostolova et al. 2010). They found that atrophy within CA1 and the subiculum predicted decline to mild cognitive impairment, and progressive CA1 and subiculum atrophy spreading into the CA2/3 subfields suggested future diagnosis of AD.

Diffusion tensor imaging

Changes to white matter microstructure can be detected using a technique called diffusion tensor imaging (DTI), which measures the diffusion of water molecules along white matter tracts (Taylor et al. 2003). Water diffusion is calculated based on the rate of diffusion along the three orthogonal axes of the diffusion ellipsoid, defined by eigenvectors (indicating diffusion direction) and their corresponding eigenvalues (reflecting diffusion magnitude) (Madden et al. 2012). Some studies suggest that DTI changes reflecting decreased white matter integrity may precede grey matter volume loss, making it a potential tool of the early detection of neurodegeneration (Hugenschmidt et al. 2008; Nir et al. 2012). The most commonly reported DTI measures are mean diffusivity (MD) and fractional anisotropy (FA). MD is the average amount of water diffusion calculated as the average diffusivity across all three principal axes of diffusion, where higher MD denotes an increased rate of diffusion (Madden et al. 2012). MD depends on the integrity of physical obstructions, such as membranes, and the resultant diffusion rate of water molecules between different cell compartments (Beaulieu 2002). FA is a value between zero and one that measures the degree of anisotropy of a diffusion process, or directionality of water diffusion. Specifically, a value of zero corresponds to isotropic diffusion (it is unrestricted or equally restricted in all directions), whereas a value of one corresponds to complete anisotropic diffusion (diffusion occurs along a single axis) (Hashemi et al. 2012). A lower FA is thought to reflect a loss of white matter integrity that may be a result of myelin or axonal membrane damage (Kubicki et al. 2007). A higher MD and/or lower FA would signify

a breakdown in white matter integrity. More recently, studies have also started to look at DTI diffusion measures of water movement parallel (axial diffusivity, AxD) and perpendicular (radial diffusivity, RD) to the primary diffusion axis to provide more specific information about white matter integrity (Madden et al. 2012). Decreased AxD and increased RD values are thought to reflect axonal damage (Concha et al. 2006; Sun et al. 2006) and loss of myelin integrity (Song et al. 2003; Song et al. 2005; Sun et al. 2006), respectively. While the diffusion tensor model provides useful summary measures of regions containing mainly single fibres where there is one major fibre direction in a voxel (O'Donnell and Westin 2011), there are several limitations that are important to be aware of when interpreting diffusion data findings. For instance, DTI has limitations in regions with more complex microstructure within voxels containing multiple fibre populations (i.e., crossing-fibre tracts) (Curran et al. 2016). Several studies have demonstrated that FA, MD, RD, and AxD are all susceptible to the effects of crossing-fibres (Pierpaoli and Basser 1996; Wheeler-Kingshott and Cercignani 2009; Vos et al. 2012). Furthermore, although FA, MD, RD, and AxD quantify different properties of white matter microstructure, they are not completely independent of each other (O'Donnell and Westin 2011). All four diffusion measures are calculated from mathematical equations using different combinations of the three mutually perpendicular eigenvectors and their corresponding eigenvalues (Soares et al. 2013).

DTI studies have shown that there are declines in white integrity as early as in the preclinical stages of AD (Kantarci et al. 2014; Prescott et al. 2014; Fischer et al. 2015). Lower FA in the parahippocampal gyrus white matter is associated with presence of APOE e4 (Nierenberg et al. 2005; Honea et al. 2010). With disease progression, white matter alterations spread from association tracts within the limbic system to temporal and parietal areas (Kantarci et al. 2010; Nowrangi et al. 2013). Cognitively normal participants with preclinical AD pathology show lower integrity in frontal, parietal, temporal, and cingulate cortex white matter,

in regions known to be involved in the early stages of AD, compared to individuals without AD pathology (Hoy et al. 2017). Both APOE e4 and parental family history of AD have been associated with microstructural white matter differences in cognitively healthy adults (Bendlin et al. 2010; Westlye et al. 2012; Adluru et al. 2014). Several major white matter tracts within the brain have been linked to preclinical AD, many of which were previously reported to be affected in mild cognitive impairment and early AD. Older participants (over 65 years of age) who are APOE e4 carriers showed higher MD in the superior longitudinal fasciculus (SLF) and cingulum bundle, and higher RD in the genu of the corpus callosum, compared to non-carriers (Adluru et al. 2014). Similar results were reported in another study, with APOE e4 carriers having increased RD and MD in the forceps minor (anterior radiation of the genu of the corpus callosum) and SLF (Westlye et al. 2012). Parental family history of AD has also been associated with lower FA in the cingulum, corpus callosum, uncinate fasciculus (UF), and hippocampus (Bendlin et al. 2010). This study further demonstrated that FA is correlated with increased risk load, where possessing both positive family history and being an APOE e4 carrier was associated with the lowest FA compared to possessing only one or no risk factors. Cognitively healthy women at increased risk for AD, based on a positive family history and have an APOE e4 allele, showed decreased white matter integrity in the inferior longitudinal fasciculus (ILF), inferior fronto-occipital fasciculus (IFOF), UF, genu of the corpus callosum, and cingulum, compared to women with a low-AD risk (Gold et al. 2010). Specifically, they had decreased FA in the ILF, IFOF, and UF, increased MD in the corpus callosum, ILF, and IFOF, decreased AxD in the cingulum, and increased RD in the ILF, IFOF, and UF. Similarly, decreased FA values in the IFOF, ILF, corpus callosum, and cingulum have been shown in cognitively healthy women with a family history of AD and who are APOE e4 carriers, compared to women without either AD risk factor (Smith et al. 2010).

Therefore, the major white matter tracts that appear to show decreased integrity in preclinical AD across multiple studies are the corpus callosum, cingulum, UF, ILF, SLF, and IFOF. The corpus callosum connects the two cerebral hemispheres thus facilitating interhemispheric integration, and atrophy leads to functional disability (Ardekani et al. 2014). The cingulum interconnects frontal, parietal, and MTL regions, as well as subcortical nuclei to the cingulate cortex (Bubb et al. 2018). The UF connects Brodmann area 10 and the lateral orbitofrontal cortex with the anterior temporal lobes (Von Der Heide et al. 2013). Both the cingulum and UF are implicated in episodic memory (Von Der Heide et al. 2013; Bubb et al. 2018), with the cingulum also involved in visuospatial memory, and damage to these tracts in preclinical AD may potentially explain the memory impairments seen in the later stages of AD. The ILF is an associative white matter tract that connects the occipital lobe with the inferior temporal lobe and MTL, and is involved in visually-guided decisions and behaviours (Waller et al. 2017; Herbet et al. 2018). The IFOF extends from areas of the occipital and parietal lobes to the inferior frontal lobe (Waller et al. 2017). The ILF and IFOF both facilitate goal-directed behaviour. The SLF is actually made up of three parallel segments – dorsal SLF I, middle SLF II, and ventral SLF III (de Schotten et al. 2011). The SLF connects the SPL, IPL, and areas of the frontal cortex, and is involved in orienting spatial attention toward visual targets, and redirecting goal-directed attention to events it identifies as salient.

Resting state functional MRI

Changes in the brain's functional connectivity associated with AD can be assessed using functional MRI (fMRI) (Ewers et al. 2011). Functional MRI is based on a blood-oxygen-level-dependent (BOLD) contrast, which is associated with neural activity at the population level. Resting state fMRI examines task-independent spontaneous BOLD signal fluctuations, which are specifically correlated between anatomically separated but functionally connected brain

regions, and reflect known anatomical systems (Fox and Raichle 2007). A particular resting functional network of interest in AD patients is the DMN, an anatomically defined network of interconnected brain regions which are preferentially active when an individual is not focused on the external environment, and shows reduced activity during cognitive task performance (Shulman et al. 1997; Buckner et al. 2008; Sperling et al. 2010). The core areas of the DMN include the posteromedial cortex (comprising the retrosplenial cortex, posterior cingulate cortex, and precuneus) (Parvizi et al. 2006), medial prefrontal cortex, and IPL extending into posterior temporal areas (Sperling et al. 2010; Márquez and Yassa 2019). In addition to these, the hippocampus and surrounding regions of the MTL are also a part of the DMN. Structural and functional MRI, as well as lesion studies in animals, have demonstrated that core areas of the DMN (particularly areas of the posteromedial cortex) have extensive connections to the MTL, a region of the brain important for episodic memory encoding (Meguro et al. 1999; Kobayashi and Amaral 2007). The DMN has also been implicated in memory formation, where successful memory formation required coordinated activation in the hippocampal, prefrontal, and parietal regions, and that age-related memory problems may be primarily due to a loss of deactivation in regions of the posteromedial cortex (Miller et al. 2008). Importantly, regions of the DMN including the MTL, posterior cingulate cortex, and retrosplenial cortex overlap with some of the earliest brain regions to show abnormal Aβ deposition and structural atrophy (Buckner et al. 2005; Bokde et al. 2009).

In preclinical AD, studies have demonstrated that disruptions in the DMN precede neurodegeneration (Sheline and Raichle 2013). Lower connectivity within the DMN was found in healthy older APOE e4 carriers, with a sex interaction in the precuneus (a major region of the DMN) (Riedel et al. 2016). Female e4 carriers showed significantly reduced functional connectivity in the precuneus compared with female e3 homozygotes and male e4 carriers (Damoiseaux et al. 2012). Significantly decreased DMN connectivity has been observed in

cognitively normal older adults with elevated Aβ levels, with decreased functional connectivity from the posterior regions (precuneus and posterior cingulate cortex) to the anterior regions (anterior cingulate cortex), as well as from the precuneus to the hippocampus (Hedden et al. 2009; Sheline, Raichle, et al. 2010). Cognitively normal individuals with a family history of LOAD have reduced connectivity between particular nodes of the DMN, namely the MTL and posterior cingulate cortex, compared to those with no family history (Wang, Catherine M. Roe, et al. 2012). Importantly, a family history effect on connectivity within the DMN was seen in APOE e4 non-carriers. Taken together these studies of resting state functional connectivity implicate regions of the posteromedial cortex within the DMN, particularly the precuneus and posterior cingulate cortex, to be especially vulnerable to early AD pathology. The precuneus and posterior cingulate cortex have reciprocal connections to the MTL (Braak and Braak 1991b), which is involved in memory function and is one of the first regions of the brain to exhibit AD tau pathology and reduced glucose metabolism in AD (Braak and Braak 1991a; Adams et al. 2019). AD patients have demonstrated less coordinated activity in the DMN, as well as less deactivation in the medial parietal and posterior cingulate cortex during memory encoding (Lustig et al. 2003). Although considerably less studied, recent studies suggest that the integrity of other resting state networks is also affected in preclinical AD and have reported alterations in functional connectivity within the dorsal attention network, frontoparietal control network, and salience network (Machulda et al. 2011; Brier et al. 2012; Brier et al. 2014; Elman et al. 2016; Buckley et al. 2017; Liang et al. 2017).

Collectively, these structural and functional imaging studies provide potential MRI biomarkers for preclinical AD. However, while minimally invasive, neuroimaging is expensive and requires extensive personnel and infrastructure to administer. The findings from these neuroimaging studies demonstrate characteristic patterns of disruption to the structural and functional integrity of brain networks, suggesting the AD is a disconnection syndrome

(Delbeuck et al. 2003). Using a task that requires successful communication across multiple brain regions is one way to test the integrity of brain networks. Behavioural tasks that involve sensory and motor regions of the brain have been shown to be affected by AD pathology (Albers et al. 2015). For instance, performance deficits of visuomotor tasks requiring communication of widespread brain regions making up the frontoparietal network (Caminiti et al. 2017) have been demonstrated in individuals with AD-related dementia risk (Hawkins and Sergio 2014; Hawkins et al. 2015; Hawkins and Sergio 2016; Rogojin et al. 2019; Lu et al. 2021), mild cognitive impairment (Salek et al. 2011), and dementia due to AD (Tippett et al. 2012; de Boer et al. 2014; de Boer et al. 2015; de Boer et al. 2016). Together with the recognition that AD pathology develops over several decades, these findings suggest that the use of early noninvasive behavioural biomarkers for AD, such as tasks involving visuomotor integration discussed in detail below, could provide an exciting possibility for early AD detection.

1.3. Sensorimotor transformations in unimanual visually-guided movements

Imagine that you'd like to take a sip from the mug of tea that may be steaming on the table in front of you as you read this. When you reach towards the cup, it involves first looking at the object before initiating the reaching movement. Your brain then automatically transforms any relevant visuospatial information into a motor output for you to successfully pick up the mug. Eye-hand coordination is an important aspect of our ability to interact with the world around us in our everyday lives. In most reaching movements, the visual stimulus and required motor action are aligned, as with the mug of tea. These types of movements are referred to as *standard* "coupled" visuomotor transformations (Wise et al. 1996). This action involves the spatially congruent guidance of the eyes, limbs, and body directly towards a visual target of a reach. In other words, the eyes are directed towards the object and the hand moves to the same

spatial location occupied by that. This process is automatic because the brain's default visuomotor mapping is thought to have the gaze and hand spatially aligned (Gielen et al. 1984; Helsen et al. 1998). However, primates have evolved to use tools and movements have become more complex, with many learned movements having an element of dissociation or "decoupling" between the targets of gaze, attention, and reach. There is an integration of some form of cognitive information into the visuomotor transformation (Wise et al. 1996). This form of visuomotor guidance depends on *non-standard* "decoupled" visuomotor transformations, and involves thinking and moving at the same time. This is also known as non-standard visuomotor integration. For non-standard visuomotor integration, the mapping between the visual stimulus and response must be learned and calibrated.

Non-standard mapping is used in situations when there is some level of dissociation between the target of a reach and the motor output. There are two categories of non-standard visuomotor mapping: 1) *arbitrary*, and 2) *transformational*. Non-standard *arbitrary* mapping involves, as the name suggests, selection of motor behaviour based on arbitrary sensory stimuli (Murray et al. 2000). Nonspatial properties of a visual stimulus, such as colour, provide information about the target for the motor output. For instance, when driving a car, a red traffic light means the person driving must step on the brake pedal to stop the car. The stimulus (red light) is arbitrary in the sense that the action it leads to has no relationship to the stimulus itself other than an associative link formed through learning to drive. Non-standard *transformational* mapping also involves dissociated visual cues and motor outputs; however, unlike in arbitrary mapping, it uses spatial information to relate the position of the visual target to the direction of an action. Non-standard *transformational* mapping is itself further broken down into two forms: 1) *sensorimotor recalibration*, and 2) *strategic control* (Wise et al. 1996). *Sensorimotor recalibration* is used when the spatial location of a visual target and the required movement are in different planes. When using a laptop trackpad, the visual target (cursor on the computer

monitor) is in a different plane from the required movement (trackpad on a horizontal surface). This type of non-standard mapping is also used for laparoscopic surgeries. There needs to be a coordinated remapping of the visual target and hand representation in one plane, onto the target representation and true location of the hand in another plane (Bedford FL 1993; Lackner and Dizio 1994; Clower and Boussaoud 2000). For the movement to be successful, there also needs to be constant feedback and updating of the hand relative to the target location. *Strategic control* is used in movements where an explicit rule needs to be applied in order to move correctly (Redding and Wallace 1996; Redding et al. 2005). Going back to the laptop trackpad example, this is seen in certain laptops where in order to scroll down, you need to slide your fingers up. There is a 180^{o} rotation, where your motor output (hand moving up) needs to go in the opposite direction of the target (page scrolling down) to successfully complete the task. Sensorimotor recalibration is implicit, whereas strategic control uses explicit rules. The projects within this dissertation involve the study of non-standard *transformational* mapping, as it requires non-standard visuomotor integration which has been shown to differ between healthy and clinical populations, discussed in more detail below.

1.3.1. Brain networks involved in unimanual visuomotor integration

Movements directed by vision require a transformation of sensory information about body and target positions into appropriate motor outputs - in other words, sensorimotor transformation. While the underlying neurological computations are not yet fully understood, a visually guided movement involves a transformation from extrinsic (using external cues) to intrinsic (the required joint and muscle activations) reference frames (Kalaska and Crammond 1992; Kalaska et al. 1997; Kakei et al. 2003). Specifically, an eye-centered coordinate frame (i.e., internal representation of a target in space using its position on the retina) needs to be transformed to an effector-centered motor coordinate frame (i.e., position of muscles and joints

performing the movement) (Andersen et al. 1985; Soechting and Flanders 1989a; Soechting and Flanders 1989b; Flanders et al. 1992; Kalaska and Crammond 1992; Ghilardi et al. 1995). In a visually-guided reaching task, this sensorimotor transformation is known as visuomotor integration. There needs to be a transformation from extrinsic visuospatial information to intrinsic muscle and joint representations (Kalaska et al. 1997; Kalaska et al. 1998; Battaglia-Mayer et al. 2000; Sergio and Kalaska 2003; Crawford et al. 2011).

It has been well established that visuomotor integration relies on a network of brain regions within the frontoparietal reach network (Wise et al. 1996; Sabes 2000; Caminiti et al. 2017). Interconnected neuronal populations from parietal, premotor, and primary motor areas forming the frontoparietal network have been established as brain areas necessary for visuomotor integration (Wise et al. 1997; Sabes 2000). The following outlines a simplified flow of information through the frontoparietal network necessary for visuomotor transformations (see **Figure 3**) (Alexander and Crutcher 1990; Kalaska and Crammond 1992; Kalaska et al. 1997; Sabes 2000). Visual information comes in through the primary visual cortex in the occipital lobe, and is further processed through the parieto-occipital region. Information then flows to the posterior parietal cortex (PPC), containing the superior parietal lobule (SPL), IPL, and areas of the intraparietal sulcus. These areas are called the anterior, medial, lateral, and ventral intraparietal areas. Neurons within the PPC are important for visuomotor transformations as they discharge in response to both sensation and movement (Kalaska 1996; Blangero et al. 2009). From the PPC, information is sent to the premotor cortex, which includes areas responsible for motor planning. These areas are the medial supplementary motor area, cingulate motor area, lateral dorsal (PMd) and ventral (PMv) premotor areas. The motor plan is then executed when these areas output information to the primary motor cortex.

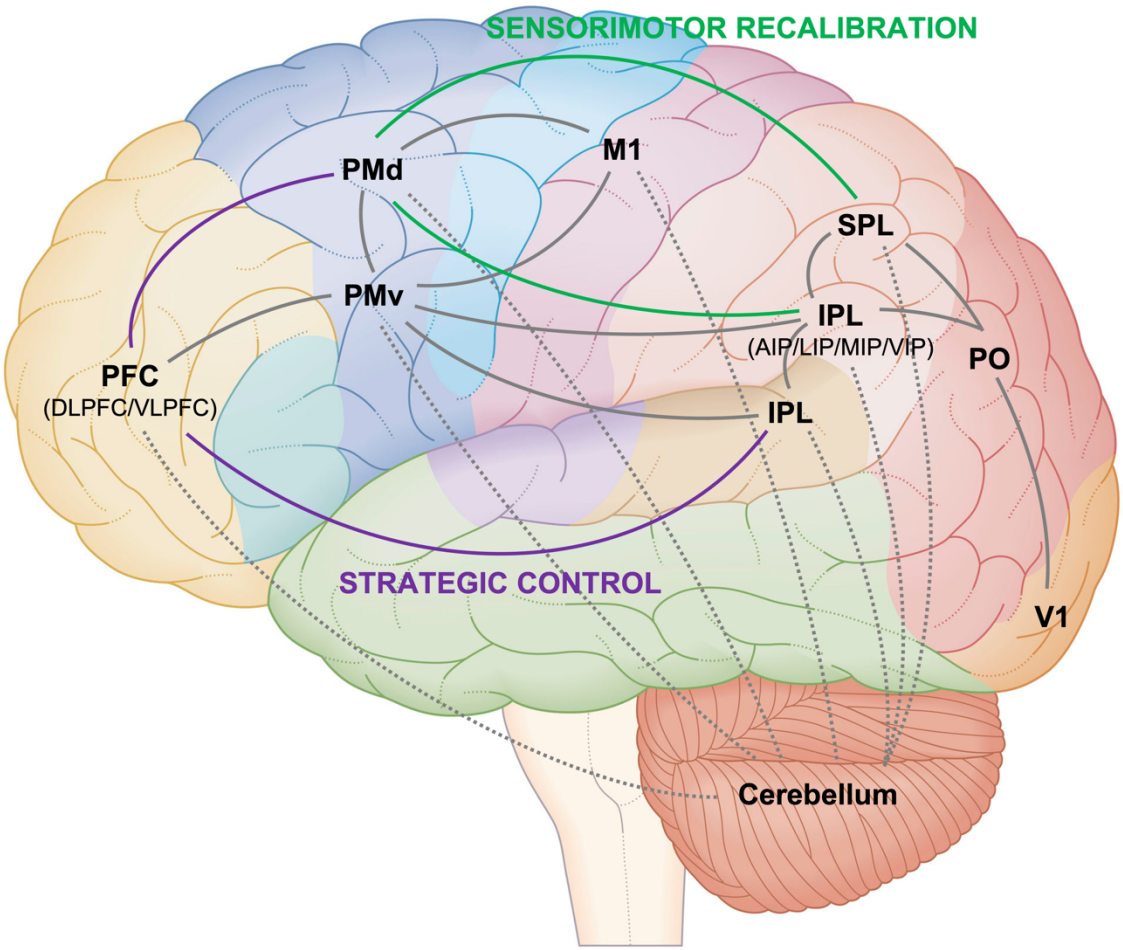

Figure 3. Putative cortical networks required for non-standard visuomotor integration (Granek and Sergio 2015). The simplified schematic diagram depicts the possible cortical connections involved in strategic control (purple lines) and sensorimotor recalibration (green lines). Other intermediate connections in the networks are indicated with grey lines, and connections to the cerebellum are shown with dashed grey lines. Most cortico-cortical connections are reciprocal. The prefrontal cortex (PFC) consists of the ventrolateral (VLPFC) and dorsolateral (DLPFC) prefrontal cortices. The posterior parietal cortex (PPC) includes the superior parietal lobule (SPL) and inferior parietal lobule (IPL). The SPL and IPL are separated by the intraparietal sulcus (IPS), which contains anterior (AIP), lateral (LIP), medial (MIP), and ventral (VIP) subdivisions. The occipital cortex includes the primary visual cortex (V1). Dorsal premotor cortex (PMd), ventral premotor cortex (PMv), parieto-occipital region (PO), and primary motor cortex (M1) are shown as well.

Both single-unit and local field potential activity within parietal and premotor areas of the frontoparietal network is modulated when there is a decoupling between the actions of the eyes and the hand (reaching on a horizontal plane while viewing a guiding stimulus on a vertical place) (Hawkins et al. 2013; Sayegh et al. 2013; Sayegh et al. 2014). Standard reaches show enhanced activity within SPL regions surrounding the medial intraparietal sulcus, and the caudal PMd (Sayegh et al. 2017). In contrast, caudal SPL and rostral PMd show enhanced activity during non-standard reaches where there is a decoupling of the eyes and hand. These results demonstrate a separation by region in the SPL and PMd during standard versus non-standard visuomotor tasks. Results from other studies have further suggested the existence of distinct neurological processes between implicit (sensorimotor recalibration) versus explicit (strategic control) non-standard transformational mapping (Taylor et al. 2014; McDougle et al. 2015). Recent neuroimaging studies in humans have characterized the brain areas required for standard versus implicit and explicit non-standard mapping (Gorbet and Sergio 2016; Gorbet and Sergio 2018). Relative to standard mapping, incorporation of an explicit rule (a visuomotor rotation of 180°) resulted in significantly different activity in the cuneus and medial premotor regions during the preparatory phase of the movement (Gorbet and Sergio 2016). During movement execution, there was greater activity within the right IPL and left superior posterior cerebellum for the non-standard task. The right IPL in particular appears to play an important role in maintaining spatial attention on current task goals, as well as adapting to changing circumstances and responding to salient new information in the environment (Singh-Curry and Husain 2009). Lesions to the right IPL result in disorders of attention and neglect, and deficits in sustaining attention and detecting salient events (Husain and Nachev 2007). Damage to the left IPL is not associated with the same deficits in attention, instead typically leading to the syndrome of apraxia. Discrimination between standard mapping and implicit (arm movements made in a different spatial plane relative to the guiding visual stimulus) non-standard mapping

early in movement planning involved the anterior prefrontal cortex and precuneus (Gorbet and Sergio 2018). As motor execution approached, activity in areas of the premotor, primary motor and somatosensory, posterior parietal, middle occipital, and medial occipital cortices, as well as the anterior lobe of the cerebellum, was able to discriminate between the two conditions.

1.3.2. Effects of healthy aging versus Alzheimer's disease on unimanual visuomotor integration

There are reductions in movement speed and accuracy, as well as difficulties in processing complex visual scenes, that come with healthy aging (Stelmach et al. 1987; Darling et al. 1989; Munoz et al. 1998; Sekuler et al. 2000; Ketcham et al. 2002). Healthy younger and older adults have shown declines in performance of increasingly dissociated reaching tasks requiring non-standard mapping (Hawkins and Sergio 2014). Reaction times and movement times were both significantly longer in the older adults when compared to younger adults in the non-standard conditions. In clinical populations, structural brain changes precede significant memory deficits typically associated with AD. Brain autopsies of demented patients showed widespread Aβ deposits and characteristic distribution patterns of neurofibrillary tangles in frontal and parietal lobes (Braak and Braak 1991a), which are part of the frontoparietal reach network required for visuomotor integration (Caminiti et al. 2017). Damage to white matter tracts has been found in and between brain areas affected in AD, such as in the posterior cingulum, between the prefrontal cortex and MTL, and between the prefrontal cortex and parietal lobe (Adlard et al. 2014). Preclinical AD has been shown to cause visuomotor deficits, where having a family history of dementia and being an APOE e4 carrier were significant predictors of poorer non-standard visuomotor integration performance (Rogojin et al. 2019). Behavioural studies looking at AD patients found performance declines of eye-hand coordination in plane change tasks requiring non-standard mapping (Ghilardi et

al. 1999; Ghilardi et al. 2000). Individuals with mild cognitive impairment and early-stage AD patients show difficulties in movements requiring the integration of cognitive information (Tippett and Sergio 2006; Tippett et al. 2007; Salek et al. 2011; Tippett et al. 2012). Interestingly, these clinical populations performed no differently compared to healthy age-matched controls on a standard mapping task, but only showed significant declines in task performance once an element of decoupling was introduced between gaze and movement (i.e., tasks requiring non-standard visuomotor integration).

While it's the hippocampus that appears to be most severely affected by structural alterations in early AD, glucose hypometabolism is seen predominantly in the temporoparietal area, including the posterior cingulate gyrus, precuneus, and IPL (Schroeter et al. 2009). One theory to explain this discrepancy is that hypometabolism in the parietal cortex is the result of a disconnection from the hippocampus due to cingulum bundle atrophy. In support of this theory, a study looking at patients with early AD found that hippocampal atrophy was correlated with cingulum bundle disruption, which in turn was correlated to hypometabolism of the posterior cingulate cortex, parahippocampal gyrus, hippocampus, and right temporoparietal associative cortex (Villain et al. 2008). These results provide the first direct evidence supporting the disconnection hypothesis as a major factor contributing to the early posterior hypometabolism in AD. Imaging studies have demonstrated that disruption of the precuneus is involved in deficits in visually-guided behaviour (Cavanna and Trimble 2006), and the precuneus has been shown to be involved in movement planning for non-standard tasks requiring a plane change (Gorbet and Sergio 2018). The precuneus, a core node within the DMN, has decreased functional connectivity in healthy older APOE e4 carriers (Riedel et al. 2016). Cognitively healthy older adults with elevated Aβ levels also show decreased DMN connectivity, specifically between the precuneus and the hippocampus (Hedden et al. 2009; Sheline, Raichle, et al. 2010). The right IPL is important for movement planning of tasks

involving a visual feedback reversal (Gorbet and Sergio 2016), and earlier research has shown that the IPL has reciprocal connections with the CA1 subregion of the hippocampus (Rockland and Van Hoesen 1999; Clower et al. 2001). In humans, there is increasing evidence that hippocampal subregions are differentially affected by AD, with atrophy seen in the subiculum and CA1 in preclinical AD (Apostolova et al. 2010; Donix, Burggren, Suthana, Siddarth, Ekstrom, Krupa, Jones, Rao, et al. 2010; Donix, Burggren, Suthana, Siddarth, Ekstrom, Krupa, Jones, Martin-Harris, et al. 2010). Damage to the hippocampus early on in disease progression may therefore affect IPL function. Both the precuneus and IPL show hypometabolism and grey matter atrophy early in AD (Schroeter et al. 2009; Honea et al. 2010). The IFOF and SLF white matter tracts are involved in visuospatial attention and goal-directed behavior (de Schotten et al. 2011; Waller et al. 2017; Herbet et al. 2018), and have connections with the IPL (de Schotten et al. 2011; Conner et al. 2018). Thus, atrophy in the precuneus and right IPL may underlie some of the early visuomotor impairments seen in preclinical AD, mild cognitive impairment, and AD for tasks requiring non-standard mapping.

1.4. Behavioural principles of bimanual coordination

Interlimb movements are those in which two limbs move simultaneously in order to perform a task, such as when buttoning up one's shirt or driving a car. Interlimb movements can involve coordination between homologous limb pairs (i.e., between both arms or both legs), or between non-homologous limb pairs (e.g., the simultaneous movements of the forearm and lower leg, or the wrist and ankle) (Swinnen 2002). Healthy older adults predominantly use interlimb movements over unimanual movements as the majority of everyday tasks require some degree of collaboration between the upper limbs (Kilbreath and Heard 2005; Vega-González and Granat 2005). The final project in this dissertation will focus on fundamental

research investigating interlimb coordination of homologous limb pairs, specifically the upper limbs in bimanual movements.

Performing tasks that require moving more than one limb together introduces constraints or limitations on bimanual movements that don't exist when performing unimanual movements. The most intensively studied have been neuromuscular constraints on bimanual coordination related to the relative timing of homologous muscle activation (Swinnen and Gooijers 2015) which as a result of different coordination modes. Although other modes exist, humans show a tendency towards in-phase or anti-phase (180° phase-shift) coordination modes (Swinnen 2002; Swinnen and Wenderoth 2004). In-phase movements involve both hands moving in mirror-symmetrical patterns with respect to the mid-sagittal plane, and correspond to simultaneous activation of bilateral homologous muscle groups (e.g., simultaneous flexion and extension of both hands at the wrist). Anti-phase patterns of coordination, or parallel asymmetrical movements, arise from non-homologous muscle activation where homologous muscle groups are activated in an alternating fashion (e.g., one hand flexes at the wrist while the other hand extends at the wrist). In-phase and anti-phase movements are spontaneously stable and can generally be performed without practice (Kelso 1984; Lee et al. 1995). In-phase coordination patterns are the more precise and stable of the two, while anti-phase patterns are increasingly unstable when performed at higher frequencies (Kelso 1984; Tuller and Kelso 1989; Wenderoth et al. 2009). For example, in a bimanual four finger tapping tasks, a mirror symmetric pattern of movements with respect to the midline of the body (in-phase) was found to be more stable than a parallel coordination pattern where fingers tapped either to the left or to the right together on both hands (anti-phase) (Mechsner et al. 2001; Mechsner and Knoblich 2004). When movement frequency is increased, the coordination mode will spontaneously switch from anti-phase to in-phase, while the opposite transition does not occur (Kelso 1984; Kelso et al. 1986; Scholz and Kelso 1989). Bimanual coupling of both arms is higher during

in-phase movements, demonstrated by a lower inter-limb phase difference, greater inter-limb synchronization, and similar acceleration profiles (Shih et al. 2019). These spatiotemporal relationships suggest that in-phase movements are controlled by a common neural generator (i.e., the dominant hemisphere), while in anti-phase movements the two limbs are controlled more independently. Phase patterns that deviate from in-phase or anti-phase coordination can be performed, however they are more difficult and require practice (Smethurst and Carson).

There is also a bimanual coupling effect that takes place such that the two hands become constrained either spatially or temporally (Swinnen 2002). Imagine for a moment that there are two cups sitting on the table in front of you, one slightly closer and one slightly further away. If you were asked to unimanually reach out and grasp each cup separately, you would likely predict that it would take less time to grasp the cup that is closer to you. If you were then asked to perform this task bimanually (i.e., perform the two unimanual tasks simultaneously), would you still conclude that you would grasp the closer cup in less time? Previous research suggests that actually you would likely reach and grasp both cups at approximately the same time (Kelso et al. 1979; Crites and Gorman 2017). This is an example of temporal bimanual coupling. Another example of temporal coupling was shown in a bimanual finger tapping study, where most individuals were not able to successfully tap rhythms of non-harmonic relations without interference between the two hands (Peters 1977).

In the spatial domain, the bimanual coupling effect has mostly been investigated through the simultaneous performance of incongruent actions, such as movements with different spatial forms (Franz et al. 1996; Franz 1997), directions (Swinnen et al. 2001), or amplitudes (Sherwood 1994a; Sherwood 1994b; Spijkers and Heuer 1995). For instance, have you ever tried to simultaneously tap the top of your head with one hand while rubbing your stomach in a circular motion with the other? In a similar task, when participants were asked to draw a line with one hand and a circle with the other hand, this resulted in cross-talk between the two

effectors and produced somewhat line-like circle and circle-like lines (Franz et al. 1991). Various combinations of these neuromuscular, temporal, and spatial constraints can further mediate bimanual control. For example, in-phase movements (homologous muscle activation) in the same direction (i.e., curling and uncurling the fingers by flexing and extending them) were performed with greater stability and accuracy than non-isodirectional in-phase movements (i.e., mirror-symmetrical abduction and adduction of the index fingers with respect to the midline of the body) (Swinnen et al. 1998).

1.4.1. Neural correlates of bimanual movements in healthy adults

Bimanual movements are not coordinated by a specific brain area, but rather require an involvement or collaboration among regions of a distributed motor network of cortical and subcortical areas that are important for general motor control (Debaere et al. 2001). These brain regions include the dorsal premotor cortex (PMd), primary sensorimotor cortex (M1 and S1), supplementary motor area (SMA), cingulate motor area (CMA), posterior parietal cortex (PPC), and the cerebellum, and show greater activation during bimanual tasks compared to unimanual tasks (Jancke et al. 2000; Tracy et al. 2001; Swinnen 2002; Lin et al. 2017). Differential activation levels were revealed in non-isodirectional bimanual coordination patterns compared to isodirectional coordination patterns, with greater activation in medial frontal areas including the SMA and CMA (Debaere et al. 2001). Studies have further addressed the distinction in neural activity underlying in-phase (symmetrical) and anti-phase (asymmetrical) coordination modes. In right-handed individuals, the left dominant hemisphere plays a key role in the execution of in-phase movements, resembling the combined activity patterns of right and left unimanual movements (Stephan et al. 1999). Meanwhile, there is greater activity in the right non-dominant hemisphere when performing anti-phase movements. Anti-phase bimanual movements, when compared to in-phase movements, show further

increased activation in the PMd (Sadato et al. 1997; Immisch et al. 2001; Ullén et al. 2003; Debaere et al. 2004a; Wu et al. 2010), SMA (Sadato et al. 1997; Debaere et al. 2001; Immisch et al. 2001; Ullén et al. 2003; Debaere et al. 2004b; Wu et al. 2010), CMA (Immisch et al. 2001; Lin et al. 2017), PPC (Nair et al. 2003; Ullén et al. 2003; Wu et al. 2010; Kiyama et al. 2014), and cerebellum (Debaere et al. 2004a; Kraft et al. 2007; Wu et al. 2010; Lin et al. 2017). Specifically, increasing spatiotemporal complexity of bimanual hand movements (i.e., moving from unimanual, to bimanual in-phase, to bimanual anti-phase, to bimanual 90° out-of-phase tasks) resulted in increases in activity in anterior and posterior hemisphere (lobule V, VIII) and vermis (V, VI, and VIII) regions of the cerebellum (Debaere et al. 2004a). Other studies have reported the importance of cerebellar lobules IV and VI in successful bimanual control (Debaere et al. 2004b; Boisgontier et al. 2018).

The cerebellum is organized into two cerebellar hemispheres which are separated by an unpaired medial structure called the vermis (Klein et al. 2016). There are 10 lobules in the two hemispheres of the cerebellar cortex (lobules I-X), with lobules I-V constituting the anterior cerebellar lobe, lobules VI-IX the posterior cerebellar lobe, and lobule X the flocculonodular lobe, with corresponding vermal regions (vermis I-X). Cerebellar lobules IV-VI both receive input from and project to the arm area of M1 (Kelly and Strick 2003). Converging evidence suggests that parts of the anterior lobe (lobule V) and posterior lobe (lobules VI and VIII) constitute the sensorimotor cerebellum, showing greater activation during sensorimotor tasks (Habas et al. 2009; Stoodley and Schmahmann 2009; Stoodley and Schmahmann 2010). Human neuroimaging studies have also demonstrated somatomotor representations within the cerebellum, with representation of the arm and fingers localized to lobules V and VIII (Grodd et al. 2001; Wiestler et al. 2011). Together with findings from bimanual studies, these studies suggest the importance of specific cerebellar lobules (i.e., lobules IV-VI and VIII) in visuomotor and bimanual control.

1.4.2. Sex differences and their potential neural correlates in bimanual coordination performance

Few studies have investigated sex effects on bimanual coordination, and those that have report contradictory findings with some studies demonstrating a slight female advantage (Albines et al. 2016; Khanjari and Arabameri 2021) while others found a slight male advantage (Mickevičienė et al. 2011; Shetty et al. 2014). These discrepancies may be due to differences in the tasks used to investigate bimanual coordination as sex effects have been shown to depend strongly on task symmetry, for instance, where women had better performance of some bimanual tasks and worse performance in others compared to men (Rudisch et al. 2020). The neural activity underlying sex-differences in bimanual movement production have not been explicitly studied. Bimanual performance asymmetries between women and men may arise from sex differences in interhemispheric connectivity. As discussed in the subsection above, different intra- and interhemispheric neural networks are necessary for successfully performing bimanual tasks. Greater within-hemisphere connectivity and cross-hemispheric cerebellar connectivity in men may confer a more efficient system for coordinated action (Ingalhalikar et al. 2014). Bimanual movements result in greater activation of the cerebellum compared to unimanual movements (Swinnen et al. 2002; Debaere et al. 2004a), with further increased cerebellar activity associated with increasingly complex bimanual tasks (Debaere et al. 2004a). Greater cross-hemispheric cerebellar connectivity in men may explain the male bimanual advantage demonstrated in some studies (Mickevičienė et al. 2011; Shetty et al. 2014).

Conversely, women have greater interhemispheric connectivity (Ingalhalikar et al. 2014) and sex-differences in functional activity associated with visually-guided arm movements have been demonstrated using both fMRI (Gorbet and Sergio 2007) and EEG (Gorbet et al. 2010). These functional studies showed that during the preparatory phase of the movement, activity

in the PMd and PPC occurred mainly contralateral to the arm movement in men but showed a more bilateral activation in women. Greater interhemispheric connectivity and more bilateral activation in women suggests there is greater transmission of information across hemispheres and a greater capacity for one hemisphere to inhibit another. This may allow for an enhanced ability to decouple the arms in bimanual movements and translate into better bimanual coordination performance in women reported by other studies (Albines et al. 2016; Khanjari and Arabameri 2021). The contradictory results of sex-differences in bimanual performance and lack of studies explicitly investigating potential sex-differences in bimanual neural activity highlight a gap in the literature trying to understand the neural correlates of bimanual movements.

1.5. A brief overview of the three projects described in this dissertation

There were a number of objectives that drove the following projects, where the broad aim of the research discussed in this dissertation was to understand the neural mechanisms controlling voluntary movement. The first general objective was to examine the impact of early Alzheimer's disease pathology on neural networks underlying complex visuomotor transformations in unimanual reaching movements. Previous work from our laboratory demonstrated that a tablet-based visuomotor transformation task may be used as a cost-effective and clinically accessible assessment tool for the early detection of dementia likely due to Alzheimer's disease (Rogojin et al. 2019). The first two projects described in this dissertation were a direct extension of these previous findings, and examined the neural anatomy (**chapter two**) and resting functional connectivity (**chapter three**) underlying impaired visuomotor performance in individuals with an increased genetic (APOE e4) risk for Alzheimer's disease. The second general objective was more fundamental in nature, and sought to elucidate the neural correlates of previously observed sex differences in bimanual task

performance in healthy adults (Mickevičienė et al. 2011; Shetty et al. 2014; Albines et al. 2016; Khanjari and Arabameri 2021). While the underlying brain activity associated with completing the unimanual task has been extensively studied and shown to differ between the sexes (Gorbet and Sergio 2007; Gorbet et al. 2010; Gorbet and Staines 2011), there is a gap in the literature investigating potential sex-differences in the neural correlates underlying bimanual performance. The final project in this dissertation characterized the differences in the neural control of bimanual movement between males and females (**chapter four**).

Chapter Two

Structural MRI and diffusion tensor imaging: Effects of APOE status, family history of dementia, and sex on non-standard visuomotor performance

Alica Rogojin, Diana J. Gorbet, Kara M. Hawkins, and Lauren E. Sergio

ABSTRACT

Introduction: Visuomotor impairments have been demonstrated in preclinical AD in individuals with a positive family history of dementia and APOE e4 carriers. Previous behavioural findings have also reported sex-differences in performance of visuomotor tasks involving a visual feedback reversal. The current study investigated the relationship between grey and white matter changes and non-standard visuomotor performance, as well as the effects of APOE status, family history of dementia, and sex on these brain-behaviour relationships. **Methods:** Older adults (n = 49) with no cognitive impairments completed non-standard visuomotor tasks involving a visual feedback reversal, plane-change, or combination of the two. Participants with a family history of dementia or who were APOE e4 carriers were considered at an increased risk for AD. T1-weighted anatomical scans were used to quantify grey matter volume and thickness, and diffusion tensor imaging measures were used to quantify white matter integrity. **Results:** In APOE e4 carriers, grey and white matter structural measures were associated with visuomotor performance. Regression analyses showed that visuomotor deficits were predicted by lower grey matter thickness and volume in areas of the medial temporal lobe previously implicated in visuomotor control (entorhinal and parahippocampal cortices). This finding was replicated in the diffusion data, where regression analyses revealed that lower white matter integrity (lower FA, higher MD, higher RD, higher AxD) was a significant predictor of worse visuomotor performance in the forceps minor, forceps major, cingulum, inferior fronto-occipital fasciculus (IFOF), inferior longitudinal fasciculus (ILF), superior longitudinal fasciculus (SLF), and uncinate fasciculus (UF). Some of these tracts overlap with those important for visuomotor integration, namely the forceps minor, forceps major, SLF, IFOF, and ILF. **Conclusions:** These findings suggest that measuring the dysfunction of brain networks underlying visuomotor control in early-stage AD may provide a novel behavioural target for dementia risk detection that is easily accessible, non-invasive, and cost-effective. The results also provide insight into the structural differences in inferior parietal lobule that may underlie previously reported sex-differences in performance of the visual feedback reversal task.

1. INTRODUCTION

Alzheimer's disease (AD) is a slowly progressive neurodegenerative disease and the most common cause of dementia in older adults. AD pathology begins several decades before the onset of clinical dementia, and symptoms appear only after there has already been significant damage to the brain (Morris 2005), which means the assessment of increased dementia risk in the early stages of AD is crucial. Recently published guidelines suggest that effective interventions could be initiated during this early stage of disease progression (Dubois et al. 2016). Even in the absence of effective disease-modifying treatments that prevent neuronal loss and resultant cognitive decline (Vaz and Silvestre 2020), the early recognition of dementia risk is important for improving patient outcomes now and in the future when effective therapies become available. Current clinical diagnosis of AD involves procedures that can be invasive, expensive, and time-ineffective (such as cerebrospinal fluid analysis, blood tests, and neuroimaging), making their use as frontline screening tools limited. Furthermore, studies have shown that dementia is under-diagnosed in primary care (Connolly et al. 2011; Lang et al. 2017; Amjad et al. 2018) even as the prevalence of AD is projected to rise due to increased life expectancy (Alzheimer's Association 2019). A number of medical, environmental, and lifestyle factors have been associated with an increased risk for developing mild cognitive impairment and dementia, some of which include modifiable risk factors such as diabetes, tobacco use, physical inactivity, obesity, and social isolation (Livingston et al. 2020; Litke et al. 2021). These factors highlight the need for the development of a non-invasive and cost-effective assessment tool for those at increased dementia risk. By identifying individuals at a greater risk for developing dementia, healthcare providers can provide evidence-based recommendations on lifestyle changes, interventions, and management of physical and mental health conditions to delay or slow down the progression of AD (World Health Organization 2019).

As an alternative to current diagnostic tools and procedures, measuring the dysfunction of brain networks underlying visuomotor transformations in early-stage AD may provide a novel behavioural target for dementia risk detection that is easily accessible and cost-effective. Default or "standard" visually-guided arm movements typically involve looking towards the intended target of a reach, followed by an arm movement to the same location (Gielen et al. 1984; Wise et al. 1996; Helsen et al. 1998). For example, reaching directly towards a cup of tea to pick it up. However, many tasks in our everyday lives require us to spatially dissociate the targets of the eye and arm movements, such as during a plane-change or a visual feedback reversal. A common example of a plane-change is using a computer with a mouse or trackpad. Arm movements controlling the mouse or trackpad are made along the horizontal plane in order to move a cursor on the vertical computer screen. An example of a visual feedback reversal is seen when using some computer trackpads, where sliding up on the trackpad scrolls the page down. Another example would be the use of a car's rear-view camera (or, rear-view mirror) while backing up. To avoid hitting any objects, one must turn the steering wheel leftward in a vertical plane while the object on the screen (or, in the mirror) moves to the right. Here, the plane of limb movement is decoupled from the guiding visual information, and there is a visual feedback reversal as well. These decoupled or "non-standard" visually-guided arm movements require the integration of some form of cognitive information into the visuomotor transformation, and the mapping between the visual stimulus and response must be learned and calibrated (Wise et al. 1996). Some patient populations show an impaired ability to successfully perform non-standard visuomotor tasks, even while their performance on standard mapping tasks remains unaffected. These impairments have been observed in patients with mild cognitive impairment (Salek et al. 2011), in the early stages of dementia due to AD (Tippett et al. 2012; de Boer et al. 2014; de Boer et al. 2015; de Boer et al. 2016), and in individuals at an increased risk for future dementia (due to a dementia family history, or a genetic risk due to

being an APOE e4 carrier) who did not yet show any cognitive deficits (Hawkins and Sergio 2014; Lu et al. 2021).

Visuomotor integration relies on interconnected brain regions within the frontoparietal network (Wise et al. 1997; Sabes 2000; Filimon 2010; Caminiti et al. 2017). There are some areas of activity common to both standard and non-standard visuomotor reaching tasks including the contralateral primary, premotor, and medial motor regions, as well as the postcentral gyrus (Gorbet et al. 2004). Additional brain regions become active during non-standard reaching tasks as visuomotor transformations become increasingly dissociated. These brain areas include the anterior prefrontal cortex, precuneus, and large regions of the occipital lobe for non-standard visuomotor integration involving a plane-change (Gorbet and Sergio 2018), as well as areas of the premotor, primary motor and somatosensory, posterior parietal, middle occipital, and medial occipital cortices during a visual feedback reversal task (Gorbet and Sergio 2016). When contrasting a standard task with a non-standard task involving both a feedback reversal and plane-change using a joystick, the non-standard task showed increased activity in the left precuneus, the right superior frontal and middle temporal gyri, and bilaterally in the angular gyri (Gorbet et al. 2004). The precuneus and inferior parietal lobule in particular appear to be important for discriminating between standard and non-standard task conditions (Gorbet and Sergio 2016; Gorbet and Sergio 2018).

Given the known functional substrates of non-standard visuomotor transformations, several white matter tracts that connect these areas of the frontoparietal network may be implicated in visually-guided reaching. The superior longitudinal fasciculus (SLF) has been shown to be important for visuomotor integration (Rodríguez-Herreros et al. 2015; Budisavljevic et al. 2017) and to a lesser extent, the inferior fronto-occipital fasciculus (IFOF) which has been implicated in visuospatial attention and goal-directed behaviour (de Schotten et al. 2011; Waller et al. 2017; Herbet et al. 2018). Both the SLF and IFOF have connections

with the inferior parietal lobule (de Schotten et al. 2011; Burks et al. 2017), which is one of the regions important for non-standard visuomotor mapping. The inferior longitudinal fasciculus (ILF) runs between the anterior temporal and posterior occipital lobes (Bennett et al. 2012; Wycoco et al. 2013), and is involved in processing visual cues and thus also in visually-guided decisions and goal-oriented behaviours (Waller et al. 2017; Herbet et al. 2018). A meta-analysis reported that the corpus callosum also plays a central role in visuomotor integration, as well as in higher-order cognitive functions such as spatial attention and executive control (Schulte and Müller-Oehring 2010).

Little evidence exists regarding the role of the medial temporal lobe in visual guidance of movements and in visuomotor or motor tasks. Some areas of the medial temporal lobe have been implicated in visuomotor coordination. The parahippocampal cortex may be an important relay for the transformation between visual inputs and hand kinematics (outputs), and the hippocampus, parahippocampus, and entorhinal cortex appear to encode the position of the hand in space (Tankus and Fried 2012). The retrosplenial cortex has extensive connections with the parietal cortex (Vann et al. 2009), playing a central role in the coordination of information between internal and external spatial frames of reference (Clark et al. 2018) which is important for visually-guided movements. Although dramatic neuronal loss is not observed in preclinical AD, there is mild grey matter atrophy in areas of the medial temporal lobe including the entorhinal, perirhinal, hippocampal, and parahippocampal cortical regions during this stage (Honea et al. 2009; Honea et al. 2011). There is increasing evidence that hippocampal subregions are differentially affected by AD progression, with the earliest atrophy found in the subiculum and CA1 subfields in preclinical AD (Apostolova et al. 2010; Donix, Burggren, Suthana, Siddarth, Ekstrom, Krupa, Jones, Martin-Harris, et al. 2010; Donix, Burggren, Suthana, Siddarth, Ekstrom, Krupa, Jones, Rao, et al. 2010). The CA1 has reciprocal

connections with the inferior parietal lobule (Rockland and Van Hoesen 1999; Clower et al. 2001). The retrosplenial cortex is also affected early in AD progression (Nestor et al. 2003).

Diffusion tensor imaging measures (fractional anisotropy, FA; mean diffusivity, MD; radial diffusivity, RD; and axial diffusivity, AxD) provide information about white matter microstructure and pathology (Song et al. 2002; Song et al. 2003), and have been used as an index of white matter integrity (Pfefferbaum et al. 2000; Acosta-Cabronero and Nestor 2014; Molloy et al. 2021). Several studies have suggested that white matter damage may precede grey matter atrophy in AD (Hong et al. 2016; Hoy et al. 2017; Dadar et al. 2020). White matter integrity declines have been found in several major white matter tracts including the corpus callosum, cingulum, SLF, IFOF, ILF, and uncinate fasciculus (UF) in cognitively healthy adults who are APOE e4 carriers and have a parental family history of AD (Bendlin et al. 2010; Gold et al. 2012; Westlye et al. 2012; Adluru et al. 2014). Some of these tracts overlap with those mentioned previously to be involved in visuomotor integration. Known early AD pathology (Thal et al. 2002; Mintun et al. 2006; Pletnikova et al. 2018) and atrophy (Chételat, Villemagne, Bourgeat, et al. 2010; Jacobs et al. 2011; Doré et al. 2013) in frontal and parietal regions, combined with frontoparietal tract involvement in healthy rule-based visuomotor integration, suggest that reduced communication along these tracts may underlie impaired performance in those at an increased risk for dementia.

In the present study, we first examined whether individuals at an increased risk for AD (due to a family history or a genetic risk) showed grey matter atrophy or declines in white matter integrity in brain regions and tracts typically affected early in disease progression. However, the main objective was to explore the neural underpinnings to previous behavioural findings, where individuals with a positive family history of dementia and APOE e4 carriers demonstrated performance deficits on non-standard visuomotor tasks (Rogojin et al. 2019). There were also sex-related differences in performance of the non-standard visuomotor task

involving a feedback reversal. In the current study, we examined the neural anatomy underlying impaired non-standard visuomotor performance, and whether this impairment is affected by family history of AD, APOE e4 status, or sex. We hypothesized a positive relationship between brain structural and white matter integrity measures and visuomotor performance. We predicted grey matter atrophy within the inferior parietal lobule, precuneus, and retrosplenial cortex to be associated with deficits in non-standard visuomotor integration. We were also interested in exploring whether atrophy in the areas of the medial temporal lobe that have been previously implicated in visuomotor coordination would be predictive of worse visuomotor task performance. Based on the importance of the SLF, IFOF, ILF, and corpus callosum in visuomotor integration and goal-directed behaviour, we also predicted that white matter integrity declines in these tracts would similarly be associated with declines in non-standard visuomotor integration performance. An exploratory component to the study was to explore the effects of family history, APOE status, and sex on these brain-behaviour relationships.

2. METHODS

2.1. Participants

Forty-nine right-handed older adults aged 49 to 69 were included in the current study: 25 individuals with a positive family history of dementia but with no cognitive impairment (n = 12 females), and 24 individuals with no family history of dementia (n = 12 females) (see **Table 1** for demographic information). Classification of a positive family history of dementia was based on self-reported maternal or multiple family history (including at least one first-degree relative) of late-onset AD or probable AD. Cognitive function was measured with the Montreal Cognitive Assessment (MoCA), where scoring at or above education-adjusted norms of 26 or higher indicated no cognitive impairment. A higher risk for AD is associated with a maternal history of dementia, while paternal history does not confer the same increased risk and was

therefore not used for high-dementia risk classification (Honea et al. 2010; Honea et al. 2011). Participants were excluded if their parents were deceased at a young age before dementia could be detected, or if the participant was estranged from either of their biological parents and did not know their medical history. Classification of no family history of dementia was based on participants having no family history of AD or any other type of dementia, not demonstrating memory impairments outside of their age range norm, and scoring at or above age-average on the MoCA. Participants with a positive family history of dementia were age-balanced with participants without a family history of dementia. At present, the apolipoprotein E (APOE) e4 allele represents the strongest and best-established genetic risk factor for progression to clinical AD (Reitz and Mayeux 2014; Dubois et al. 2016). Participants with a family history of dementia or who were APOE e4 carriers were considered at an increased risk for AD. The exclusion criteria included uncorrected visual impairments, upper-limb impairments, any medical conditions that would hinder motor task performance (e.g., severe arthritis or dystonia), neurological illnesses (e.g., Parkinson's disease, depression, schizophrenia, alcoholism, epilepsy), history of head injury (e.g., mild, severe), stroke, and medical diagnoses that might impact white matter integrity and brain connectivity (i.e., hypertension or diabetes). The study protocol was approved by the Human Participants Review Sub-Committee of York University's Ethics Review Board.

Table 1. Participant demographic features.

	APOE e4 positive	APOE e4 negative	FH+	FH-	Females	Males
Demographics						
n	16	31	25	24	24	25
Age (years)	59.3 ± 5.30	58.4 ± 5.99	58.5 ± 6.10	58.8 ± 5.29	58.4 ± 5.81	58.8 ± 5.63
Range	*51 - 68*	*49 - 69*	*51 - 69*	*49 - 67*	*50 - 68*	*49 - 69*
FH+	11 (69%)	14 (45%)			12 (50%)	13 (52%)
APOE e4 positive			11 (69%)	5 (31%)	11 (46%)	5 (20%)
MoCA score	27.9 ± 1.5	28 ± 1.56	27.8 ± 1.52	28 ± 1.56	28.2 ± 1.53	27.6 ± 1.5
Range	*26 - 30*	*26 - 30*	*26 - 30*	*26 - 30*	*26 - 30*	*26 - 30*
Years of education	16.0 ± 3.70	17.7 ± 3.15	17.3 ± 3.52	16.8 ± 3.19	17.3 ± 3.07	16.7 ± 3.61
Range	*11 - 23*	*12 - 24*	*11 - 23*	*12 - 24*	*12 - 24*	*11 - 22*

FH+, positive family history of dementia; FH-, no family history of dementia; APOE, apolipoprotein E; MoCA, Montreal Cognitive Assessment.

2.2. APOE genotyping

A total of 2 mL of saliva were collected from each participant in microtubes from Diamed Lab Supplies Inc. using collection aids from Cedarlane Labs. Samples were sent to DNA Genotek Inc. (Ottawa, ON, Canada) for DNA extraction and APOE genotyping. DNA was isolated from samples according to the manufacturer's protocols. Genotyping for APOE involved single nucleotide polymorphism (SNP) genotyping, and tested for SNPs rs429358 and rs7412. The proteins that are produced by the APOE gene are either E2, E3, or E4 combinations (for instance, E2/E3).

2.3. Behavioural data

2.3.1. Behavioural data acquisition

A detailed description of our visuomotor assessment has been previously published (Rogojin et al. 2019). Briefly, all subjects completed four visuomotor transformation tasks, similar to those previously used by our laboratory (Tippett and Sergio 2006; Tippett et al. 2007; Salek et al. 2011; Tippett et al. 2012; Hawkins and Sergio 2014; Hawkins et al. 2015; Hawkins and Sergio 2016). These tasks were found to discriminate between women at high- and low-AD risk with a classification accuracy of 86.4% (sensitivity: 81.8%, specificity: 90.9%) (Hawkins and Sergio 2014). The tasks involved making simple sliding finger movements between targets displayed on an Acer Iconia 6120 dual-touchscreen tablet. These tasks were divided into one standard mapping condition (gaze and movement were coupled) and three different non-standard mapping conditions (gaze and movement were decoupled). In all four conditions, participants were instructed to slide the index finger of their right hand along the touch screen (either the vertical or horizontal screen depending on the condition) in order to displace the cursor from a central target to one of four peripheral targets (up, down, left, right) as quickly and as accurately as possible. In the standard mapping task (S), the spatial location of the visual

target and the required hand movement were the same. The non-standard mapping tasks involved the finger movements being made either on a different plane (plane-change, PC), in the opposite direction (feedback reversal, FR), or both (PC+FR), from the spatial target location (see **Fig. 1a** for depictions of all four visuomotor transformation task conditions). Eye movements were the same across all conditions (i.e., always to the guiding visual target on the vertical screen).

The four conditions were presented in randomized blocks, each consisting of five pseudo-randomly presented trials to each of the four peripheral targets. Peripheral targets were located 75 mm from the central target, with target diameters set to 20 mm. The tasks were displayed on a 170 x 170 mm black square and a surrounding grey background. There was a total of 20 trials per condition, and thus each participant completed a total of 80 trials across the four conditions. To ensure task comprehension, each participant was given two practice trials per peripheral target prior to each of the four conditions. The trial timings and participant movements consisted of the following steps: 1) a yellow central (home) target was presented on the vertical tablet, 2) participants moved a white cursor to the central target, changing its colour to green once they reached it, 3) after holding the central target for 4000 ms, one of four red peripheral targets appeared and the central target disappeared, serving as the 'Go' signal for initiation of a movement, 4) participants were told to look towards the visual target and slide their finger along the touchscreen to direct the cursor towards the target, 5) once the peripheral target was reached and the participant held it for 500 ms, it disappeared, signaling the end of the trial, 5) the next trial began with the presentation of the central target after an inter-trial interval of 2000 ms (see **Fig. 1b** for visual representations of a single trial completion).

In the standard condition, participants were asked to slide their finger directly to the target on the vertical screen (the cursor was directly under their finger). In the PC condition (non-

standard), participants needed to move on the horizontal screen while looking at the vertical screen in order to direct the cursor towards the visual target displayed on the vertical screen. In the FR condition (non-standard), the cursor moved in the opposite direction of the participant's finger movements, requiring them to slide their finger on the vertical screen away from the visual target in order to move the cursor towards it. Finally, in the PC+FR condition (non-standard), movements needed to be made in the opposite direction and on a different plane from the visual target in order to direct the cursor towards it.

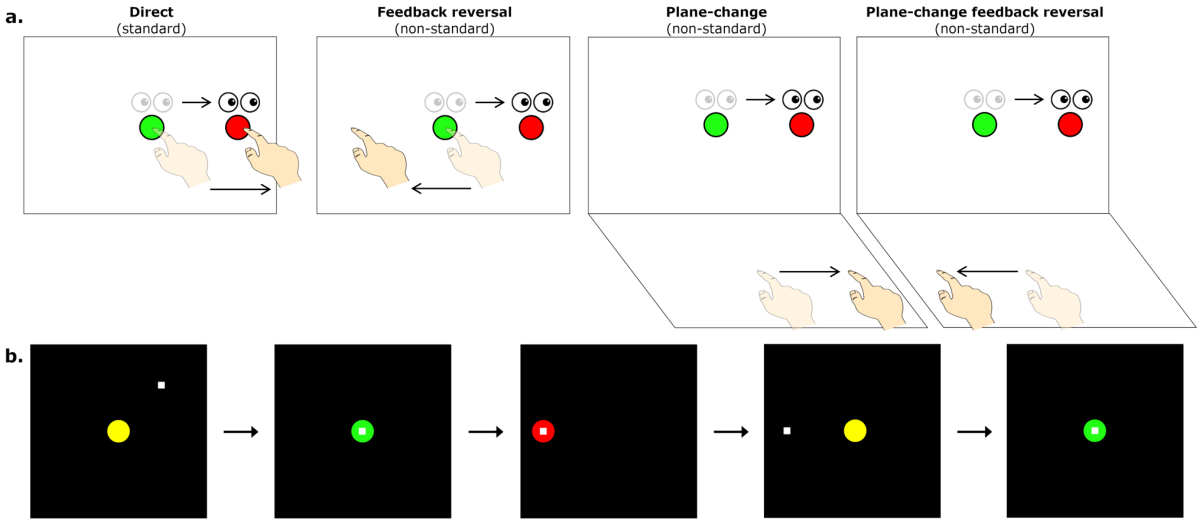

Figure 1. a) Schematic drawing of the visuomotor task conditions. Lighter eye and hand symbols denote the starting position for each trial (green central target). Darker eye and hand symbols denote the instructed eye and hand movements for each task. Red circles denote the peripheral (reach) target, presented randomly in one of four locations (left, up, right, or down relative to the central target). The direct interaction task requires standard mapping, where participants slide their finger on a touch screen to move a cursor from a central target to one of four peripheral targets. The other three conditions involve non-standard visuomotor integration, where targets either have a 180° feedback reversal (feedback reversal), are spatially dissociated from the plane of hand motion (plane-change), or both (plane-change + feedback reversal). **b)** Sequence of events during one trial of the visuomotor task. All trials begin in the central (home) target. Once the participant moves the cursor (denoted by the white square) into the central target, the target changes from yellow to green to signify a movement preparation period. After 4000 ms, a red peripheral target appears in one of four directions (up, down, left, or right of the centre) and serves as the 'Go' signal. Once the peripheral target is acquired and held for 500 ms it disappears, signaling the end of the trial. After an inter-trial interval of 2000 ms, the central yellow target reappears, and the participant moves back to the central target to initiate the next trial.

2.3.2. Behavioural data preprocessing

Kinematic measures, including timing, finger position (x, y coordinates; 50 Hz sampling rate), and error data were recorded for each trial and converted into a MATLAB readable format using a custom written (C++) application. Custom analysis software (Matlab, Mathworks Inc.) was used to process individuals' finger trajectories with a fourth-order (dual pass) low-pass Butterworth filter at 10 Hz. Finger trajectories were generated from these filtered paths for each successful trial and displayed on a Cartesian plot illustrating finger location data superimposed on central and peripheral target locations. Movement onsets and ballistic movement offsets (the initial movement prior to any corrective movements) were scored at 10% peak velocity. Total movement offsets were scored as the final 10% peak velocity point once the finger position was within the correct peripheral target. If the initial movement successfully resulted in the finger reaching the peripheral target, then ballistic and total movement offsets were the same. These movement profiles were then verified by visual inspection, and manually corrected when necessary. Unsuccessful trials (error data) were detected by the data collection software by meeting the following criteria: finger left the home target too early (<4000 ms), reaction time (RT) was <150 ms or >8000 ms, or total movement time was >10 000 ms. Trials in which the first ballistic movement exited the boundaries of the central target in the wrong direction (>90^{o} in either direction from a straight line to the target) were coded as direction reversals. Direction reversals were not included in metrics from correct trials, but instead were analyzed as a separate variable. All scored data were then processed to compute 7 different timing, accuracy, and precision measures described below. Any trials exceeding 2 standard deviations from the participant's mean for any of the outcome measures were eliminated from final outcome calculations.

The kinematic outcome measures were as follows: 1) Reaction time (RT), the time interval (in ms) between the central target disappearance and movement onset; 2) Full

movement time (MTf), the time (in ms) between movement onset and offset; 3) Peak velocity (PV), the maximum velocity obtained during the ballistic movement, and used to calculate the 10% threshold used for determining movement onsets and offsets; 4) Path length (PL), the total distance (in mm, calculated from the x and y trajectories) travelled between movement onset and offset; 5) Absolute error (AE), a measure of end-point accuracy, and the average distance (in mm) from the individual ballistic movement endpoints ($\sum$ x/n, $\sum$ y/n) to the actual target location; 6) Variable error (VE), a measure of end-point precision, and the distance (in mm) between the individual ballistic movement endpoints (σ) from their mean movement; and 7) Direction reversals (DR), recorded as a percentage of total completed trials. Corrective path length (CPL) represents corrective movements and was quantified by subtracting the PLb (initial movement offset) from the PLf (full movement offset).

2.4. Magnetic resonance imaging

2.4.1. Image acquisition

MRI data were acquired using a 3 Tesla (3T) Siemens Trio scanner at York University. Participants received a T1-weighted anatomical scan using a sagittal volumetric magnetization-prepared rapid gradient echo (MP-RAGE) sequence. The MP-RAGE consisted of the following acquisition parameters: 192 sagittal slices (slice thickness of 1 mm, with no gap), field of view (FOV) of 256 x 256 mm, matrix size of 256 x 256 resulting in a voxel resolution of 1 x 1 x 1 mm, echo time (TE) = 2.96 ms, repetition time (TR) = 2300 ms, flip angle = 9^{o}. The MP-RAGE scan was used to quantify grey matter volume and thickness. For assessing white matter integrity, a whole-brain diffusion-weighted scan was acquired with 64 encoding directions using diffusion-weighted spin-echo single-shot echo planar imaging. The diffusion tensor imaging (DTI) sequence used the following acquisition parameters: 56 axial slices (slice thickness of 2 mm, with no gap), FOV of 192 x 192 mm, matrix size of 128 x 128 resulting in

a voxel resolution of 1.5 x 1.5 x 2.0 mm, TE = 86 ms, TR = 6900 ms, b-value = 1000 s/mm^2 (including one volume with no diffusion gradient, b = 0 s/mm^2).

2.4.2. Structural MRI

Preprocessing: The cortical surface was reconstructed using FreeSurfer 7.1 (Harvard Medical School, Boston, USA; https://surfer.nmr.mgh.harvard.edu/) with individual T1-weighted MR images serving as input. The main Freesurfer reconstruction pipeline ("*recon-all*") was used to parcellate and segment the brain into anatomically distinct regions of the cortex and subcortical nuclei, respectively. Visual inspection of each participant's parcellation and segmentation was performed to ensure that there were no obvious errors.

Grey matter volume and thickness (Fig. 2a,b): Volume and thickness measures for the precuneus, inferior parietal lobule, and parahippocampal cortex were obtained from the Desikan-Killiany atlas (Desikan et al. 2006) used in *recon-all*. Volume and thickness measures for the entorhinal cortex and perirhinal cortex were obtained from the cytoarchitecturally-defined ex vivo labels in FreeSurfer. The retrosplenial cortex was defined as the posterior-ventral part of the cingulate gyrus, or the isthmus of the cingulate gyrus, from the Destrieux atlas (Destrieux et al. 2010) used in *recon-all*. The posterior-ventral part of the cingulate gyrus provides a mask slightly larger than Brodmann areas 29 and 30 (i.e., the retrosplenial cortex proper) (Shine et al. 2016; Calati et al. 2018).

Hippocampal subfield segmentation (Fig. 2c,d,e): Segmentation of the hippocampus into its subfields was performed with the FreeSurfer hippocampal module using the T1-weighted volumes processed with recon-all (Iglesias et al. 2015). This tool uses a probabilistic atlas constructed from *ex vivo* MRI data and a separate *in vivo* MRI dataset to automatically segment the hippocampal substructures. The resultant hippocampal subfields are the parasubiculum, presubiculum, subiculum, CA1, CA2/3, CA4/dentate gyrus (DG), molecular layer, fimbria,

hippocampal fissure, hippocampus-amygdala-transition-area (HATA), and hippocampal tail. Visual inspection of each participants' hippocampal subfield segmentation was performed to ensure that there were no obvious errors, with the caveat that precise visualization of the distinct subfield boundaries at the spatial resolution used in this study is difficult. The following subfields were excluded: the parasubiculum (volume of <100 µl and may be more prone to noise), the molecular later (at risk of partial volume effects), HATA (volume of <100 µl and may be more prone to noise), fimbria (thin white matter whose segmentation is less reliable and is at risk of partial volume effects), the hippocampal fissure (a sulcus containing a thin layer of cerebrospinal fluid, rather than a hippocampal substructure exactly, whose segmentation is less reliable), and the hippocampal tail (a region where the subfields are not histologically distinct and discernible from each other) (Van Leemput et al. 2009; Kühn et al. 2012; Iglesias et al. 2015; Parker et al. 2019). The following 5 subfields were therefore used for the final analysis: the presubiculum, the subiculum, CA1, CA2/3, and CA4/DG.

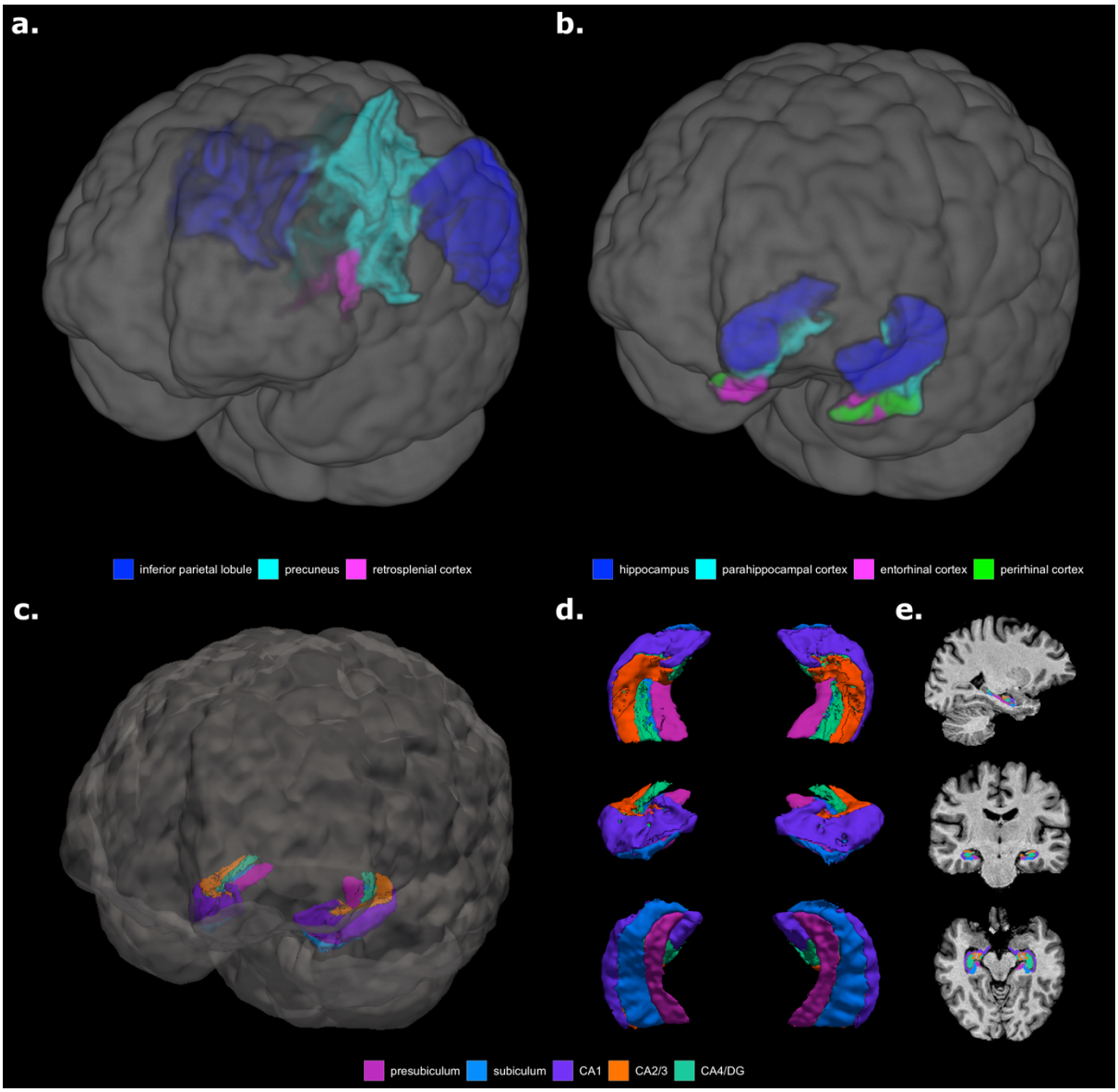

Figure 2. 3D depictions of **a)** areas important for non-standard visuomotor integration, and **b)** areas of the medial temporal lobe, used for grey matter volume and cortical thickness analyses. Hippocampal subfields obtained from FreeSurfer segmentation and used for analysis are shown in **c)** a 3D brain, **d)** 3D superior, anterior, and inferior views, and **e)** sagittal, coronal, and axial slices.

Intracranial volume adjustment: Intracranial volume (ICV) adjustment is an important step as it takes individuals' variations in head size into account (i.e., the confound that subjects with large ICV and/or of younger age would be expected to have a larger hippocampus). ICV was calculated from the T1-weighted images using Statistical Parametric Mapping (SPM) 12 software. The hippocampal subfield, parahippocampal, entorhinal, perirhinal, precuneus, inferior parietal lobule, and retrosplenial cortical volumes of interest (VOI) were ICV-corrected using the residuals method. This method was originally described by (Mathalon et al. 1993) and it aims to remove the ICV-VOI relationship. The residuals method obtains estimates of the ICV-VOI regression model parameters based on information solely from the control group, and these estimates are then used to compute residuals for the entire dataset (O'Brien et al. 2011). The assumption behind this method is that the regression slope β is representative of a non-pathological relationship between VOI and ICV (Voevodskaya 2014). Thus, in studies where there is suspected brain atrophy (e.g., due to having a family history of dementia and being APOE e4-positive), the VOI-ICV regression line is calculated from controls (i.e., for the current study, controls are individuals who do not have a family history of dementia and who are also APOE-e4 non-carriers). Cortical thickness was not normalized as thickness measures do not scale linearly with head size.

2.4.3. Diffusion-weighted imaging

Preprocessing: T1-weighted images for each participant were aligned into AC-PC space to provide a common orientation for brain visualization and tractography. This alignment involved manually defining several anatomical landmarks in the T1 images: the AC (anterior commissure), the PC (posterior commissure), and the mid-sagittal plane. Diffusion-weighted images were preprocessed in FMRIB's Software Library (FSL) using FMRIB's Diffusion Toolbox (FDT) for eddy current correction and head motion correction. The preprocessed

diffusion-weighted images and the ACPC-aligned T1-weighted images were then input into the automated fibre quantification (AFQ) software (Yeatman et al. 2012). AFQ, a software package implemented in MATLAB, was used to identify the core of 20 major white matter tracts in each subject's brain and then quantified the tissue properties of voxels near the core of the estimated tracts (Yeatman et al. 2012). The AFQ procedure is based on a combination of the methods described by (Hua et al. 2008) and (Zhang et al. 2008), and can be summarized in 6 steps: 1) *Whole-brain tractography* is done for each subject, where all fibers are tracked with a white matter mask defined as all the voxels with an FA value >0.3; 2) *Fiber tract segmentation* is performed based on the waypoint ROI procedure described in (Wakana et al. 2007). Fibers are assigned as candidates to a specific fiber tract if they pass through two waypoint ROIs that define the central portion of the tract; 3) *Fiber tract refinement* involves scoring each candidate fiber based on its similarity to a standard fiber tract probability map from (Hua et al. 2008). Fibers with high probability scores are retained, thus defining the fiber tract core; 4) *Fiber tract cleaning* filters out stray fibers that deviate substantially from the core of a fiber group represented as a 3-dimensional Gaussian distribution; 5) *Fiber tract clipping* to the central portion that spans between the two defining ROIs for that tract; and finally 6) *Fiber tract quantification* to calculate diffusion measures at 100 equidistant nodes along the trajectory of the fiber group. The diffusion measures are calculated at each node by taking the weighted average of each fiber making up the tract based on its distance from the tract core. Thus, the AFQ pipeline produces a set of "tract profiles" that measure the tissue properties (FA, RD, AxD, and MD) at equidistant sample positions (100 nodes were used for our analysis) from the start to the end of the tract core. There is one profile for each tract and tissue property combination (e.g., FA along the inferior fronto-occipital fasciculus). The 20 fiber tracts identified with AFQ are: bilateral anterior thalamic radiation, bilateral corticospinal tract, bilateral cingulum cingulate, bilateral cingulum hippocampus, callosum forceps minor,

callosum forceps major, bilateral inferior fronto-occipital fasciculus, bilateral inferior longitudinal fasciculus, bilateral superior longitudinal fasciculus, bilateral uncinate fasciculus, and bilateral arcuate fasciculus (Hua et al. 2008). The literature has shown that the cingulum bundle, corpus callosum, inferior fronto-occipital fasciculus, inferior longitudinal fasciculus, superior longitudinal fasciculus, and uncinate fasciculus are affected early in AD progression. The corpus callosum, inferior fronto-occipital fasciculus, inferior longitudinal fasciculus, and superior longitudinal fasciculus have also been implicated in non-standard visuomotor transformations. We excluded the cingulum hippocampus which could not be properly tracked and was missing diffusion measures in over 5 subjects. The following 12 tracts of interest were therefore used in the final analysis: left (n = 47) and right (n = 46) cingulum cingulate (CGC), callosum forceps minor (n = 49), callosum forceps major (n = 49), left (n = 48) and right (n = 47) inferior fronto-occipital fasciculus (IFOF), left (n = 48) and right (n = 49) inferior longitudinal fasciculus (ILF), left (n = 49) and right (n = 48) superior longitudinal fasciculus (SLF), and left (n = 48) and right (n = 49) uncinate fasciculus (UF) (**Fig. 3**).

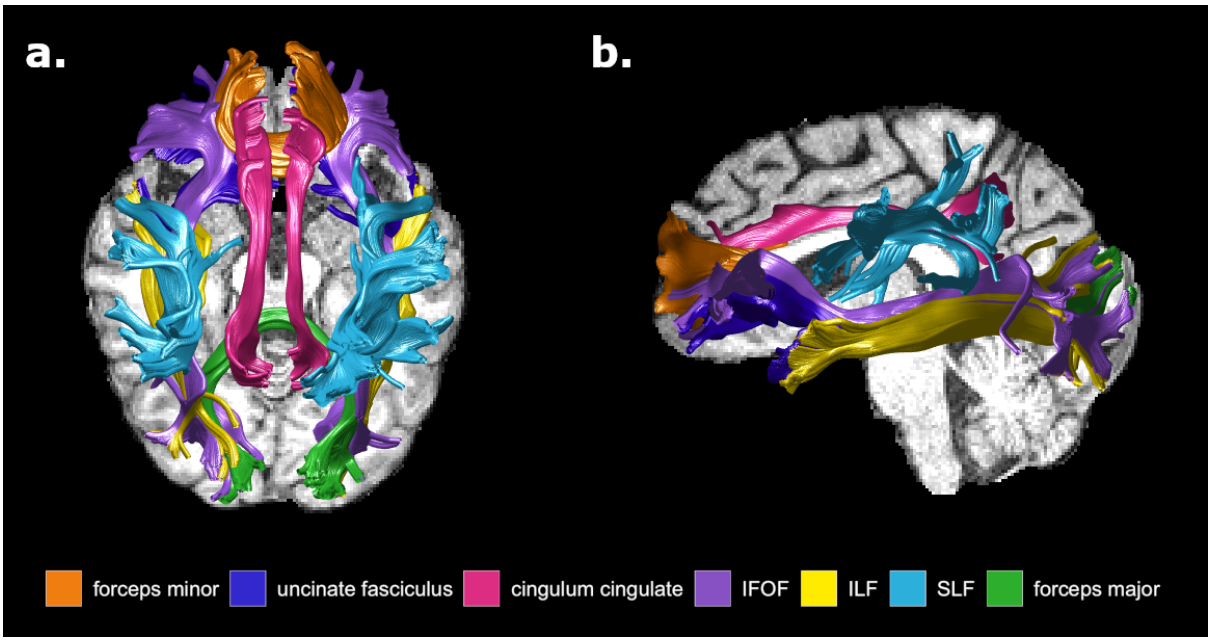

Figure 3. White matter tracts of interest obtained from Automated Fibre Quantification software and used for analysis, shown in **a)** sagittal, and **b)** axial view. IFOF, inferior fronto-occipital fasciculus; ILF, inferior longitudinal fasciculus; SLF, superior longitudinal fasciculus.

2.5. Statistical analysis

All statistical analyses were carried out using open-source R software v4.1.0 (R Core Team 2021).

2.5.1. Differences in structural MRI and DTI measures between groups

Three-way ANOVAs were used to compare differences in structural MRI and DTI measures between three groups: 1) individuals with a family history of dementia and individuals without a family history of dementia, 2) females and males, and 3) APOE e4 carriers and non-carriers. Specifically, the neuroimaging measures being compared were 1) grey matter volumes of the hippocampal subfields, parahippocampal cortex, entorhinal cortex, perirhinal cortex, retrosplenial cortex, inferior parietal lobule, and precuneus, 2) grey matter thickness of the parahippocampal cortex, entorhinal cortex, perirhinal cortex, retrosplenial cortex, inferior parietal lobule, and precuneus, and 3) mean diffusivity measures (i.e., FA, MD, RD, AxD) across the white matter tracts of interest. Post-hoc analyses were adjusted for multiple comparisons using the Holm correction method. Corrections were considered statistically significant at an alpha of $p < 0.05$.

2.5.2. Effects of structural MRI and DTI measures on visuomotor performance

Some of the kinematic measures were combined into composite scores to decrease the number of comparisons made in the data analysis, and the procedure was previously described in detail (Rogojin et al. 2019). Briefly, all kinematic measures were standardized using z-scores and composite scores were then created using simple averaging. The timing score was a composite score of RT, MTf, and PV, and the endpoint error score was a composite score of AE and VE. The Cronbach's alpha values for the timing and endpoint error scores were 0.897 and 0.772, respectively, indicating a high internal consistency.

Multiple regression analyses previously revealed both sex and family history as significant predictors of greater endpoint error scores (indicative of worse visuomotor performance) in the visual feedback reversal condition. The regression analyses also provided preliminary evidence that having an APOE e4 allele was a significant predictor of greater endpoint error scores in the plane-change feedback reversal condition, and greater corrective path lengths (indicative of worse visuomotor performance) in both plane-change conditions. Based on these previous behavioural findings, the current study used multiple linear regression analysis to explore whether visuomotor performance declines are associated with grey and white matter structural neuroimaging measures. The white matter tracts of interest were the cingulum cingulate, callosum forceps minor, callosum forceps major, IFOF, ILF, SLF, and UF. The grey matter regions of interest were the retrosplenial cortex, inferior parietal lobule, and precuneus, all shown to be involved in visually-guided reaching. Regression models were set up with grey or white matter measures as the predictor variable, visuomotor performance measures as the dependent variable, and were controlled for 1) sex and family history in the feedback reversal condition, and 2) APOE e4 status in the two plane-change conditions. The p-values were adjusted for multiple comparisons using the Holm correction method and were considered statistically significant at $p < 0.05$. For example, the regression models in the plane-change feedback reversal condition were set up as follows:

$$Y = \beta_1 X + \beta_2 Z + \beta_3 X \cdot Z + \beta_0$$

where: Y is the continuous dependent variable,
X is the continuous independent variable,
Z is the dichotomous independent variable,
X*Z is the interaction term calculated as X multiplied by Z,
β_0 is the intercept,
β_1 is the effect of X on Y,
β_2 is the effect of Z on Y, and
β_3 is the effect of XZ on Y.

A sample model looking at whether FA in the right ILF is predictive of endpoint error scores in the plane-change feedback reversal condition, moderated by APOE e4 status:

$$Endpoint\ error\ score = \beta_1 Right\ ILF + \beta_2 APOE\ e4\ status + \beta_3 Right\ ILF \cdot APOE\ e4\ status + \beta_0$$

If a significant moderated relationship has been identified (i.e., significant interaction X*Z), we used simple slopes analysis to examine the effects of X on Y within the individual levels of Z. A simple slope is the regression of Y on X at a specific value of Z. In this study, all moderator variables (family history of dementia, sex, and APOE e4 status) were binary - therefore, we tested the regression of Y on X at 0 (no family history, female, APOE e4 non-carrier) and 1 (family history of dementia, male, APOE e4 carriers). Simple slopes analysis was used to determine whether either of the slopes differed significantly from zero (the horizontal).

3. RESULTS

3.1. Grey matter volume and thickness

There was a significant main effect of family history on retrosplenial cortical volume (**Fig. 4a**), where individuals with a family history of dementia had lower grey matter volumes in the left retrosplenial cortex compared to individuals without a family history of dementia ($F_{1,43} = 6.903$, $p < 0.05$). There was a significant main effect of family history on parahippocampal cortical volume (**Fig. 4b**), where individuals with a family history of dementia had greater grey matter volumes in the right parahippocampal cortex compared to individuals without a family history of dementia ($F_{1,43} = 14.2647$, $p < 0.01$). Conversely, there was a significant main effect of APOE status on parahippocampal cortical volume (**Fig. 4c**), where APOE e4 carriers had lower grey matter volumes in the right parahippocampal cortex

compared to individuals without an APOE e4 allele ($F_{1,43} = 5.4288$, $p < 0.05$). Lastly, there was a significant main effect of sex on inferior parietal lobule thickness (**Fig. 4d**), where males had lower cortical thickness in the left inferior parietal lobule compared to females ($F_{1,43} = 10.1512$, $p < 0.01$). There were no statistically significant differences between 1) positive and negative family history, 2) females and males, and 3) APOE e4 carriers and non-carriers found for grey matter volume or thickness in the hippocampal subfields, entorhinal cortex, and perirhinal cortex.

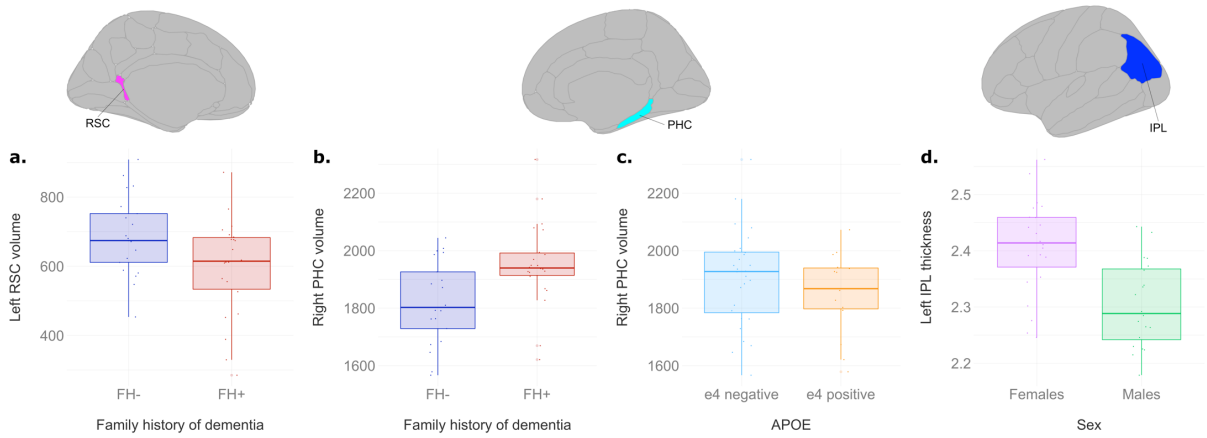

Figure 4. Grey matter volume and thickness differences between participant groups. Significant results shown from three-way ANOVAs. Individuals with a family history of dementia had **a)** lower left retrosplenial volumes ($F_{1,43} = 6.903$, $p < 0.05$), but **b)** greater right parahippocampal volumes compared to individuals without a family history of dementia ($F_{1,43} = 14.2647$, $p < 0.01$). **c)** APOE e4 carriers had lower right parahippocampal volumes compared to non-carriers ($F_{1,43} = 5.4288$, $p < 0.05$). **d)** Males had lower cortical thickness in the left inferior parietal lobule compared to females ($F_{1,43} = 10.1512$, $p < 0.01$). Brain figures made with "ggseg" R package (Mowinckel and Vidal-Piñeiro 2020). RSC, retrosplenial cortex; PHC, parahippocampal cortex; IPL, inferior parietal lobule; FH+, positive family history of dementia; FH-, no family history of dementia; APOE, apolipoprotein E.

3.2. Relationship between grey matter measures and non-standard visuomotor performance

There were no significant interaction effects between the inferior parietal lobule, precuneus, or restrosplenial cortex and family history, sex, or APOE status in the multiple regression models that were based on previous behavioural findings. Multiple linear regression analyses revealed that presubiculum, subiculum, and parahippocampal volumes, as well as entorhinal cortical thickness were predictors of visuomotor performance in several of the non-standard conditions.

Hippocampal subfields (Fig. 5a,b,c): There was a significant interaction effect of left presubiculum volume and sex (β = -0.054317, $p < 0.05$) on endpoint error scores in the feedback reversal condition. The results of the regression indicated that the predictors explained 35.8% of variance ($R^2_{adj} = 0.3584$, $F_{5,39} = 5.915$, $p < 0.001$). Simple slopes analysis showed that smaller left presubiculum volume was a significant predictor of greater endpoint error scores only in males (simple slope = -0.06, S.E. = 0.02, $p < 0.01$). There was a significant interaction effect between right presubiculum volume and APOE status (β = 0.042356, $p < 0.01$) on corrective path length in the plane-change condition, where the two predictors explained 43.1% of variance ($R^2_{adj} = 0.4312$, $F_{3,39} = 11.61$, $p < 0.0001$). Simple slopes analysis showed that larger left presubiculum volume was a significant predictor of greater corrective path length only in APOE e4 carriers (simple slope = 0.04, S.E. = 0.01, $p < 0.01$). There was a significant interaction effect between right subiculum volume and APOE status (β = 0.02861, $p < 0.05$) on corrective path length in the plane-change condition, where the two predictors explained 32.5% of variance ($R^2_{adj} = 0.3248$, $F_{3,39} = 7.736$, $p < 0.001$). Simple slopes analysis showed that larger right subiculum volume was a significant predictor of greater endpoint error scores only in APOE e4 carriers (simple slope = 0.02, S.E. = 0.01, $p < 0.01$).

Entorhinal cortex (Fig. 5d): There was a significant interaction effect of right entorhinal thickness and APOE status ($\beta = -7.759$, $p < 0.05$) on endpoint error scores in the plane-change feedback reversal condition. The results of the regression indicated that the predictors explained 34.8% of variance ($R^2_{adj} = 0.3479$, $F_{3,43} = 9.181$, $p < 0.0001$). Simple slopes analysis showed that smaller right entorhinal thickness was a significant predictor of greater endpoint error scores only in APOE e4 carriers (simple slope = -6.32, S.E. = 2.70, $p = 0.02$).

Parahippocampal cortex (Fig. 5e): There was a significant interaction effect of left parahippocampal volume and APOE status ($\beta = -0.0044851$, $p < 0.05$) on corrective path length in the plane-change condition. The results of the regression indicated that the predictors explained 35.2% of variance ($R^2_{adj} = 0.3519$, $F_{3,39} = 8.601$, $p < 0.001$). Simple slopes analysis showed that smaller left parahippocampal volume was a significant predictor of greater corrective path length only in APOE e4 carriers (simple slope = -0.004, S.E. = 0.001, $p < 0.01$). There was also a significant interaction effect of left parahippocampal volume and APOE status ($\beta = -0.02192$, $p < 0.05$) on corrective path length in the plane-change feedback reversal condition. The results of the regression indicated that the predictors explained 36.2% of variance ($R^2_{adj} = 0.3616$, $F_{3,43} = 9.686$, $p < 0.0001$), however simple slopes analysis was not significant, indicating that APOE e4 carriers and non-carriers were significantly different from each other but not from zero.

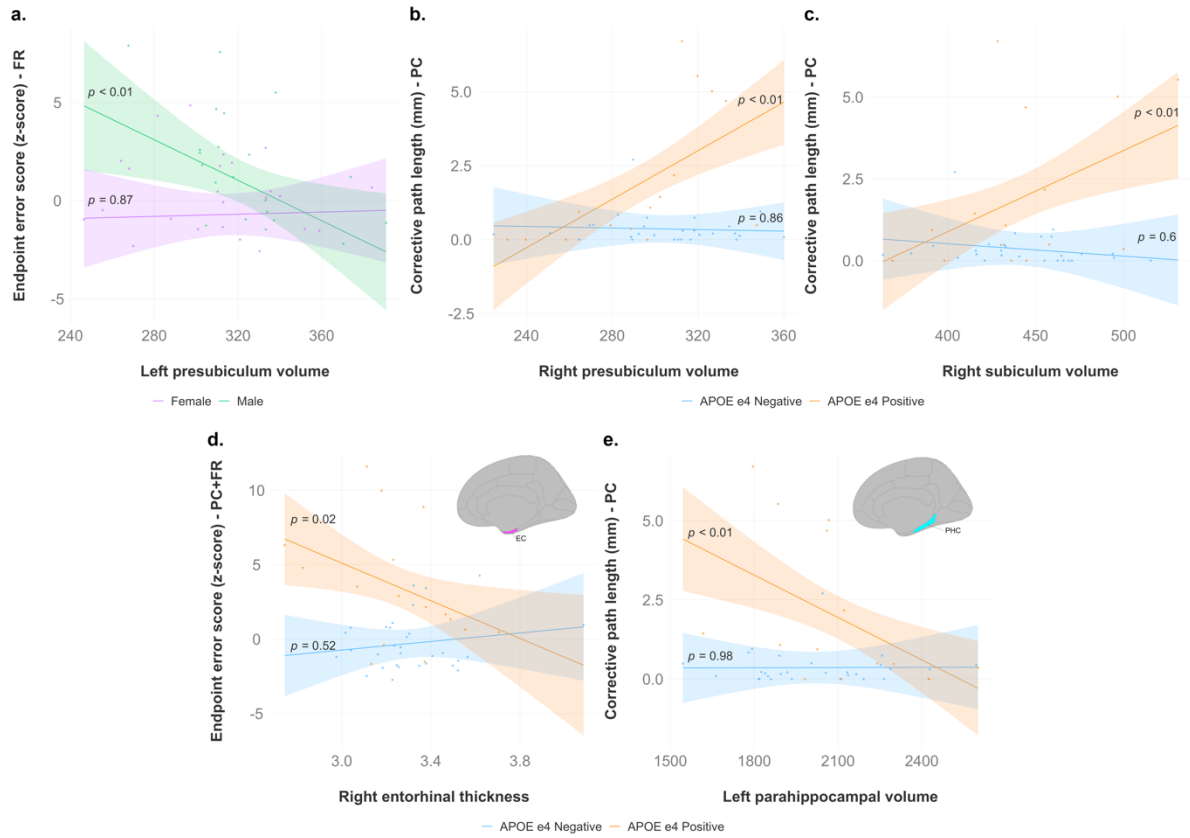

Figure 5. Significant results from hippocampal subfield, entorhinal, and parahippocampal multiple regression and simple slopes analyses. Top panel (a,b,c): Hippocampal subfield volumes predict non-standard visuomotor task performance in the feedback reversal and the plane-change conditions. **a)** Higher endpoint error scores, reflecting worse visuomotor performance, were associated with smaller left presubiculum volumes (simple slope = -0.06, S.E. = 0.02, $p < 0.01$) only in males. Higher corrective path lengths, reflecting worse visuomotor performance, were associated with **b)** greater right presubiculum volume (simple slope = 0.04, S.E. = 0.01, $p < 0.01$), and **c)** greater right subiculum volume (simple slope = 0.02, S.E. = 0.01, $p < 0.01$) only in APOE e4 carriers. Bottom panel (d,e): Entorhinal thickness and parahippocampal volume predict non-standard visuomotor task performance. **d)** Higher endpoint error scores, reflecting worse visuomotor performance, were associated with lower right entorhinal cortical thickness in the plane-change feedback reversal condition (simple slope = -6.32, S.E. = 2.70, $p = 0.02$) only in APOE e4 carriers. **e)** Higher corrective path lengths, reflecting worse visuomotor performance, were associated with lower left parahippocampal volume in the plane-change condition (simple slope = -0.004, S.E. = 0.001, $p < 0.01$) only in APOE e4 carriers. Brain figures made with "ggseg" R package (Mowinckel and Vidal-Piñeiro 2020). EC, entorhinal cortex; PHC, parahippocampal cortex; FR, feedback reversal; PC, plane-change; PC+FR, plane-change feedback reversal; APOE, apolipoprotein E.

3.3. Diffusion measures

There were no statistically significant differences between 1) positive and negative family history, 2) females and males, and 3) APOE e4 carriers and non-carriers found for any of the diffusion measures in the major white matter tracts.

3.4. Relationship between diffusion measures and non-standard visuomotor performance

Multiple linear regression analyses revealed that lower FA, higher MD, higher RD, and higher AxD were significant predictors of worse visuomotor performance only in the plane-change feedback reversal condition. Simple slopes analyses revealed that the relationship between the diffusion measures and visuomotor performance was only statistically significant in APOE e4 carriers (summarized in **Table 2**).

Specifically, lower FA was associated with worse non-standard visuomotor performance in the forceps minor, right IFOF, and right ILF (**Fig. 6**). Higher MD was associated with worse non-standard visuomotor performance in the right cingulum cingulate, forceps major, forceps minor, and bilateral IFOF (**Fig. 7**). Higher RD was associated with worse non-standard visuomotor performance in the forceps minor, bilateral IFOF, and right ILF (**Fig. 8**). Higher AxD was associated with worse non-standard visuomotor performance in the right cingulum cingulate, bilateral IFOF, left SLF, and left UF (**Fig. 9**). Lower FA, higher MD, higher RD, and higher AxD are typically associated with damaged or impaired fibre integrity due to aging or disease pathology (Beaulieu et al. 1996; Davis et al. 2009; Acosta-Cabronero et al. 2010; Salat et al. 2010; Zhang et al. 2010; Bosch et al. 2012; Soares et al. 2013; Doan et al. 2017; Mayo et al. 2019; Bigham et al. 2020). Previous studies in preclinical Alzheimer's populations found similar patterns of changes in diffusion measure of white matter in the same tracts (Bendlin et al. 2010; Gold et al. 2012; Westlye et al. 2012; Adluru et al. 2014), some of which overlap tracts important for visuomotor integration, namely the SLF, IFOF, ILF, and corpus

callosum. Our findings support our hypothesis that white matter integrity declines in these tracts would be associated with declines in non-standard visuomotor integration performance. The statistics for these multiple linear regressions are listed in **Table 3**.

Table 2. Summary of DTI findings by tract. In APOE e4 carriers, patterns in diffusion measures shown below (lower FA, higher MD, higher RD, higher AxD) were significant predictors of worse visuomotor performance in the plane-change feedback reversal condition.

Tract		FA	MD	RD	AxD
Forceps minor	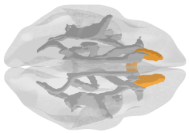	↓	↑	↑	
Forceps major	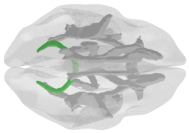		↑		
Cingulum cingulate	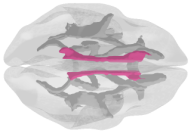		↑ right		↑ right
IFOF	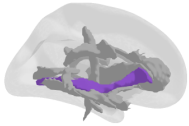	↓ right	↑ bilateral	↑ bilateral	↑ bilateral
ILF	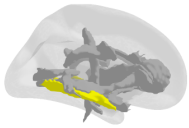	↓ right		↑ right	
SLF	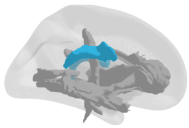				↑ left
UF	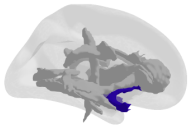				↑ left

Brain figures made with "ggseg3d" R package (Mowinckel and Vidal-Piñeiro 2020). APOE, apolipoprotein E; FA, fractional anisotropy; MD, mean diffusivity; RD, radial diffusivity; AxD, axial diffusivity; IFOF, inferior fronto-occipital fasciculus; ILF, inferior longitudinal fasciculus; SLF, superior longitudinal fasciculus; UF, uncinate fasciculus.

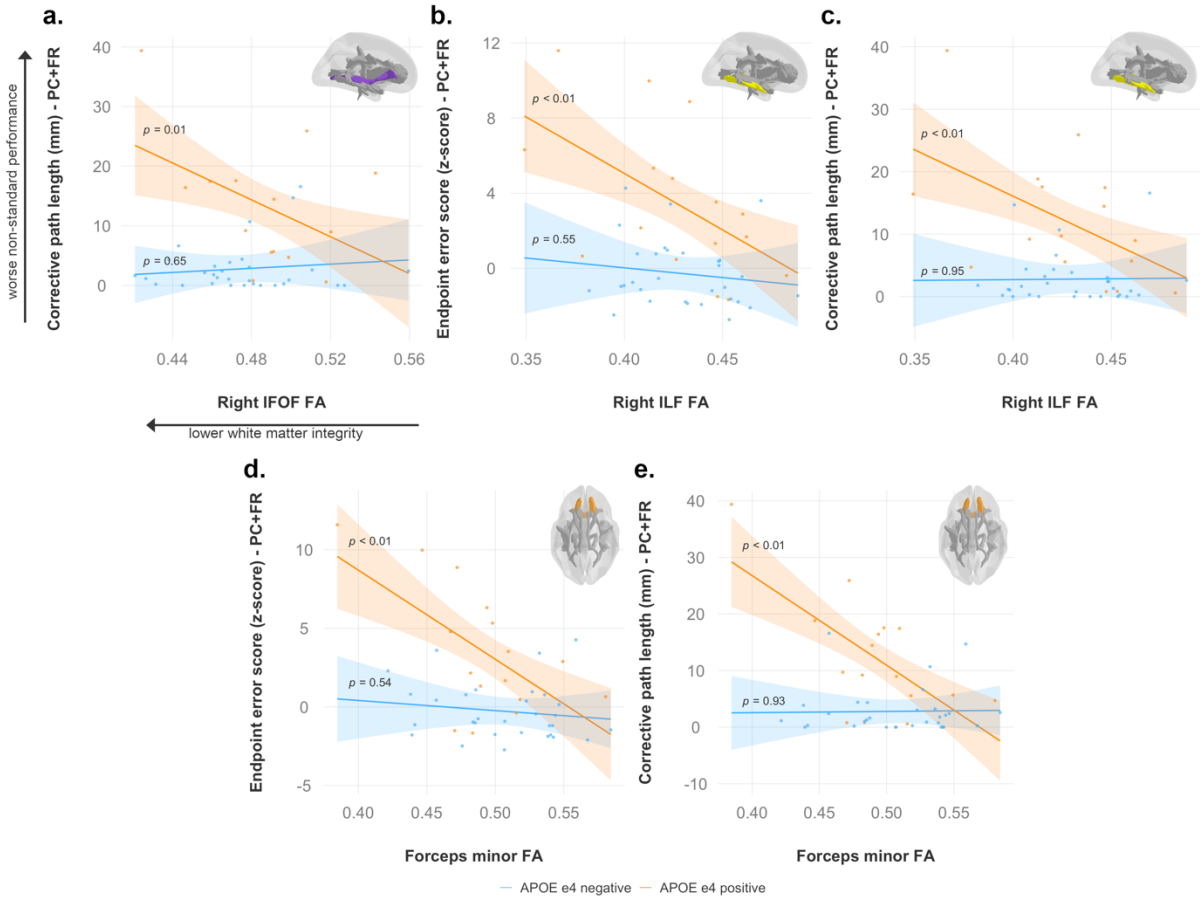

Figure 6. Lower fractional anisotropy predicts worse visuomotor performance (reflected by higher endpoint error scores or corrective path lengths) in the plane-change feedback reversal condition only in APOE e4 carriers in several major white matter tracts, including the **a)** right IFOF, **b-c)** right ILF, and **d-e)** forceps minor. Significant results shown from multiple regression and simple slopes analyses. Brain figures made with "ggseg" R package (Mowinckel and Vidal-Piñeiro 2020). PC+FR, plane change feedback reversal condition; APOE, apolipoprotein E; FA, fractional anisotropy; IFOF, inferior fronto-occipital fasciculus; ILF, inferior longitudinal fasciculus.

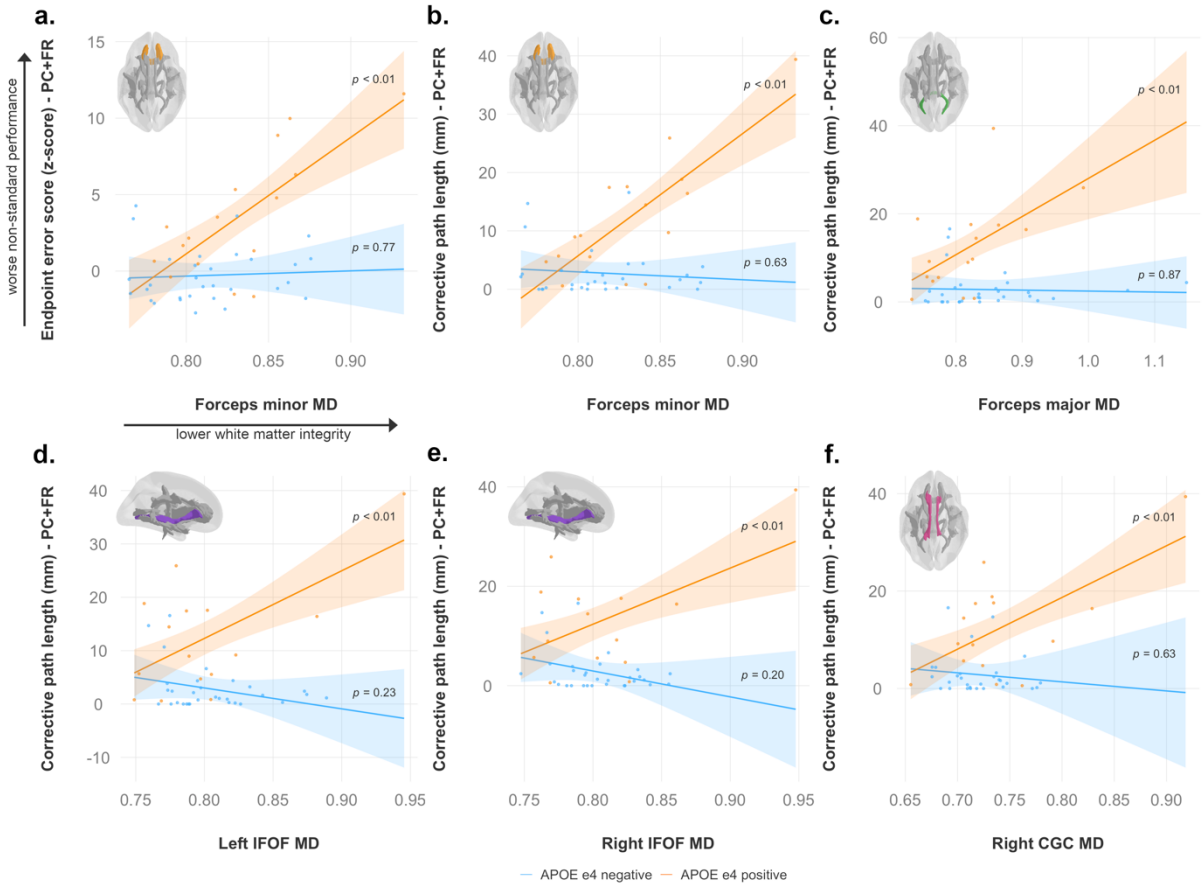

Figure 7. Higher mean diffusivity predicts worse visuomotor performance (reflected by higher endpoint error scores or corrective path lengths) in the plane-change feedback reversal condition only in APOE e4 carriers in several major white matter tracts, including the **a-b)** forceps minor, **c)** forceps major, **d)** left IFOF, **e)** right IFOF, and **f)** right CGC. Significant results shown from multiple regression and simple slopes analyses. Brain figures made with "ggseg" R package (Mowinckel and Vidal-Piñeiro 2020). PC+FR, plane change feedback reversal condition; APOE, apolipoprotein E; MD, mean diffusivity; IFOF, inferior fronto-occipital fasciculus; CGC, cingulum cingulate.

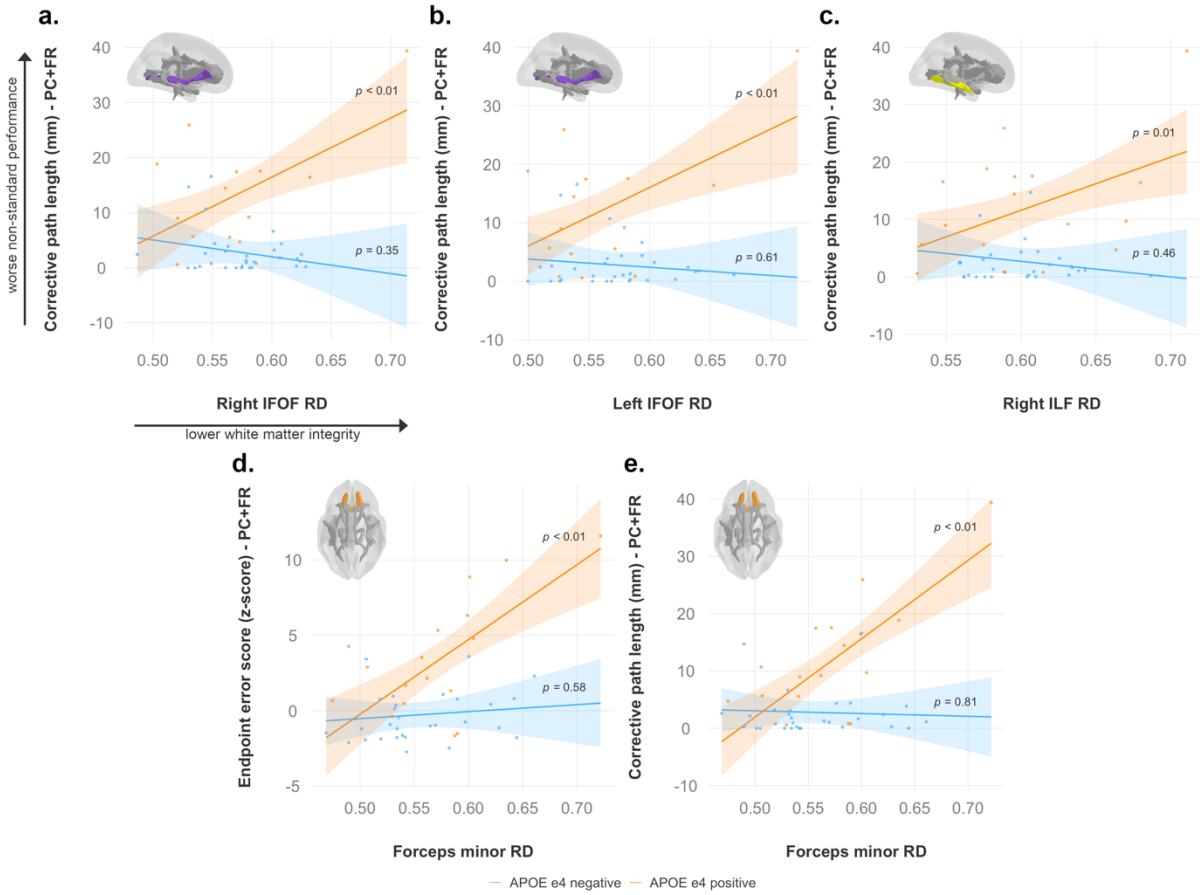

Figure 8. Higher radial diffusivity predicts worse visuomotor performance (reflected by higher endpoint error scores or corrective path lengths) in the plane-change feedback reversal condition only in APOE e4 carriers in several major white matter tracts, including the **a)** right IFOF, **b)** left IFOF, **c)** right ILF, and **d-e)** forceps minor. Significant results shown from multiple regression and simple slopes analyses. Brain figures made with "ggseg" R package (Mowinckel and Vidal-Piñeiro 2020). PC+FR, plane change feedback reversal condition; APOE, apolipoprotein E; RD, radial diffusivity; IFOF, inferior fronto-occipital fasciculus; ILF, inferior longitudinal fasciculus.

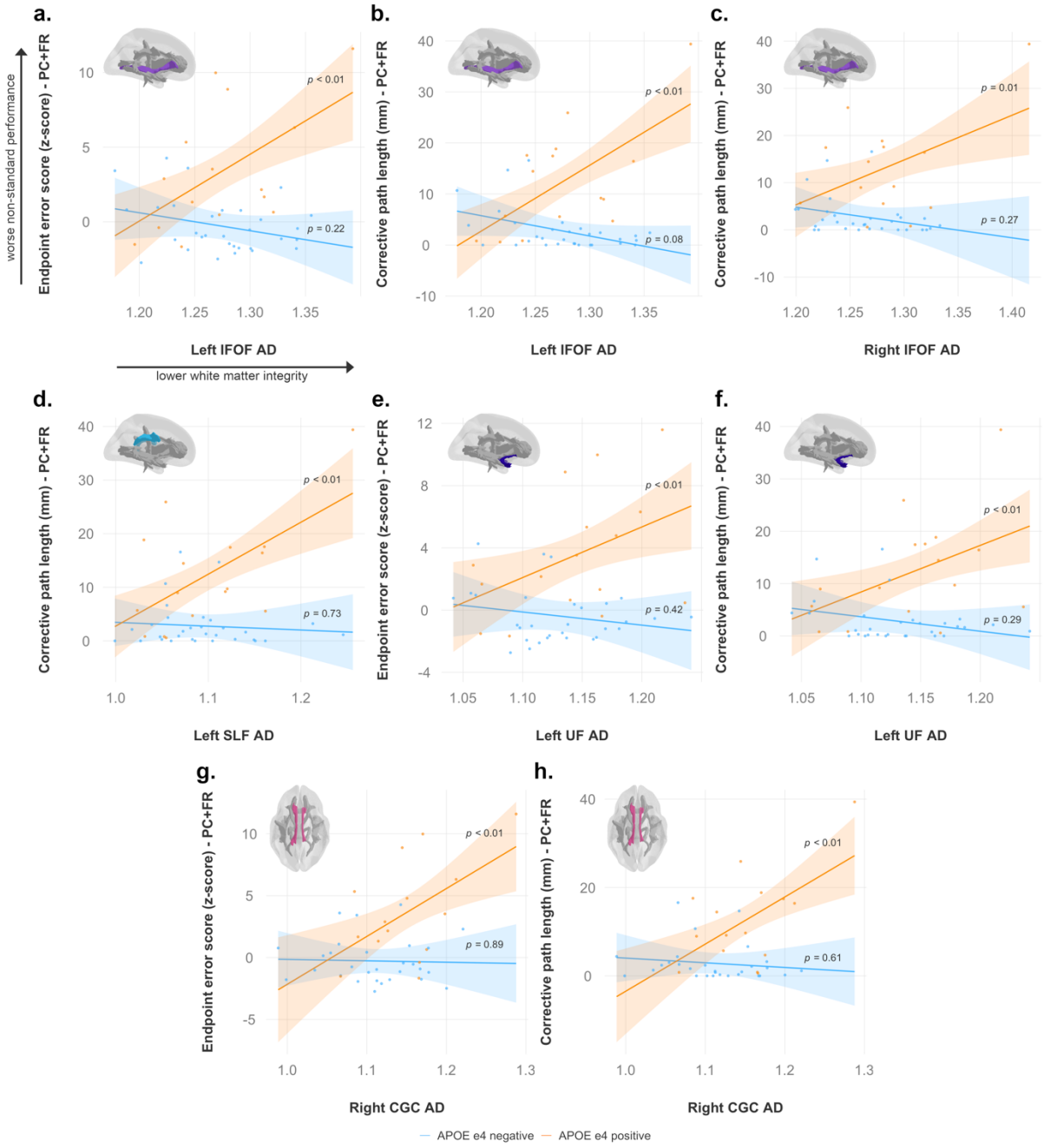

Figure 9. Higher axial diffusivity predicts worse visuomotor performance (reflected by higher endpoint error scores or corrective path lengths) in the plane-change feedback reversal condition only in APOE e4 carriers in several major white matter tracts, including the **a-b)** left IFOF, **c)** right IFOF, **d)** left SLF, **e-f)** left UF, and **g-h)** right CGC. Significant results shown from multiple regression and simple slopes analyses. Brain figures made with "ggseg" R package (Mowinckel and Vidal-Piñeiro 2020). PC+FR, plane change feedback reversal condition; APOE, apolipoprotein E; AxD, axial diffusivity; IFOF, inferior fronto-occipital fasciculus; SLF, superior longitudinal fasciculus; UF, uncinate fasciculus; CGC, cingulum cingulate.

Table 3. Multiple linear regression models used to explore whether visuomotor performance declines are associated with white matter structural neuroimaging measures. Regression models were set up with white matter measures (FA, MD, RD, AxD) as the predictor variable, APOE e4 status as the moderator variable, and visuomotor performance measures (EE score and CPL) in the plane change feedback reversal condition as the outcome variable. Models with significant interactions are shown.

Outcome	Tract	Predictor	Estimate	S.E.	t	Unadjusted *p*	Adjusted *p*
EE Score	Forceps minor	Intercept	17.19	4.42	3.89	0.00034	
		FA	-31.60	8.86	-3.57	0.00090	0.00271
		APOE	28.41	8.84	3.21	0.00248	0.00497
		FA*APOE	-50.30	17.72	-2.84	0.00689	0.00689
						$R^2_{adj} = 0.4602$, $F_{3,43} = 14.07$, $p = 0.000001574$	
						APOE e4 simple slope = -56.75, S.E. = 14.33, $p < 0.01$	
EE Score	Forceps minor	Intercept	-31.44	7.79	-4.04	0.00022	
		MD	39.80	9.44	4.22	0.00013	0.00038
		APOE	-56.72	15.58	-3.64	0.00073	0.00073
		MD*APOE	72.72	18.89	3.85	0.00039	0.00058
						$R^2_{adj} = 0.5444$, $F_{3,43} = 19.32$, $p = 0.00000004399$	
						APOE e4 simple slope = 76.16, S.E. = 14.69, $p < 0.01$	
EE Score	Forceps minor	Intercept	-13.94	3.79	-3.68	0.00065	
		RD	27.11	6.66	4.07	0.00020	0.00059
		APOE	-22.19	7.58	-2.93	0.00542	0.00542
		RD*APOE	44.96	13.31	3.38	0.00157	0.00235
						$R^2_{adj} = 0.5149$, $F_{3,43} = 17.28$, $p = 0.0000001652$	
						APOE e4 simple slope = 49.59, S.E. = 10.48, $p < 0.01$	
CPL	Forceps minor	Intercept	45.94	10.56	4.35	0.00008	
		FA	-78.17	21.17	-3.69	0.00062	0.00092
		APOE	88.46	21.13	4.19	0.00014	0.00041
		FA*APOE	-160.60	42.35	-3.79	0.00046	0.00092
						$R^2_{adj} = 0.5054$, $F_{3,43} = 16.67$, $p = 0.0000002487$	
						APOE e4 simple slope = -158.47, S.E. = 34.25, $p < 0.01$	
CPL	Forceps minor	Intercept	-73.99	18.07	-4.09	0.00018	
		MD	97.93	21.91	4.47	0.00006	0.00006
		APOE	-175.48	36.14	-4.86	0.00002	0.00002
		MD*APOE	222.80	43.82	5.09	0.00001	0.00002
						$R^2_{adj} = 0.6066$, $F_{3,43} = 24.64$, $p = 0.000000001956$	
						APOE e4 simple slope = 209.33, S.E. = 34.07, $p < 0.01$	
CPL	Forceps minor	Intercept	-30.51	8.93	-3.42	0.00139	
		RD	66.01	15.68	4.21	0.00013	0.00019
		APOE	-71.88	17.85	-4.03	0.00023	0.00023
		RD*APOE	141.56	31.37	4.51	0.00005	0.00015
						$R^2_{adj} = 0.5683$, $F_{3,43} = 21.18$, $p = 0.00000001411$	
						APOE e4 simple slope = 136.79, S.E. = 24.68, $p < 0.01$	
CPL	Forceps major	Intercept	-26.96	11.19	-2.41	0.02030	
		MD	42.21	13.52	3.12	0.00321	0.00482
		APOE	-63.20	22.37	-2.83	0.00715	0.00715
		MD*APOE	88.78	27.04	3.28	0.00205	0.00482
						$R^2_{adj} = 0.4346$, $F_{3,43} = 12.79$, $p = 0.000004156$	
						APOE e4 simple slope = 86.60, S.E. = 23.72, $p < 0.01$	
EE Score	Right CGC	Intercept	-19.91	8.45	-2.36	0.02340	
		AxD	18.76	7.41	2.53	0.01540	0.01770
		APOE	-41.81	16.90	-2.48	0.01770	0.01770

		AxD*APOE	39.80	14.82	2.69	0.01050	0.01770
						$R^2_{adj} = 0.4183$, $F_{3,40} = 11.31$, $p = 0.00001659$	
						APOE e4 simple slope = 38.66, S.E. = 12.19, $p < 0.01$	
CPL	Right CGC	Intercept	-25.00	16.70	-1.50	0.14220	
		MD	43.78	22.91	1.91	0.06320	0.06320
		APOE	-82.42	33.39	-2.47	0.01800	0.02700
		MD*APOE	124.68	45.83	2.72	0.00960	0.02700
						$R^2_{adj} = 0.4897$, $F_{3,40} = 14.75$, $p = 0.000001286$	
						APOE e4 simple slope = 106.12, S.E. = 25.49, $p < 0.01$	
CPL	Right CGC	Intercept	-47.77	20.59	-2.32	0.02549	
		AxD	48.05	18.06	2.66	0.01118	0.01118
		APOE	-124.80	41.17	-3.03	0.00426	0.00639
		AxD*APOE	117.30	36.12	3.25	0.00236	0.00639
						$R^2_{adj} = 0.4474$, $F_{3,40} = 12.61$, $p = 0.000006087$	
						APOE e4 simple slope = 106.70, S.E. = 29.70, $p < 0.01$	
EE Score	Left IFOF	Intercept	-19.29	10.07	-1.92	0.06223	
		AxD	16.35	7.89	2.07	0.04449	0.04445
		APOE	-68.60	20.13	-3.41	0.00146	0.00219
		AxD*APOE	56.71	15.78	3.59	0.00085	0.00219
						$R^2_{adj} = 0.4325$, $F_{3,42} = 12.43$, $p = 0.000005912$	
						APOE e4 simple slope = 44.70, S.E. = 12.49, $p < 0.01$	
CPL	Left IFOF	Intercept	-27.39	17.72	-1.55	0.12964	
		MD	43.80	22.02	1.99	0.05324	0.05324
		APOE	-123.46	35.43	-3.48	0.00117	0.00175
		MD*APOE	165.93	44.04	3.77	0.00051	0.00152
						$R^2_{adj} = 0.4872$, $F_{3,42} = 15.25$, $p = 0.0000007371$	
						APOE e4 simple slope = 126.76, S.E. = 30.43, $p < 0.01$	
CPL	Left IFOF	Intercept	-16.57	11.39	-1.46	0.15316	
		RD	42.97	20.00	2.15	0.03749	0.03749
		APOE	-54.78	22.78	-2.41	0.02067	0.03101
		RD*APOE	114.04	40.00	2.85	0.00673	0.02019
						$R^2_{adj} = 0.4236$, $F_{3,42} = 12.02$, $p = 0.000008145$	
						APOE e4 simple slope = 99.99, S.E. = 29.01, $p < 0.01$	
CPL	Left IFOF	Intercept	-49.43	23.42	-2.11	0.04080	
		AxD	44.72	18.36	2.44	0.01920	0.01920
		APOE	-206.24	46.85	-4.40	0.00007	0.00011
		AxD*APOE	169.32	36.72	4.61	0.00004	0.00011
						$R^2_{adj} = 0.5198$, $F_{3,42} = 17.23$, $p = 0.0000001911$	
						APOE e4 simple slope = 129.37, S.E. = 29.06, $p < 0.01$	
CPL	Right IFOF	Intercept	41.57	16.58	2.51	0.01625	
		FA	-68.66	34.23	-2.01	0.05146	0.05146
		APOE	94.14	33.17	2.84	0.00702	0.02106
		FA*APOE	-172.21	68.45	-2.52	0.01589	0.03178
						$R^2_{adj} = 0.4094$, $F_{3,41} = 11.17$, $p = 0.00001727$	
						APOE e4 simple slope = -154.77, S.E. = 57.00, $p = 0.01$	
CPL	Right IFOF	Intercept	-16.66	20.80	-0.80	0.42761	
		MD	30.40	25.80	1.18	0.24549	0.24549
		APOE	-122.55	41.59	-2.95	0.00528	0.00792
		MD*APOE	164.96	51.61	3.20	0.00268	0.00792
						$R^2_{adj} = 0.4717$, $F_{3,41} = 14.09$, $p = 0.000001858$	
						APOE e4 simple slope = 112.88, S.E. = 33.18, $p < 0.01$	
CPL	Right IFOF	Intercept	-13.76	12.94	-1.06	0.29385	
		RD	38.32	22.57	1.70	0.09706	0.09706
		APOE	-68.10	25.89	-2.63	0.01195	0.01794

		RD*APOE	137.62	45.13	3.05	0.00401	0.01203
						R^2_{adj} = 0.4648, $F_{3,41}$ = 13.74, p = 0.000002407	
						APOE e4 simple slope = 107.13, S.E. = 31.27, $p < 0.01$	
CPL	Right IFOF	Intercept	-32.43	28.96	-1.12	0.26925	
		AxD	31.24	22.71	1.38	0.17628	0.17628
		APOE	-152.27	57.92	-2.63	0.01200	0.01800
		AxD*APOE	127.33	45.41	2.80	0.00768	0.01800
						R^2_{adj} = 0.4224, $F_{3,41}$ = 11.72, p = 0.00001109	
						APOE e4 simple slope = 94.91, S.E. = 34.80, p = 0.01	
EE Score	Right ILF	Intercept	16.64	5.29	3.14	0.00302	
		FA	-35.26	12.34	-2.86	0.00657	0.01971
		APOE	24.94	10.59	2.36	0.02314	0.04628
		FA*APOE	-49.78	24.69	-2.02	0.05002	0.05000
						R^2_{adj} = 0.4212, $F_{3,43}$ = 14.07, p = 0.000006795	
						APOE e4 simple slope = -60.15, S.E. = 17.56, $p < 0.01$	
CPL	Right ILF	Intercept	38.52	13.31	2.89	0.00596	
		FA	-72.82	31.04	-2.35	0.02365	0.03880
		APOE	73.67	26.63	2.77	0.00831	0.02493
		FA*APOE	-150.79	62.08	-2.43	0.01940	0.03880
						R^2_{adj} = 0.4129, $F_{3,43}$ = 11.79, p = 0.000009155	
						APOE e4 simple slope = -148.21, S.E. = 44.16, $p < 0.01$	
CPL	Right ILF	Intercept	-12.50	14.42	-0.87	0.39050	
		RD	32.76	23.92	1.37	0.17800	0.17800
		APOE	-63.00	28.83	-2.19	0.03440	0.05160
		RD*APOE	119.83	47.84	2.51	0.01610	0.04830
						R^2_{adj} = 0.3905, $F_{3,43}$ = 10.83, p = 0.00002004	
						APOE e4 simple slope = 92.67, S.E. = 31.40, p = 0.01	
CPL	Left SLF	Intercept	-41.76	17.49	-2.39	0.02140	
		AxD	44.87	15.93	2.82	0.00731	0.00731
		APOE	-104.73	34.97	-2.99	0.00455	0.00683
		AxD*APOE	104.03	31.87	3.26	0.00216	0.00648
						R^2_{adj} = 0.4582, $F_{3,43}$ = 13.97, p = 0.000001699	
						APOE e4 simple slope = 96.88, S.E. = 24.47, $p < 0.01$	
EE Score	Left UF	Intercept	-12.26	9.27	-1.32	0.19320	
		AxD	12.04	8.14	1.48	0.14660	0.14660
		APOE	-42.87	18.55	-2.31	0.02580	0.03870
		AxD*APOE	40.99	16.29	2.52	0.01580	0.03870
						R^2_{adj} = 0.379, $F_{3,42}$ = 10.16, p = 0.00003728	
						APOE e4 simple slope = 32.54, S.E. = 12.55, p = 0.01	
CPL	Left UF	Intercept	-27.72	22.90	-1.21	0.23297	
		AxD	30.68	20.11	1.53	0.13460	0.13460
		APOE	-123.68	45.80	-2.70	0.00995	0.01493
		AxD*APOE	116.73	40.22	2.90	0.00588	0.01493
						R^2_{adj} = 0.3899, $F_{3,42}$ = 10.59, p = 0.00002596	
						APOE e4 simple slope = 89.05, S.E. = 30.98, p = 0.01	

Unadjusted and adjusted p-values reported. Values were adjusted for multiple comparisons using the Holm correction method and were considered statistically significant at $p < 0.05$. S.E., standard error; EE score, endpoint error score; CPL, corrective path length; APOE, apolipoprotein E; FA, fractional anisotropy; MD, mean diffusivity; RD, radial diffusivity; AxD, axial diffusivity; CGC, cingulum cingulate; IFOF, inferior fronto-occipital fasciculus; ILF, inferior longitudinal fasciculus; SLF, superior longitudinal fasciculus; UF, uncinate fasciculus.

4. DISCUSSION

The main interest of this study was to investigate the grey and white matter neural anatomy underlying impaired visuomotor performance, and to explore the effects of family history of dementia, APOE genotype, and sex. Our key findings suggest that there is a relationship between the APOE e4 genotype and structural brain changes that predicts poorer visuomotor performance. This relationship was demonstrated in our grey matter structural findings, where lower thickness and volume in areas of the medial temporal lobe predicted visuomotor deficits, and then replicated in our diffusion data, where declines in white matter integrity also predicted impaired non-standard visuomotor performance. These visuomotor performance deficits in APOE e4 carriers were detectable using our non-standard visuomotor tasks in the absence of any measurable purely cognitive issues. We also found sex-differences in grey matter thickness and volume in areas of the posterior parietal cortex and hippocampus that are important for visuospatial processing, which may explain the poorer visual feedback reversal task performance we previously reported in males.

4.1. Grey matter measures underlying visuomotor deficits in individuals with an increased risk for Alzheimer's disease

We first examined group differences in grey matter volume and thickness. Individuals with a family history of dementia had greater grey matter volumes in the right parahippocampal cortex compared to those without a family history of dementia. Conversely, APOE e4 carriers had lower grey matter volumes in the right parahippocampal cortex compared to individuals without an APOE e4 allele. Individuals with a family history of dementia also had lower grey matter volumes in the left retrosplenial cortex. Our main interest, however, was exploring whether structural differences in the inferior parietal lobule, precuneus, retrosplenial cortex, and areas of the medial temporal lobe may underlie visuomotor integration deficits in

individuals at an increased risk for AD. Our results for hippocampal subfield volumes were surprising. We found that poorer non-standard visuomotor performance was associated with greater grey matter volumes in the right presubiculum and right subiculum. This relationship was only significant for APOE e4 carriers and is contrary to our hypothesis that atrophy within the hippocampus, one of the medial temporal lobe regions involved in visuomotor control (Tankus and Fried 2012), may be predictive of worse visuomotor task performance. However, it should be noted that the automated hippocampal subfield segmentation module in FreeSurfer has not been validated against histological annotations within the same subjects, nor against manual segmentation on the same MRI scans. (Wisse et al. 2021) caution against using 1 x 1 x 1 mm^3 T1 scans for automatic segmentation of the hippocampus as the subfields are difficult to discern at this resolution. Studies that used automatic hippocampal segmentation have been shown to report contradictory and sometimes neurobiologically unexpected results (Haukvik et al. 2018; Wisse et al. 2021). Indeed, (Iglesias et al. 2015) themselves mention that the volumetric results from individual subfields automatically segmented in FreeSurfer using only standard resolution (1 mm) T1 data must be interpreted with caution.

In APOE e4 carriers, a lower left parahippocampal volume and lower right entorhinal thickness were associated with worse non-standard visuomotor task performance. As mentioned previously, the hippocampal, parahippocampal, entorhinal, and retrosplenial cortices have been implicated in visuospatial processing and visuomotor control (Vann et al. 2009; Tankus and Fried 2012). In addition to prominent memory declines, AD patients also show impairments in visuospatial processing and skilled eye-hand coordination performance (Ghilardi et al. 1999; Tippett and Sergio 2006; Tippett et al. 2007). Apraxia, a disorder of skilled movements, is seen in some AD patients and is included as one of the criteria for AD (Lesourd et al. 2013; Dubois et al. 2014; Smits et al. 2014). Regions of the medial temporal lobe, including the hippocampus (subiculum, presubiculum, and parasubiculum) and

parahippocampus, are interconnected with the parietal cortex via the retrosplenial cortex, which itself is involved in episodic memory, navigation, and translation between different frames of reference (Vann et al. 2009). Thus, early dysfunction in not only medial temporal regions but also in regions involved in visuomotor control could prove to be useful for understanding the underlying pathophysiology of AD and predicting AD risk.

Some of our findings showed increased volumes in regions of medial temporal lobe in individuals at an increased risk for AD, both in group differences (family history versus no family history of dementia) as well as associated with non-standard visuomotor deficits. Converging evidence suggests that by the time clinical impairment is detectable in AD, extensive neurodegeneration has already taken place (Morris 2005). However, the relationship between AD pathology and brain atrophy in preclinical AD is still under debate (Chételat et al. 2013). Grey matter atrophy has been reported in cognitively healthy individuals positive for amyloid pathology (Fagan et al. 2009; Mormino et al. 2009; Villeneuve et al. 2014) and tau pathology (Wang et al. 2016; Scott et al. 2020; Xie et al. 2020), family history of dementia (Honea et al. 2010; Honea et al. 2011; Mosconi et al. 2014), and the APOE e4 allele (O'Dwyer et al. 2012; Haller et al. 2017; Veldsman et al. 2021). Conversely, other studies have reported increased volumes in areas of the medial temporal lobe in preclinical AD (Chételat, Villemagne, Pike, et al. 2010; Gispert et al. 2015). Therefore, the changes in grey matter volume in preclinical AD may not necessarily be linear.

4.2. Pattern of white matter integrity declines are generally consistent with the literature and predict visuomotor deficits in APOE e4 carriers

Studies examining white matter diffusion characteristics have demonstrated that white matter may be independently affected from amyloid pathology (Rabin et al. 2019) and grey matter atrophy (Amlien and Fjell 2014) early in the pathological process, emphasizing the

importance of investigating white matter changes underlying disease progression. White matter microstructural reductions have been shown in cognitively healthy individuals at an increased risk for AD (due to family history of dementia and having an APOE e4 allele) in the absence of medial temporal lobe atrophy (Gold et al. 2010). In the current study, we found no differences in white matter diffusion measures between groups (i.e., family history status, sex, or APOE e4 status). While there were no group differences in white matter integrity alone, we did observe that in APOE e4 carriers, diffusion measures of several major white matter tracts were predictive of non-standard visuomotor performance. Specifically, we found that lower FA (in the forceps minor, right IFOF, and right ILF), higher MD (in the right cingulum cingulate, forceps major, forceps minor, and bilateral IFOF), higher RD (in the forceps minor, right ILF, and bilateral IFOF), and higher AxD (in the cingulum cingulate, bilateral IFOF, left SLF, and left UF) were predictive of worse performance in the most cognitively demanding non-standard visuomotor condition (plane-change feedback reversal). Our findings are consistent with the literature, where white matter alterations have previously been detected in cognitively healthy individuals with the APOE e4 allele, with similar patterns of reduced white matter microstructure (i.e., reduced FA, and increased MD, RD, AxD) in some of the same tracts affected in our results, including the cingulum cingulate, forceps minor, IFOF, SLF, and ILF (Westlye et al. 2012; Adluru et al. 2014; Cavedo et al. 2018; Operto et al. 2018).

Our findings suggest that lower white matter integrity in several major tracts in the brain may underlie the non-standard visuomotor deficits we previously demonstrated in APOE e4 carriers compared to non-carriers. In the brain, the APOE protein plays a central role in cholesterol transport (Mahley and Rall 2000), which is essential for axonal growth as well as synaptic formation and remodelling (Liu et al. 2013). APOE may affect white matter microstructure due to the e4 isoform having a reduced capacity of keeping cholesterol homeostasis in the brain, leading to disruptions of the myelin sheath (Operto et al. 2018).

Vulnerability to the degradation of white matter microstructure may therefore be particularly high or accelerated in APOE e4 carriers. The resultant myelin disruption and axonal injury in tracts projecting between brain regions necessary for non-standard visuomotor integration, a task that heavily relies on large scale frontoparietal networks, may impact effective communication across these areas and be reflected as visuomotor deficits. Indeed, the white matter tracts in which lower white matter integrity was associated with visuomotor performance declines are some of the same white matter tracts that comprise the frontoparietal network, including the SLF, IFOF, and ILF (de Schotten et al. 2011; Rodríguez-Herreros et al. 2015; Budisavljevic et al. 2017; Waller et al. 2017; Herbet et al. 2018).

4.3. Grey matter structure underlying sex-differences in non-standard visuomotor performance

We previously showed that sex was a significant predictor of visuomotor performance in the feedback reversal condition, where males had greater endpoint error scores compared to females after controlling for family history and APOE status (Rogojin et al. 2019). In the current study, we found that males had lower left inferior parietal lobule thickness compared to females. While the right inferior parietal lobule in particular appears to be involved in non-standard visuomotor transformations involving a visual feedback reversal (Gorbet and Sergio 2016) and is a crucial node in the frontoparietal network needed for maintaining spatial attention on current task goals (Singh-Curry and Husain 2009), the left inferior parietal lobule has been shown to be important for visually-guided reaches as well. There was bilateral activation in the inferior parietal lobule during a reaching task, and reaching to visual targets compared to proprioceptive targets incurred more activity in the left inferior parietal lobule (Bernier and Grafton 2010). Furthermore, the feedback reversal condition used in the current study is a version of visuomotor adaptation, and the left inferior parietal lobule is critical for

successful visuomotor adaptation (Mutha et al. 2011; Crottaz-Herbette et al. 2014). It is important to note that the lower left inferior lobule thickness found in males may just be a general structural sex-difference rather than a result of age-related atrophy, as others have previously demonstrated greater cortical thickness in the inferior parietal lobules of adult females compared to males (Sowell et al. 2007). We found that having a lower left presubiculum volume was also associated with greater endpoint error scores in the visual feedback reversal condition only in males. The presubiculum of the hippocampus has extensive interconnections with the inferior parietal lobule (Rockland and Van Hoesen 1999; Ding et al. 2000; Clower et al. 2001), and the hippocampus itself has been implicated in visuomotor coordination (Tankus and Fried 2012).

4.4. Limitations and future directions

One of the limitations of the current study was that hippocampal subfield segmentation was obtained from T1-weighted MRI scans, which have limited tissue contrast of hippocampal structures (Wisse et al. 2021). Another limitation is that this study was cross-sectional in nature. It would be interesting to conduct a longitudinal study to investigate if participants demonstrating visuomotor deficits prior to cognitive decline are more likely to develop mild cognitive impairment or dementia later in life. Preclinical AD has been hypothesized to begin decades before the onset of clinical symptoms. One proposed sequence of events leading to dementia suggests that disruptions in the default mode network may precede neurodegeneration (Sheline and Raichle 2013). Several of the core nodes of the default mode network (Parvizi et al. 2006; Sperling et al. 2010; Márquez and Yassa 2019) overlap with brain areas shown to be involved in non-standard visuomotor integration (Gorbet and Sergio 2016; Gorbet and Sergio 2018). Future work could therefore investigate whether there are differences

in default mode network connectivity between groups based on family history, genetic risk, or sex, and whether disruptions in functional connectivity underlie visuomotor deficits.

4.5. General conclusions

Our results suggest that a visuomotor task may have potential for detecting the early effects of the APOE e4 allele on white matter microstructure and medial temporal lobe grey matter early in dementia progression, as the white matter and grey matter declines observed here were associated with visuomotor difficulties only in e4 carriers. Importantly, the visuomotor deficits were seen prior to group differences in volumetric and diffusion measures due to genetic risk, and *in advance of any cognitive deficits*. We also found structural grey matter differences in the inferior parietal lobule that may underlie the sex-related differences we've previously demonstrated in non-standard visuomotor performance.

DECLARATION OF INTEREST STATEMENT

No conflicts declared.

ACKNOWLEDGEMENTS

The authors wish to thank Heather Edgell, PhD, and Michael Riddell, PhD, for providing storage for saliva samples, as well as Joy Williams, MRT(MR), for her MR image acquisition expertise. This work was supported by a Canadian Institutes of Health Research operating grant (grant number MOP-125915 to L.E.S.).

Chapter Three

Differences in resting state functional connectivity underlie visuomotor performance declines in older adults with a genetic risk (APOE e4) for Alzheimer's disease

Alica Rogojin, Diana J. Gorbet, Kara M. Hawkins, and Lauren E. Sergio

ABSTRACT

Introduction: Non-standard visuomotor integration requires the interaction of large networks in the brain. Previous findings have shown that non-standard visuomotor performance is impaired in individuals with specific dementia risk factors (family history of dementia and presence of the APOE e4 allele) in advance of any cognitive impairments. These findings suggest that visuomotor impairments are associated with early dementia-related brain changes. The current study examined the underlying resting state functional connectivity (RSFC) associated with impaired non-standard visuomotor performance, as well as the impacts of dementia family history, sex, and APOE status. **Methods:** Cognitively healthy older adults (n = 48) were tested on four visuomotor tasks using two linked touchscreens where reach and gaze were increasingly spatially dissociated (i.e., involving either visual feedback reversal, plane-change, or plane-change feedback reversal). Participants who had a family history of dementia or the APOE e4 allele were considered to be at an increased risk for AD. To quantify RSFC within networks of interest, an echo planar imaging (EPI) sequence sensitive to blood oxygenation level dependent (BOLD) contrast was collected. The networks of interest were the default mode network (DMN), somatomotor network (SMN), dorsal attention network (DAN), ventral attention network (VAN), and frontoparietal control network (FPN). **Results:** Individuals with the e4 allele showed abnormalities in RSFC between posterior DMN nodes that predicted poorer non-standard visuomotor performance. Specifically, multiple linear regression analyses revealed lower RSFC between the precuneus and posterior cingulate cortex, a posterior functional core of the DMN, and the left inferior parietal lobule and left parahippocampal cortex. Presence of the APOE e4 allele also modified the relationship between mean DAN RSFC and visuomotor performance for two of the behavioural measures in the plane-change feedback reversal condition. There was a significant interaction effect of mean RSFC in the DAN and APOE status on endpoint error score and corrective path length, both indicative of worse visuomotor performance, only in APOE e4 carriers. There were otherwise no effects of family history, APOE e4 status, or sex on the relationship between RSFC and visuomotor performance for any of the other resting networks. **Conclusions:** The preliminary findings provide insight into the impact of Alzheimer's disease pathology on neural networks underlying complex visuomotor transformations, and demonstrate that the non-standard visuomotor task paradigm discussed in this study may be used as a non-invasive, easily accessible assessment tool for dementia risk.

1. INTRODUCTION

Alzheimer's disease (AD) related brain changes are thought to begin several decades before the onset of clinical symptoms (Morris 2005). Early identification of preclinical AD can allow for healthcare providers to make recommendations on lifestyle changes to mitigate modifiable risk factors such as diabetes, physical inactivity, and social isolation (Xu et al. 2015; Livingston et al. 2020; Litke et al. 2021) in order to delay or slow down disease progression. One of the important challenges facing AD clinical management today is the early detection or measure of small changes in behaviour or clinical signs in at-risk individuals that could accurately predict their likelihood of future disease-related impairment (Dubois et al. 2016). Current methods for detecting biomarkers of AD are expensive or invasive, such as abnormal amyloid, tau, or [18F]-fluorodeoxyglucose positron emission tomography (FDG-PET), atrophy in the brain using magnetic resonance imaging (MRI), and lumbar puncture for cerebrospinal fluid analysis (Rice and Bisdas 2017; Jack et al. 2018; Shaw et al. 2018; Ou et al. 2019). Blood-based biomarkers are a more affordable option, however they are still invasive and require extensive laboratory resources (Nabers et al. 2018; Milà-Alomà et al. 2019; Otto et al. 2019). Behavioural measures that detect dysfunction of brain networks due to AD pathology may be a more affordable and easily accessible alternative to current diagnostic and risk assessment tools.

Converging evidence suggests that AD is a disconnection syndrome (Delbeuck et al. 2003), showing characteristic patterns of disruption to both structural (Filippi and Agosta 2011; Gold et al. 2012; Shao et al. 2012; Peraza et al. 2019) and functional connectivity (Wang et al. 2007; Brier et al. 2012; Vemuri et al. 2012; Sheline and Raichle 2013) between brain regions. In particular, the default mode network (DMN) has been a focus of AD biomarker research as regions of the default mode network largely overlap with regions showing earliest signs of AD pathology (Buckner et al. 2005; Palmqvist et al. 2017). Decreased functional connectivity

between areas of the DMN has been demonstrated in cognitively healthy individuals with increased amyloid deposition (Hedden et al. 2009; Sheline, Raichle, et al. 2010), a family history of AD (Wang, Catherine M. Roe, et al. 2012), and presence of the APOE e4 allele (Sheline, Morris, et al. 2010; Wang et al. 2015; Liang et al. 2017). In addition to the DMN, other resting state functional networks have also been shown to have altered functional connectivity in preclinical AD. Cognitively normal older adults with amyloid burden have exhibited decreased functional connectivity in the frontoparietal control network (Elman et al. 2016; Buckley et al. 2017), dorsal attention network (Elman et al. 2016), and salience network (Buckley et al. 2017). Decreased functional connectivity was found in cognitively normal APOE e4 carriers in the prefrontal cortex, cingulate cortex, and visual areas (McKenna et al. 2016), as well as in posterior regions of the DMN (Machulda et al. 2011). Other studies have reported increased functional connectivity within the salience network in older APOE e4 carriers (Machulda et al. 2011; Liang et al. 2017). One study investigating resting functional connectivity with disease progression found initial hyperconnectivity in resting state networks in the very early stages of AD progression, followed by consistent reductions in functional connectivity in all networks with increasing AD severity (Brier et al. 2012).

One way to test the functional integrity of networks is to use a task that requires the integration of different domains (e.g., sensory, cognitive, and motor) and requires communication across multiple brain regions. Visuomotor tasks involving an element of dissociation or "decoupling" between the visual stimulus and target of the reach may present a novel behavioural target for dementia risk detection. Most everyday "standard" visually-guided arm movements involve a direct interaction with an object, such as picking up a mug of tea, and are automatic because the brain's default visuomotor mapping is thought to have the gaze and hand spatially aligned (Gielen et al. 1984; Helsen et al. 1998). With the advent of tool use, humans can also perform decoupled or "non-standard" visually-guided arm movements that

are more cognitively demanding as they must be learned or calibrated and involve the integration of some form of cognitive information into the movement (Wise et al. 1996). An example would be the increasingly common use of a rear-view camera (or the more traditional rear-view mirror) while backing up one's car. To avoid an object, one needs to spin the wheel in a vertical plane leftward while viewing the object on the screen moving to the right; in this scenario the plane of limb motion is decoupled from guiding visual information, and there is a reversal of visual feedback. These more cognitively demanding non-standard tasks require sound connections between disparate brain regions within the frontoparietal network (Wise et al. 1997; Sabes 2000; Filimon 2010; Caminiti et al. 2017), and an inhibition of the default standard visuomotor control network (Gorbet et al. 2004). Impairments in performance of increasingly dissociated visuomotor tasks have been reported in the early stages of AD-related dementia (Tippett et al. 2012; de Boer et al. 2014; de Boer et al. 2015; de Boer et al. 2016), in patients with mild cognitive impairment (Salek et al. 2011), and in cognitively healthy individuals at an increased risk for dementia (Hawkins and Sergio 2014; Lu et al. 2021). Notably, these groups do not necessarily display large impairments in function when domains (sensory, cognitive, motor) are tested individually.

Initial findings on the structural neural correlates underlying visuomotor impairments in APOE e4 carriers without cognitive decline showed an association between reduced structural integrity in several major white matter tracts (Rogojin et al., in preparation). In the present study, we test the hypothesis that visuomotor impairments in cognitively healthy individuals with specific dementia risk factors (positive family history of dementia and presence of the APOE e4 allele) may also be associated with reduced functional connectivity in the DMN, and altered functional connectivity in other resting state networks. As an exploratory component, we were also interested in exploring whether differences in functional connectivity of resting state networks may underlie previously reported sex-differences in visuomotor control

(Rogojin et al. 2019) as sex-differences in resting brain connectivity have previously been demonstrated in the default mode, frontoparietal control, and sensorimotor networks (Zhang et al. 2018). Investigating the relationship between measures of network connectivity and visuomotor control in preclinical AD will provide insight into the potential utility of a clinically accessible behavioural assessment of dementia risk.

2. METHODS

2.1. Participants

Forty-eight right-handed older adults with no cognitive impairments were included in the current study: 24 individuals with a positive family history of dementia (n = 11 females) and 24 individuals with no family history of dementia (n = 12 females) (see **Table 1** for demographic information). All subjects scored at or above education-adjusted norms of 26 or higher on the Montreal Cognitive Assessment (MoCA), indicating no cognitive impairment. A positive family history of dementia was determined based on self-reported maternal or multiple family history (with at least one first-degree relative) of late-onset AD as a higher risk for AD is associated with a maternal or multiple, but not paternal, family history of dementia (Honea et al. 2010; Honea et al. 2011). Classification of no family history of dementia was based on having no family history of AD or any other type of dementia. Participants were excluded if their parents were deceased at a young age before dementia could be detected, or if they were estranged from either biological parent and did not know their medical history. Participants with a positive family history of dementia were age-balanced with those without a family history of dementia. The apolipoprotein E (APOE) e4 allele is the only gene that has been consistently associated with late-onset AD, representing the best-established genetic risk factor for progression to clinical AD (Reitz and Mayeux 2014; Dubois et al. 2016). Participants who were APOE e4 carriers were considered to be at an increased risk for AD. The exclusion criteria

included uncorrected visual impairments, upper-limb impairments or medical conditions that could hinder motor task performance (e.g., severe arthritis or dystonia), any neurological or psychiatric illnesses (e.g., Parkinson's disease, depression, schizophrenia, alcoholism, epilepsy), any history of head injury (e.g., mild, severe) or stroke, and medical diagnoses that might impact brain connectivity (i.e., hypertension or diabetes). The study protocol was approved by the Human Participants Review Sub-Committee of York University's Ethics Review Board.

Table 1. Participant demographic features.

	APOE e4 positive	APOE e4 negative	FH+	FH-	Females	Males
Demographics						
n	15	31	24	24	23	25
Age (years)	59.8 ± 4.99	58.4 ± 5.99	58.8 ± 6.03	58.8 ± 5.29	58.7 ± 5.71	58.8 ± 5.63
Range	*51 - 68*	*49 - 69*	*51 - 69*	*49 - 67*	*50 - 68*	*49 - 69*
FH+	10 (67%)	14 (45%)			11 (48%)	13 (52%)
APOE e4 positive			10 (67%)	5 (33%)	10 (43%)	5 (20%)
MoCA score	27.7 ± 1.44	28 ± 1.56	27.8 ± 1.48	28 ± 1.56	28.1 ± 1.51	27.6 ± 1.5
Range	*26 - 30*	*26 - 30*	*26 - 30*	*26 - 30*	*26 - 30*	*26 - 30*
Years of education	16.2 ± 3.78	17.7 ± 3.15	17.4 ± 3.52	16.8 ± 3.19	17.5 ± 3.06	16.7 ± 3.61
Range	*11 - 23*	*12 - 24*	*11 - 23*	*12 - 24*	*12 - 24*	*11 - 22*

FH+, positive family history of dementia; FH-, no family history of dementia; APOE, apolipoprotein E; MoCA, Montreal Cognitive Assessment.

2.2. APOE genotyping

A total of 2 mL of saliva were collected from each subject in microtubes from Diamed Lab Supplies Inc. using collection aids from Cedarlane Labs. Saliva samples were sent to DNA Genotek Inc. (Ottawa, ON, Canada) for APOE genotyping. DNA was extracted from samples according to the manufacturer's protocols. Genotyping for APOE involved single nucleotide polymorphism (SNP) genotyping, and samples were tested for SNPs rs429358 and rs7412. The proteins that are produced by the APOE gene are either E2, E3, or E4 combinations (for instance, E2/E3). For the current study, subjects were categorized as either having a presence (APOE e4 positive) or absence (APOE e4 negative) of the APOE e4 allele.

2.3. Behavioural data

2.3.1. Behavioural data acquisition

Our visuomotor assessment and behavioural data preprocessing have been described in detail in previous publications (Rogojin et al. 2019). Briefly, all subjects completed four visuomotor transformation tasks which involved making simple sliding finger movements between targets displayed on an Acer Iconia 6120 dual-touchscreen tablet. These tasks were divided into one standard condition (where gaze and movement were coupled) and three more cognitively demanding non-standard conditions (where gaze and movement were decoupled). Participants were instructed to slide the index finger of their right hand along the vertical or horizontal touchscreen (depending on the condition) in order to displace the cursor from a central target to one of four peripheral targets (to the top, bottom, left, or right of centre) as quickly and as accurately as possible. In the standard mapping condition (S), the spatial location of the visual target and the required hand movement were the same. The non-standard mapping conditions required the finger movements to be made either on a different plane (plane-change, PC), in the opposite direction (feedback reversal, FR), or both (PC+FR), from

the spatial peripheral target location (see **Fig. 1a** for depictions of all four visuomotor transformation task conditions). Eye movements were the same across all conditions (i.e., always to the guiding visual peripheral target on the vertical screen). The four conditions were presented in randomized blocks, each consisting of five pseudo-randomly presented trials to each of the four peripheral targets for a total of 20 trials per condition, and thus 80 trials per participant across the four conditions. Each participant was also given two practice trials per peripheral target prior to each of the four conditions to ensure task comprehension. See **Fig. 1b** for visual representations of a single trial completion, including trial timings.

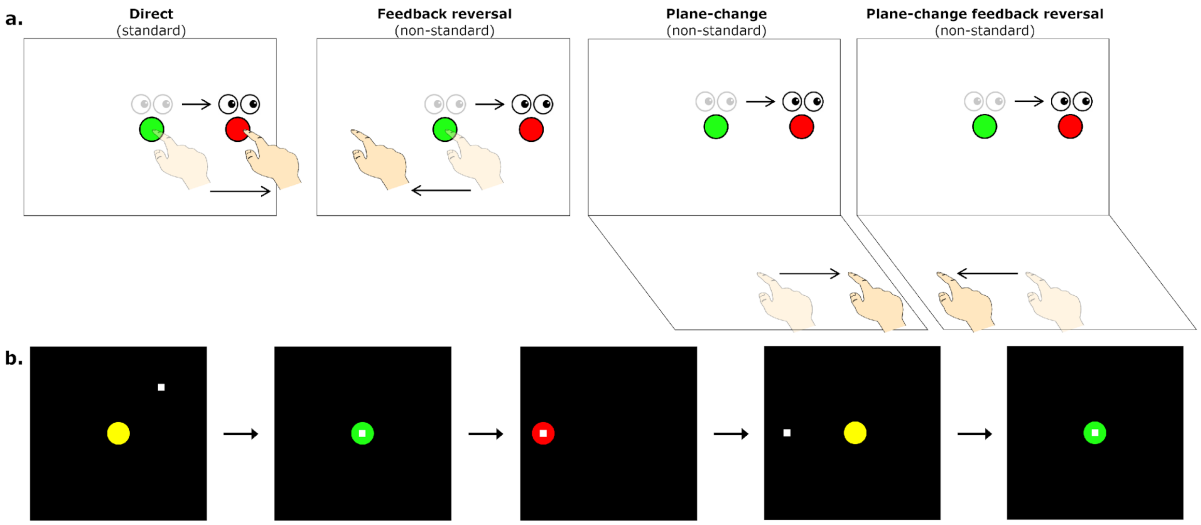

Figure 1. a) Schematic drawing of the visuomotor task conditions. Lighter eye and hand symbols denote the starting position for each trial (green central target). Darker eye and hand symbols denote the instructed eye and hand movements for each task. Red circles denote the peripheral (reach) target, presented randomly in one of four locations (left, up, right, or down relative to the central target). The direct interaction task requires standard mapping, where participants slide their finger on a touch screen to move a cursor from a central target to one of four peripheral targets. The other three conditions involve non-standard visuomotor integration, where targets either have a 180° feedback reversal (feedback reversal), are spatially dissociated from the plane of hand motion (plane-change), or both (plane-change + feedback reversal). **b)** Sequence of events during one trial of the visuomotor task. All trials begin in the central (home) target. Once the participant moves the cursor (denoted by the white square) into the central target, the target changes from yellow to green to signify a movement preparation period. After 4000 ms, a red peripheral target appears in one of four directions (up, down, left, or right of the centre) and serves as the 'Go' signal. Once the peripheral target is acquired and held for 500 ms it disappears, signaling the end of the trial. After an inter-trial interval of 2000 ms, the central yellow target reappears, and the participant moves back to the central target to initiate the next trial.

2.3.2. Behavioural data preprocessing

Kinematic measures, including timing, finger position (x, y coordinates; 50 Hz sampling rate), and error data were recorded for each trial and converted into a MATLAB readable format using a custom written (C++) application. Custom analysis software (Matlab, Mathworks Inc.) was used to process individuals' finger trajectories and generate movement profiles that were then verified by visual inspection, and manually corrected when necessary. All data were processed to compute timing, accuracy, and precision measures. These kinematic outcome measures were as follows: 1) Reaction time (RT), the time interval (in ms) between the central target disappearance and movement onset; 2) Full movement time (MTf), the time (in ms) between movement onset and offset; 3) Peak velocity (PV), the maximum velocity obtained during the ballistic movement, and used to calculate the 10% threshold used for determining movement onsets and offsets; 4) Path length (PL), the total distance (in mm, calculated from the x and y trajectories) travelled between movement onset and offset; 5) Absolute error (AE), a measure of end-point accuracy, and the average distance (in mm) from the individual ballistic movement endpoints ($\sum x/n, \sum y/n$) to the actual target location; and 6) Variable error (VE), a measure of end-point precision, and the distance (in mm) between the individual ballistic movement endpoints (σ) from their mean movement. Corrective path length (CPL) represents corrective movements and was quantified by subtracting the PLb (initial movement offset) from the PLf (full movement offset). The procedure for combining some of the kinematic measures into composite scores to decrease the number of comparisons made in the data analysis was previously described (Rogojin et al. 2019). Briefly, all kinematic measures were standardized using z-scores and the composite scores were then created using simple averaging. A "timing score" was created as a composite score of RT, MTf, and PV, and an "endpoint error score" was a composite score of AE and VE. The timing and endpoint error scores had a high internal consistency, as indicated by Cronbach's alpha values of 0.897 and

0.772, respectively. The corrective path lengths, timing scores, and endpoint error scores were then used for statistical analysis.

2.4. Magnetic resonance imaging

2.4.1. Image acquisition

MRI data were acquired using a 3 Tesla (3T) Siemens Trio scanner at York University. Participants received a T1-weighted anatomical scan using a sagittal volumetric magnetization-prepared rapid gradient echo (MP-RAGE) sequence. The MP-RAGE consisted of the following acquisition parameters: 192 sagittal slices (slice thickness of 1 mm, with no gap), field of view (FOV) of 256 x 256 mm, matrix size of 256 x 256 resulting in a voxel resolution of 1 x 1 x 1 mm, echo time (TE) = 2.96 ms, repetition time (TR) = 2300 ms, flip angle = 9^{o}. To quantify resting state functional connectivity (RSFC) within networks of interest, an echo planar imaging (EPI) sequence sensitive to blood oxygenation level dependent (BOLD) contrast was collected. Participants were asked to lie still with their eyes closed, letting their mind wander for six minutes in the scanner during the functional sequence with the following acquisition parameters: 35 axial slices (slice thickness of 4 mm, with no gap), field of view (FOV) of 210 x 210 mm, matrix size of 70 x 70 resulting in a voxel resolution of 3 x 3 x 4 mm, echo time (TE) = 30 ms, repetition time (TR) = 2000 ms, flip angle = 90^{o}.

2.4.2. MR image preprocessing

Preprocessing of the neuroimaging data was done using FreeSurfer 7.1 (Harvard Medical School, Boston, USA; http://www.surfer.nmr.mgh.harvard.edu) and Analysis of Functional NeuroImages (AFNI) software (version 21.3.07 'Trajan') (Cox 1996). The T1-weighted MR images were used as input to the main Freesurfer reconstruction pipeline ("*recon-all*") to parcellate and segment the brain into anatomically distinct regions of the cortex and subcortical

nuclei, respectively. Each individual's parcellation and segmentation was visually inspected to ensure that there were no obvious errors. AFNI was used for preprocessing of the resting state data. For every participant, the first 2 image-volumes were removed. Functional preprocessing steps included despiking (3dDespike), slice timing correction (3dTshift), coregistration of the rest run with the subject's T1-weighted anatomical image (3dAllineate), and motion correction (3dVolreg). ANATICOR (Jo et al. 2010) was used for nuisance variable regression (removal of ventricle/white matter tissue-based signals). The ventricle and white matter masks used for nuisance regression by ANATICOR were created from Freesurfer's segmentation of the T1-weighted data and were visually-inspected for quality control. Within AFNI, these masks were eroded to prevent inclusion of voxels containing gray matter. Motion censoring was applied such that successive functional volumes containing >0.25 mm of head motion, as well as volumes containing >5% of voxels as outliers, were removed. At each voxel, the data was detrended using the default polynomial degree based on the duration of the resting state run. A voxel was labelled an outlier if the signal was outside of a defined number of mean absolute deviations (MAD) from the trend, calculated based on the number of TRs in the dataset. To account for older adults' tendency to move more in the scanner (Pardoe et al. 2016; Savalia et al. 2017; Madan 2018), the motion censor threshold used in the current study was less conservative than that typically used in resting state fMRI preprocessing pipelines for younger participants (>0.2 mm) (Power et al. 2014). Average motion after censoring was <0.15 mm for all participants. The percentage of censored volumes and average censored motion did not differ significantly between groups (family history positive vs. no family history, males vs. females, APOE e4 positive vs. APOE e4 negative). In addition to nuisance variables created via ANATICOR, nuisance variables for the time-series of each voxel also included estimates of head motion in 6 directions and the temporal derivative of each of these six head motion estimates. Least-squares model fitted time-series of all nuisance variables were subtracted from

the voxel time-series resulting in a residual time-series that was used in subsequent analyses. As a data quality assessment procedure, the precuneus was used as a seed region in the preprocessed functional data (i.e., the residual time-series) in order to verify that the DMN looked reasonable in every subject. The seed region was selected within the left hemisphere precuneus, 2-3 slices away from the mid-sagittal plane, central to the region bordered by the pars marginalis of the cingulate sulcus, the subparietal sulcus, and the parieto-occipital fissure. Following preprocessing, one participant was excluded due to missing resting state data, and 48 participants were used in the final analysis.

2.4.3. Functional connectivity parcellation

An individualized functional parcellation approach was used to identify subject-specific functional resting state network nodes in the preprocessed data (Chong et al. 2017). Functional parcellation of resting state networks refers to the identification of cortical areas, or 'parcels' that exhibit functionally similar properties (Raichle et al. 2001; Sporns et al. 2005; Kim et al. 2010; Eickhoff et al. 2011; Smith et al. 2013; Eickhoff et al. 2015). The most common approach to parcellation relies on a mean functional resting state network parcellation common to a group of subjects (i.e., the group average network), which is then projected back onto individual subject data (Yeo et al. 2011; Wig et al. 2014). These population-average networks have provided important information on the large-scale functional organization of the brain (Buckner et al. 2013; Wig 2017). However, population-average networks may obscure individual-specific network organization and thus lead to inaccuracies at the level of individual subjects (Chong et al. 2017). Thus, there is a growing focus on person-specific parcellation to define functional parcels independently for each participant. Group prior individual parcellation (GPIP) was implemented to automatically perform parcellation of resting functional data into functional networks at the level of individual subjects (Chong et al. 2017).

GPIP is a novel cortical parcellation method that initializes parcellation using an atlas template. This initial parcellation is then refined for each subject using the subject's functional data to allow individual variability across subjects in the boundaries of these parcels (Chong et al. 2017). The use of a template atlas for parcellation initialization results in all subjects having corresponding functional regions (aiding group analysis), while functional parcel boundaries can vary from subject to subject. GPIP iterates between two steps to continuously update parcel labels until convergence: 1) each participant's parcel boundaries (first obtained from the initialization to the Schaefer atlas) are refined relative to their resting functional data, and 2) the concentration (inverse covariance/partial correlation) matrices from all individuals are then jointly estimated using a group sparsity constraint (Chong et al. 2017). Specifically, for the results presented in the current study, the preprocessed and denoised resting state functional data were first initialized with the 200-parcel Schaefer atlas (Schaefer et al. 2018), corresponding to the 7 functional networks atlas (Yeo et al. 2011).

Prior to GPIP initialization, the functional data were registered to the corresponding FreeSurfer anatomical images for each subject, converted from volumetric to surface space, and resampled to the FreeSurfer cortical surface template (fsaverage5). Spatial smoothing of 6 mm was applied to the anatomically-aligned data in surface space. Visual inspection was used to verify proper coregistration of functional data with the T1-weighted anatomical images. Values from vertices located in the medial wall were resampled into the surface data as they are removed by FreeSurfer but are needed for running GPIP. The functional time-series data were normalized by scaling to a mean value of 0 and a standard deviation of 1. The normalized functional time-series data were then used in subsequent steps for GPIP analysis. GPIP performed its two-step iterative process 20 times for each subject resulting in increasingly refined functional network parcellations with optimal segmentation with respect to the cortical surface. Each participant's final parcellation was plotted and inspected to verify the quality of

the parcellation (an example of a single subject's final parcellation is shown in **Fig. 2**). To further assess the quality of the parcellations, homogeneity was calculated as the mean temporal correlation coefficient between all pairs of vertices within each GPIP parcel, where a large value suggests that the vertices included in a particular parcel have similar time-series (i.e., are homogeneous) and therefore correctly assigned to that parcel. The homogeneity value was calculated for the whole brain as a mean value across all parcels for each GPIP iteration to verify that these values increased with each iteration before plateauing prior to the final iterations, suggesting stable and accurate parcellations. Further, cross-correlation matrices including all GPIP parcels were plotted and visually inspected to verify reasonable patterns of whole-brain connectivity in each participant (see **section 2.4.4** below for specific details on matrix construction).

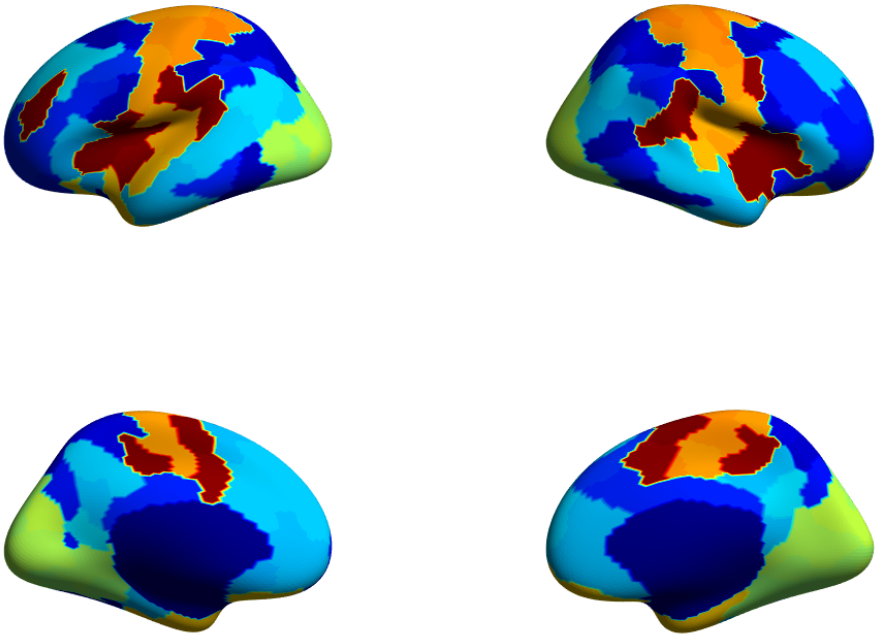

Figure 2. Example parcellation from a single subject initialized with the 200-parcel 7-network Schaefer atlas (Schaefer et al. 2018) with refined parcel borders that functionally correspond to the subject's resting state data as a result of the GPIP process.

2.4.4. Resting state functional connectivity matrix

A functional connectivity matrix was created for each participant based on their individualized parcellation. The mean BOLD signal time-series data was extracted from each parcel and pairwise correlations were computed between each parcel pair. The correlation coefficients were then converted to z-scores using Fisher's r-to-z transformation to normalize the distribution of correlation values, resulting in a 200 x 200 functional connectivity matrix for each subject. A growing body of research has implicated the DMN as being particularly vulnerable to AD pathology beginning in the preclinical stage (Hedden et al. 2009; Sheline, Raichle, et al. 2010; Sheline and Raichle 2013; Riedel et al. 2016; Hampton et al. 2020). Functional nodes of the DMN include the posterior cingulate cortex, retrosplenial cortex, precuneus, medial prefrontal cortex, inferior parietal lobes, temporal pole extending into the lateral temporal cortex, and regions of the medial temporal lobe (including the hippocampal and parahippocampal cortices) (Parvizi et al. 2006; Uddin et al. 2009; Andrews-Hanna et al. 2010; Sperling et al. 2011; Márquez and Yassa 2019). Previous studies have further identified two functional cores of the DMN: the medial prefrontal cortex within the anterior medial portion of the DMN, and the precuneus and posterior cingulate cortex in the posterior medial portion of the DMN (Buckner et al. 2008; Fransson and Marrelec 2008; Andrews-Hanna et al. 2010; Utevsky et al. 2014). These regions represent core hubs to which all other regions of the DMN are correlated (Buckner et al. 2008). As previously mentioned, functional connectivity in the DMN is disrupted in preclinical AD including prominently in the posterior medial regions (precuneus and posterior cingulate cortex) and the medial prefrontal cortex (Hedden et al. 2009; Damoiseaux et al. 2012; Wang, Catherine M Roe, et al. 2012; Riedel et al. 2016), as well as between posterior medial regions and other posterior areas of the DMN, namely the medial temporal lobe and inferior parietal lobule (Sheline, Raichle, et al. 2010; López-Sanz et al. 2017). Therefore, instead of examining the DMN as a whole, homogeneous network, it was

assessed based on the functional connectivity between and within the anterior and posterior core hubs, as well as the connectivity of these regions to other functional nodes within the DMN. The Schaefer parcellation was visually inspected to assign GPIP parcels of the DMN to the following network nodes: precuneus/posterior cingulate cortex (pCun/PCC), medial prefrontal cortex (mPFC), left and right lateral prefrontal cortex (llPFC, rlPFC), left and right inferior parietal lobe (lIPL, rIPL), left and right lateral temporal cortex (lLTC, rLTC), and left parahippocampal cortex (lPHC) (**Fig. 3a**). The IPL consisted largely of the angular and supramarginal gyri, and the LTC consisted of the temporal pole extending into the inferior, middle, and superior temporal gyri. Each participant's mean Fisher z-transformed RSFC values were also extracted for several other resting state networks of interest as a measure of overall within-network functional connectivity. The networks of interest were the somatomotor network (SMN), dorsal attention network (DAN), ventral attention network (VAN), and frontoparietal control network (FPN) (**Fig. 3b-e**).

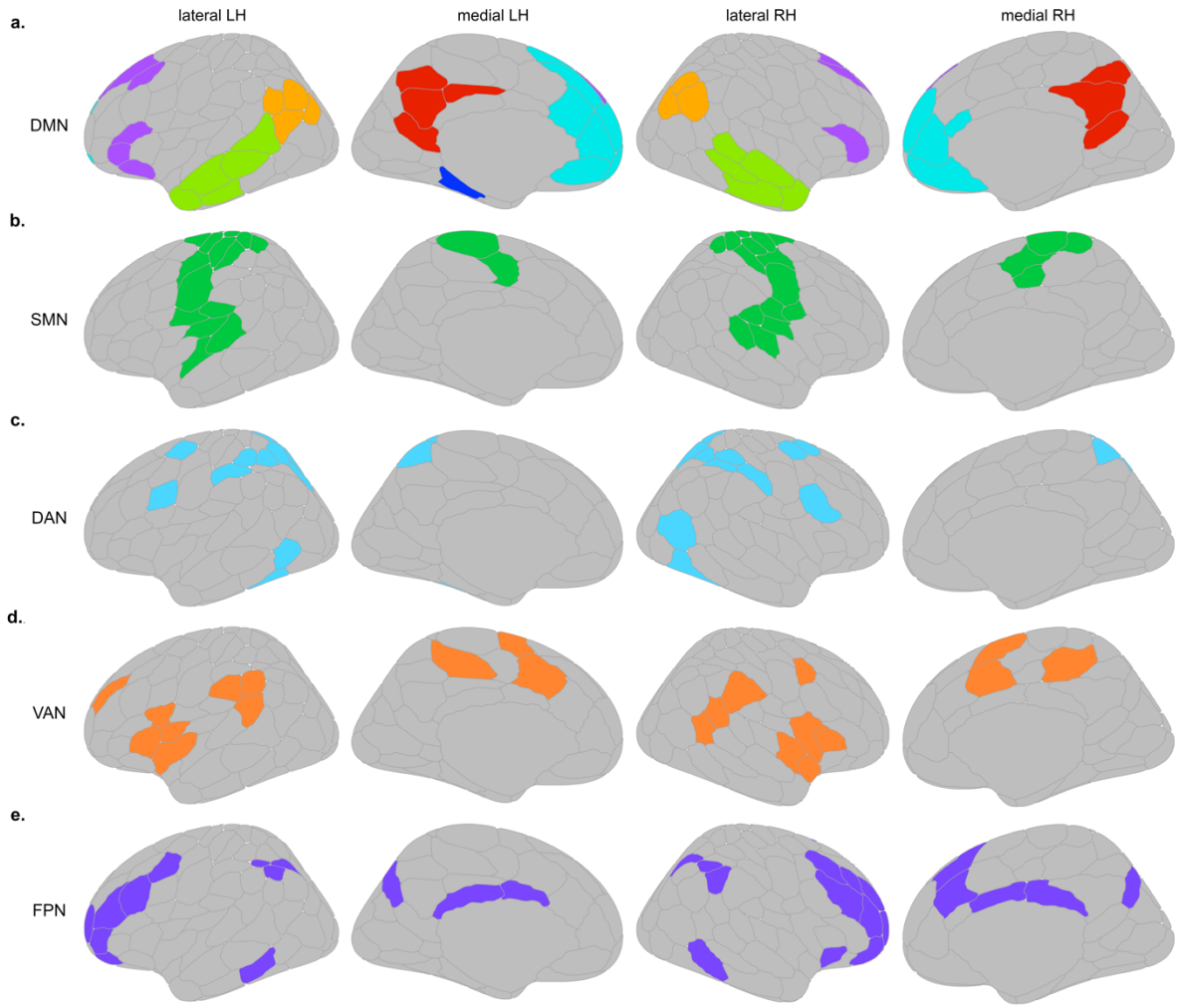

Figure 3. a) Parcels from GPIP parcellation of the default mode network (DMN) were visually inspected and assigned to the following DMN nodes: precuneus/posterior cingulate cortex (pCun/PCC; red), medial prefrontal cortex (mPFC; cyan), left and right lateral prefrontal cortex (llPFC, rlPFC; purple), left and right inferior parietal lobe (lIPL, rIPL; orange), left and right lateral temporal cortex (lLTC, rLTC; lime green), and left parahippocampal cortex (lPHC; dark blue). Resting state networks used for mean resting state functional connectivity (RSFC) analysis, with corresponding nodes assigned by GPIP to the **b)** somatomotor network (SMN; green), **c)** dorsal attention network (DAN; blue), **d)** ventral attention network (VAN; orange), and **e)** frontoparietal control network (FPN; purple). LH, left hemisphere; RH, right hemisphere. Brain figures made with "ggseg" R package (Mowinckel and Vidal-Piñeiro 2020).

2.5. Statistical analysis

All statistical analyses were carried out using open-source R software v4.1.0 (R Core Team 2021).

2.5.1. Family history of dementia, APOE status, and sex effects on functional connectivity

Three-way ANOVAs were used to compare differences in RSFC between: 1) individuals with a family history of dementia and individuals without a family history of dementia, 2) APOE e4 carriers and non-carriers, and 3) females and males. The RSFC measures being compared were pairwise parcel FC values for select DMN nodes, as well as mean within-network RSFC in the SMN, DAN, VAN, and FPN. The pairwise comparisons for the DMN were performed between the following nodes: pCun/PCC and mPFC; pCun/PCC and bilateral lPFC, bilateral IPL, bilateral LTC, and left PHC; mPFC and bilateral lPFC, bilateral IPL, bilateral LTC, and left PHC. Post-hoc analyses were adjusted for multiple comparisons using the Holm correction method, and were considered statistically significant at an alpha of $p < 0.05$.

2.5.2. Family history of dementia, APOE status, sex, and functional connectivity effects on visuomotor integration performance

Previous behavioural findings revealed that significant predictors of worse visuomotor performance were 1) a family history of dementia (greater endpoint error scores in the visual feedback reversal condition), 2) having the APOE e4 allele (greater endpoint error scores in the plane-change feedback reversal condition, and greater corrective path lengths in both of the plane-change conditions), and 3) sex (greater endpoint error scores in the visual feedback reversal condition) (Rogojin et al. 2019). The current study used multiple linear regression analysis to assess whether these performance declines are associated with RSFC. The RSFC

measures being compared were pairwise parcel FC values for select DMN nodes, as well as for mean within-network FC for the SMN, DAN, VAN, and FPN. The pairwise comparisons for the DMN were performed between the following nodes: pCun/PCC and mPFC; pCun/PCC and bilateral lPFC, bilateral IPL, bilateral LTC, and left PHC; mPFC and bilateral lPFC, bilateral IPL, bilateral LTC, and left PHC. Regression models were set up with RSFC as the predictor variable, one of the visuomotor performance measures as the dependent variable, and based on the previous findings they were controlled for 1) sex and family history in the feedback reversal condition, and 2) APOE e4 status in the two plane-change conditions. Specifically, the visuomotor performance measures used in this study were endpoint error scores in the feedback reversal condition (controlled for sex and family history), endpoint error scores in the plane-change feedback reversal condition (controlled for APOE status), and corrective path lengths in both of the plane-change conditions (controlled for APOE status). The p-values were adjusted for multiple comparisons using the Holm correction method. Corrections were considered statistically significant at $p < 0.05$.

3. RESULTS

3.1. No general effects of family history of dementia, APOE status, and sex on functional connectivity

There were no statistically significant differences between 1) positive and negative dementia family history, 2) APOE e4 carriers and non-carriers, and 3) females and males found between pairwise parcel FC values for the DMN nodes of interest, or for mean within-network FC in the SMN, DAN, VAN, and FPN.

3.2. Modifying effects of the APOE e4 allele on the relationship between visuomotor performance and connectivity between the posterior medial DMN with other DMN nodes

Presence of the APOE e4 allele modified the relationship between visuomotor performance in the plane-change feedback reversal condition and RSFC between the pCun/PCC and two other nodes in the left hemisphere (**Table 2**). There was a significant interaction effect of pCun/PCC to left IPL RSFC and APOE status ($\beta = -16.303$, $p < 0.05$) on endpoint error scores (**Fig. 4a**). The results of the regression analysis indicated that the predictors explained 37% of variance ($R^2_{adj} = 0.3696$, $F_{3,42} = 9.796$, $p < 0.01$). Simple slopes analysis revealed that a lower RSFC between the pCun/PCC and left IPL (**Fig. 3a**, red/orange) was a significant predictor of greater corrective path length (indicative of worse visuomotor performance) only in APOE e4 carriers (simple slope = -11.43, S.E. = 4.43, $p = 0.01$). Similarly, there was a significant interaction effect of pCun/PCC to left PHC RSFC and APOE status ($\beta = -27.278$, $p < 0.05$) on corrective path length (**Fig. 4b**). The results of the regression analysis indicated that the predictors explained 35.3% of variance ($R^2_{adj} = 0.3532$, $F_{3,42} = 9.192$, $p < 0.01$). Simple slopes analysis revealed that a lower RSFC between the pCun/PCC and left PHC (**Fig. 3a**, red/dark blue) was a significant predictor of greater corrective path length (indicative of worse visuomotor performance) only in APOE e4 carriers (simple slope = -21.86, S.E. = 8.20, $p = 0.01$).

3.3. Modifying effects of the APOE e4 allele on the relationship between mean intra-DAN functional connectivity and visuomotor performance

Presence of the APOE e4 allele modified the relationship between mean intra-DAN RSFC and visuomotor performance for two of the behavioural measures in the plane-change feedback reversal condition (**Fig. 5**). There was a significant interaction effect of mean RSFC in the DAN and APOE status ($\beta = -25.543$, $p < 0.01$) on endpoint error scores. The results of the regression analysis indicated that the predictors explained 41.5% of variance ($R^2_{adj} = 0.4148$, $F_{3,42} = 11.63$, $p < 0.001$). Simple slopes analysis revealed that a lower mean RSFC in

the DAN was a significant predictor of greater endpoint error scores (indicative of worse visuomotor performance) only in APOE e4 carriers (simple slope = -23.41, S.E. = 6.81, $p < 0.01$). Similarly, there was also a significant interaction effect of mean RSFC in the DAN and APOE status ($\beta = -59.268$, $p < 0.05$) on corrective path length. The results of the regression analysis indicated that the predictors explained 38% of variance ($R^2_{adj} = 0.3799$, $F_{3,42} = 5.915$, $p < 0.001$). Simple slopes analysis revealed that a lower mean RSFC in the DAN was a significant predictor of greater corrective path length (indicative of worse visuomotor performance) only in APOE e4 carriers (simple slope = -53.40, S.E. = 17.23, $p < 0.01$). The statistics for these multiple linear regressions are listed in **Table 2**. There were otherwise no effects of family history, APOE e4 status, or sex on the relationship between mean within-network functional connectivity and visuomotor performance for any of the other resting networks.

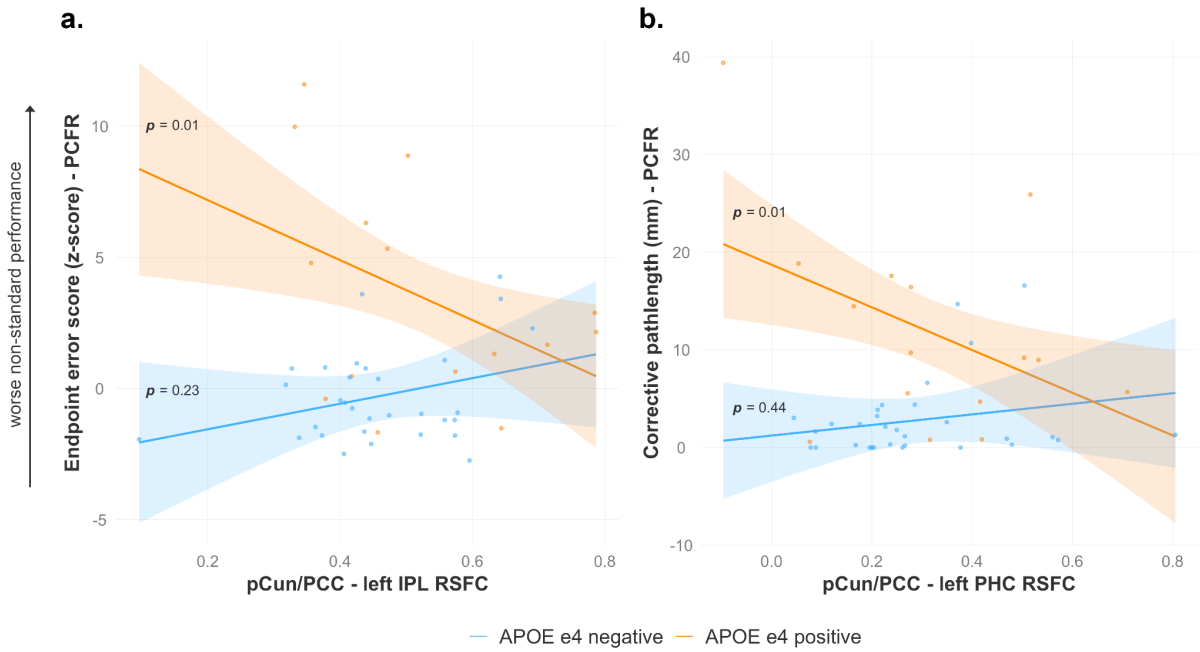

Figure 4. Lower RSFC between several DMN nodes predicts worse visuomotor performance (reflected by higher endpoint error scores or corrective path lengths) in the plane-change feedback reversal condition only in APOE e4 carriers. Specifically, lower RSFC between the **a)** pCun/PCC and left IPL, and **b)** pCun/PCC and left PHC predicts worse non-standard visuomotor performance. Significant results shown from multiple regression and simple slopes analyses. RSFC, resting state functional connectivity; APOE, apolipoprotein E; pCun/PCC, precuneus/posterior cingulate cortex; IPL, inferior parietal lobule; PHC, parahippocampal cortex; PC+FR, plane change feedback reversal condition.

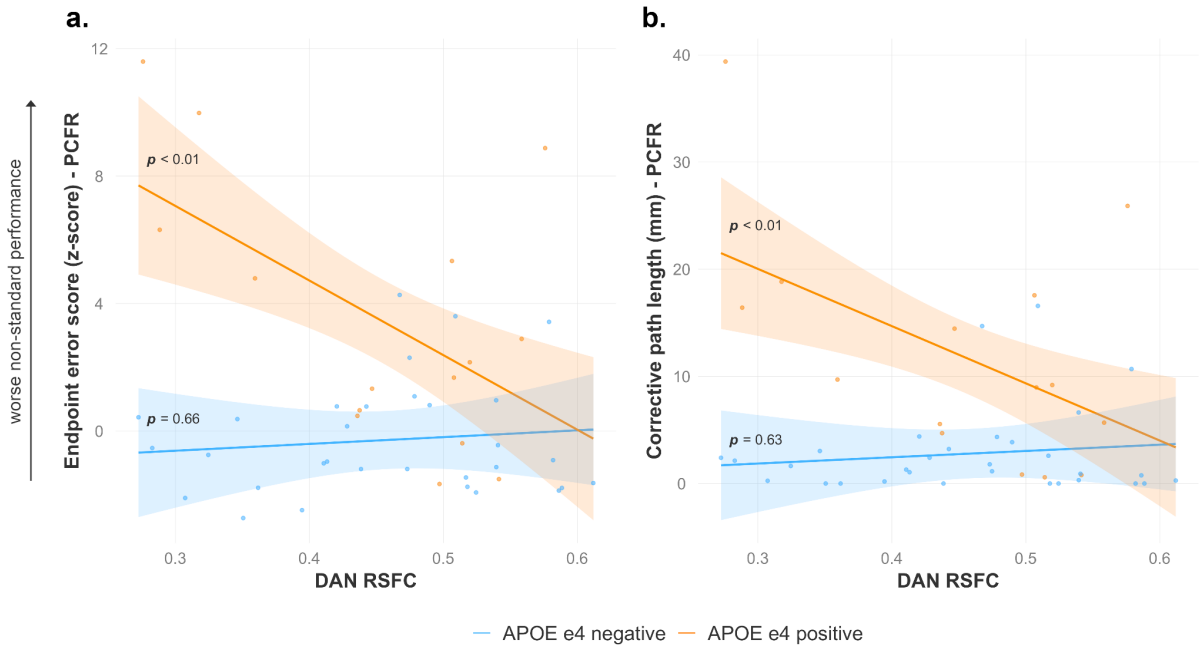

Figure 5. Lower intra-DAN mean RSFC predicts worse visuomotor performance in the plane-change feedback reversal condition only in APOE e4 carriers. Worse non-standard visuomotor performance is reflected by **a)** higher endpoint error scores, and **b)** greater corrective path lengths. Significant results shown from multiple regression and simple slopes analyses. RSFC, resting state functional connectivity; APOE, apolipoprotein E; DAN, dorsal attention network; PC+FR, plane change feedback reversal condition.

Table 2. Multiple linear regression models used to assess whether non-standard visuomotor performance declines are associated with resting state functional connectivity (RSFC). Regression models were set up with RSFC as the predictor variable, APOE e4 status as the moderator variable, and visuomotor performance measures (EE score and CPL) in the plane-change feedback reversal condition as the outcome variable. Models with significant interactions are shown.

Outcome	Network	Predictor	Estimate	S.E.	t	Unadjusted *p*	Adjusted *p*
EE Score	pCun/PCC – left IPL	Intercept	3.474	1.531	2.268	0.028508	
		RSFC	-3.283	2.979	-1.102	0.276775	0.276775
		APOE	11.991	3.063	3.915	0.000326	0.000978
		RSFC*APOE	-16.303	5.958	-2.736	0.009068	0.018136
						R^2_{adj} = 0.3696, $F_{3,42}$ = 9.796, p = 0.00005061	
						APOE e4 simple slope = -11.43, S.E. = 4.43, $p < 0.01$	
CPL	pCun/PCC – left PHC	Intercept	9.972	1.927	5.174	6.03E-06	
		RSFC	-8.219	5.397	-1.523	0.1353	0.1353
		APOE	17.498	3.854	4.54	4.67E-05	0.0001401
		RSFC*APOE	-27.278	10.795	-2.527	0.0154	0.0308
						R^2_{adj} = 0.3532, $F_{3,42}$ = 9.192, p = 0.000008531	
						APOE e4 simple slope = -21.86, S.E. = 8.20, $p < 0.01$	
EE Score	Mean DAN	Intercept	6.41	1.934	3.314	0.001898	
		RSFC	-10.638	4.168	-2.552	0.014422	0.014422
		APOE	15.345	3.868	3.967	0.000278	0.000834
		RSFC*APOE	-25.543	8.336	-3.064	0.003802	0.007604
						R^2_{adj} = 0.4148, $F_{3,42}$ = 11.63, p = 0.0000111	
						APOE e4 simple slope = -23.41, S.E. = 6.81, $p < 0.01$	
CPL	Mean DAN	Intercept	18.08	4.895	3.694	0.000632	
		RSFC	-23.771	10.547	-2.254	0.02949	0.02949
		APOE	35.948	9.789	3.672	0.000674	0.002022
		RSFC*APOE	-59.268	21.094	-2.81	0.007498	0.014996
						R^2_{adj} = 0.3799, $F_{3,42}$ = 10.19, p = 0.00003623	
						APOE e4 simple slope = -53.40, S.E. = 17.23, p < 0.01	

Unadjusted and adjusted p-values reported. Values were adjusted for multiple comparisons using the Holm correction method and were considered statistically significant at $p < 0.05$. S.E., standard error; EE score, endpoint error score; CPL, corrective path length; RSFC, resting state functional connectivity; APOE, apolipoprotein E; DAN, dorsal attention network; pCun/PCC, precuneus/posterior cingulate cortex; IPL, inferior parietal lobule; PHC, parahippocampal cortex.

4. DISCUSSION

The main goal of this study was to assess whether disrupted RSFC may underlie impaired visuomotor abilities in individuals with specific dementia risk factors (positive family history of dementia, or presence of the APOE e4 allele). A secondary goal was to investigate whether differences in RSFC may also explain previously demonstrated sex-differences in non-standard visuomotor performance. We previously found that e4-carriers performed significantly worse on visuomotor tasks under increasing cognitively-demanding conditions (Rogojin et al. 2019), and that this impaired performance was associated with lower white matter integrity in the brain (Rogojin et al., in preparation). Our key novel findings in the current study demonstrate that the e4 allele also modified the relationship between RSFC and visuomotor performance, where lower RSFC in the DMN and the DAN predicted poorer non-standard performance. Notably, these visuomotor deficits in APOE e4 carriers were detectable using our non-standard visuomotor tasks *in advance of any measurable cognitive issues*. There were no significant relationships between RSFC and family history of dementia or sex to explain previously reported differences in visuomotor task performance.

4.1. Reduced resting state functional connectivity in the posterior DMN and the DAN predict visuomotor deficits in APOE e4 carriers

Individuals with the e4 allele showed abnormalities in RSFC between posterior DMN nodes that predicted poorer non-standard visuomotor performance. Specifically, there was lower RSFC between the precuneus and posterior cingulate cortex, the posterior functional core of the DMN (Buckner et al. 2008; Fransson and Marrelec 2008; Andrews-Hanna et al. 2010; Utevsky et al. 2014), and the left IPL and left parahippocampal cortex. Our findings are consistent with the literature, where reduced functional connectivity was demonstrated in the DMN between the precuneus and left parahippocampal cortex specifically, among several

other DMN nodes, in cognitively normal individuals with amyloid pathology (Sheline, Raichle, et al. 2010). These findings were then replicated in APOE e4 carriers without any cognitive impairments and prior to the onset of amyloid pathology, where e4 carriers had lower RSFC of the precuneus to bilateral hippocampus and left parahippocampus compared to non-carriers (Sheline, Morris, et al. 2010). Several other studies have similarly found reduced RSFC within the posterior DMN in APOE e4 carriers compared to non-carriers, including in the precuneus (Fleisher et al. 2009; Patel et al. 2013; Su et al. 2017), posterior cingulate cortex (Patel et al. 2013; Su et al. 2017), and between the pCun/PCC and hippocampus (Heise et al. 2014). Our findings are further supported by other studies showing decreased functional connectivity in the angular gyrus (a region of the IPL) in APOE e4 carriers (Wu et al. 2016). Patients with mild cognitive impairment who later develop AD, compared to mild cognitive impairment patients who remain stable in follow-up, also demonstrate significantly decreased RSFC in bilateral IPL (Li et al. 2016).

Additionally, lower RSFC in the DAN was also a predictor of worse non-standard visuomotor performance in APOE e4 carriers. The DAN, composed bilaterally of the intraparietal sulcus and frontal eye fields, is involved in goal-driven "top-down" orienting of attention toward behaviourally relevant stimuli (Fox et al. 2006). The influence of the e4 allele on the DAN is not widely studied (Foo et al. 2020). One paper looking at structural MRI found cortical thinning in APOE e4 carriers in the frontoparietal regions that form DAN functional nodes (Wolk and Dickerson 2010). Most studies on the DAN and its relation to AD are from clinical populations with either mild cognitive impairment or dementia, demonstrating that "top-down" attention processing mediated by the DAN is impaired by mild cognitive impairment and AD with decreased RSFC observed in both populations (Li et al. 2012; Qian et al. 2015; Zhang et al. 2015; Mcdonough et al. 2019; Wang et al. 2022).

There are several brain regions that are activated during non-standard visuomotor movements, with the precuneus and IPL in particular appearing to be crucial for discriminating between standard and non-standard task conditions (Gorbet and Sergio 2016; Gorbet and Sergio 2018). Other studies have further demonstrated the importance of the IPL in visuomotor control (Bernier and Grafton 2010; Mutha et al. 2011; Crottaz-Herbette et al. 2014). Regions of the medial temporal lobe, including the hippocampus, parahippocampus, and entorhinal cortex, are involved in encoding hand position in space, and the parahippocampal cortex may be particularly important for sensorimotor transformations between visual inputs and hand kinematics (Tankus and Fried 2012). The involvement of these regions in visuomotor integration may therefore explain the reduced RSFC that we see between several regions of the DMN including the pCun/PCC, IPL, and parahippocampal cortex in e4 carriers associated with deficits in non-standard visuomotor movements. Further, the intraparietal sulcus of the DAN is located within the PPC, which is activated during visuomotor transformations (Blangero et al. 2009). Taken together, our findings from the DMN and DAN demonstrate a relationship between parietal-frontal and parietal-temporal functional connectivity and visuomotor performance. This is consistent with the important role of reciprocal cortical networks involving frontal, parietal, and temporal regions in visuomotor transformations required for successful execution of goal-directed movements (Gorbet et al. 2004; Gorbet and Sergio 2016; Caminiti et al. 2017; Gorbet and Sergio 2018).

4.2. Potential mechanisms of APOE e4 effects on resting state functional connectivity

The APOE e4 allele has been proposed to reduce protection or increase toxicity compared to the e3 and e2 alleles in most AD pathogenic pathways. One potential mechanism of APOE e4 action is via Aβ-induced neurotoxicity (Mahley and Rall 2000; Manelli et al. 2004). Histopathological studies demonstrated that APOE e4 carriers have a higher Aβ plaque density

and burden compared to non-carriers (Rebeck et al. 1993; Tiraboschi et al. 2004; Reiman et al. 2009; Caselli et al. 2010). In cognitively normal individuals, biomarkers of Aβ accumulation were present at a frequency that corresponded to their APOE genotype, with the highest frequency found in APOE e4 carriers (Castellano et al. 2011). The APOE E4 protein appears to bind with less affinity to Aβ (LaDu et al. 1994), and may therefore prevent effective clearance of neurotoxic Aβ species compared to other APOE variants (LaDu et al. 1997). Indeed, Aβ complexes formed with the E2 and E3 proteins are cleared more rapidly from the brain compared to complexes with the E4 variant (Deane et al. 2008). Several studies have demonstrated decreased functional connectivity in the DMN in cognitively normal subjects with high amyloid burden (Hedden et al. 2009; Sperling et al. 2009; Sheline, Raichle, et al. 2010; Mormino et al. 2011). Multiple studies have found a general spatial-temporal pattern of amyloid deposition in AD with earliest accumulation in the medial frontal and cingulate regions (Fantoni et al. 2020), which overlap with the core functional nodes of the DMN (Buckner et al. 2008; Fransson and Marrelec 2008; Andrews-Hanna et al. 2010; Utevsky et al. 2014). A recent study investigating the effects of APOE e4 on Aβ spatial distribution patterns found highest amyloid accumulation in the medial temporal lobe (hippocampal, parahippocampal, and entorhinal cortices) and inferior parietal regions (Cacciaglia et al. 2022). These are some of the same regions between which we reported lower RSFC that predicted poorer visuomotor performance in e4 carriers. In addition to amyloid plaques, systemic inflammation has been implicated in AD pathogenesis with activation of inflammatory responses observed in the brains of AD patients (Bales et al. 2000). APOE may modulate the neuroinflammatory response in AD pathology, as the e4 allele has been associated with a greater pro-inflammatory response compared to the e3 allele (Guo et al. 2004). Lower RSFC in the DMN and DAN was linked to peripheral pro-inflammatory signalling in older adults without dementia, and was further magnified in APOE e4 carriers (Walker et al. 2020). Therefore, the APOE e4 allele may

compromise the functional integrity of resting cortical networks through both Aβ-related and non-Aβ related pathways early in disease progression.

4.3. General conclusions

Sensory and motor regions in the brain are affected by AD pathology, and sensorimotor deficits may precede the onset of cognitive symptoms of AD by several years (Albers et al. 2015). These findings raise the possibility that sensory and motor changes may be an early non-invasive biomarker for AD, and even a target for intervention in the treatment of AD (de Boer et al. 2018; Echlin et al. 2020). Our findings support the potential use of a simple behavioural task that requires communication across brain regions processing visual, cognitive, and motor information to detect sensorimotor (more specifically, visuomotor) impairments. The visuomotor paradigm requiring cognitive rule integration used in the current study may be sensitive to the presence of the APOE e4 allele, the greatest genetic risk factor for AD (Farrer et al. 1997; Bekris et al. 2010; Karch and Goate 2015). Such a behavioural testing approach could have potential for detecting sensory and motor changes that are specific to AD in the preclinical stage. While the generalizability of these findings is limited by the relatively small sample size and the study being cross-sectional in nature, they provide important insights into the relationship between visuomotor dysfunctions and preclinical AD. Future work should investigate if individuals demonstrating visuomotor impairments on a non-standard task prior to cognitive decline are more likely to then develop mild cognitive impairment or dementia later in life.

ACKNOWLEDGEMENTS

The authors wish to thank Heather Edgell, PhD, and Michael Riddell, PhD, for providing storage for saliva samples, as well as Joy Williams, MRT(MR), for her MR image acquisition

expertise. This work was supported by a Canadian Institutes of Health Research operating grant (grant number MOP-125915 to L.E.S.).

Chapter Four

Sex differences in the neural underpinnings of unimanual and bimanual control in adults

Alica Rogojin, Diana J. Gorbet, and Lauren E. Sergio

ABSTRACT

Introduction: While many of the movements we make throughout our day involve just one upper limb, most daily movements require a certain degree of coordination between both upper limbs. Historically, sex differences in eye-hand coordination have been observed. As well, there are demonstrated sex-specific differences in hemisphere symmetry, interhemispheric connectivity, and motor cortex organization. While it has been suggested that these anatomical differences may underlie sex-related differences in performance, sex differences in the functional neural correlates underlying bimanual performance have not been explicitly investigated. In the current study we tested the hypothesis that the functional connectivity underlying bimanual movement control differed depending on the sex of an individual. **Methods:** Participants underwent MRI scanning to acquire anatomical and functional brain images. During the functional runs, participants performed unimanual and bimanual coordination tasks using two button boxes. The tasks included pressing the buttons in time to an auditory cue with either their left or their right hand individually (unimanual), or with both hands simultaneously (bimanual). The bimanual task was further divided into either an in-phase (mirror/symmetrical) or anti-phase (parallel/asymmetrical) condition. Participants were trained until behavioural task performance was equivalent between men and women. A generalized psychophysiological interaction (gPPI) analysis was implemented to examine how functional connectivity in each condition was modulated by sex. **Results:** In support of our hypothesis, women and men demonstrated differences in the neural correlates underlying unimanual and bimanual movements. In line with previous literature, functional connectivity patterns showed sex-related differences for right- vs left-hand movements. Sex-specific functional connectivity during bimanual movements was not a sum of the functional connectivity underlying right- and left-hand unimanual movements. Further, women generally showed greater interhemispheric functional connectivity across all conditions compared to men and had greater connectivity between task-related cortical areas, while men had greater connectivity involving the cerebellum. **Conclusions:** With equivalent performance, sex differences in brain connectivity were associated with both unimanual and bimanual movement control. Not only do these findings provide novel insight into the fundamentals of how the brain controls bimanual movements in both women and men, they also present potential clinical implications on how bimanual movement training used in rehabilitation can best be tailored to the needs of individuals.

1. INTRODUCTION

Bimanual coordination is essential for performing many everyday movements that require successful spatiotemporal interactions between both arms, such as typing or picking up a box (Kilbreath and Heard 2005; Howard et al. 2009). Indeed, healthy adults use both hands together in everyday functional activities more than either hand alone (Kilbreath and Heard 2005; Stone et al. 2013). Thus, gaining a better understanding of how the brain controls these movements is both important fundamentally, and could provide a basis for clinical applications. For instance, bimanual movement training is being increasingly used as a potential post-stroke rehabilitation technique (Rose and Winstein 2004; Stewart et al. 2006; Kang and Cauraugh 2014; Wolf et al. 2014), although the results have been inconsistent (Cauraugh et al. 2010). Fundamental studies investigating sex differences in bimanual performance report contradictory findings with some showing better performance in men (Mickevičienė et al. 2011; Shetty et al. 2014) and others a better performance in women (Albines et al. 2016; Khanjari and Arabameri 2021). These inconsistencies may be a result of the type of bimanual task used, as there appears to be a female advantage in some bimanual tasks and a male advantage in others (Rudisch et al. 2020). However, the neural underpinnings of these observed bimanual sex differences have never been examined. Thus, understanding how the neural correlates underlying bimanual movements differ between the sexes is not only important for expanding on motor control research, but may inform clinical practices as sex may be a potential factor in determining bimanual training success.

Bimanual coordination is associated with activation within a widespread network of brain regions similar to that involved in unimanual movements, including the primary sensorimotor cortex (S1/M1), dorsal premotor cortex (PMd), supplementary motor area (SMA), cingulate motor area (CMA), posterior parietal cortex (PPC), and the cerebellum (Jancke et al. 2000; Tracy et al. 2001; Swinnen 2002; Debaere et al. 2004b; Lin et al. 2017). There is a further

increased activation in the PMd, SMA, CMA, PPC, and cerebellum during more complex anti-phase (asymmetrical/parallel) compared to in-phase (symmetrical/mirror) bimanual tasks (Sadato et al. 1997; Debaere et al. 2001; Immisch et al. 2001; Nair et al. 2003; Ullén et al. 2003; Debaere et al. 2004b; Kraft et al. 2007; Wu et al. 2010; Kiyama et al. 2014; Lin et al. 2017). The importance of intact interhemispheric connectivity for successful bimanual coordination comes from imaging studies investigating the integrity of the corpus callosum.

The corpus callosum is a major white matter tract that connects the two hemispheres and facilitates interhemispheric communication (Bloom and Hynd 2005), crucial for motor control involving bimanual coordination (Gooijers et al. 2014; Rudisch et al. 2018) and damage to transcallosal pathways impairs bimanual performance (Serrien et al. 2001; Larson et al. 2002; Caeyenberghs et al. 2011). Increased bimanual performance of a finger tapping task was associated with increased white matter integrity (measured as greater fractional anisotropy) in the corpus callosum, likely reflecting increased myelination of the corpus callosum and consequently more efficient neuronal signal transmission (Muetzel et al. 2008). Callosal regions where white matter integrity was correlated with bimanual performance gave rise to pathways connecting the SMA and CMA between the two hemispheres (Johansen-Berg et al. 2007), both medial wall regions that are important for complex bimanual coordination. Together, these findings suggest that greater interhemispheric connectivity between brain regions involved in bimanual coordination is especially important for successful bimanual control.

There is direct evidence of a greater amount of interhemispheric connectivity in women, especially in the splenium (posterior portion of the corpus callosum) (Allen et al. 1991; Dubb et al. 2003), while men show greater intrahemispheric connectivity (Ingalhalikar et al. 2014). The corpus callosum specifically has been shown to have structural differences related to sex, where women have a significantly larger corpus callosum compared to men after adjusting for

brain size (Shiino et al. 2017). Functional neuroimaging and electrophysiological studies have demonstrated that even when men and women show equal performance of complex unimanual visuomotor tasks, the underlying brain activity associated with completing the tasks differs between the sexes with a more bilateral pattern of visuomotor brain activity in women relative to men (Grön et al. 2000; Gorbet and Sergio 2007; Gorbet et al. 2010; Gorbet and Staines 2011). Collectively, these findings predict sex-related differences in interhemispheric connectivity associated with bimanual movement coordination. In the current study, we directly tested the hypothesis that the neural correlates underlying the control of unimanual and bimanual movements differ in women and men. As mentioned above, sex differences in the neural underpinning of unimanual control have been reported in a variety of paradigms. Here, we were interested in comparing the sex differences in functional connectivity of unimanual and bimanual movements on comparable tasks. We predicted that regions known to be important for unimanual and bimanual control would be significantly more bilaterally connected in women compared to men.

2. METHODS

2.1. Participants

Thirty right-handed participants were included in the experiment. Participants of the study were 15 women (mean age 25.3 ± SD 6.2 years) and 15 men (mean age 24.9 ± SD 4.7 years). Handedness was verified using the Edinburgh inventory (Oldfield 1971). Participants were asked to self-report sex on a binary scale (female/male). In the current study, female/male and woman/man labels both refer to self-reported sex, as gender was not explored in the analysis. None of the participants had any known neurological issues. All subjects had normal or corrected-to-normal vision. The study protocol was approved by the Human Participants

Review Sub-Committee of York University's Ethics Review Board, and all participants provided informed written consent before data collection.

2.2. Apparatus and MRI acquisition

MRI data were acquired using a 3 Tesla (3T) Siemens Magnetom Prisma Fit scanner at York University. Participants lay in a supine position in the scanner with a vertical screen behind them in the magnet bore. A mirror was attached to the MRI head coil in front of the participant's eyes to allow participants to view a fixation target being presented on the screen behind them. Participants wore MRI compatible headphones (MR Confon audio system) to hear auditory cues, and eye movements were monitored using an MRI-compatible eye tracking system (Avotec Eye Tracking System RE-5721) solely to verify gaze fixation. Two button boxes with 4 buttons in a curved line (Current Designs fORP SKU#HHSC-2x4-C) were placed under the right and left hand in a position that allowed participants to press appropriate buttons using their fingers with minimal wrist and lower arm movements.

T1-weighted anatomical images were collected using a sagittal volumetric magnetization-prepared rapid gradient echo (MP-RAGE) sequence. The MP-RAGE consisted of 192 sagittal slices (slice thickness of 1 mm, with no gap), TR = 2300 ms, TE = 2.26 ms, flip angle = 8^{o}, FoV = 256 mm, and voxel dimension of 1 x 1 x 1 mm. Functional images covered the entire brain and cerebellum, and were acquired using an echo planar imaging (EPI) sequence with TR = 1200 ms, TE = 30 ms, flip angle = 66^{o}, and FoV = 240 mm. Fifty-four, 3.0-mm thick slices with a voxel dimension of 2.5 x 2.5 x 3.0 mm were collected with an interleaved acquisition sequence and zero gap between slices.

2.3. Experimental paradigm

All participants were trained on the experimental tasks prior to scanning. After a demonstration of how to perform the tasks by the experimenter (DG), participants performed two blocks of each of the four task conditions (two unimanual and two bimanual) to ensure task comprehension. In addition, participants were provided with an illustrated description of the tasks several days prior to scanning. During MRI data collection, each participant performed five experimental runs. Each run consisted of a randomized order of four conditions, each presented twice, for a total of eight blocks. Each run began with 30 s of baseline data collection where participants fixated on a central dot. Each block was preceded by a 6 s instruction screen which informed participants which of the four conditions they would be performing in the following block. Instruction screens were followed by another 15.6 s central fixation trial to allow brain activity to return to baseline levels. There was then a 30 s experimental block where participants performed one of the four conditions, followed by a 15.6 s inter-block central fixation. The next instruction screen was presented for the next block condition.

The four conditions were two unimanual and two bimanual coordination tasks using two button boxes. The conditions involved pressing the buttons in time to an auditory cue presented at 1 s intervals with just their left hand (unimanual), pressing the buttons with just their right hand (unimanual), or using both hands to press buttons simultaneously (bimanual) for a total of 7 repetitions of the full movement pattern for each condition (**Fig. 1**). The auditory cue ensured that all participants pressed the buttons at the same rate. The bimanual coordination task was further divided into two conditions, in-phase (mirror/symmetrical) or anti-phase (parallel/asymmetrical). The symmetrical bimanual condition involved the same fingers moving on both hands simultaneously (i.e., index, middle, ring, pinky). The asymmetrical bimanual condition involved both hands moving fingers from the left side of the hand to the right simultaneously (i.e., left pink + right index, left ring + right middle, left middle + right

ring, left index +right pinky). For all four conditions, hand positions were kept constant with both hands resting over both button boxes regardless of condition. As both the unimanual and bimanual task conditions were easy following training and had an auditory cue to guide the rate of button presses, behavioural task performance was expected to be equivalent between men and women. During scanning, participants were monitored to ensure they were correctly completing the tasks by monitoring both eye position as well as accuracy of button presses. Men and women did not differ in their ability to successfully perform each condition.

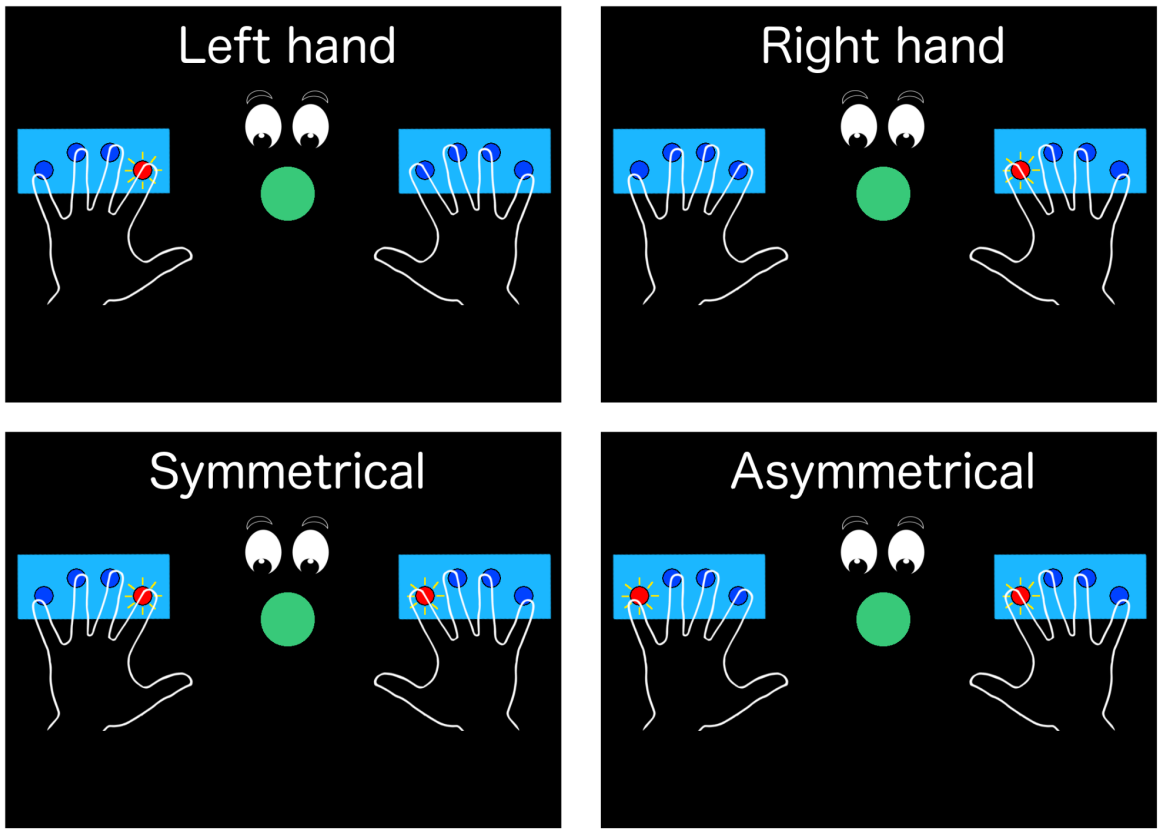

Figure 1. Schematic representation of the four task conditions. Participants pressed buttons on two button boxes in time to an auditory stimulus. The two unimanual tasks involved using either the left hand, or right hand. The two bimanual tasks involved using both hands simultaneously in a symmetrical pattern (same fingers moving on both hands), or asymmetrical pattern (both hands moving fingers from the left side of the hand to the right simultaneously).

2.4. Preprocessing of MRI data

MRI data were analysed with the CONN toolbox (version 21a; https://www.nitrc.org/projects/conn) in Matlab R2019a (Mathworks Inc., Natick, MA) using the default preprocessing pipeline and denoising procedure (Whitfield-Gabrieli and Nieto-Castanon 2012). The pipeline included realignment of the functional data using the SPM12 *realign & unwrap procedure* (Andersson et al. 2001) to coregister and resample all scans to a reference image (first scan of the first session). Temporal distortions between slices in the functional data were corrected using the SPM12 *slice-timing correction procedure* (Henson et al. 1999). Scans with a framewise displacement >0.9mm or global BOLD signal changes of >5 SD were identified and flagged as outliers. Functional and anatomical data were then normalized into MNI space and segmented into grey matter, white matter, and cerebrospinal fluid tissue classes based on the SPM12 unified segmentation and normalization procedure (Ashburner and Friston 2005). Smoothing of fMRI data was performed by applying a spatial convolution with a Gaussian kernel of 8mm full-width half-maximum (FWHM).

Functional data were then denoised using Ordinary Least Squares (OLS) regression to remove the following confounding effects for each voxel's time-series: (a) White matter and cerebrospinal fluid areas that were computed by applying a one-voxel binary erosion to the masks of voxels with values above 50% in white matter and cerebrospinal fluid posterior probability maps. Within each of these two regions, 5 potential noise components were estimated. These included the average BOLD signal and the first four components in a Principal Component Analysis of the covariance within the subspace orthogonal to the average BOLD signal; (b) 12 head motion parameter estimates (3 translation, 3 rotation, and their associated first-order derivatives); (c) all identified outlier scans from the preprocessing pipeline (i.e., scans with a framewise displacement >0.9 mm or global BOLD signal changes >5 SD); and

(d) linear BOLD signal trends within each session. Last, following nuisance regression, functional data were temporally filtered by applying a bandpass of 0.008 - 0.09 Hz.

2.5. Generalized psychophysiological interaction (gPPI) analysis to measure functional connectivity

Several brain regions of interest (ROIs) were chosen for this study based on their importance in bimanual coordination, or that have demonstrated sex-related differences associated with motor control. Neuroimaging studies have identified a distributed sensorimotor network involved in bimanual coordination consisting of the dorsal premotor cortex (PMd), primary sensorimotor cortex (S1/M1), supplementary motor area (SMA), cingulate motor area (CMA), superior parietal lobule (SPL), inferior parietal lobule (IPL), and cerebellum (Sadato et al. 1997; Jancke et al. 2000; Immisch et al. 2001; Tracy et al. 2001; Swinnen 2002; Nair et al. 2003; Ullén et al. 2003; Debaere et al. 2004b; Kraft et al. 2007; Wu et al. 2010; Lin et al. 2017). Within the cerebellum, cerebellar lobules IV, V, VI, and VIII, and vermis regions V, VI, and VIII were specifically identified as being involved in bimanual coordination (Debaere et al. 2004b; Debaere et al. 2004a; Boisgontier et al. 2018). Sex-differences have been reported in premotor regions, S1, SPL, and regions of the lateral sulcus (superior temporal gyrus (STG) and parietal operculum (PO)) during eye-hand coordination tasks (Gorbet and Sergio 2007). The CONN toolbox uses the FSL Harvard-Oxford atlas (distributed with FSL http://www.fmrib.ox.ac.uk/fsl/) and AAL atlas (Tzourio-Mazoyer et al. 2002) for cortical and cerebellar parcellation, respectively. Therefore, the following cortical regions from the FSL Harvard-Oxford atlas were used as seed regions for analysis: right/left precentral gyrus, right/left postcentral gyrus, right/left superior parietal lobule, right/left supramarginal gyrus, right/left angular gyrus, right/left supplementary motor cortex, right/left parietal operculum cortex, and right/left superior temporal gyrus. The following cerebellar regions from the AAL

atlas were chosen as seed regions: right/left lobule IV/V, right/left lobule VI, right/left lobule VIII, vermis IV/V, vermis VI, and vermis VIII.

First-level seed-to-voxel generalized psychophysiological interaction (gPPI) analysis was then implemented in CONN to examine how sex modulates functional connectivity during bimanual coordination. A gPPI analysis computes how functional association strength between a seed region and all other voxels in the brain covaries with an external or experimental factor (in this case, task condition). In CONN, gPPI analysis involves computation of separate multiple regression models for each target voxel BOLD time series, and included a) all of the selected task effects convolved with a canonical hemodynamic response function (psychological term), b) seed ROI BOLD time-series (physiological term), and c) the interaction term specified as the product of (a) and (b) (PPI term). Second-level analyses were then performed to control for multiple comparisons at the level of individual clusters using parametric statistics based on Gaussian Random Field Theory (Worsley et al. 1996). Sex was used as a covariate in the second-level analysis, with a contrast of female > male set for each of the seed regions for all four task conditions (left unimanual, right unimanual, in-phase/symmetrical, anti-phase/asymmetrical). Active clusters were reported only when surviving a voxel-level a priori $p < 0.001$ uncorrected height threshold and a false discovery rate (FDR)-corrected cluster-level $p < 0.05$ threshold. The uncorrected height threshold p-value is defined as the likelihood of a randomly selected cluster being its size or higher and the FDR-corrected p-value is defined as the expected proportion of false discoveries among all clusters of this size or larger over the entire analysis volume, both under the null hypothesis.

3. RESULTS

Functional connectivity between our seed ROIs and the whole brain differed between men and women during our four task conditions (see **Table 1**). During the right-hand

unimanual condition (**Fig. 2a**), women demonstrated increased connectivity relative to men between the right SPL (seed) and voxels covering the right central opercular cortex/PMd, as well as between the left SPL (seed) and bilateral anterior CMA. Men showed greater functional connectivity between the anterior CMA (seed) and voxels covering the right lateral occipital cortex/IPL (angular gyrus), and between the right cerebellar lobule VIII (seed) and right lateral occipital cortex/precuneus. During the left-hand unimanual condition (**Fig. 2b**), women had increased functional connectivity between the right SMA (seed) and voxels covering bilateral IPL (supramarginal gyrus) and primary sensorimotor cortex (S1/M1). Vermis VI (seed) also had greater connectivity to the left lateral occipital cortex and left lingual gyrus/cerebellar lobule IV/V. In men, greater functional connectivity was demonstrated between right STG to the right lateral occipital cortex/precuneus, left cerebellar lobule IV/V (seed) to the left frontal cortex and left IPL (angular gyrus/supramarginal gyrus), between right cerebellar lobule VI (seed) to left PMd, and between vermis VIII (seed) to left middle temporal gyrus. In the in-phase (symmetrical/mirror) condition (**Fig. 2c**), women showed greater functional connectivity between the right IPL (supramarginal gyrus; seed) and the left CMA. Women also had higher connectivity between vermis IV/V (seed) and other subcortical structures in the left hemisphere (including the left cerebellar Crus I and II, thalamus, and hippocampus). Men had greater functional connectivity between right PMd (seed) and right PMd/SMA, as well as right SMA (seed) and left lingual gyrus/occipital fusiform gyrus. In the anti-phase (asymmetrical/parallel) condition (**Fig. 2d**), women had greater functional connectivity between the right SMA (seed) and left insular cortex.

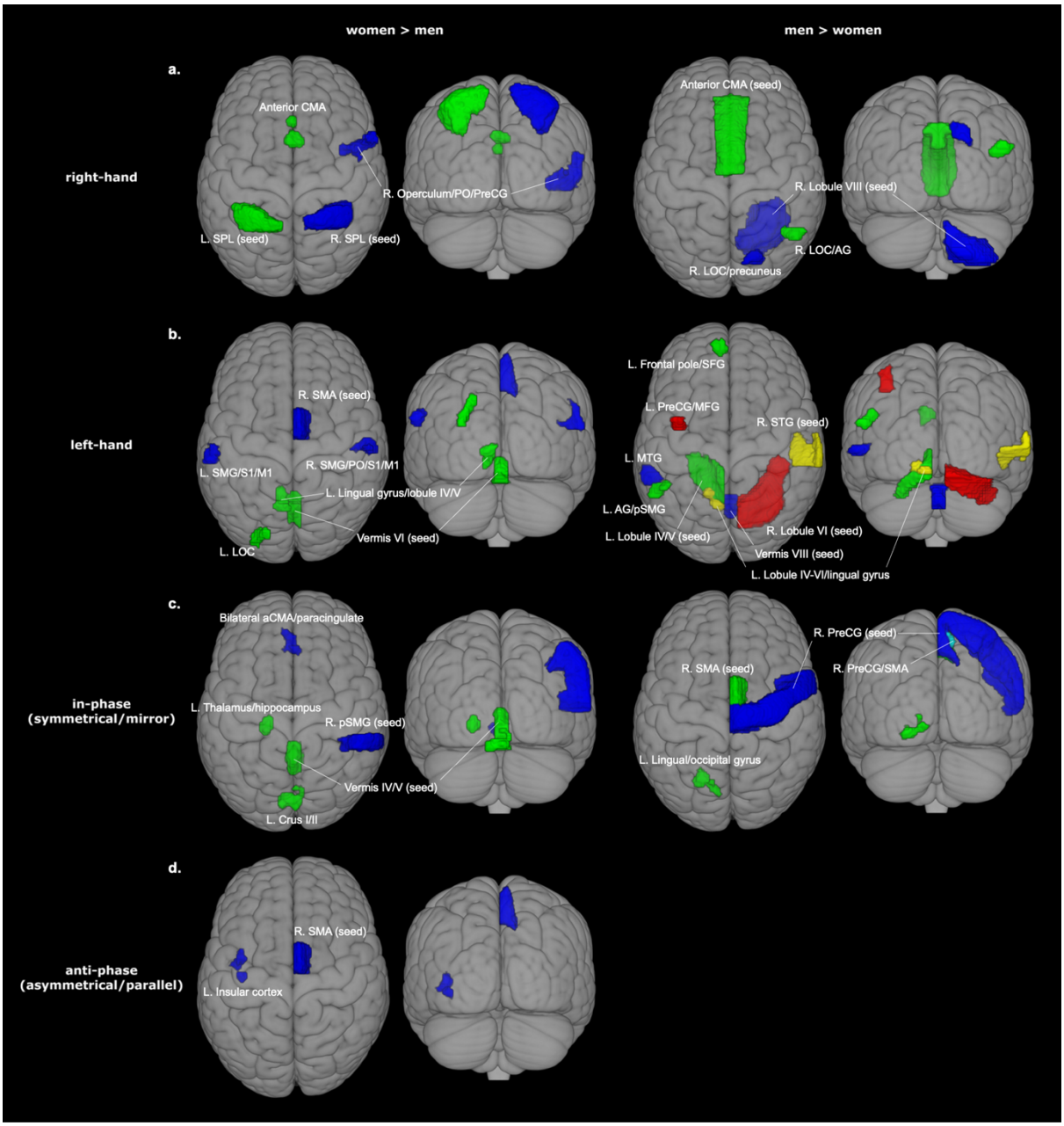

Figure 2. Regions of interest (seeds) and the corresponding significant clusters showing increased functional connectivity with that seed for the contrast female vs male. Colours of the seed regions match their respective target regions. Women > male indicate regions that showed increased functional connectivity in women and men > women indicate regions that showed increased functional connectivity in men in the **a)** right-hand unimanual, **b)** left-hand unimanual, **c)** in-phase (symmetrical/mirror) bimanual, and **d)** anti-phase (asymmetrical/parallel) bimanual conditions. CMA, cingulate motor area; SPL, superior parietal lobule; PO, parietal operculum; PreCG, precentral gyrus; LOC, lateral occipital cortex; AG, angular gyrus; SMG, supramarginal gyrus; SMA, supplementary motor area; S1/M1, primary sensorimotor cortex; SFG, superior frontal gyrus; MFG, middle frontal gyrus; MTG, middle temporal gyrus; STG, superior temporal gyrus.

Table 1. Results of the seed-based generalized psychophysiological interaction (gPPI) analysis for the contrast female vs male. Percentages in the Target column indicate what percentage of that significant cluster corresponds to regions in the Harvard-Oxford atlas.

Condition	Seed (hemi)	Target (hemi)	**Cluster size** (no. of voxels)	**MNI coordinates** (x, y, z)	p-FDR*	**Higher connectivity**
Right	Superior parietal lobule (right)	26% Central opercular cortex (right); 20% Inferior frontal gyrus, pars opercularis (right); 20% Precentral gyrus (right)	429	48, 6, 4	0.000026	Women
	Superior parietal lobule (left)	99% Cingulate gyrus, anterior division (mid)	165	-2, 10, 36	0.011294	Women
	Cingulate gyrus, anterior division (mid)	50% Lateral occipital cortex, superior division (right); 39% Angular gyrus (right)	155	42, -58, 24	0.017527	Men
	Cerebellar lobule VIII (right)	66% Lateral occipital cortex, superior division (right); 10% Precuneus (mid); 6% Cuneus (right)	163	18, -78, 40	0.024667	Men
Left	Superior temporal gyrus, posterior division (right)	55% Cerebellar lobule 6 (left); 28% Lingual gyrus (left); 15% Cerebellar lobule 4/5 (left)	101	-10, -64, -14	0.04938	Men
	Supplementary motor area (right)	31% Supramarginal gyrus, anterior division (right); 24% Parietal operculum (right); 18% Postcentral gyrus (right)	193	56, -16, 22	0.009355	Women
		70% Supramarginal gyrus, anterior division (left); 27% Postcentral gyrus (left)	149	-62, -26, 24	0.017063	Women
	Cerebellar lobule IV/V (left)	50% Frontal pole (left); 34% Superior frontal gyrus (left)	137	-6, 56, 28	0.017648	Men
		65% Angular gyrus (left); 20% Supramarginal gyrus, posterior division (left)	130	-56, -54, 22	0.017648	Men
	Cerebellar lobule VI (right)	57% Precentral gyrus (left); 38% Middle frontal gyrus (left)	136	-38, -4, 54	0.024313	Men
	Cerebellar vermis VI (mid)	64% Lateral occipital cortex, superior division (left); 34% Occipital pole (left)	173	-26, -90, 30	0.007001	Women
		71% Lingual gyrus (left); 25% Cerebellar lobule 4/5 (left)	150	-8, -54, -8	0.0071	Women
	Cerebellar vermis VIII (mid)	51% Middle temporal gyrus, posterior division (left); 35% Middle temporal gyrus, temporooccipital part (left)	137	-58, -44, 2	0.008737	Men
In-phase	Precentral gyrus (right)	60% Precentral gyrus (right); 9% Supplementary motor cortex (right)	134	10, -18, 56	0.033101	Men
	Supramarginal gyrus, posterior division (right)	34% Paracingulate gyrus (left); 30% Subcallosal cortex; 23% Cingulate gyrus, anterior division (mid); 3% Paracingulate gyrus (right)	145	-6, 42, -8	0.029083	Women
	Supplementary motor area (right)	55% Lingual gyrus (left); 43% Occipital fusiform gyrus (left)	155	-20, -79, -10	0.04926	Men

	Cerebellar vermis IV/V (mid)	18% Cerebellar Crus 2 (left); 16% Cerebellar Crus 1 (left)	180	-2, -84, -18	0.017758	Women
		37% Thalamus (left); 20% Hippocampus (left)	126	-20, -28, -4	0.044482	Women
Anti-phase	Supplementary motor area (right)	77% Insular cortex (left); 12% Planum polare (left)	131	-38, -18, -86	0.031629	Women

*False discovery rate (FDR)-corrected cluster-level $p < 0.05$ threshold.

4. DISCUSSION

The main goal of the current study was to assess whether there were sex differences in the functional connectivity underlying bimanual control even in the absence of behavioural performance differences. The key findings of this paper were as follows: (1) functional connectivity sex differences exist during unimanual movements, and are distinct for right- vs left-hand movements; (2) sex-related functional connectivity during bimanual movement did not reflect the sum of sex differences in functional connectivity underlying right- and left-hand unimanual movements; (3) women generally showed greater interhemispheric functional connectivity across all conditions compared to men; and (4) functional connectivity differences where women had greater connectivity than men tended to involve cortical areas, while functional connectivity differences where men had greater connectivity than women were more likely to involve the cerebellum.

4.1. Functional connectivity is distinct for right- vs left-hand unimanual conditions in women and men

It has been well established that unimanual movements rely on a bilateral motor network (Chettouf et al. 2020) where right-handed movements typically involve greater activity within the contralateral motor areas whereas a greater engagement of the ipsilateral hemisphere has been shown during left-hand movements (Kawashima et al. 1993; Kim et al. 1993; Li et al. 1996; Stephan et al. 1999). The sex differences observed in the current study in the right-hand condition suggest that it is connectivity within the ipsilateral hemisphere that largely differs between men and women. Different regions of the lateral and medial PPC, including the SPL, IPL (composed of the angular and supramarginal gyri), and precuneus, are important for both men and women in performing the right-hand condition. The PPC plays an important role in

multiple cognitive and motor processes including planned movements, sensorimotor integration, and spatial attention (Whitlock 2017).

Women had greater functional connectivity between bilateral SPL and motor regions including the anterior CMA and right PMd. Similar to this increased connectivity between right parietal and right premotor regions we reported in women, a study looking at visually guided arm movements demonstrated that activity in parietal and premotor regions tended to be more bilateral in women with greater activation of the right (ipsilateral) hemisphere during right-handed movements (Gorbet and Sergio 2007). They also found that the right PMd was more active in women than in men. The SPL in particular was previously shown to be more activated for simple finger sequencing in girls compared to boys (Richards et al. 2009) and more bilaterally activated in women compared to men during various motor tasks (Jordan et al. 2002; Gorbet and Sergio 2007). When tapping with the dominant hand, women showed higher activation in contralateral parietal cortex, ipsilateral premotor cortex, and ipsilateral anterior CMA (Lissek et al. 2007). Findings from these studies align with the greater connectivity between bilateral SPL and motor regions we reported in women when performing a right-handed finger pressing task. Findings from the right-hand condition revealed that men had greater functional connectivity between anterior CMA and the right angular gyrus extending into the right lateral occipital cortex, as well as between the right cerebellar lobule VIII and the precuneus extending into the right lateral occipital cortex. Relative to a rest control, right-hand finger tapping produced activation in lobule VIII, with greater activation occurring ipsilaterally (Desmond et al. 1997). In another study that looked only at male participants, activation during right-hand movements was observed in the ipsilateral cerebellar hemisphere of lobule VIII (Habas et al. 2004). These findings coincide well with our results showing greater connectivity between this area and medial PPC in men performing the right-hand condition.

Production of right-hand unimanual movement involved sex differences in connectivity between brain regions that was distinct from, and not a mirror of, the functional connectivity differences observed for left-hand unimanual movement. Previous findings suggest that activity in the left hemisphere is essential for controlling more complex movements, such as left-hand use in right-handed individuals (Serrien and Spapé 2009). There was greater involvement of the left hemisphere in both men and women in the left-hand condition, and taken together with findings from the right-hand condition suggests that sex differences are more prominent in functional connectivity with the ipsilateral hemisphere to the movement. Women generally showed significantly greater connectivity between ipsi- and contralateral task-related cortical areas than men, while men mainly had greater connectivity involving the cerebellum and this connectivity was mainly ipsilateral. The right SMA was bilaterally connected to the parietal and sensorimotor regions to a greater degree in women, and has been shown to be a brain area with increased activation during motor and sensory tasks using the left hand (Chung et al. 2005). Men had greater connectivity between the contralateral STG and precuneus/lateral occipital cortex, and regions of the cerebellum with the ipsilateral frontal cortex, IPL (angular and supramarginal gyri), and MTG. The connectivity between these regions is very similar to patterns of activation previously reported in men during tapping sequences with the non-dominant hand, where there was higher activation in ipsilateral IPL, STG, MTG, and regions of the frontal gyrus (Lissek et al. 2007).

Both men and women showed greater involvement of the cerebellum in left-handed movements, with more cerebellar regions showing distinct functional connectivity in men compared to women suggesting that the cerebellum is especially important for left-handed movements in men. The cerebellar motor regions span the hemispheres of lobules IV-VIII (Habas et al. 2009; Krienen and Buckner 2009; Stoodley and Schmahmann 2009; Stoodley and Schmahmann 2010), corresponding to hand representation in these lobules (Grodd et al. 2001;

Wiestler et al. 2011). Activation in these regions has been reported during different finger movement tasks including tapping and flexion/extension (Rijntjes et al. 1999; Ramnani et al. 2001; Blouin et al. 2004). Sex differences have also been reported in the cerebellum, where cerebellar lobule and vermis VIII have a larger relative volume in men compared to women (Steele and Chakravarty 2018) and may explain the greater involvement of this motor cerebellar lobule in the two unimanual tasks in men.

4.2. Sex differences in the functional connectivity underlying bimanual control

The two bimanual conditions were not a combination of results from the two unimanual conditions, suggesting that different neural activity underlies unimanual and bimanual tasks in men and women. This coincides with other studies suggesting that while there is overlap in areas activated during bimanual and unimanual tasks, bimanual movements show distinct patterns of activation and are not simply a summation of independent movements (Jancke et al. 2000; Cardoso de Oliveira et al. 2001; Swinnen 2002; Walsh et al. 2008; Lin et al. 2017). In the current study, the regions showing differences in functional connectivity tended to be in the opposite hemisphere to the seed region rather than within the same hemisphere as the seed. This in part supported our hypothesis as women showed greater interhemispheric functional connectivity in both bimanual conditions, although we report that men did also have greater interhemispheric connectivity during the in-phase task. Sex differences in functional connectivity existed between distinct regions depending on the bimanual mode used.

In the in-phase task, women had increased functional connectivity between the right supramarginal gyrus and left anterior CMA. Women also showed greater connectivity between vermis IV/V and left cerebellar Crus I/II, thalamus, and hippocampus in the in-phase condition. To perform bimanual movement, online monitoring of finger positions is necessary (Sadato et al. 1997) and suggests that activation of brain regions involved in spatial attention and spatial

working memory may therefore be important for successful bimanual control. The cerebellum has been shown to be important in the visual guidance of movement, as well as for feedback loops and online correction and control of movement (Bastian 2006; Manto et al. 2012; Patel and Zee 2015). Women have larger cerebellar Crus II volumes compared to men (Steele and Chakravarty 2018), which along with Crus I is a cerebellar region implicated in spatial processing (Stoodley and Schmahmann 2009). There is increased activation of cerebellar lobules IV/VI during successful bimanual control (Debaere et al. 2004b; Boisgontier et al. 2018), with lobules V/VIII and vermis V/VI/VIII increasingly activated in more complex bimanual tasks (Tracy et al. 2001; Blouin et al. 2004; Debaere et al. 2004a). This may explain the increased connectivity between vermis IV/V and Crus II that we saw in women.

The SMA participates in the execution of sequential unimanual and bimanual movements (Shibasaki et al. 1993; Gerloff et al. 1997; Sadato et al. 1997), demonstrating further increased activity during more complex bimanual movements such as in anti-phase compared to in-phase tasks (Sadato et al. 1997; Debaere et al. 2001; Immisch et al. 2001; Ullén et al. 2003; Debaere et al. 2004b; Wu et al. 2010). Men had greater functional connectivity between the right SMA and left lingual gyrus/occipital fusiform gyrus in the in-phase condition, as well as greater within-seed region functional connectivity in the right PMd with the significant target cluster further overlapping with the right SMA. Interestingly, the right SMA had greater interhemispheric connectivity with the left insular cortex in the anti-phase task in women. Our data are therefore concurrent with previous findings suggesting that the right SMA is particularly important for bimanual movements in both men and women, and further demonstrates that it has different interhemispheric connectivity patterns with the rest of the brain depending on the type of bimanual task used.

Thus, women showed overall greater bilateral connectivity not only in the left-hand condition, but in the two bimanual conditions as well. Although there is still some debate as to

whether sex contributes to cerebral lateralization, sex has been found to be associated with functional asymmetry with stronger laterality in men than in women (Liu et al. 2009). In cerebral regions, males have shown greater within-hemispheric connectivity, while females had predominantly between-hemispheric connectivity (Ingalhalikar et al. 2014). This relationship was reversed in the cerebellum, with greater interhemispheric cerebellar connectivity in men. These findings were supported by graph theory measures demonstrating that male brains generally had higher clustering coefficients and higher local efficiency in nodes within the cerebral cortex, while these measures were higher for female participants only in the cerebellum (Zhang et al. 2016). The findings from these studies support the notion that within females, connections are more widespread between the two hemispheres and the network is less modular thus facilitating functional integration, whereas men prevail in functional segregation.

In conclusion, the observed sex differences in functional connectivity included differences with respect to intra- vs interhemispheric connectivity, differences in supra- vs infratentorial connectivity, and differences in lateralization of areas in one sex compared to the other. These between-sex differences in cerebral and cerebellar activation patterns during unimanual and bimanual movements existed even when performance is equivalent, suggesting that patterns of brain activity differ in women and men even when performing equivalent movements. Gaining knowledge of how neural activity may differ between men and women during bimanual movement is important not only for our fundamental understanding of how the brain works, but also from a clinical perspective. Stroke is the leading cause of long-term motor impairments, with approximately 80% of unilateral stroke patients initially experiencing hemiparesis (a weakness of one side of the body) in their contralesional upper extremities (Virani et al. 2021). Bimanual movement training has been tested for many years as a promising rehabilitation technique for hemiparesis (Rose and Winstein 2004; Wolf et al. 2014). The goal

of this approach is to encourage corresponding intact brain regions in the undamaged brain hemisphere to stimulate damaged areas via interhemispheric connections. However, many studies have produced inconsistent results (Cauraugh et al. 2010) and, to our knowledge, no studies have examined sex as a potential factor in bimanual training success. Understanding how the sex of an individual contributes to the neural control of different bimanual movements could inform clinical practice regarding how approaches can best be tailored to the needs of individuals, by individualizing the types of tasks used in bimanual movement training.

4.3. Limitations and future directions

The results presented in this study should be considered preliminary, as the data set used was relatively small due to the financial costs associated with MRI not allowing for additional subjects to be recruited. Despite these constraints on the number of participants that could be included, we have tried to eliminate as many differences between the two experimental groups as possible. Mean ages of men and women did not differ significantly, subjects' eye movements were tracked, and behavioural performance between groups did not differ. While it is difficult to eliminate all non-sex-related differences between groups, we argue that the findings presented here are largely attributable to sex-specific group differences. As mentioned in the introductory section of this study, sex-related discrepancies in bimanual coordination performance that have been reported in the literature may be due to differences in the bimanual tasks used (Rudisch et al. 2020). While we acknowledge that we have used two very simple paradigms to investigate the neural underpinnings of bimanual control, we argue that this is an advantage as it allows for clear interpretation of the results and we believe that the findings in this study represent an important starting point. Although gender and its impact on functional connectivity underlying motor control was beyond the scope of the current study, we hope to investigate this relationship in the future. We have also collected diffusion-weighted scans for

all subjects in the study that could potentially be used to expand on previous reports of greater interhemispheric structural connectivity in women (Allen et al. 1991; Dubb et al. 2003) by exploring potential sex-related differences in structural connectivity underlying bimanual movement control.

ACKNOWLEDGEMENTS

The authors wish to thank Joy Williams, MRT(MR), for her MR image acquisition expertise. This work was supported by a Natural Sciences and Engineering Research Council of Canada (NSERC) Discovery grant (grant number RG-2016-05336 to L.E.S.).

Chapter Five

General Discussion

5.1. Summary and conclusions

The basic skills of unimanual and bimanual eye-hand coordination are carried out by widespread but interconnected areas of the brain (Debaere et al. 2001). While many everyday unimanual movements involve a direct ("standard") interaction with the object that is being viewed (Gielen et al. 1984; Wise et al. 1996; Helsen et al. 1998), humans have also evolved an ability to indirectly interact with objects via tools ("non-standard") (Johnson et al. 1996; Wise et al. 1996). When using tools, the direction of the gaze and the object being manipulated can be in different spatial planes (such as using a trackpad on a laptop) or involve a feedback reversal (such as scrolling up on a computer in order to move the page down). These types of reaches are not innate and must be learned and calibrated over time (Neggers et al. 2000; Bo et al. 2006; Sergio et al. 2009). While deterioration of non-standard performance has been reported in individuals at an increased risk for dementia (Hawkins and Sergio 2014; Rogojin et al. 2019), how the underlying neural correlates are altered by dementia risk in both men and women has not yet been fully characterized. In addition to unimanual movements, most daily movements actually involve bimanual control requiring coordination between both upper limbs (Kilbreath and Heard 2005; Vega-González and Granat 2005). Although neuroimaging studies have investigated the neural activity underlying unimanual and bimanual movements (Grön et al. 2000; Jancke et al. 2000; Sadato et al. 2000; Tracy et al. 2001; Jordan et al. 2002; Swinnen 2002; Weiss et al. 2003; Debaere et al. 2004b; Seurinck et al. 2004; Lin et al. 2017), there is a lack of literature on the sex-related differences in functional connectivity underlying these movements. Thus, each of the three studies in this dissertation provided additional insight into the structural and functional cortical networks responsible for different types of complex eye-hand coordination tasks across different populations.

The first two studies (**chapter 2** and **chapter 3**) provide fundamental knowledge concerning the mechanisms of unimanual visuomotor control in aging in women and men, and

applied knowledge around the consequences of increased dementia risk on activities of daily living. Few laboratories study the neural control of rule-based skilled movement as it applies to functional daily activity. The overarching aim of the first two studies was to examine changes brought on by AD in brain networks responsible for transforming visual and cognitive information into goal-directed movements. An exploratory component of these studies was to investigate the neural correlates of previously reported sex differences in non-standard unimanual movements. To address these goals, we recruited older adults who were either at an increased risk for dementia (based on having a positive family history of dementia, or presence of the APOE e4 allele) or low risk for dementia (no family history of dementia and no APOE e4 allele). Female and male participants performed coupled (standard) and decoupled (non-standard) reaching movements on a dual-screen laptop.

The objective in **chapter 2** was to examine the impact of early Alzheimer's disease pathology on the *structural* integrity of brain networks underlying complex visuomotor transformations in unimanual reaching movements. The findings demonstrated that there was a relationship between the APOE e4 genotype and structural brain changes that predict poorer non-standard visuomotor performance. Specifically, the grey matter structural findings showed that lower thickness and volume in areas of the medial temporal lobe predicted visuomotor deficits. This finding was replicated in the diffusion-weighted imaging data, where declines in white matter integrity also predicted impaired non-standard visuomotor performance. Sex differences were found in structural grey matter in areas of the posterior parietal cortex that are important for visuospatial processing (Singh-Curry and Husain 2009; Singh-Curry and Husain 2009; Mutha et al. 2011; Crottaz-Herbette et al. 2014; Gorbet and Sergio 2016), providing insight into the previously reported behavioural performance sex differences in the visual feedback reversal task.

The objective in **chapter 3** was to examine the impact of early Alzheimer's disease pathology on the *functional* integrity of resting state brain networks underlying complex visuomotor transformations in unimanual reaching movements. Similarly to the structural findings, there was a relationship between the APOE e4 genotype and resting state functional connectivity that predicted declines in non-standard visuomotor performance. Specifically, in the default mode network there was lower functional connectivity between the precuneus/posterior cingulate cortex and two other nodes, the left inferior parietal lobule and left parahippocampal cortex. These regions have all been previously described as integral to performance of visuomotor tasks (Tankus and Fried 2012; Gorbet and Sergio 2016; Gorbet and Sergio 2018). There was also decreased functional connectivity in the dorsal attention network, which is involved in goal-driven orienting of attention toward relevant stimuli (Fox et al. 2006). The key findings from these two studies suggest that a visuomotor task may have potential for detecting the early effects of genetic risk on structural and functional integrity in dementia progression *in advance of any measurable cognitive deficits*.

The third study was more fundamental in nature, and **chapter 4** primarily sought to address the gap in the literature looking at sex differences in the functional connectivity underlying bimanual control. Participants were trained on and performed comparable unimanual and bimanual coordination tasks using two button boxes while undergoing a functional MRI scan. Task performance was equivalent between men and women, and included pressing buttons in time to an auditory cue using either just their left or their right hand (unimanual), or using both hands simultaneously in a simpler in-phase (mirror/symmetrical) or more complex anti-phase (parallel/asymmetrical) bimanual task. Functional connectivity sex differences were distinct for right- vs left-hand movements, the sum of which did not reflect sex differences in functional connectivity underlying bimanual movements. The findings demonstrated sex differences in functional connectivity with respect to intra- vs

interhemispheric connectivity, supra- vs infratentorial connectivity, and lateralization of brain regions.

Taken collectively, these three projects provide novel insight into the cortical networks involved in unimanual and bimanual movement control, and how they differ based on various factors including sex and dementia risk. Importantly, the results reported in this dissertation have the potential to translate into clinical practice, discussed in more detail below, by highlighting the importance of eye-hand coordination in evaluating everyday functional abilities.

5.2. Limitations and future directions

Due to the high costs inherent in neuroimaging studies the three studies in this dissertation have a small sample size per participant group, and were also cross-sectional in nature. As in most experiments, the results presented in the current dissertation have raised a few more questions. Due to their cross-sectional nature, it was not possible to test whether poorer non-standard visuomotor integration performance on non-standard tasks reported in **chapter 2** and **chapter 3** is predictive of future conversion from dementia risk to dementia. Longitudinal studies monitoring a larger sample of both men and women over the span of several years are required to fully elucidate the use of a simple visuomotor task in predicting future cognitive and functional decline. The preclinical studies in the current dissertation focused on risk for probable AD based on family history and the AD-related APOE e4 risk allele. Future research may also consider the potential use of non-standard visuomotor tasks in distinguishing between different types of dementia, or even different types of damage to the brain such as from concussion (Hurtubise et al. 2016; Hurtubise et al. 2020). Given a large enough sample size from different clinical populations, it may be possible to determine different kinematic profiles based on different kinds of neurological conditions.

The paradigm used for the first two projects was initially studied in healthy young adult populations, looking at both behavioural performance measures and the underlying neural correlates of task performance. The findings from these more fundamental studies were then extended to use in clinical (mild cognitive impairment and dementia) and preclinical populations. Similarly, the fundamental characterization of the sex differences in the functional connectivity underlying bimanual movements in **chapter 4** has potential clinical importance. An increasing amount of evidence supports the idea that sex-related differences in brain structure are clinically relevant. The prevalence, rate of recovery, and efficacy of interventions have been shown to differ between women and men for a number of neurological conditions including, but not limited to, dementia, stroke, Parkinson's disease, and multiple sclerosis (Wooten et al. 2004; Cahill 2006; Clayton 2016; Laws et al. 2018). Therefore, a better understanding of sex-specific differences in the brain are critical for the development of targeted and effective treatment strategies for neurological conditions.

In summary, this dissertation provided novel information about the neural correlates underlying one of our most fundamental human behaviours, eye-hand coordination involving one or both hands, in different populations (younger and older adults) and how these are affected by sex and genetic risk for dementia.

REFERENCES

Acosta-Cabronero J, Nestor PJ. 2014. Diffusion tensor imaging in Alzheimer's disease: Insights into the limbic-diencephalic network and methodological considerations. Frontiers in Aging Neuroscience. 6(SEP):1–21. doi:10.3389/fnagi.2014.00266.

Acosta-Cabronero J, Williams GB, Pengas G, Nestor PJ. 2010. Absolute diffusivities define the landscape of white matter degeneration in Alzheimer's disease. Brain. 133(2):529–539. doi:10.1093/brain/awp257.

Adams JN, Lockhart SN, Li L, Jagust WJ. 2019. Relationships between tau and glucose metabolism reflect Alzheimer's disease pathology in cognitively normal older adults. Cerebral Cortex. 29(5):1997–2009. doi:10.1093/cercor/bhy078.

Adlard PA, Tran BA, Finkelstein DI, Desmond PM, Johnston LA, Bush AI, Egan GF. 2014. A review of β-amyloid neuroimaging in Alzheimer's disease. Frontiers in Neuroscience. 8:327. doi:10.3389/fnins.2014.00327.

Adluru N, Destiche DJ, Yuan-Fu Lu S, Doran ST, Birdsill AC, Melah KE, Okonkwo OC, Alexander AL, Maritza Dowling N, Johnson SC, et al. 2014. White matter microstructure in late middle-age: Effects of apolipoprotein E4 and parental family history of Alzheimer's disease. NeuroImage: Clinical. 4:730–742. doi:10.1016/j.nicl.2014.04.008.

Albers MW, Gilmore GC, Kaye J, Murphy C, Wingfield A, Bennett DA, Boxer AL, Buchman AS, Cruickshanks KJ, Devanand DP, et al. 2015. At the interface of sensory and motor dysfunctions and Alzheimer's disease. Alzheimer's and Dementia. 11(1):70–98. doi:10.1016/j.jalz.2014.04.514.

Albines D, Granek JA, Gorbet DJ, Sergio LE. 2016. Bimanual Coordination Development Is Enhanced in Young Females and Experienced Athletes. Journal of Motor Learning and Development. 4(2):274–286. doi:10.1123/jmld.2015-0038.

Alexander GE, Crutcher MD. 1990. Neural representations of the target (goal) of visually guided arm movements in three motor areas of the monkey. Journal of Neurophysiology. 64(1):164–178. doi:doi.org/10.1152/jn.1990.64.1.164.

Allen LS, Richey MF, Chai YM, Gorski RA. 1991. Sex Differences in the Corpus Callosum of the Living Human Being. The Journal of Neuroscience. 1(4):933–942. doi:doi.org/10.1523/JNEUROSCI.11-04-00933.1991.

Alonso Vilatela ME, López-López M, Yescas-Gómez P. 2012. Genetics of Alzheimer's disease. Archives of Medical Research. 43(8):622–631. doi:10.1016/j.arcmed.2012.10.017.

Alzheimer's Association. 2019. 2019 Alzheimer's disease facts and figures. Alzheimer's & Dementia. 15(3):321–387. doi:10.1016/j.jalz.2019.01.010.

Amjad H, Roth DL, Sheehan OC, Lyketsos CG, Wolff JL, Samus QM. 2018. Underdiagnosis of Dementia: an Observational Study of Patterns in Diagnosis and Awareness in US Older Adults. Journal of General Internal Medicine. 33(7):1131–1138. doi:10.1007/s11606-018-4377-y.

Amlien IK, Fjell AM. 2014. Diffusion tensor imaging of white matter degeneration in Alzheimer's disease and mild cognitive impairment. Neuroscience. 276:206–215. doi:10.1016/j.neuroscience.2014.02.017.

Amunts K, Jancke B L, Mohlberg H, Steinmetz H, Zilles K. 2000. Interhemispheric asymmetry of the human motor cortex related to handedness and gender. Neuropsychologia. 38(3):304–312. doi:https://doi.org/10.1016/S0028-3932(99)00075-5.

Andersen RA, Essick GK, Siegel RM. 1985. Encoding of spatial location by posterior parietal neurons. Science. 230:456–458. doi:10.1126/science.4048942.

Andersson JLR, Hutton C, Ashburner J, Turner R, Friston K. 2001. Modeling geometric deformations in EPI time series. NeuroImage. 13(5):903–919. doi:10.1006/nimg.2001.0746.

Andrews-Hanna JR, Reidler JS, Sepulcre J, Poulin R, Buckner RL. 2010. Functional-anatomic fractionation of the brain's Default Network. Neuron. 65(4):550–562. doi:10.1016/j.neuron.2010.02.005.

Apostolova LG, Dutton RA, Dinov ID, Hayashi M, Toga AW, Cummings JL, Thompson PM. 2006. Conversion of Mild Cognitive Impairment to Alzheimer disease predicted by hippocampal atrophy maps. Archives of Neurology. 63(5):693–699. doi:doi:10.1001/archneur.63.5.693.

Apostolova LG, Mosconi L, Thompson PM, Green AE, Hwang KS, Ramirez A, Mistur R, Tsui WH, de Leon MJ. 2010. Subregional hippocampal atrophy predicts Alzheimer's dementia in the cognitively normal. Neurobiology of Aging. 31(7):1077–1088. doi:10.1016/j.neurobiolaging.2008.08.008.

Ardekani BA, Bachman AH, Figarsky K, Sidtis JJ. 2014. Corpus callosum shape changes in early Alzheimer's disease: an MRI study using the OASIS brain database. Brain Structure and Function. 2019(1):1–21. doi:10.1038/jid.2014.371.

Ashburner J, Friston KJ. 2005. Unified segmentation. NeuroImage. 26(3):839–851. doi:10.1016/j.neuroimage.2005.02.018.

Bales KR, Du Y, Holtzman D, Cordell B, Paul SM. 2000. Neuroinflammation and Alzheimer's disease: Critical roles for cytokine/Aβ-induced glial activation, NF-κB, and apolipoprotein E. Neurobiology of Aging. 21(3):427–432. doi:10.1016/S0197-4580(00)00143-3.

Bastian AJ. 2006. Learning to predict the future: the cerebellum adapts feedforward movement control. Current Opinion in Neurobiology. 16(6):645–649. doi:10.1016/j.conb.2006.08.016.

Bateman RJ, Xiong C, Benzinger TLS, Fagan AM, Goate A, Fox NC, Marcus DS, Cairns NJ, Xie X, Blazey TM, et al. 2012. Clinical and biomarker changes in dominantly inherited Alzheimer's disease. New England Journal of Medicine. 367(9):795–804. doi:10.1056/NEJMoa1202753.

Battaglia-Mayer A, Ferraina S, Mitsuda T, Marconi B, Genovesio A, Onorati P, Lacquaniti F, Caminiti R. 2000. Early coding of reaching in the parietooccipital cortex. Journal of Neurophysiology. 83(4):2374–2391. doi:doi.org/10.1152/jn.2000.83.4.2374.

Beaulieu C. 2002. The basis of anisotropic water diffusion in the nervous system - A technical review. NMR in Biomedicine. 15(7–8):435–455. doi:10.1002/nbm.782.

Beaulieu C, Does MD, Snyder RE, Allen PS. 1996. Changes in Water Diffusion Due to Wallerian Degeneration in Peripheral Nerve. Magnetic Resonance in Medicine. 36(4):627–631. doi:doi.org/10.1002/mrm.1910360419.

Bedford FL. 1993. Perceptual and cognitive spatial learning. J Exp Psychol Hum Percept Perform. 19(3):517–530. doi:doi.org/10.1037/0096-1523.19.3.517.

Bekris LM, Yu CE, Bird TD, Tsuang DW. 2010. Genetics of Alzheimer disease. Journal of Geriatric Psychiatry and Neurology. 23(4):213–227. doi:10.1177/0891988710383571.

Belleville S, Fouquet C, Duchesne S, Collins DL, Hudon C. 2014. Detecting early preclinical Alzheimer's disease via cognition, neuropsychiatry, and neuroimaging: Qualitative review and recommendations for testing. Journal of Alzheimer's Disease. 42:375–382. doi:10.3233/JAD-141470.

Bendlin BB, Ries ML, Canu E, Sodhi A, Lazar M, Alexander AL, Carlsson CM, Sager MA, Asthana S, Johnson SC. 2010. White matter is altered with parental family history of Alzheimer's disease. Alzheimer's & Dementia. 6(5):394–403. doi:10.1016/j.jalz.2009.11.003.

Bennett IJ, Motes MA, Rao NK, Rypma B. 2012. White matter tract integrity predicts visual search performance in young and older adults. Neurobiology of Aging. 33(2):433.e21-433.e31. doi:10.1016/j.neurobiolaging.2011.02.001.

Bernier PM, Grafton ST. 2010. Human posterior parietal cortex flexibly determines reference frames for reaching based on sensory context. Neuron. 68(4):776–788. doi:10.1016/j.neuron.2010.11.002.

Bigham B, Zamanpour SA, Zemorshidi F, Boroumand F, Zare H. 2020. Identification of Superficial White Matter Abnormalities in Alzheimer's Disease and Mild Cognitive Impairment Using Diffusion Tensor Imaging. Journal of Alzheimer's Disease Reports. 4(1):49–59. doi:10.3233/ADR-190149.

Binder LI, Frankfurter A, Rebhun LI. 1995. The distribution of tau in the mammalian central nervous system. Journal of Cell Biology. 101(4):1371–1378. doi:doi.org/10.1083/jcb.101.4.1371.

Blangero A, Menz MM, McNamara A, Binkofski F. 2009. Parietal modules for reaching. Neuropsychologia. 47(6):1500–1507. doi:10.1016/j.neuropsychologia.2008.11.030.

Bloom GS. 2014. Amyloid-β and tau: The trigger and bullet in Alzheimer disease pathogenesis. JAMA Neurology. 71(4):505–508. doi:10.1001/jamaneurol.2013.5847.

Bloom JS, Hynd GW. 2005. The role of the corpus callosum in interhemispheric transfer of information: Excitation or inhibition? Neuropsychology Review. 15(2):59–71. doi:10.1007/s11065-005-6252-y.

Blouin JS, Bard C, Paillard J. 2004. Contribution of the cerebellum to self-initiated synchronized movements: A PET study. Experimental Brain Research. 155(1):63–68. doi:10.1007/s00221-003-1709-9.

Bo J, Contreras-Vidal JL, Kagerer FA, Clark JE. 2006. Effects of increased complexity of visuo-motor transformations on children's arm movements. Human Movement Science. 25(4–5):553–567. doi:10.1016/j.humov.2006.07.003.

de Boer C, Echlin HV, Rogojin A, Baltaretu BR, Sergio LE. 2018. Thinking-while-moving exercises may improve cognition in elderly with mild cognitive deficits: A proof-of-principle study. Dementia and Geriatric Cognitive Disorders Extra. 8(2):248–258. doi:10.1159/000490173.

de Boer C, Mattace-Raso F, van der Steen J, Pel JJM. 2014. Mini-Mental State Examination subscores indicate visuomotor deficits in Alzheimer's disease patients: A cross-sectional study in a Dutch population. Geriatrics and Gerontology International. 14(4):880–885. doi:10.1111/ggi.12183.

de Boer C, Pel JJM, Van Der Steen J, Mattace-Raso F. 2015. Delays in manual reaching are associated with impaired functional abilities in early dementia patients. Dementia and Geriatric Cognitive Disorders. 40(1–2):63–71. doi:10.1159/000377674.

de Boer C, Van Der Steen J, Mattace-Raso F, Boon AJW, Pel JJM. 2016. The effect of neurodegeneration on visuomotor behavior in Alzheimer's disease and Parkinson's disease. Motor Control. 20(1):1–20. doi:10.1123/mc.2014-0015.

Boisgontier MP, Cheval B, van Ruitenbeek P, Cuypers K, Leunissen I, Sunaert S, Meesen R, Zivari Adab H, Renaud O, Swinnen SP. 2018. Cerebellar gray matter explains bimanual coordination performance in children and older adults. Neurobiology of Aging. 65:109–120. doi:10.1016/j.neurobiolaging.2018.01.016.

Bokde ALW, Ewers M, Hampel H. 2009. Assessing neuronal networks: Understanding Alzheimer's disease. Progress in Neurobiology. 89(2):125–133. doi:10.1016/j.pneurobio.2009.06.004.

Bosch B, Arenaza-Urquijo EM, Rami L, Sala-Llonch R, Junqué C, Solé-Padullés C, Peña-Gómez C, Bargalló N, Molinuevo JL, Bartrés-Faz D. 2012. Multiple DTI index analysis in normal aging, amnestic MCI and AD. Relationship with neuropsychological performance. Neurobiology of Aging. 33(1):61–74. doi:10.1016/j.neurobiolaging.2010.02.004.

Boyles JK, Pitas RE, Wilson E, Mahley RW, Taylor JM. 1985. Apolipoprotein E associated with astrocytic glia of the central nervous system and with nonmyelinating glia of the peripheral nervous system. The Journal of Clinical Investigation. 76(4):1501–1513. doi:doi.org/10.1172/JCI112130.

Braak H, Braak E. 1991a. Neuropathological stageing of Alzheimer-related changes. Acta Neuropathol. 82(4):239–259. doi:doi.org/10.1007/BF00308809.

Braak H, Braak E. 1991b. Alzheimer's disease affects limbic nuclei of the thalamus. Acta Neuropathol. 81:261–268.

Braak H, Thal DR, Ghebremedhin E, Del Tredici K. 2011. Stages of the pathologic process in alzheimer disease: Age categories from 1 to 100 years. Journal of Neuropathology and Experimental Neurology. 70(11):960–969. doi:10.1097/NEN.0b013e318232a379.

Brier MR, Thomas JB, Snyder AZ, Benzinger TL, Zhang D, Raichle ME, Holtzman DM, Morris JC, Ances BM. 2012. Loss of intranetwork and internetwork resting state functional connections with Alzheimer's disease progression. Journal of Neuroscience. 32(26):8890–8899. doi:10.1523/JNEUROSCI.5698-11.2012.

Brier MR, Thomas JB, Snyder AZ, Wang L, Fagan AM, Benzinger T, Morris JC, Ances BM. 2014. Unrecognized preclinical Alzheimer disease confounds rs-fcMRI studies of normal aging. Neurology. 83(18):1613–1619. doi:doi.org/10.1212/WNL.0000000000000939.

Bubb EJ, Metzler-Baddeley C, Aggleton JP. 2018. The cingulum bundle: Anatomy, function, and dysfunction. Neuroscience and Biobehavioral Reviews. 92:104–127. doi:10.1016/j.neubiorev.2018.05.008.

Buckley RF, Schultz AP, Hedden T, Papp KV, Hanseeuw BJ, Marshall G, Sepulcre J, Smith EE, Rentz DM, Johnson KA, et al. 2017. Functional network integrity presages cognitive decline in preclinical Alzheimer disease. Neurology. 89(1):29–37. doi:10.1212/WNL.0000000000004059.

Buckner RL, Andrews-Hanna JR, Schacter DL. 2008. The brain's default network: Anatomy, function, and relevance to disease. Annals of the New York Academy of Sciences. 1124:1–38. doi:10.1196/annals.1440.011.

Buckner RL, Krienen FM, Yeo BTT. 2013. Opportunities and limitations of intrinsic functional connectivity MRI. Nature Neuroscience. 16(7):832–837. doi:10.1038/nn.3423.

Buckner RL, Snyder AZ, Shannon BJ, LaRossa G, Sachs R, Fotenos AF, Sheline YI, Klunk WE, Mathis CA, Morris JC, et al. 2005. Molecular, structural, and functional characterization of Alzheimer's disease: Evidence for a relationship between default activity, amyloid, and memory. Journal of Neuroscience. 25(34):7709–7717. doi:10.1523/JNEUROSCI.2177-05.2005.

Budisavljevic S, Dell'Acqua F, Zanatto D, Begliomini C, Miotto D, Motta R, Castiello U. 2017. Asymmetry and Structure of the Fronto-Parietal Networks Underlie Visuomotor Processing in Humans. Cerebral Cortex. 27(2):1532–1544. doi:10.1093/cercor/bhv348.

Burks JD, Boettcher LB, Conner AK, Glenn CA, Bonney PA, Baker CM, Briggs RG, Pittman NA, O'Donoghue DL, Wu DH, et al. 2017. White matter connections of the inferior parietal lobule: A study of surgical anatomy. Brain and Behavior. 7(4):e00640. doi:10.1002/brb3.640.

Burns A, Iliffe S. 2009. Dementia. BMJ. 338(7691):405–409. doi:10.1136/bmj.b75.

Cacciaglia R, Salvadó G, Molinuevo JL, Shekari M, Falcon C, Operto G, Suárez-Calvet M, Milà-Alomà M, Sala A, Rodriguez-Vieitez E, et al. 2022. Age, sex and APOE-ε4 modify the balance between soluble and fibrillar β-amyloid in non-demented individuals: topographical patterns across two independent cohorts. Molecular Psychiatry. 27(4):2010–2018. doi:10.1038/s41380-022-01436-7.

Caeyenberghs K, Leemans A, Coxon J, Leunissen I, Drijkoningen D, Geurts M, Gooijers J, Michiels K, Sunaert S, Swinnen SP. 2011. Bimanual coordination and corpus callosum microstructure in young adults with traumatic brain injury: A diffusion tensor imaging study. Journal of Neurotrauma. 28(6):897–913. doi:10.1089/neu.2010.1721.

Cahill L. 2006. Why sex matters for neuroscience. Nature Reviews Neuroscience. 7(6):477–484. doi:10.1038/nrn1909.

Calati R, Maller JJ, Meslin C, Lopez-Castroman J, Ritchie K, Courtet P, Artero S. 2018. Repatriation is associated with isthmus cingulate cortex reduction in community-dwelling elderly. World Journal of Biological Psychiatry. 19(6):421–430. doi:10.1080/15622975.2016.1258490.

Caminiti R, Borra E, Visco-Comandini F, Battaglia-Mayer A, Averbeck BB, Luppino G. 2017. Computational architecture of the parieto-frontal network underlying cognitive-motor control in monkeys. eNeuro. 4(1). doi:10.1523/ENEURO.0306-16.2017.

Canadian Institute for Health Information. 2019. Young-onset dementia. [accessed 2020 Mar 15]. https://www.cihi.ca/en/dementia-in-canada/spotlight-on-dementia-issues/young-onset-dementia.

Canevari L, Abramov AY, Duchen MR. 2004. Toxicity of amyloid β peptide: Tales of calcium, mitochondria, and oxidative stress. Neurochemical Research. 29(3):637–650. doi:10.1023/B:NERE.0000014834.06405.af.

Cardoso de Oliveira S, Gribova A, Donchin O, Bergman H, Vaadia E. 2001. Neural interactions between motor cortical hemispheres during bimanual and unimanual arm movements. European Journal of Neuroscience. 14(11):1881–1896. doi:doi.org/10.1046/j.0953-816x.2001.01801.x.

Caselli RJ, Walker D, Sue L, Sabbagh M, Beach T. 2010. Amyloid load in nondemented brains correlates with APOE e4. Neuroscience Letters. 473(3):168–171. doi:10.1016/j.neulet.2010.02.016.

Castellano JM, Kim J, Stewart FR, Jiang H, DeMattos RB, Patterson BW, Fagan AM, Morris JC, Mawuenyega KG, Cruchaga C, et al. 2011. Human apoE isoforms differentially regulate brain amyloid-β peptide clearance. Science Translational Medicine. 3(89):1–11. doi:10.1126/scitranslmed.3002156.

Cauraugh JH, Lodha N, Naik SK, Summers JJ. 2010. Bilateral movement training and stroke motor recovery progress: A structured review and meta-analysis. Human Movement Science. 29(5):853–870. doi:10.1016/j.humov.2009.09.004.

Cavanna AE, Trimble MR. 2006. The precuneus: A review of its functional anatomy and behavioural correlates. Brain. 129(3):564–583. doi:10.1093/brain/awl004.

Cavedo E, Chiesa PA, Houot M, Ferretti MT, Grothe MJ, Teipel SJ, Lista S, Habert MO, Potier MC, Dubois B, et al. 2018. Sex differences in functional and molecular neuroimaging biomarkers of Alzheimer's disease in cognitively normal older adults with subjective memory complaints. Alzheimer's and Dementia. 14(9):1204–1215. doi:10.1016/j.jalz.2018.05.014.

Chen GF, Xu TH, Yan Y, Zhou YR, Jiang Y, Melcher K, Xu HE. 2017. Amyloid beta: Structure, biology and structure-based therapeutic development. Acta Pharmacologica Sinica. 38(9):1205–1235. doi:10.1038/aps.2017.28.

Chételat G, La Joie R, Villain N, Perrotin A, De La Sayette V, Eustache F, Vandenberghe R. 2013. Amyloid imaging in cognitively normal individuals, at-risk populations and preclinical Alzheimer's disease. NeuroImage: Clinical. 2(1):356–365. doi:10.1016/j.nicl.2013.02.006.

Chételat G, Villemagne VL, Bourgeat P, Pike KE, Jones G, Ames D, Ellis KA, Szoeke C, Martins RN, O'Keefe GJ, et al. 2010. Relationship between atrophy and β-amyloid deposition in Alzheimer disease. Annals of Neurology. 67(3):317–324. doi:10.1002/ana.21955.

Chételat G, Villemagne VL, Pike KE, Baron JC, Bourgeat P, Jones G, Faux NG, Ellis KA, Salvado O, Szoeke C, et al. 2010. Larger temporal volume in elderly with high versus low beta-amyloid deposition. Brain. 133(11):3349–3358. doi:10.1093/brain/awq187.

Chettouf S, Rueda-Delgado LM, de Vries R, Ritter P, Daffertshofer A. 2020. Are unimanual movements bilateral? Neuroscience and Biobehavioral Reviews. 113:39–50. doi:10.1016/j.neubiorev.2020.03.002.

Chong M, Bhushan C, Joshi AA, Choi S, Haldar JP, Shattuck DW, Spreng RN, Leahy RM. 2017. Individual parcellation of resting fMRI with a group functional connectivity prior. NeuroImage. 156:87–100. doi:10.1016/j.neuroimage.2017.04.054.

Chung G, Han YM, Jeong SH, Jack CR. 2005. Functional Heterogeneity of the Supplementary Motor Area. American Journal of Neuroradiology. 26(7):1819–1823.

Clark BJ, Simmons CM, Berkowitz LE, Wilber AA. 2018. The retrosplenial-parietal network and reference frame coordination for spatial navigation. Behavioral Neuroscience. 132(5):416–429. doi:10.1037/bne0000260.

Clayton JA. 2016. Sex influences in neurological disorders: Case studies and perspectives. Dialogues in Clinical Neuroscience. 18(4):357–360. doi:10.31887/dcns.2016.18.4/jclayton.

Clower DM, Boussaoud D. 2000. Selective use of perceptual recalibration versus visuomotor skill acquisition. Journal of Neurophysiology. 84(5):2703–2708. doi:10.1152/jn.2000.84.5.2703.

Clower DM, West RA, Lynch JC, Strick PL. 2001. The inferior parietal lobule is the target of output from the superior colliculus, hippocampus, and cerebellum. Journal of Neuroscience. 21(16):6283–6291. doi:10.1523/jneurosci.21-16-06283.2001.

Concha L, Gross DW, Wheatley BM, Beaulieu C. 2006. Diffusion tensor imaging of time-dependent axonal and myelin degradation after corpus callosotomy in epilepsy patients. NeuroImage. 32(3):1090–1099. doi:10.1016/j.neuroimage.2006.04.187.

Conner AK, Briggs RG, Sali G, Rahimi M, Baker CM, Burks JD, Glenn CA, Battiste JD, Sughrue ME. 2018. A Connectomic Atlas of the Human Cerebrum - Chapter 13: Tractographic Description of the Inferior Fronto-Occipital Fasciculus. Operative neurosurgery (Hagerstown, Md). 15(1):S436–S443. doi:10.1093/ons/opy267.

Connolly A, Gaehl E, Martin H, Morris J, Purandare N. 2011. Underdiagnosis of dementia in primary care: Variations in the observed prevalence and comparisons to the expected prevalence. Aging and Mental Health. 15(8):978–984. doi:10.1080/13607863.2011.596805.

Corder EH, Saunders AM, Strittmatter WJ, Schmechel DE, Gaskell PC, Small GW, Roses AD, Haines JL, Pericak-Vance MA. 1993. Gene dose of apolipoprotein E type 4 allele and the risk of Alzheimer's disease in late onset families. Science. 261(5123):921–923. doi:10.1126/science.8346443.

Cox RW. 1996. AFNI: Software for Analysis and Visualization of Functional Magnetic Resonance Neuroimages. Computers and Biomedical Research. 29(3):162–173. doi:https://doi.org/10.1006/cbmr.1996.0014.

Crawford JD, Henriques DYP, Medendorp WP. 2011. Three-dimensional transformations for goal-directed action. Annual Review of Neuroscience. 34(1):309–331. doi:10.1146/annurev-neuro-061010-113749.

Crean S, Ward A, Mercaldi CJ, Collins JM, Cook MN, Baker NL, Arrighi HM. 2011. Apolipoprotein E ε4 prevalence in Alzheimer's disease patients varies across global populations: A systematic literature review and meta-analysis. Dementia and Geriatric Cognitive Disorders. 31(1):20–30. doi:10.1159/000321984.

Crites MJ, Gorman JC. 2017. Bimanual coupling and the intermanual speed advantage. In: Proceedings of the Human Factors and Ergonomics Society. Vol. 2017-October. Human Factors an Ergonomics Society Inc. p. 1385–1389.

Crottaz-Herbette S, Fornari E, Clarke S. 2014. Prismatic adaptation changes visuospatial representation in the inferior parietal lobule. Journal of Neuroscience. 34(35):11803–11811. doi:10.1523/JNEUROSCI.3184-13.2014.

Curran KM, Emsell L, Leemans A. 2016. Quantitative DTI Measures. In: Van Hecke W, Emsell L, Sunaert S, editors. Diffusion Tensor Imaging. New York, NY: Springer New York. p. 65–87.

Dadar M, Camicioli R, Duchesne S, Collins DL. 2020. The temporal relationships between white matter hyperintensities, neurodegeneration, amyloid beta, and cognition.

Alzheimer's and Dementia: Diagnosis, Assessment and Disease Monitoring. 12(1):1–11. doi:10.1002/dad2.12091.

Damoiseaux JS, Seeley WW, Zhou J, Shirer WR, Coppola G, Karydas A, Rosen HJ, Miller BL, Kramer JH, Greicius MD. 2012. Gender modulates the APOE ε4 effect in healthy older adults: Convergent evidence from functional brain connectivity and spinal fluid tau levels. Journal of Neuroscience. 32(24):8254–8262. doi:10.1523/JNEUROSCI.0305-12.2012.

Darling WG, Cooke IJD, Brown SH, Cooke JD. 1989. Control of Simple Arm Movements in Elderly Humans. Neurobiology of Aging. 10:149–157. doi:doi.org/10.1016/0197-4580(89)90024-9.

Davis SW, Dennis NA, Buchler NG, White LE, Madden DJ, Cabeza R. 2009. Assessing the effects of age on long white matter tracts using diffusion tensor tractography. NeuroImage. 46(2):530–541. doi:10.1016/j.neuroimage.2009.01.068.

Deane R, Sagare A, Hamm K, Parisi M, Lane S, Finn MB, Holtzman DM, Zlokovic BV. 2008. ApoE isoform-specific disruption of amyloid β peptide clearance from mouse brain. Journal of Clinical Investigation. 118(12):4002–4013. doi:10.1172/JCI36663.

Debaere F, Swinnen SP, Béatse E, Sunaert S, Van Hecke P, Duysens J. 2001. Brain areas involved in interlimb coordination: A distributed network. NeuroImage. 14(5):947–958. doi:10.1006/nimg.2001.0892.

Debaere F, Wenderoth N, Sunaert S, Van Hecke P, Swinnen SP. 2004a. Cerebellar and premotor function in bimanual coordination: Parametric neural responses to spatiotemporal complexity and cycling frequency. NeuroImage. 21(4):1416–1427. doi:10.1016/j.neuroimage.2003.12.011.

Debaere F, Wenderoth N, Sunaert S, Van Hecke P, Swinnen SP. 2004b. Changes in brain activation during the acquisition of a new bimanual coordination task. Neuropsychologia. 42(7):855–867. doi:10.1016/j.neuropsychologia.2003.12.010.

DeCarli C, Frisoni GB, Clark CM, Harvey D, Grundman M, Petersen RC, Thal LJ, Jin S, Jack CR, Scheltens P. 2007. Qualitative estimates of medial temporal atrophy as a predictor of progression from mild cognitive impairment to dementia. Archives of Neurology. 64(1):108–115. doi:10.1001/archneur.64.1.108.

Delbeuck X, Van Der Linden M, Collette F. 2003. Alzheimer's disease as a disconnection syndrome? Neuropsychology Review. 13(2):79–92. doi:https://doi.org/10.1023/A:1023832305702.

Desikan RS, Ségonne F, Fischl B, Quinn BT, Dickerson BC, Blacker D, Buckner RL, Dale AM, Maguire RP, Hyman BT, et al. 2006. An automated labeling system for subdividing the human cerebral cortex on MRI scans into gyral based regions of interest. NeuroImage. 31(3):968–980. doi:10.1016/j.neuroimage.2006.01.021.

Desmond JE, Gabrieli JDE, Wagner AD, Ginier BL, Glover GH. 1997. Lobular Patterns of Cerebellar Activation in Verbal Working-Memory and Finger-Tapping Tasks as

Revealed by Functional MRI. Journal of Neuroscience. 17(24):9676–9685. doi:doi.org/10.1523/JNEUROSCI.17-24-09675.1997.

Destrieux C, Fischl B, Dale A, Halgren E. 2010. Automatic parcellation of human cortical gyri and sulci using standard anatomical nomenclature. NeuroImage. 53(1):1–15. doi:10.1016/j.neuroimage.2010.06.010.

Devi L, Prabhu BM, Galati DF, Avadhani NG, Anandatheerthavarada HK. 2006. Accumulation of amyloid precursor protein in the mitochondrial import channels of human Alzheimer's disease brain is associated with mitochondrial dysfunction. Journal of Neuroscience. 26(35):9057–9068. doi:10.1523/JNEUROSCI.1469-06.2006.

Ding S-L, Van Hoesen G, Rockland KS. 2000. Inferior Parietal Lobule Projections to the Presubiculum and Neighboring Ventromedial Temporal Cortical Areas. Journal of Comparative Neurology. 425(4):510–530. doi:doi.org/10.1002/1096-9861(20001002)425:4<510::AID-CNE4>3.0.CO;2-R.

Doan NT, Engvig A, Persson K, Alnæs D, Kaufmann T, Rokicki J, Córdova-Palomera A, Moberget T, Brækhus A, Barca ML, et al. 2017. Dissociable diffusion MRI patterns of white matter microstructure and connectivity in Alzheimer's disease spectrum. Scientific Reports. 7(45131):1–12. doi:10.1038/srep45131.

Donix M, Burggren AC, Suthana NA, Siddarth P, Ekstrom AD, Krupa AK, Jones M, Martin-Harris L, Ercoli LM, Miller KJ, et al. 2010. Family history of Alzheimer's disease and hippocampal structure in healthy people. American Journal of Psychiatry. 167(11):1399–1406. doi:10.1176/appi.ajp.2010.09111575.

Donix M, Burggren AC, Suthana NA, Siddarth P, Ekstrom AD, Krupa AK, Jones M, Rao A, Martin-Harris L, Ercoli LM, et al. 2010. Longitudinal changes in medial temporal cortical thickness in normal subjects with the APOE-4 polymorphism. NeuroImage. 53(1):37–43. doi:10.1038/jid.2014.371.

Doré V, Villemagne VL, Bourgeat P, Fripp J, Acosta O, Chetélat G, Zhou L, Martins R, Ellis KA, Masters CL, et al. 2013. Cross-sectional and longitudinal analysis of the relationship between aβ deposition, cortical thickness, and memory in cognitively unimpaired individuals and in alzheimer disease. JAMA Neurology. 70(7):903–911. doi:10.1001/jamaneurol.2013.1062.

Dorszewska J, Prendecki M, Oczkowska A, Dezor M, Kozubski W. 2016. Molecular basis of familial and sporadic Alzheimer's disease. Current Alzheimer Research. 13(9):952–963. doi:10.2174/1567205013666160314150501.

Dubb A, Gur R, Avants B, Gee J. 2003. Characterization of sexual dimorphism in the human corpus callosum. NeuroImage. 20(1):512–519. doi:10.1016/S1053-8119(03)00313-6.

Dubois B, Feldman HH, Jacova C, Hampel H, Molinuevo JL, Blennow K, Dekosky ST, Gauthier S, Selkoe D, Bateman R, et al. 2014. Advancing research diagnostic criteria for Alzheimer's disease: The IWG-2 criteria. Lancet Neurology. 13(6):614–629. doi:10.1016/S1474-4422(14)70090-0.

Dubois B, Hampel H, Feldman HH, Scheltens P, Aisen P, Andrieu S, Bakardjian H, Benali H, Bertram L, Blennow K, et al. 2016. Preclinical Alzheimer's disease: Definition, natural history, and diagnostic criteria. Alzheimer's & Dementia. 12(3):292–323. doi:10.1016/j.jalz.2016.02.002.

Echlin HV, Gorbet DJ, Sergio LE. 2020. Assessment of a cognitive-motor training program in adults at risk for developing dementia. Canadian Geriatrics Journal. 23(2):190–198. doi:10.5770/cgj.23.394.

Eichenbaum H, Schoenbaum G, Young B, Bunsey M. 1996. Functional organization of the hippocampal memory system. Proceedings of the National Academy of Sciences of the United States of America. 93(24):13500–13507. doi:10.1073/pnas.93.24.13500.

Eickhoff SB, Bzdok D, Laird AR, Roski C, Caspers S, Zilles K, Fox PT. 2011. Co-activation patterns distinguish cortical modules, their connectivity and functional differentiation. NeuroImage. 57(3):938–949. doi:10.1016/j.neuroimage.2011.05.021.

Eickhoff SB, Thirion B, Varoquaux G, Bzdok D. 2015. Connectivity-based parcellation: Critique and implications. Human Brain Mapping. 36(12):4771–4792. doi:10.1002/hbm.22933.

Elman JA, Madison CM, Baker SL, Vogel JW, Marks SM, Crowley S, O'Neil JP, Jagust WJ. 2016. Effects of Beta-Amyloid on Resting State Functional Connectivity Within and between Networks Reflect Known Patterns of Regional Vulnerability. Cerebral Cortex. 26(2):695–707. doi:10.1093/cercor/bhu259.

Ewers M, Sperling RA, Klunk WE, Weiner MW, Hampel H. 2011. Neuroimaging markers for the prediction and early diagnosis of Alzheimer's disease dementia. Trends in Neurosciences. 34(8):430–442. doi:10.1016/j.tins.2011.05.005.

Fagan AM, Head D, Shah AR, Marcus D, Mintun M, Morris JC, Holtzman DM. 2009. Decreased cerebrospinal fluid Aβ 42 correlates with brain atrophy in cognitively normal elderly. Annals of Neurology. 65(2):176–183. doi:10.1002/ana.21559.

Fantoni E, Collij L, Alves IL, Buckley C, Farrar G. 2020. The spatial-temporal ordering of amyloid pathology and opportunities for PET imaging. Journal of Nuclear Medicine. 61(2):166–171. doi:10.2967/jnumed.119.235879.

Farrer LA, Cupples LA, Haines JL, Hyman B, Kukull WA, Mayeux R, Myers RH, Pericak-Vance MA, Risch N, Van Duijn CM. 1997. Effects of age, sex, and ethnicity on the association between apolipoprotein E genotype and Alzheimer disease: A meta-analysis. Journal of the American Medical Association. 278(16):1349–1356. doi:10.1001/jama.1997.03550160069041.

Farrer LA, Cupples LA, Van Duijn CM, Kurz A, Zimmer R, Müller U, Green RC, Clarke V, Shoffner J, Wallace DC, et al. 1995. Apolipoprotein E genotype in patients with alzheimer's disease: Implications for the risk of dementia among relatives. Annals of Neurology. 38(5):797–808. doi:10.1002/ana.410380515.

Filimon F. 2010. Human cortical control of hand movements: Parietofrontal networks for reaching, grasping, and pointing. Neuroscientist. 16(4):388–407. doi:10.1177/1073858410375468.

Filippi M, Agosta F. 2011. Structural and functional network connectivity breakdown in Alzheimer's disease studied with magnetic resonance imaging techniques. Journal of Alzheimer's Disease. 24(3):455–474. doi:10.3233/JAD-2011-101854.

Fischer FU, Wolf D, Scheurich A, Fellgiebel A. 2015. Altered whole-brain white matter networks in preclinical Alzheimer's disease. NeuroImage: Clinical. 8:660–666. doi:10.1016/j.nicl.2015.06.007.

Flanders M, Tillery SIH, Soechting JF. 1992. Early stages in a sensorimotor transformation. Behavioral and Brain Sciences. 15(2):309–320. doi:10.1017/s0140525x00068813.

Fleisher A, Sherzai A, Taylor C, Langbaum J, Chen K, Buxton R. 2009. Resting-state BOLD networks versus task-associated functional MRI for distinguishing Alzheimer's disease risk groups. NeuroImage. 47(4):1678–1690. doi:https://doi.org/10.1016/j.neuroimage.2009.06.021.

Fleisher A, Sowell B, Taylor C, Gamst A, Petersen R, Thal L. 2007. Clinical predictors of progression to Alzheimer disease in amnestic mild cognitive impairment. Neurology. 68(19):1588–1595. doi:10.1212/01.wnl.0000258542.58725.4c.

Foo H, Mather KA, Jiang J, Thalamuthu A, Wen W, Sachdev PS. 2020. Genetic influence on ageing-related changes in resting-state brain functional networks in healthy adults: A systematic review. Neuroscience and Biobehavioral Reviews. 113:98–110. doi:10.1016/j.neubiorev.2020.03.011.

Fox MD, Corbetta M, Snyder AZ, Vincent JL, Raichle ME. 2006. Spontaneous neuronal activity distinguishes human dorsal and ventral attention systems. Proceedings of the National Academy of Sciences. 103(26):10046–10051. doi:doi.org/10.1073/pnas.0604187103.

Fox MD, Raichle ME. 2007. Spontaneous fluctuations in brain activity observed with functional magnetic resonance imaging. Nature Reviews Neuroscience. 8(9):700–711. doi:10.1038/nrn2201.

Fozard JL, Vercruyssen M, Reynolds SL, Hancock PA, Quilter RE. 1994. Age Differences and Changes in Reaction Time: The Baltimore Longitudinal Study of Aging. Journal of Gerontology: Psychological Sciences. 49(4):179–189. doi:doi.org/10.1093/geronj/49.4.P179.

Fransson P, Marrelec G. 2008. The precuneus/posterior cingulate cortex plays a pivotal role in the default mode network: Evidence from a partial correlation network analysis. NeuroImage. 42(3):1178–1184. doi:10.1016/j.neuroimage.2008.05.059.

Franz EA. 1997. Spatial Coupling in the Coordination of Complex Actions. Quarterly Journal of Experimental Psychology Section A: Human Experimental Psychology. 50(3):684–704. doi:10.1080/713755726.

Franz EA, Eliassen JC, Ivry RB, Gazzaniga MS. 1996. Dissociation of Spatial and Temporal Coupling in the Bimanual Movements of Callosotomy Patients. Psychological Science. 7(5):306–310. doi:doi.org/10.1111/j.1467-9280.1996.tb00379.x.

Franz EA, Zelaznik HN, McCabe G. 1991. Spatial topological constraints in a bimanual task. Acta Psychologica. 77(2):137–151. doi:10.1016/0001-6918(91)90028-X.

Gatz M, Reynolds C a, Fratiglioni L, Johansson B, Mortimer J a, Berg S, Fiske A, Pedersen NL. 2006. Role of genes and environments for explaining Alzheimer's disease. Archives of General Psychiatry. 63(2):168–74. doi:10.1001/archpsyc.63.2.168.

Gerloff C, Corwell B, Chen R, Hallett M, Cohen LG. 1997. Stimulation over the human supplementary motor area interferes with the organization of future elements in complex motor sequences. Brain. 120(9):1587–1602. doi:doi.org/10.1093/brain/120.9.1587.

Ghilardi MF, Alberoni M, Marelli S, Rossi M, Franceschi M, Ghez C, Fazio F. 1999. Impaired movement control in Alzheimer's disease. Neuroscience Letters. 260(1):45–48. doi:10.1016/S0304-3940(98)00957-4.

Ghilardi MF, Alberoni M, Rossi M, Franceschi M, Mariani C, Fazio F. 2000. Visual feedback has differential effects on reaching movements in Parkinson's and Alzheimer's disease. Brain Research. 876(1–2):112–123. doi:10.1016/S0006-8993(00)02635-4.

Ghilardi MF, Gordon J, Ghez C. 1995. Learning a visuomotor transformation in a local area of work space produces directional biases in other areas. Journal of Neurophysiology. 74(6):2535–2539. doi:10.1152/jn.1995.73.6.2535.

Gielen CCAM, van den Heuvel PJM, van Gisbergen JAM. 1984. Coordination of fast eye and arm movements in a tracking task. Experimental Brain Research. 56(1):154–161. doi:10.1007/BF00237452.

Gispert JD, Rami L, Sánchez-Benavides G, Falcon C, Tucholka A, Rojas S, Molinuevo JL. 2015. Nonlinear cerebral atrophy patterns across the Alzheimer's disease continuum: Impact of APOE4 genotype. Neurobiology of Aging. 36(10):2687–2701. doi:10.1016/j.neurobiolaging.2015.06.027.

Gold BT, Johnson NF, Powell DK, Smith CD. 2012. White matter integrity and vulnerability to Alzheimer's disease: Preliminary findings and future directions. Biochimica et Biophysica Acta - Molecular Basis of Disease. 1822(3):416–422. doi:10.1016/j.bbadis.2011.07.009.

Gold BT, Powell DK, Andersen AH, Smith CD. 2010. Alterations in multiple measures of white matter integrity in normal women at high risk for Alzheimer's disease. NeuroImage. 52(4):1487–1494. doi:10.1016/j.neuroimage.2010.05.036.

Gómez-Tortosa E, Barquero MS, Barón M, Sainz MJ, Manzano S, Payno M, Ros R, Almaraz C, Gómez-Garré P, Jiménez-Escrig A. 2007. Variability of age at onset in siblings with familial Alzheimer disease. Archives of Neurology. 64(12):1743–1748. doi:10.1001/archneur.64.12.1743.

Gooijers J, Leemans A, Van Cauter S, Sunaert S, Swinnen SP, Caeyenberghs K. 2014. White matter organization in relation to upper limb motor control in healthy subjects: exploring the added value of diffusion kurtosis imaging. Brain structure & function. 219(5):1627–1638. doi:10.1007/s00429-013-0590-y.

Gorbet D, Mader L, Staines W. 2010. Sex-related differences in the hemispheric laterality of slow cortical potentials during the preparation of visually guided movements. Experimental Brain Research. 202(3):633–646. doi:10.1007/s00221-010-2170-1.

Gorbet D, Sergio L. 2007. Preliminary sex differences in human cortical BOLD fMRI activity during the preparation of increasingly complex visually guided movements. European Journal of Neuroscience. 25(4):1228–1239. doi:10.1111/j.1460-9568.2007.05358.x.

Gorbet D, Sergio L. 2016. Don't watch where you're going: The neural correlates of decoupling eye and arm movements. Behavioural Brain Research. 298:229–240. doi:10.1016/j.bbr.2015.11.012.

Gorbet D, Sergio L. 2018. Looking up while reaching out: the neural correlates of making eye and arm movements in different spatial planes. Experimental Brain Research. 237(1):57–70. doi:10.1007/s00221-018-5395-z.

Gorbet D, Staines W. 2011. Inhibition of contralateral premotor cortex delays visually guided reaching movements in men but not in women. Experimental Brain Research. 212(2):315–325. doi:10.1007/s00221-011-2731-y.

Gorbet D, Staines W, Sergio L. 2004. Brain mechanisms for preparing increasingly complex sensory to motor transformations. NeuroImage. 23(3):1100–1111. doi:10.1016/j.neuroimage.2004.07.043.

Granek JA, Sergio LE. 2015. Evidence for distinct brain networks in the control of rule-based motor behavior. J Neurophysiol. 114:1298–1309. doi:10.1152/jn.00233.2014.-Reach.

Grodd W, Hü E, Lotze M, Wildgruber D, Erb M. 2001. Sensorimotor Mapping of the Human Cerebellum: fMRI Evidence of Somatotopic Organization. Human Brain Mapping. 13(2):55–73. doi:doi.org/10.1002/hbm.1025.

Grön G, Wunderlich AP, Spitzer M, Tomczak R, Riepe MW. 2000. Brain activation during human navigation: Gender-different neural networks as substrate of performance. Nature Neuroscience. 3(4):404–408. doi:10.1038/73980.

Guo L, LaDu MJ, Van Eldik LJ. 2004. A dual role for apolipoprotein E in neuroinflammation: anti- and pro-inflammatory activity. Journal of molecular neuroscience : MN. 23(3):205–212. doi:10.1385/JMN:23:3:205.

Guo T, Zhang D, Zeng Y, Huang TY, Xu H, Zhao Y. 2020. Molecular and cellular mechanisms underlying the pathogenesis of Alzheimer's disease. Molecular Neurodegeneration. 15(1):1–37. doi:10.1186/s13024-020-00391-7.

Gur RC, Alsop D, Glahn D, Petty R, Swanson CL, Maldjian JA, Turetsky BI, Detre JA, Gee J, Gur RE. 2000. An fMRI study of sex differences in regional activation to a verbal and a spatial task. Brain and Language. 74(2):157–170. doi:10.1006/brln.2000.2325.

Habas C, Axelrad C, Nguyen T, Cabanis E. 2004. Specific neocerebellar activation during out-of-phase bimanual movements. Neuroreport. 15(4):595–599. doi:10.1097/01.wnr.0000117893.59944.d1.

Habas C, Kamdar N, Nguyen D, Prater K, Beckmann CF, Menon V, Greicius MD. 2009. Distinct cerebellar contributions to intrinsic connectivity networks. Journal of Neuroscience. 29(26):8586–8594. doi:10.1523/JNEUROSCI.1868-09.2009.

Hall JAY, Kimura D. 1995. Sexual Orientation and Performance on Sexually Dimorphic Motor Tasks. Archives of Sexual Behavior. 24(4):395–407. doi:doi.org/10.1007/BF01541855.

Haller S, Montandon ML, Rodriguez C, Ackermann M, Herrmann FR, Giannakopoulos P. 2017. APOE-E4 is associated with gray matter loss in the posterior cingulate cortex in healthy elderly controls subsequently developing subtle cognitive decline. American Journal of Neuroradiology. 38(7):1335–1342. doi:10.3174/ajnr.A5184.

Hampton OL, Buckley RF, Manning LK, Scott MR, Properzi MJ, Peña-Gómez C, Jacobs HIL, Chhatwal JP, Johnson KA, Sperling RA, et al. 2020. Resting-state functional connectivity and amyloid burden influence longitudinal cortical thinning in the default mode network in preclinical Alzheimer's disease. NeuroImage: Clinical. 28:102407. doi:10.1016/j.nicl.2020.102407.

Hashemi RH, Bradley WG, Lisanti CJ. 2012. MRI: The Basics. Lippincott Williams & Wilkins.

Haukvik UK, Tamnes CK, Söderman E, Agartz I. 2018. Neuroimaging hippocampal subfields in schizophrenia and bipolar disorder: A systematic review and meta-analysis. Journal of Psychiatric Research. 104:217–226. doi:10.1016/j.jpsychires.2018.08.012.

Hawkins KM, Goyal AI, Sergio LE. 2015. Diffusion tensor imaging correlates of cognitive-motor decline in normal aging and increased Alzheimer's disease risk. Journal of Alzheimer's Disease. 44(3):867–878. doi:10.3233/JAD-142079.

Hawkins KM, Sayegh P, Yan X, Crawford JD, Sergio LE. 2013. Neural activity in superior parietal cortex during rule-based visual-motor transformations. Journal of Cognitive Neuroscience. 25(3):436–454. doi:10.1162/jocn_a_00318.

Hawkins KM, Sergio LE. 2014. Visuomotor impairments in older adults at increased Alzheimer's disease risk. Journal of Alzheimer's Disease. 42(2):607–621. doi:10.3233/JAD-140051.

Hawkins KM, Sergio LE. 2016. Adults at increased Alzheimer's disease risk diplay cognitive-motor integration impairment associated with changes in resting-state functional connectivity: A preliminary study. Journal of Alzheimer's disease. 53:1161–1172. doi:10.3233/JAD-151137.

Hebert LE, Bienias JL, McCann JJ, Scherr PA, Wilson RS, Evans DA. 2010. Upper and lower extremity motor performance and functional impairment in Alzheimers disease. American Journal of Alzheimer's Disease and other Dementias. 25(5):425–431. doi:10.1177/1533317510367636.

Hedden T, Van Dijk KRA, Becker JA, Mehta A, Sperling RA, Johnson KA, Buckner RL. 2009. Disruption of functional connectivity in clinically normal older adults harboring amyloid burden. Journal of Neuroscience. 29(40):12686–12694. doi:10.1523/JNEUROSCI.3189-09.2009.

Heise V, Filippini N, Trachtenberg AJ, Suri S, Ebmeier KP, Mackay CE. 2014. Apolipoprotein E genotype, gender and age modulate connectivity of the hippocampus in healthy adults. NeuroImage. 98:23–30. doi:10.1016/j.neuroimage.2014.04.081.

Helsen WF, Elliott D, Starkes JL, Ricker KL. 1998. Temporal and spatial coupling of point of gaze and hand movements in aiming. Journal of Motor Behavior. 30(3):249–259. doi:10.1080/00222899809601340.

Henson R, Büchel C, Josephs O, Friston K. 1999. The slice-timing problem in event-related fMRI. NeuroImage. 9:125.

Herbet G, Zemmoura I, Duffau H. 2018. Functional Anatomy of the Inferior Longitudinal Fasciculus: From Historical Reports to Current Hypotheses. Frontiers in Neuroanatomy. 12:1–15. doi:10.3389/fnana.2018.00077.

Honea RA, Swerdlow DRH, Vidoni ED, Goodwin J, Burns BJM. 2010. Reduced gray matter volume in normal adults with a maternal family history of Alzheimer disease. Neurology. 74:113–120. doi:doi.org/10.1212/WNL.0b013e3181c918cb.

Honea RA, Swerdlow RH, Vidoni ED, Burns JM. 2011. Progressive regional atrophy in normal adults with a maternal history of Alzheimer disease. Neurology. 76:822–829. doi:https://doi.org/10.1212/WNL.0b013e31820e7b74.

Honea RA, Vidoni E, Harsha A, Burns JM. 2009. Impact of APOE on the healthy aging brain: A voxel-based MRI and DTI study. Journal of Alzheimer's Disease. 18(3):553–564. doi:10.3233/JAD-2009-1163.

Hong YJ, Kim CM, Jang EH, Hwang J, Roh JH, Lee JH. 2016. White matter changes may precede gray matter loss in elderly with subjective memory impairment. Dementia and Geriatric Cognitive Disorders. 42(3–4):227–235. doi:10.1159/000450749.

Howard IS, Ingram JN, Körding KP, Wolpert DM. 2009. Statistics of natural movements are reflected in motor errors. Journal of Neurophysiology. 102(3):1902–1910. doi:10.1152/jn.00013.2009.

Hoy AR, Ly M, Carlsson CM, Okonkwo OC, Zetterberg H, Blennow K, Sager MA, Asthana S, Johnson SC, Alexander AL, et al. 2017. Microstructural white matter alterations in preclinical Alzheimer's disease detected using free water elimination diffusion tensor imaging. PLoS ONE. 12(3). doi:10.1371/journal.pone.0173982.

Hua K, Zhang J, Wakana S, Jiang H, Li X, Reich DS, Calabresi PA, Pekar JJ, van Zijl PCM, Mori S. 2008. Tract probability maps in stereotaxic spaces: Analyses of white matter anatomy and tract-specific quantification. NeuroImage. 39(1):336–347. doi:10.1016/j.neuroimage.2007.07.053.

Hugenschmidt CE, Peiffer AM, Kraft RA, Casanova R, Deibler AR, Burdette JH, Maldjian JA, Laurienti PJ. 2008. Relating imaging indices of white matter integrity and volume in healthy older adults. Cerebral Cortex. 18(2):433–442. doi:10.1093/cercor/bhm080.

Hurtubise J, Gorbet D, Hamandi Y, Macpherson A, Sergio L. 2016. The effect of concussion history on cognitive-motor integration in elite hockey players. Concussion. 1(3). doi:10.2217/cnc-2016-0006.

Hurtubise JM, Gorbet DJ, Hynes LM, MacPherson AK, Sergio LE. 2020. White Matter Integrity and Its Relationship to Cognitive-Motor Integration in Females with and without Post-Concussion Syndrome. Journal of Neurotrauma. 37(13):1528–1536. doi:10.1089/neu.2019.6765.

Husain M, Nachev P. 2007. Space and the parietal cortex. Trends in Cognitive Sciences. 11(1):30–36. doi:10.1016/j.tics.2006.10.011.

Iglesias JE, Augustinack JC, Nguyen K, Player CM, Player A, Wright M, Roy N, Frosch MP, McKee AC, Wald LL, et al. 2015. A computational atlas of the hippocampal formation using ex vivo, ultra-high resolution MRI: Application to adaptive segmentation of in vivo MRI. NeuroImage. 115:117–137. doi:10.1016/j.neuroimage.2015.04.042.

Immisch I, Waldvogel D, Van Gelderen P, Hallett M. 2001. The role of the medial wall and its anatomical variations for bimanual antiphase and in-phase movements. NeuroImage. 14(3):674–684. doi:10.1006/nimg.2001.0856.

Ingalhalikar M, Smith A, Parker D, Satterthwaite TD, Elliott MA, Ruparel K, Hakonarson H, Gur RE, Gur RC, Verma R. 2014. Sex differences in the structural connectome of the human brain. Proceedings of the National Academy of Sciences of the United States of America. 111(2):823–828. doi:10.1073/pnas.1316909110.

Jack CR, Bennett DA, Blennow K, Carrillo MC, Dunn B, Haeberlein SB, Holtzman DM, Jagust W, Jessen F, Karlawish J, et al. 2018. NIA-AA Research Framework: Toward a biological definition of Alzheimer's disease. Alzheimer's and Dementia. 14(4):535–562. doi:10.1016/j.jalz.2018.02.018.

Jack CR, Bennett DA, Blennow K, Carrillo MC, Feldman HH, Frisoni GB, Hampel H, Jagust WJ, Johnson KA, Knopman DS, et al. 2016. A/T/N: An unbiased descriptive classification scheme for Alzheimer disease biomarkers. Neurology. 87(5):539–547. doi:10.1212/WNL.0000000000002923.

Jack CR, Petersen RC, Xu Y, O'Brien PC, Smith GE, Ivnik RJ, Boeve BF, Tangalos EG, Kokmen E. 2000. Rates of hippocampal atrophy correlate with change in clinical status in aging and AD. Neurology. 55(4):484–489. doi:10.1212/wnl.55.4.484.

Jacobs HIL, Van Boxtel MPJ, Uylings HBM, Gronenschild EHBM, Verhey FR, Jolles J. 2011. Atrophy of the parietal lobe in preclinical dementia. Brain and Cognition. 75(2):154–163. doi:10.1016/j.bandc.2010.11.003.

Jancke L, Peters M, Himmelbach M, Nosselt T, Shah J, Steinmetz H. 2000. fMRI study of bimanual coordination. Neuropsychologia. 38:164–174. doi:doi:10.1016/s0028-3932(99)00062-7.

Jayadev S, Steinbart EJ, Chi YY, Kukull WA, Schellenberg GD, Bird TD. 2008. Conjugal Alzheimer disease: Risk in children when both parents have Alzheimer disease. Archives of Neurology. 65(3):373–378. doi:10.1001/archneurol.2007.61.

Jo HJ, Saad ZS, Simmons WK, Milbury LA, Cox RW. 2010. Mapping sources of correlation in resting state FMRI, with artifact detection and removal. NeuroImage. 52(2):571–582. doi:10.1016/j.neuroimage.2010.04.246.

Johansen-Berg H, Della-Maggiore V, Behrens TEJ, Smith SM, Paus T. 2007. Integrity of white matter in the corpus callosum correlates with bimanual co-ordination skills. NeuroImage. 36(SUPPL. 2). doi:10.1016/j.neuroimage.2007.03.041.

Johnson PB, Ferraina S, Bianchi L, Caminiti R. 1996. Cortical networks for visual reaching: Physiological and anatomical organization of frontal and parietal lobe arm regions. Cerebral Cortex. 6(2):102–119. doi:10.1093/cercor/6.2.102.

Jordan K, Wüstenberg T, Heinze H-J, Peters M, Jäncke L. 2002. Women and men exhibit different cortical activation patterns during mental rotation tasks. Neuropsychologia. 40:2397–2408. doi:doi.org/10.1016/S0028-3932(02)00076-3.

Kakei S, Hoffman DS, Strick PL. 2003. Sensorimotor transformations in cortical motor areas. Neuroscience Research. 46(1):1–10. doi:10.1016/S0168-0102(03)00031-2.

Kalaska JF. 1996. Parietal cortex area 5 and visuomotor behavior. Canadian Journal of Physiology and Pharmacology. 74(4):483–498. doi:10.1139/y96-040.

Kalaska JF, Crammond DJ. 1992. Cerebral cortical mechanisms of reaching movements. Science. 255(5051):1517–1523. doi:10.1126/science.1549781.

Kalaska JF, Scott SH, Cisek P, Sergio LE. 1997. Cortical control of reaching movements. Current Opinion in Neurobiology. 7(6):849–859. doi:10.1016/S0959-4388(97)80146-8.

Kalaska JF, Sergio LE, Cisek P. 1998. Cortical control of whole-arm motor tasks. Novartis Foundation Symposium. 218(218):176–201. doi:10.1002/9780470515563.ch10.

Kamboh MI. 2004. Molecular genetics of late-onset Alzheimer's disease. Annals of Human Genetics. 68(4):381–404. doi:10.1046/j.1529-8817.2004.00110.x.

Kang N, Cauraugh JH. 2014. Force control improvements in chronic stroke: Bimanual coordination and motor synergy evidence after coupled bimanual movement training. Experimental Brain Research. 232(2):503–513. doi:10.1007/s00221-013-3758-z.

Kantarci K, Avula R, Senjem ML, Samikoglu AR, Zhang B, Weigand SD, Przybelski SA, Edmonson HA, Vemuri P, Knopman DS, et al. 2010. Dementia with Lewy bodies and

Alzheimer disease: Neurodegenerative patterns characterized by DTI. Neurology. 74(22):1814–1821. doi:10.1212/WNL.0b013e3181e0f7cf.

Kantarci K, Schwarz CG, Reid RI, Przybelski SA, Lesnick TG, Zuk SM, Senjem ML, Gunter JL, Lowe V, Machulda MM, et al. 2014. White matter integrity determined with diffusion tensor imaging in older adults without dementia: Influence of amyloid load and neurodegeneration. JAMA Neurology. 71(12):1547–1554. doi:10.1001/jamaneurol.2014.1482.

Karch CM, Cruchaga C, Goate AM. 2014. Alzheimer's disease genetics: From the bench to the clinic. Neuron. 83(1):11–26. doi:10.1016/j.neuron.2014.05.041.

Karch CM, Goate AM. 2015. Alzheimer's disease risk genes and mechanisms of disease pathogenesis. Biological Psychiatry. 77(1):43–51. doi:10.1016/j.biopsych.2014.05.006.

Kawashima R, Yamada K, Kinomura S, Yamaguchi T, Matsui H, Yoshioka S, Fukuda H. 1993. Regional cerebral blood flow changes of cortical motor areas and prefrontal areas in humans related to ipsilateral and contralateral hand movement. Brain Research. 623:33–40. doi:doi.org/10.1016/0006-8993(93)90006-9.

Kelly RM, Strick PL. 2003. Behavioral/Systems/Cognitive Cerebellar Loops with Motor Cortex and Prefrontal Cortex of a Nonhuman Primate. Journal of Neuroscience. 23(23):8432–8444. doi:doi.org/10.1523/JNEUROSCI.23-23-08432.2003.

Kelso J. 1984. Phase transitions and critical behavior in human bimanual coordination. American Journal of Physiology-Regulatory, Integrative and Comparative Physiology. 246(6):R1000–R1004. doi:doi.org/10.1152/ajpregu.1984.246.6.R1000.

Kelso J, Scholz JP, Schoner G. 1986. Nonequilibrium phase transitions in coordinated biological motion: critical fluctuations. Physics Letters A. 118(6):279–284. doi:doi.org/10.1016/0375-9601(86)90359-2.

Kelso J, Southard DL, Goodman D. 1979. On the coordination of two-handed movements. Journal of Experimental Psychology: Human Perception and Performance. 5(2):229–238. doi:doi.org/10.1037/0096-1523.5.2.229.

Ketcham CJ, Seidler RD, Van Gemmert AW, Stelmach GE. 2002. Age-related kinematic differences as influenced by task difficulty, target size, and movement amplitude. Journals of Gerontology - Series B Psychological Sciences and Social Sciences. 57(1):54–64. doi:10.1093/geronb/57.1.P54.

Khanjari Y, Arabameri E. 2021. Investigating the Asymmetric Bimanual Coordination Differences in Male and Female Athletes in Ball and Non-ball Sports. Journal of Sport Biomechanics. 6(4):250–263. doi:10.32598/biomechanics.6.3.4.

Kilbreath SL, Heard RC. 2005. Frequency of hand use in healthy older persons. Australian Journal of Physiotherapy. 51(2):119–122. doi:10.1016/S0004-9514(05)70040-4.

Kim J, Basak JM, Holtzman DM. 2009. The role of Apolipoprotein E in Alzheimer's disease. Neuron. 63(3):287–303. doi:10.1016/j.neuron.2009.06.026.

Kim JH, Lee JM, Jo HJ, Kim SH, Lee JH, Kim ST, Seo SW, Cox RW, Na DL, Kim SI, et al. 2010. Defining functional SMA and pre-SMA subregions in human MFC using resting state fMRI: Functional connectivity-based parcellation method. NeuroImage. 49(3):2375–2386. doi:10.1016/j.neuroimage.2009.10.016.

Kim S-G, Ashe J, Hendrich K, Ellermann JM, Merkle H, Uğurbil K, Georgopoulos AP. 1993. Functional Magnetic Resonance Imaging of Motor Cortex: Hemispheric Asymmetry and Handedness. New Series. 261(5121):615–617. doi:doi:10.1126/science.8342027.

Kimura D. 1993. Neuromotor Mechanisms in Human Communication. Oxford: Oxford University Press.

Kiyama S, Kunimi M, Lidaka T, Nakai T. 2014. Distant functional connectivity for bimanual finger coordination declines with aging: An fMRI and SEM exploration. Frontiers in Human Neuroscience. 8(1). doi:10.3389/fnhum.2014.00251.

Klein AP, Ulmer JL, Quinet SA, Mathews V, Mark LP. 2016. Nonmotor functions of the cerebellum: An introduction. American Journal of Neuroradiology. 37(6):1005–1009. doi:10.3174/ajnr.A4720.

Kobayashi Y, Amaral D. 2007. Macaque monkey retrosplenial cortex: III. Cortical efferents. Journal of Comparative Neurology. 502:810–833. doi:10.1002/cne.

Kraft E, Chen AW, Flaherty AW, Blood AJ, Kwong KK, Jenkins BG. 2007. The role of the basal ganglia in bimanual coordination. Brain Research. 1151(1):62–73. doi:10.1016/j.brainres.2007.01.142.

Krienen FM, Buckner RL. 2009. Segregated fronto-cerebellar circuits revealed by intrinsic functional connectivity. Cerebral Cortex. 19(10):2485–2497. doi:10.1093/cercor/bhp135.

Kubicki M, McCarley R, Westin CF, Park HJ, Maier S, Kikinis R, Jolesz FA, Shenton ME. 2007. A review of diffusion tensor imaging studies in schizophrenia. Journal of Psychiatric Research. 41(1–2):15–30. doi:10.1016/j.jpsychires.2005.05.005.

Kühn S, Musso F, Mobascher A, Warbrick T, Winterer G, Gallinat J. 2012. Hippocampal subfields predict positive symptoms in schizophrenia: First evidence from brain morphometry. Translational Psychiatry. 2(6):e127. doi:10.1038/tp.2012.51.

Lackner JR, Dizio P. 1994. Rapid adaptation to Coriolis force perturbations of arm trajectory. Journal of Neurophysiology. 72(1):299–313. doi:10.1152/jn.1994.72.1.299.

LaDu MJ, Falduto MT, Manelli AM, Reardon CA, Getz GS, Frail DE. 1994. Isoform-specific binding of apolipoprotein E to β-amyloid. Journal of Biological Chemistry. 269(38):23403–23406. doi:doi.org/10.1016/S0021-9258(17)31529-6.

LaDu MJ, Lukens JR, Reardon CA, Getz GS. 1997. Association of human, rat, and rabbit apolipoprotein E with β-amyloid. Journal of Neuroscience Research. 49(1):9–18. doi:10.1002/(SICI)1097-4547(19970701)49:1<9::AID-JNR2>3.0.CO;2-H.

LaDu MJ, Shah JA, Reardon CA, Getz GS, Bu G, Hu J, Guo L, Van Eldik LJ. 2000. Apolipoprotein E receptors mediate the effects of β-amyloid on astrocyte cultures. Journal of Biological Chemistry. 275(43):33974–33980. doi:10.1074/jbc.M000602200.

Lahiri D, Maloney B, Riyaz Basha M, Wen Ge Y, Zawia N. 2007. How and when environmental agents and dietary factors affect the course of Alzheimer's disease: the "LEARn" model (latent early-life associated regulation) may explain the triggering of AD. Current Alzheimer Research. 4(2):219–228. doi:10.2174/156720507780362164.

Lang L, Clifford A, Wei L, Zhang D, Leung D, Augustine G, Danat IM, Zhou W, Copeland JR, Anstey KJ, et al. 2017. Prevalence and determinants of undetected dementia in the community: a systematic literature review and a meta-analysis. Open. 7:11146. doi:10.1136/bmjopen-2016.

Larson EB, Burnison DS, Brown WS. 2002. Callosal Function in Multiple Sclerosis: Bimanual Motor Coordination. Cortex. 38(2):201–214. doi:doi.org/10.1016/S0010-9452(08)70650-6.

Lautenschlager NT, Cupples LA, Rao VS, Auerbach SA, Becker R, Burke J, Chui H, Duara R, Foley EJ, Glatt SL, et al. 1996. Risk of dementia among relatives of Alzheimer's disease patients in the MIRAGE study: What is in store for the oldest old? Neurology. 46(3):641–650. doi:10.1212/WNL.46.3.641.

Laws KR, Irvine K, Gale TM. 2018. Sex differences in Alzheimer's disease. Current Opinion in Psychiatry. 31(2):133–139. doi:10.1097/YCO.0000000000000401.

Lee TD, Swinnen SP, Verschueren S. 1995. Relative phase alterations during bimanual skill acquisition. Journal of Motor Behavior. 27(3):263–274. doi:10.1080/00222895.1995.9941716.

Lesourd M, Le Gall D, Baumard J, Croisile B, Jarry C, Osiurak F. 2013. Apraxia and Alzheimer's disease: Review and perspectives. Neuropsychology Review. 23(3):234–256. doi:10.1007/s11065-013-9235-4.

Li A, Yetkin FZ, Cox R, Haughton VM. 1996. Ipsilateral Hemisphere Activation during Motor and Sensory Tasks. American Journal of Neuroradiology. 17(4):651–655.

Li JQ, Tan Lan, Wang HF, Tan MS, Tan Lin, Xu W, Zhao QF, Wang J, Jiang T, Yu JT. 2016. Risk factors for predicting progression from mild cognitive impairment to Alzheimer's disease: A systematic review and meta-analysis of cohort studies. Journal of Neurology, Neurosurgery and Psychiatry. 87(5):476–484. doi:10.1136/jnnp-2014-310095.

Li R, Wu X, Fleisher AS, Reiman EM, Chen K, Yao L. 2012. Attention-related networks in Alzheimer's disease: A resting functional MRI study. Human Brain Mapping. 33(5):1076–1088. doi:10.1002/hbm.21269.

Liang Y, Li Z, Wei J, Li C, Zhang X. 2017. Frequency Specific Effects of ApoE ϵ 4 Allele on Resting-State Networks in Nondemented Elders. BioMed Research International. doi:10.1155/2017/9823501.

Lin Q, Li H, Mao YR, Lo WL, Zhao JL, Chen L, Leng Y, Huang DF, Li L. 2017. The Difference of Neural Networks between Bimanual Antiphase and In-Phase Upper Limb Movements: A Preliminary Functional Magnetic Resonance Imaging Study. Behavioural Neurology. doi:10.1155/2017/8041962.

Lissek S, Hausmann M, Knossalla F, Peters S, Nicolas V, Güntürkün O, Tegenthoff M. 2007. Sex differences in cortical and subcortical recruitment during simple and complex motor control: An fMRI study. NeuroImage. 37(3):912–926. doi:10.1016/j.neuroimage.2007.05.037.

Litke R, Garcharna LC, Jiwani S, Neugroschl J. 2021. Modifiable Risk Factors in Alzheimer Disease and Related Dementias: A Review. Clinical Therapeutics. 43(6):953–965. doi:10.1016/j.clinthera.2021.05.006.

Liu CC, Kanekiyo T, Xu H, Bu G. 2013. Apolipoprotein E and Alzheimer disease: Risk, mechanisms and therapy. Nature Reviews Neurology. 9(2):106–118. doi:10.1038/nrneurol.2012.263.

Liu H, Stufflebeam SM, Sepulcre J, Hedden T, Buckner RL, Raichle ME. 2009. Evidence from intrinsic activity that asymmetry of the human brain is controlled by multiple factors. Proceedings of the national academy of sciences. 106(48):20499–20503. doi:doi.org/10.1073/pnas.0908073106.

Livingston G, Huntley J, Sommerlad A, Ames D, Ballard C, Banerjee S, Brayne C, Burns A, Cohen-Mansfield J, Cooper C, et al. 2020. Dementia prevention, intervention, and care: 2020 report of the Lancet Commission. Lancet. 396(10248):413–446. doi:10.1016/S0140-6736(20)30367-6.

López-Sanz D, Bruña R, Garcés P, Martín-Buro MC, Walter S, Delgado ML, Montenegro M, Higes RL, Marcos A, Maestú F. 2017. Functional connectivity disruption in subjective cognitive decline and mild cognitive impairment: A common pattern of alterations. Frontiers in Aging Neuroscience. 9. doi:10.3389/fnagi.2017.00109.

Lu K, Nicholas JM, Weston PSJ, Stout JC, O'Regan AM, James S-N, Buchanan SM, Lane CA, Parker TD, Keuss SE, et al. 2021. Visuomotor integration deficits are common to familial and sporadic preclinical Alzheimer's disease. Brain Communications. 3(1):1–12. doi:10.1093/braincomms/fcab003.

Lustig C, Snyder AZ, Bhakta M, O'Brien KC, McAvoy M, Raichle ME, Morris JC, Buckner RL. 2003. Functional deactivations: Change with age and dementia of the Alzheimer type. Proceedings of the National Academy of Sciences of the United States of America. 100:14504–14509. doi:10.1073/pnas.2235925100.

Machulda MM, Jones DT, Vemuri P, McDade E, Avula R, Przybelski S, Boeve BF, Knopman DS, Petersen RC, Jack CR. 2011. Effect of APOE ε4 status on intrinsic network connectivity in cognitively normal elderly subjects. Archives of Neurology. 68(9):1131–1136. doi:10.1001/archneurol.2011.108.

Madan CR. 2018. Age differences in head motion and estimates of cortical morphology. PeerJ. 6(7):e5176. doi:10.7717/peerj.5176.

Madden DJ, Bennett IJ, Burzynska A, Potter GG, Chen N kuei, Song AW. 2012. Diffusion tensor imaging of cerebral white matter integrity in cognitive aging. Biochimica et Biophysica Acta - Molecular Basis of Disease. 1822(3):386–400. doi:10.1016/j.bbadis.2011.08.003.

Mahley RW, Rall SC. 2000. Apolipoprotein E: Far more than a lipid transport protein. Annual Review of Genomics and Human Genetics. 1(1):507–537. doi:10.1146/annurev.genom.1.1.507.

Manelli AM, Stine WB, Van Eldik LJ, LaDu MJ. 2004. ApoE and Abeta1-42 interactions: effects of isoform and conformation on structure and function. Journal of molecular neuroscience. 23(3):235–246. doi:10.1385/JMN:23:3:235.

Manto M, Bower JM, Conforto AB, Delgado-García JM, Da Guarda SNF, Gerwig M, Habas C, Hagura N, Ivry RB, Marien P, et al. 2012. Roles of the cerebellum in motor control-the diversity of ideas on cerebellar involvement in movement. Cerebellum. 11(2):457–487. doi:10.1007/s12311-011-0331-9.

Márquez F, Yassa MA. 2019. Neuroimaging biomarkers for Alzheimer's disease. Molecular Neurodegeneration. 14(21):1–14. doi:10.1186/s13024-019-0325-5.

Mathalon DH, Sullivan EV, Rawles JM, Pfefferbaum A. 1993. Correction for Head Size in Brain-Imaging Measurements. Psychiatry Research: Neuroimaging. 50(2):121–139. doi:doi:10.1016/0925-4927(93)90016-b.

Mattson MP. 2004. Pathways towards and away from Alzheimer's disease. Nature. 430(7000):631–639. doi:10.1038/nature02621.

Mayo CD, Garcia-Barrera MA, Mazerolle EL, Ritchie LJ, Fisk JD, Gawryluk JR. 2019. Relationship between DTI metrics and cognitive function in Alzheimer's disease. Frontiers in Aging Neuroscience. 11:436. doi:10.3389/fnagi.2018.00436.

Mcdonough IM, Wood MM, Miller WS. 2019. A Review on the Trajectory of Attentional Mechanisms in Aging and the Alzheimer's Disease Continuum through the Attention Network Test. Yale Journal of Biology and Medicine. 92:37–51.

McDougle SD, Bond KM, Taylor JA. 2015. Explicit and implicit processes constitute the fast and slow processes of sensorimotor learning. Journal of Neuroscience. 35(26):9568–9579. doi:10.1523/JNEUROSCI.5061-14.2015.

McKenna F, Koo BB, Killiany R, for the Alzheimer's Disease Neuroimaging Initiative. 2016. Comparison of ApoE-related brain connectivity differences in early MCI and normal aging populations: an fMRI study. Brain Imaging and Behavior. 10(4):970–983. doi:10.1007/s11682-015-9451-z.

Mechsner F, Kerzel D, Knoblich G, Prinz W. 2001. Perceptual basis of bimanual coordination. Nature. 414(6859):69–73. doi:doi.org/10.1038/35102060.

Mechsner F, Knoblich G. 2004. Do muscles matter for coordinated action? Journal of Experimental Psychology: Human Perception and Performance. 30(3):490–503. doi:10.1037/0096-1523.30.3.490.

Meguro K, Blaizot X, Kondoh Y, Le Mestric C, Baron JC, Chavoix C. 1999. Neocortical and hippocampal glucose hypometabolism following neurotoxic lesions of the entorhinal and perirhinal cortices in the non-human primate as shown by PET Implications for Alzheimer's disease. Brain. 122:1519–1531. doi:doi.org/10.1093/brain/122.8.1519.

Mickevičienė D, Motiejūnaitė K, Karanauskienė D, Skurvydas A, Vizbaraitė D, Krutulytė G, Rimdeikienė I. 2011. Gender-Dependent Bimanual Task Performance. Investigations Medicina (Kaunas). 47(9):497–503. doi:doi.org/10.3390/medicina47090073.

Milà-Alomà M, Suárez-Calvet M, Molinuevo JL. 2019. Latest advances in cerebrospinal fluid and blood biomarkers of Alzheimer's disease. Therapeutic Advances in Neurological Disorders. 12:1756286419888819. doi:10.1177/1756286419888819.

Miller SL, Celone K, DePeau K, Diamond E, Dickerson BC, Rentz D, Pihlajamäki M, Sperling RA. 2008. Age-related memory impairment associated with loss of parietal deactivation but preserved hippocampal activation. Proceedings of the National Academy of Sciences of the United States of America. 105(6):2181–2186. doi:10.1073/pnas.0706818105.

Mintun MA, Larossa GN, Sheline YI, Dence CS, Lee SY, MacH RH, Klunk WE, Mathis CA, Dekosky ST, Morris JC. 2006. [11C]PIB in a nondemented population: Potential antecedent marker of Alzheimer disease. Neurology. 67(3):446–452. doi:10.1212/01.wnl.0000228230.26044.a4.

Molloy CJ, Nugent S, Bokde ALW. 2021. Alterations in diffusion measures of white matter integrity associated with healthy aging. Journals of Gerontology: Biological Sciences. 76(6):945–954. doi:10.1093/gerona/glz289.

Mormino EC, Kluth JT, Madison CM, Rabinovici GD, Baker SL, Miller BL, Koeppe RA, Mathis CA, Weiner MW, Jagust WJ. 2009. Episodic memory loss is related to hippocampal-mediated β-amyloid deposition in elderly subjects. Brain. 132(5):1310–1323. doi:10.1093/brain/awn320.

Mormino EC, Smiljic A, Hayenga AO, H. Onami S, Greicius MD, Rabinovici GD, Janabi M, Baker SL, V. Yen I, Madison CM, et al. 2011. Relationships between beta-amyloid and functional connectivity in different components of the default mode network in aging. Cerebral Cortex. 21(10):2399–2407. doi:10.1093/cercor/bhr025.

Morris JC. 2005. Early-stage and preclinical Alzheimer disease. Alzheimer Disease and Associated Disorders. 19(3):163–165. doi:10.1097/01.wad.0000184005.22611.cc.

Mosconi L. 2005. Brain glucose metabolism in the early and specific diagnosis of Alzheimer's disease: FDG-PET studies in MCI and AD. European Journal of Nuclear Medicine and Molecular Imaging. 32(4):486–510. doi:10.1007/s00259-005-1762-7.

Mosconi L, Berti V, Swerdlow RH, Pupi A, Duara R, de Leon M. 2010. Maternal transmission of Alzheimer's disease: prodromal metabolic phenotype and the search for genes. Human genomics. 4(3):170–193. doi:10.1186/1479-7364-4-3-170.

Mosconi L, Brys M, Switalski R, Mistur R, Glodzik L, Pirraglia E, Tsui W, De Santi S, de Leon MJ. 2007. Maternal family history of Alzheimer's disease predisposes to reduced

brain glucose metabolism. Proceedings of the National Academy of Sciences. 104(48):19067–19072. doi:10.1073/pnas.0705036104.

Mosconi L, Murray J, Tsui W, Li Y, Spector N, Goldowsky A, Williams S, Osorio R, McHugh P, Glodzik L, et al. 2014. Brain imaging of cognitively normal individuals with 2 parents affected by late-onset AD. Neurology. 82(9):752–760. doi:10.1212/WNL.0000000000000181.

Mowinckel AM, Vidal-Piñeiro D. 2020. Visualization of Brain Statistics With R Packages ggseg and ggseg3d. Advances in Methods and Practices in Psychological Science. 3(4):466–483. doi:10.1177/2515245920928009.

Muetzel RL, Collins PF, Mueller BA, M. Schissel A, Lim KO, Luciana M. 2008. The development of corpus callosum microstructure and associations with bimanual task performance in healthy adolescents. NeuroImage. 39(4):1918–1925. doi:10.1016/j.neuroimage.2007.10.018.

Munoz DP, Broughton JR, Goldring JE, Armstrong IT. 1998. Age-related performance of human subjects on saccadic eye movement tasks. Experimental Brain Research. 121(4):391–400. doi:10.1007/s002210050473.

Murray EA, Bussey TJ, Wise SP. 2000. Role of prefrontal cortex in a network for arbitrary visuomotor mapping. Experimental Brain Research. 133(1):114–129. doi:10.1007/s002210000406.

Mutha PK, Sainburg RL, Haaland KY. 2011. Left parietal regions are critical for adaptive visuomotor control. Journal of Neuroscience. 31(19):6972–6981. doi:10.1523/JNEUROSCI.6432-10.2011.

Nabers A, Perna L, Lange J, Mons U, Schartner J, Güldenhaupt J, Saum K, Janelidze S, Holleczek B, Rujescu D, et al. 2018. Amyloid blood biomarker detects Alzheimer's disease. EMBO Molecular Medicine. 10(5). doi:10.15252/emmm.201708763.

Nair DG, Purcott KL, Fuchs A, Steinberg F, Kelso JAS. 2003. Cortical and cerebellar activity of the human brain during imagined and executed unimanual and bimanual action sequences: a functional MRI study. Cognitive Brain Research. 15:250–260. doi:doi.org/10.1016/S0926-6410(02)00197-0.

Nathan BP, Chang KC, Bellosta S, Brisch E, Ge N, Mahley RW, Pitas RE. 1995. The inhibitory effect of apolipoprotein E4 on neurite outgrowth is associated with microtubule depolymerization. Journal of Biological Chemistry. 270(34):19791–19799. doi:10.1074/jbc.270.34.19791.

Neggers S, Bekkering H, Bekkering Ocular H. 2000. Ocular Gaze is Anchored to the Target of an Ongoing Pointing Movement. Journal of Neurophysiology. 83(2):639–651. doi:doi.org/10.1152/jn.2000.83.2.639.

Nestor PJ, Fryer TD, Ikeda M, Hodges JR. 2003. Retrosplenial cortex (BA 29/30) hypometabolism in mild cognitive impairment (prodromal Alzheimer's disease). European Journal of Neuroscience. 18(9):2663–2667. doi:10.1046/j.1460-9568.2003.02999.x.

Nierenberg J, Pomara N, Hoptman MJ, Sidtis JJ, Ardekani BA, Lim KO. 2005. Abnormal white matter integrity in healthy apolipoprotein E epsilon4 carriers. NeuroReport. 16(12):1369–1372. doi:10.1097/01.wnr.0000174058.49521.16.

Nir T, Prasad G, Joshi S, Villalon J, Jahanshad N, Toga A, Jack C, Weiner M, Thompson P. 2012. Predicting future brain atrophy from DTI-based maximum density path analysis in mild cognitive impairment and Alzheimer's disease. Medical Image Computing and Computer-Assisted Intervention Workshop on Novel Imaging Biomarkers for Alzheimer's Disease and Related Disorders.:178–189.

Nowrangi MA, Lyketsos CG, Leoutsakos JMS, Oishi K, Albert M, Mori S, Mielke MM. 2013. Longitudinal, region-specific course of diffusion tensor imaging measures in mild cognitive impairment and Alzheimer's disease. Alzheimer's and Dementia. 9(5):519–528. doi:10.1016/j.jalz.2012.05.2186.

O'Brien LM, Ziegler DA, Deutsch CK, Frazier JA, Herbert MR, Locascio JJ. 2011. Statistical adjustments for brain size in volumetric neuroimaging studies: Some practical implications in methods. Psychiatry Research - Neuroimaging. 193(2):113–122. doi:10.1016/j.pscychresns.2011.01.007.

O'Donnell LJ, Westin C-F. 2011. An Introduction to Diffusion Tensor Image Analysis. Neurosurgery Clinics of North America. 22(2):185–196. doi:10.1016/j.nec.2010.12.004.

O'Dwyer L, Lamberton F, Matura S, Tanner C, Scheibe M, Miller J, Rujescu D, Prvulovic D, Hampel H. 2012. Reduced Hippocampal Volume in Healthy Young ApoE4 Carriers: An MRI Study. PLoS ONE. 7(11). doi:10.1371/journal.pone.0048895.

Oldfield R. 1971. The assessment and analysis of handedness: the Edinburgh inventory. Neuropsychologia. 9(1):97–113. doi:https://doi.org/10.1016/0028-3932(71)90067-4.

Operto G, Cacciaglia R, Grau-Rivera O, Falcon C, Brugulat-Serrat A, Ródenas P, Ramos R, Morán S, Esteller M, Bargalló N, et al. 2018. White matter microstructure is altered in cognitively normal middle-aged APOE-ϵ4 homozygotes. Alzheimer's Research and Therapy. 10(1). doi:10.1186/s13195-018-0375-x.

Otto POM, Oeckl P, Otto ÁM. 2019. A Review on MS-Based Blood Biomarkers for Alzheimer's Disease. Neurology and Therapy. 8(2):113–127. doi:10.6084/m9.figshare.9792635.

Ou YN, Xu W, Li JQ, Guo Y, Cui M, Chen KL, Huang YY, Dong Q, Tan L, Yu JT. 2019. FDG-PET as an independent biomarker for Alzheimer's biological diagnosis: A longitudinal study. Alzheimer's Research and Therapy. 11(1):1–11. doi:10.1186/s13195-019-0512-1.

Palmqvist S, Schöll M, Strandberg O, Mattsson N, Stomrud E, Zetterberg H, Blennow K, Landau S, Jagust W, Hansson O. 2017. Earliest accumulation of β-amyloid occurs within the default-mode network and concurrently affects brain connectivity. Nature Communications. 8(1). doi:10.1038/s41467-017-01150-x.

Pardoe HR, Kucharsky Hiess R, Kuzniecky R. 2016. Motion and morphometry in clinical and nonclinical populations. NeuroImage. 135:177–185. doi:10.1016/j.neuroimage.2016.05.005.

Parker TD, Cash DM, Lane CAS, Lu K, Malone IB, Nicholas JM, James SN, Keshavan A, Murray-Smith H, Wong A, et al. 2019. Hippocampal subfield volumes and preclinical Alzheimer's disease in 408 cognitively normal adults born in 1946. PLoS ONE. 14(10). doi:10.1371/journal.pone.0224030.

Parvizi J, Van Hoesen GW, Buckwalter J, Damasio A. 2006. Neural connections of the posteromedial cortex in the macaque. Proceedings of the National Academy of Sciences of the United States of America. 103(5):1563–1568. doi:10.1073/pnas.0507729103.

Patel KT, Stevens MC, Pearlson GD, Winkler AM, Hawkins KA, Skudlarski P, Bauer LO. 2013. Default mode network activity and white matter integrity in healthy middle-aged ApoE4 carriers. Brain Imaging and Behavior. 7(1):60–67. doi:10.1007/s11682-012-9187-y.

Patel VR, Zee DS. 2015. The cerebellum in eye movement control: Nystagmus, coordinate frames and disconjugacy. Eye. 29(2):191–195. doi:10.1038/eye.2014.271.

Pennanen C, Kivipelto M, Tuomainen S, Hartikainen P, Hänninen T, Laakso MP, Hallikainen M, Vanhanen M, Nissinen A, Helkala EL, et al. 2004. Hippocampus and entorhinal cortex in mild cognitive impairment and early AD. Neurobiology of Aging. 25(3):303–310. doi:10.1016/S0197-4580(03)00084-8.

Peraza LR, Díaz-Parra A, Kennion O, Moratal D, Taylor JP, Kaiser M, Bauer R. 2019. Structural connectivity centrality changes mark the path toward Alzheimer's disease. Alzheimer's and Dementia: Diagnosis, Assessment and Disease Monitoring. 11:98–107. doi:10.1016/j.dadm.2018.12.004.

Peters M. 1977. Simultaneous performance of two motor activities: The factor of timing. Neuropsychologia. 15:461–465. doi:doi.org/10.1016/0028-3932(77)90099-9.

Pfefferbaum A, Sullivan EV, Hedehus M, Lim KO, Adalsteinsson E, Moseley M. 2000. Age-Related Decline in Brain White Matter Anisotropy Measured With Spatially Corrected Echo-Planar Diffusion Tensor Imaging. Magnetic Resonance in Medicine. 44:259–268. doi:doi.org/10.1002/1522-2594(200008)44:2<259::AID-MRM13>3.0.CO;2-6.

Pierpaoli C, Basser PJ. 1996. Toward a quantitative assessment of diffusion anisotropy. Magn Reson Med. 36(6):893–906. doi:10.1002/mrm.1910360612.

Pletnikova O, Kageyama Y, Rudow G, LaClair KD, Albert M, Crain BJ, Tian J, Fowler D, Troncoso JC. 2018. The spectrum of preclinical Alzheimer's disease pathology and its modulation by ApoE genotype. Neurobiology of Aging. 71:72–80. doi:10.1016/j.neurobiolaging.2018.07.007.

Poirier J, Bertrand P, Poirier J, Kogan S, Gauthier S, Poirier J, Gauthier S, Davignon J, Bouthillier D, Davignon J. 1993. Apolipoprotein E polymorphism and Alzheimer's disease. The Lancet. 342(8873):697–699. doi:10.1016/0140-6736(93)91705-Q.

Power JD, Mitra A, Laumann TO, Snyder AZ, Schlaggar BL, Petersen SE. 2014. Methods to detect, characterize, and remove motion artifact in resting state fMRI. NeuroImage. 84:320–341. doi:10.1016/j.neuroimage.2013.08.048.

Prescott JW, Guidon A, Doraiswamy PM, Choudhury KR, Liu C, Petrella JR. 2014. The alzheimer structural connectome: Changes in cortical network topology with increased amyloid plaque burden. Radiology. 273(1):175–184. doi:10.1148/radiol.14132593.

Prince M, Knapp M, Guerchet M, McCrone P, Prina M, Comas-Herrera A, Wittenberg R, Adelaja B, Hu B, King D, et al. 2014. Dementia UK: Update. Alzheimer's Society.

Public Health Agency of Canada. 2017. Dementia in Canada, including Alzheimer's disease.

Qian S, Zhang Z, Li B, Sun G. 2015. Functional-structural degeneration in dorsal and ventral attention systems for Alzheimer's disease, amnestic mild cognitive impairment. Brain Imaging and Behavior. 9(4):790–800. doi:10.1007/s11682-014-9336-6.

R Core Team. 2021. R: A language and environment for statistical computing. http://www.r-project.org/.

Rabin JS, Perea RD, Buckley RF, Neal TE, Buckner RL, Johnson KA, Sperling RA, Hedden T. 2019. Global white matter diffusion characteristics predict longitudinal cognitive change independently of amyloid status in clinically normal older adults. Cerebral Cortex. 29(3):1251–1262. doi:10.1093/cercor/bhy031.

Raichle ME, MacLeod AM, Snyder AZ, Powers WJ, Gusnard DA, Shulman GL. 2001. A default mode of brain function. Proceedings of the National Academy of Sciences of the United States of America. 98(2):676–682. doi:10.1073/pnas.98.2.676.

Räihä I, Kaprio J, Koskenvuo M, Rajala T, Sourander L. 1996. Alzheimer's disease in Finnish twins. Lancet. 347(9001):573–578. doi:10.1016/S0140-6736(96)91272-6.

Ramnani N, Toni I, Passingham RE, Haggard P. 2001. The cerebellum and parietal cortex play a specific role in coordination: A pet study. NeuroImage. 14(4):899–911. doi:10.1006/nimg.2001.0885.

Raz N, Lindenberger U, Rodrigue KM, Kennedy KM, Head D, Williamson A, Dahle C, Gerstorf D, Acker JD. 2005. Regional brain changes in aging healthy adults: General trends, individual differences and modifiers. Cerebral Cortex. 15(11):1676–1689. doi:10.1093/cercor/bhi044.

Rebeck GW, Reiter JS, Strickland DK, Hyman BT. 1993. Apolipoprotein E in Sporadic Alzheimer's Disease: Allelic Variation and Receptor Interactions. Neuron. 11:575–580. doi:doi.org/10.1016/0896-6273(93)90070-8.

Redding GM, Rossetti Y, Wallace B. 2005. Applications of prism adaptation: A tutorial in theory and method. Neuroscience and Biobehavioral Reviews. 29(3):431–444. doi:10.1016/j.neubiorev.2004.12.004.

Redding GM, Wallace B. 1996. Adaptive spatial alignment and strategic perceptual-motor control. Journal of Experimental Psychology: Human Perception and Performance. 22(2):379–394. doi:10.1037/0096-1523.22.2.379.

Reiman EM, Chen K, Liu X, Bandy D, Yu M, Lee W, Ayutyanont N, Keppler J, Reeder SA, Langbaum JBS, et al. 2009. Fibrillar amyloid-burden in cognitively normal people at 3 levels of genetic risk for Alzheimer's disease. Proceedings of the National Academy of Sciences. 106(16):6820–6825. doi:doi.org/10.1073/pnas.0900345106.

Reitz C, Mayeux R. 2014. Alzheimer disease: Epidemiology, diagnostic criteria, risk factors and biomarkers. Biochemical Pharmacology. 88(4):640–651. doi:10.1016/j.bcp.2013.12.024.

Rice L, Bisdas S. 2017. The diagnostic value of FDG and amyloid PET in Alzheimer's disease—A systematic review. European Journal of Radiology. 94:16–24. doi:10.1016/j.ejrad.2017.07.014.

Richards TL, Berninger VW, Stock P, Altemeier L, Trivedi P, Maravilla K. 2009. Functional magnetic resonance imaging sequential-finger movement activation differentiating good and poor writers. Journal of Clinical and Experimental Neuropsychology. 31(8):967–983. doi:10.1080/13803390902780201.

Riedel BC, Daianu M, Ver Steeg G, Mezher A, Salminen LE, Galstyan A, Thompson PM. 2018. Uncovering biologically coherent peripheral signatures of health and risk for Alzheimer's disease in the aging brain. Frontiers in Aging Neuroscience. 10:390. doi:10.3389/fnagi.2018.00390.

Riedel BC, Thompson PM, Brinton RD. 2016. Age, APOE and sex: Triad of risk of Alzheimer's disease. Journal of Steroid Biochemistry and Molecular Biology. 160:134–147. doi:10.1016/j.jsbmb.2016.03.012.

Rijntjes M, Buechel C, Kiebel S, Weiller C. 1999. Motor Systems: Multiple somatotopic representations in the human cerebellum. NeuroReport. 10(17):3653–3658. doi:doi:10.1097/00001756-199911260-00035.

Risacher S, Saykin A, Wes J, Shen L, Firpi H, McDonald B. 2009. Baseline MRI predictors of conversion from MCI to probable AD in the ADNI cohort. Current Alzheimer Research. 6(4):347–361. doi:10.2174/156720509788929273.

Rockland KS, Van Hoesen GW. 1999. Some temporal and parietal cortical connections converge in CA1 of the primate hippocampus. Cerebral Cortex. 9(3):232–237. doi:10.1093/cercor/9.3.232.

Rodrigue KM, Raz N. 2004. Shrinkage of the entorhinal cortex over five years predicts memory performance in healthy adults. Journal of Neuroscience. 24(4):956–963. doi:10.1523/JNEUROSCI.4166-03.2004.

Rodríguez-Herreros B, Amengual JL, Gurtubay-Antolín A, Richter L, Jauer P, Erdmann C, Schweikard A, López-Moliner J, Rodríguez-Fornells A, Münte TF. 2015. Microstructure of the superior longitudinal fasciculus predicts stimulation-induced interference with on-line motor control. NeuroImage. 120:254–265. doi:10.1016/j.neuroimage.2015.06.070.

Rogaeva E. 2002. The solved and unsolved mysteries of the genetics of early-onset Alzheimer's disease. NeuroMolecular Medicine. 2(1):1–10. doi:10.1385/nmm:2:1:01.

Rogojin A, Gorbet DJ, Hawkins KM, Sergio LE. 2019. Cognitive-motor integration performance is affected by sex, APOE status, and family history of dementia. Journal of Alzheimer's Disease. 71(2):685–701. doi:10.3233/JAD-190403.

Rose DK, Winstein CJ. 2004. Bimanual training after stroke: Are two hands better than one? Topics in Stroke Rehabilitation. 11(4):20–30. doi:10.1310/NCB1-JWAA-09QE-7TXB.

Rosen AC, Prull MW, Gabrieli JDE, Stoub T, O'Hara R, Friedman L, Yesavage JA, DeToledo-Morrell L. 2003. Differential associations between entorhinal and hippocampal volumes and memory performance in older adults. Behavioral Neuroscience. 117(6):1150–1160. doi:10.1037/0735-7044.117.6.1150.

Rossor MN, Fox NC, Mummery CJ, Schott JM, Warren JD. 2010. The diagnosis of young-onset dementia. The Lancet Neurology. 9(8):793–806. doi:10.1016/S1474-4422(10)70159-9.

Rudisch J, Butler J, Izadi H, Birtles D, Green D. 2018. Developmental Characteristics of Disparate Bimanual Movement Skills in Typically Developing Children. Journal of Motor Behavior. 50(1):8–16. doi:10.1080/00222895.2016.1271302.

Rudisch J, Müller K, Kutz DF, Brich L, Sleimen-Malkoun R, Voelcker-Rehage C. 2020. How Age, Cognitive Function and Gender Affect Bimanual Force Control. Frontiers in Physiology. 11:245. doi:10.3389/fphys.2020.00245.

Sabes PN. 2000. The planning and control of reaching movements. Current Opinion in Neurobiology. 10(6):740–746. doi:10.1016/S0959-4388(00)00149-5.

Sadato N, Ibañez V, Deiber MP, Hallett M. 2000. Gender difference in premotor activity during active tactile discrimination. NeuroImage. 11(5 I):532–540. doi:10.1006/nimg.2000.0566.

Sadato N, Yonekura Y, Waki A, Yamada H, Ishii Y. 1997. Role of the Supplementary Motor Area and the Right Premotor Cortex in the Coordination of Bimanual Finger Movements. The Journal of Neuroscience. 17(24):9667–9674. doi:doi.org/10.1523/JNEUROSCI.17-24-09667.1997.

Salat DH, Tuch DS, van der Kouwe AJW, Greve DN, Pappu V, Lee SY, Hevelone ND, Zaleta AK, Growdon JH, Corkin S, et al. 2010. White matter pathology isolates the hippocampal formation in Alzheimer's disease. Neurobiology of Aging. 31(2):244–256. doi:10.1016/j.neurobiolaging.2008.03.013.

Salek Y, Anderson ND, Sergio L. 2011. Mild cognitive impairment is associated with impaired visual-motor planning when visual stimuli and actions are incongruent. European Neurology. 66(5):283–293. doi:10.1159/000331049.

Sanan DA, Weisgraber KH, Russell SJ, Mahley RW, Huang D, Saunders A, Schmechel D, Wisniewski T, Frangione B, Roses AD, et al. 1994. Apolipoprotein E associates with β amyloid peptide of Alzheimer's disease to form novel monofibrils. Journal of Clinical Investigation. 94(2):860–869. doi:10.1172/JCI117407.

dos Santos Picanco LC, Ozela PF, de Fatima de Brito Brito M, Pinheiro AA, Padilha EC, Braga FS, de Paula da Silva CHT, dos Santos CBR, Rosa JMC, da Silva Hage-Melim LI. 2016. Alzheimer's Disease: A Review from the Pathophysiology to Diagnosis, New Perspectives for Pharmacological Treatment. Current Medicinal Chemistry. 25(26):3141–3159. doi:10.2174/0929867323666161213101126.

Savalia NK, Agres PF, Chan MY, Feczko EJ, Kennedy KM, Wig GS. 2017. Motion-related artifacts in structural brain images revealed with independent estimates of in-scanner head motion. Human Brain Mapping. 38(1):472–492. doi:10.1002/hbm.23397.

Sayegh PF, Gorbet DJ, Hawkins KM, Hoffman KL, Sergio LE. 2017. The contribution of different cortical regions to the control of spatially decoupled eye-hand coordination. Journal of Cognitive Neuroscience. 29(7):1194–1211. doi:10.1162/jocn_a_01111.

Sayegh PF, Hawkins KM, Hoffman KL, Sergio LE. 2013. Differences in spectral profiles between rostral and caudal premotor cortex when hand-eye actions are decoupled. Journal of Neurophysiology. 110(4):952–963. doi:10.1152/jn.00764.2012.

Sayegh PF, Hawkins KM, Neagu B, Crawford JD, Hoffman KL, Sergio LE. 2014. Decoupling the actions of the eyes from the hand alters beta and gamma synchrony within SPL. Journal of Neurophysiology. 111(11):2210–2221. doi:10.1152/jn.00793.2013.

Schaefer A, Kong R, Gordon EM, Laumann TO, Zuo X-N, Holmes AJ, Eickhoff SB, Yeo BTT. 2018. Local-Global Parcellation of the Human Cerebral Cortex from Intrinsic Functional Connectivity MRI. Cerebral Cortex. 28(9):3095–3114. doi:10.1093/cercor/bhx179.

Scholz JP, Kelso JAS. 1989. A quantitative approach to understanding the formation and change of coordinated movement patterns. Journal of Motor Behavior. 21(2):122–144. doi:10.1080/00222895.1989.10735470.

de Schotten MT, Dell'Acqua F, Forkel SJ, Simmons A, Vergani F, Murphy DGM, Catani M. 2011. A lateralized brain network for visuospatial attention. Nature Neuroscience. 14(10):1245–1246. doi:10.1038/nn.2905.

Schroeter ML, Stein T, Maslowski N, Neumann J. 2009. Neural correlates of Alzheimer's disease and mild cognitive impairment: A systematic and quantitative meta-analysis involving 1351 patients. NeuroImage. 47(4):1196–1206. doi:10.1016/j.neuroimage.2009.05.037.

Schulte T, Müller-Oehring EM. 2010. Contribution of callosal connections to the interhemispheric integration of visuomotor and cognitive processes. Neuropsychology Review. 20(2):174–190. doi:10.1007/s11065-010-9130-1.

Scott MR, Hampton OL, Buckley RF, Chhatwal JP, Hanseeuw BJ, Jacobs HIL, Properzi MJ, Sanchez JS, Johnson KA, Sperling RA, et al. 2020. Inferior temporal tau is associated with accelerated prospective cortical thinning in clinically normal older adults. NeuroImage. 220:116991. doi:10.1016/j.neuroimage.2020.116991.

Sekuler AB, Bennett PJ, Mamelak M. 2000. Effects of aging on the useful field of view. Experimental Aging Research. 26(2):103–120. doi:10.1080/036107300243588.

Sergio LE, Gorbet DJ, Tippett WJ, Yan X, Neagu B. 2009. Cortical mechanisms of vision for complex action. In: Jenkins M, Harris L, editors. Cortical mechanisms of vision. Cambridge: Cambridge University Press.

Sergio LE, Kalaska JF. 2003. Systematic changes in motor cortex cell activity with arm posture during directional isometric force generation. Journal of Neurophysiology. 89(1):212–228. doi:10.1152/jn.00016.2002.

Serrien DJ, Nirkko AC, Wiesendanger M. 2001. Role of the corpus callosum in bimanual coordination: A comparison of patients with congenital and acquired callosal damage. European Journal of Neuroscience. 14(11):1897–1905. doi:10.1046/j.0953-816X.2001.01798.x.

Serrien DJ, Spapé MM. 2009. The role of hand dominance and sensorimotor congruence in voluntary movement. Experimental Brain Research. 199(2):195–200. doi:10.1007/s00221-009-1998-8.

Seurinck R, Vingerhoets G, De Lange FP, Achten E. 2004. Does egocentric mental rotation elicit sex differences? NeuroImage. 23(4):1440–1449. doi:10.1016/j.neuroimage.2004.08.010.

Shao J, Myers N, Yang Q, Feng J, Plant C, Böhm C, Förstl H, Kurz A, Zimmer C, Meng C, et al. 2012. Prediction of Alzheimer's disease using individual structural connectivity networks. Neurobiology of Aging. 33(12):2756–2765. doi:10.1016/j.neurobiolaging.2012.01.017.

Shaw LM, Arias J, Blennow K, Galasko D, Molinuevo JL, Salloway S, Schindler S, Carrillo MC, Hendrix JA, Ross A, et al. 2018. Appropriate use criteria for lumbar puncture and cerebrospinal fluid testing in the diagnosis of Alzheimer's disease. Alzheimer's and Dementia. 14(11):1505–1521. doi:10.1016/j.jalz.2018.07.220.

Sheline YI, Morris JC, Snyder AZ, Price JL, Yan Z, D'Angelo G, Liu C, Dixit S, Benzinger T, Fagan A, et al. 2010. APOE4 allele disrupts resting state fMRI connectivity in the absence of amyloid plaques or decreased CSF Aβ42. Journal of Neuroscience. 30(50):17035–17040. doi:10.1523/JNEUROSCI.3987-10.2010.

Sheline YI, Raichle ME. 2013. Resting state functional connectivity in preclinical Alzheimer's disease. Biological Psychiatry. 74(5):340–347. doi:10.1016/j.biopsych.2012.11.028.

Sheline YI, Raichle ME, Snyder AZ, Morris JC, Head D, Wang S, Mintun MA. 2010. Amyloid Plaques Disrupt Resting State Default Mode Network Connectivity in Cognitively Normal Elderly. Biological Psychiatry. 67(6):584–587. doi:10.1016/j.biopsych.2009.08.024.

Sherwood DE. 1994a. Hand preference, practice order, and spatial assimilations in rapid bimanual movement. Journal of Motor Behavior. 26(2):123–134. doi:10.1080/00222895.1994.9941667.

Sherwood DE. 1994b. Interlimb amplitude differences, spatial assimilations, and the temporal structure of rapid bimanual movements. Human Movement Science. 13:841–860. doi:doi.org/10.1016/0167-9457(94)90021-3.

Shetty AK, Vinutha Shankar MS, Annamalai N. 2014. Bimanual coordination: Influence of age and gender. Journal of Clinical and Diagnostic Research. 8(2):15–16. doi:10.7860/JCDR/2014/7333.3994.

Shibasaki H, Sadato N, Lyshkow H, Yonekura Y, Honda M, Nagamine T, Suwazono S, Magata Y, Ikeda A, Miyazaki M, et al. 1993. Both primary motor cortex and supplementary motor area play an important role in complex finger movement. Brain. 116(6):1387–1398. doi:doi.org/10.1093/brain/116.6.1387.

Shih PC, Steele CJ, Nikulin V, Villringer A, Sehm B. 2019. Kinematic profiles suggest differential control processes involved in bilateral in-phase and anti-phase movements. Scientific Reports. 9(1). doi:10.1038/s41598-019-40295-1.

Shiino A, Chen YW, Tanigaki K, Yamada A, Vigers P, Watanabe T, Tooyama I, Akiguchi I. 2017. Sex-related difference in human white matter volumes studied: Inspection of the corpus callosum and other white matter by VBM. Scientific Reports. 7. doi:10.1038/srep39818.

Shine JP, Valdés-Herrera JP, Hegarty M, Wolbers T. 2016. The human retrosplenial cortex and thalamus code head direction in a global reference frame. Journal of Neuroscience. 36(24):6371–6381. doi:10.1523/JNEUROSCI.1268-15.2016.

Shulman GL, Corbetta M, Buckner RL, Fiez JA, Miezin FM, Raichle ME, Petersen SE. 1997. Common blood flow changes across visual tasks: I. Increases in subcortical structures and cerebellum but not in nonvisual cortex. Journal of Cognitive Neuroscience. 9(5):624–647. doi:10.1162/jocn.1997.9.5.624.

Silverman JM, Li G, Zaccario ML, Smith CJ, Schmeidler J, Mohs RC, Davis KL. 1994. Patterns of risk in first-degree relatives of patients with Alzheimer's disease. Archives of General Psychiatry. 51(7):577–586. doi:10.1001/archpsyc.1994.03950070069012.

Singh PP, Singh M, Mastana SS. 2006. APOE distribution in world populations with new data from India and the UK. Annals of Human Biology. 33(3):279–308. doi:10.1080/03014460600594513.

Singh-Curry V, Husain M. 2009. The functional role of the inferior parietal lobe in the dorsal and ventral stream dichotomy. Neuropsychologia. 47(6):1434–1448. doi:10.1016/j.neuropsychologia.2008.11.033.

Skoog I, Hesse C, Aevarsson Ó, Landahl S, Wahlström J, Fredman P, Blennow K. 1998. A population study of apoE genotype at the age of 85: Relation to dementia, cerebrovascular disease, and mortality. Journal of Neurology Neurosurgery and Psychiatry. 64(1):37–43. doi:10.1136/jnnp.64.1.37.

Smith CD, Chebrolu H, Andersen AH, Powell DA, Lovell MA, Xiong S, Gold BT. 2010. White matter diffusion alterations in normal women at risk of Alzheimer's disease. Neurobiology of Aging. 31(7):1122–1131. doi:10.1016/j.neurobiolaging.2008.08.006.

Smith SM, Vidaurre D, Beckmann CF, Glasser MF, Jenkinson M, Miller KL, Nichols TE, Robinson EC, Salimi-Khorshidi G, Woolrich MW, et al. 2013. Functional connectomics from resting-state fMRI. Trends in Cognitive Sciences. 17(12):666–682. doi:10.1016/j.tics.2013.09.016.

Smits LL, Flapper M, Sistermans N, Pijnenburg YAL, Scheltens P, Van Der Flier WM. 2014. Apraxia in mild cognitive impairment and Alzheimer's disease: Validity and reliability of the van heugten test for apraxia. Dementia and Geriatric Cognitive Disorders. 38(1–2):55–64. doi:10.1159/000358168.

Soares JM, Marques P, Alves V, Sousa N. 2013. A hitchhiker's guide to diffusion tensor imaging. Frontiers in Neuroscience. 7:31. doi:10.3389/fnins.2013.00031.

Soechting JF, Flanders M. 1989a. Errors in pointing are due to approximations in sensorimotor transformations. Journal of Neurophysiology. 62(2):595–608. doi:10.1152/jn.1989.62.2.595.

Soechting JF, Flanders M. 1989b. Sensorimotor representations for pointing to targets in three-dimensional space. Journal of Neurophysiology. 62(2):582–594. doi:10.1152/jn.1989.62.2.582.

Song SK, Sun SW, Ju WK, Lin SJ, Cross AH, Neufeld AH. 2003. Diffusion tensor imaging detects and differentiates axon and myelin degeneration in mouse optic nerve after retinal ischemia. NeuroImage. 20(3):1714–1722. doi:10.1016/j.neuroimage.2003.07.005.

Song SK, Sun SW, Ramsbottom MJ, Chang C, Russell J, Cross AH. 2002. Dysmyelination revealed through MRI as increased radial (but unchanged axial) diffusion of water. NeuroImage. 17(3):1429–1436. doi:10.1006/nimg.2002.1267.

Song SK, Yoshino J, Le TQ, Lin SJ, Sun SW, Cross AH, Armstrong RC. 2005. Demyelination increases radial diffusivity in corpus callosum of mouse brain. NeuroImage. 26(1):132–140. doi:10.1016/j.neuroimage.2005.01.028.

Sowell ER, Peterson BS, Kan E, Woods RP, Yoshii J, Bansal R, Xu D, Zhu H, Thompson PM, Toga AW. 2007. Sex differences in cortical thickness mapped in 176 healthy individuals between 7 and 87 years of age. Cerebral Cortex. 17(7):1550–1560. doi:10.1093/cercor/bhl066.

Sperling R, Chua E, Cocchiarella A, Rand-Giovannetti E, Poldrack R, Schacter DL, Albert M. 2003. Putting names to faces: Successful encoding of associative memories activates the anterior hippocampal formation. NeuroImage. 20(2):1400–1410. doi:10.1016/S1053-8119(03)00391-4.

Sperling RA, Aisen PS, Beckett LA, Bennett DA, Craft S, Fagan AM, Iwatsubo T, Jack CR, Kaye J, Montine TJ, et al. 2011. Toward defining the preclinical stages of Alzheimer's disease: Recommendations from the National Institute on Aging-Alzheimer's Association workgroups on diagnostic guidelines for Alzheimer's disease. Alzheimer's and Dementia. 7(3):280–292. doi:10.1016/j.jalz.2011.03.003.

Sperling RA, Bates JF, Cocchiarella AJ, Schacter DL, Rosen BR, Albert MS. 2001. Encoding novel face-name associations: A functional MRI study. Human Brain Mapping. 14(3):129–139. doi:10.1002/hbm.1047.

Sperling RA, Dickerson BC, Pihlajamaki M, Vannini P, LaViolette PS, Vitolo OV, Hedden T, Becker JA, Rentz DM, Selkoe DJ, et al. 2010. Functional alterations in memory networks in early Alzheimer's disease. NeuroMolecular Medicine. 12(1):27–43. doi:10.1007/s12017-009-8109-7.

Sperling RA, LaViolette PS, O'Keefe K, O'Brien J, Rentz DM, Pihlajamaki M, Marshall G, Hyman BT, Selkoe DJ, Hedden T, et al. 2009. Amyloid Deposition Is Associated with Impaired Default Network Function in Older Persons without Dementia. Neuron. 63(2):178–188. doi:10.1016/j.neuron.2009.07.003.

Spijkers W, Heuer H. 1995. Structural Constraints on the Performance of Symmetrical Bimanual Movements with Different Amplitudes. The Quarterly Journal of Experimental Psychology Section A. 48(3):716–740. doi:10.1080/14640749508401412.

Sporns O, Tononi G, Kötter R. 2005. The human connectome: A structural description of the human brain. PLoS Computational Biology. 1(4):0245–0251. doi:10.1371/journal.pcbi.0010042.

Steele CJ, Chakravarty MM. 2018. Gray-matter structural variability in the human cerebellum: Lobule-specific differences across sex and hemisphere. NeuroImage. 170:164–173. doi:10.1016/j.neuroimage.2017.04.066.

Stelmach GE, Goggin NL, García-Colera A. 1987. Movement specification time with age. Experimental Aging Research. 13(1):39–46. doi:10.1080/03610738708259298.

Stephan K, Binkofski F, Halsband U, Dohle C, Wunderlich G, Schnitzler A, Tass P, Posse S, Herzog H, Sturm V, et al. 1999. Cerebral midline structures in bimanual coordination. Brain. 122(2):351–368. doi:https://doi.org/10.1093/brain/122.2.351.

Stewart KC, Cauraugh JH, Summers JJ. 2006. Bilateral movement training and stroke rehabilitation: A systematic review and meta-analysis. Journal of the Neurological Sciences. 244(1–2):89–95. doi:10.1016/j.jns.2006.01.005.

Stone KD, Bryant DC, Gonzalez CLR. 2013. Hand use for grasping in a bimanual task: Evidence for different roles? Experimental Brain Research. 224(3):455–467. doi:10.1007/s00221-012-3325-z.

Stoodley CJ, Schmahmann JD. 2009. Functional topography in the human cerebellum: A meta-analysis of neuroimaging studies. NeuroImage. 44(2):489–501. doi:10.1016/j.neuroimage.2008.08.039.

Stoodley CJ, Schmahmann JD. 2010. Evidence for topographic organization in the cerebellum of motor control versus cognitive and affective processing. Cortex. 46(7):831–844. doi:10.1016/j.cortex.2009.11.008.

Strittmatter WJ, Saunders AM, Goedert M, Weisgraber KH, Dong LM, Jakes R, Huang DY, Pericak-Vance M, Schmechel D, Roses AD. 1994. Isoform-specific interactions of apolipoprotein E with microtubule-associated protein tau: Implications for Alzheimer disease. Proceedings of the National Academy of Sciences of the United States of America. 91(23):11183–11186. doi:10.1073/pnas.91.23.11183.

Su YY, Zhang XD, Schoepf UJ, Varga-Szemes A, Stubenrauch A, Liang X, Zheng LJ, Zheng G, Kong X, Xu Q, et al. 2017. Lower functional connectivity of default mode network in cognitively normal young adults with mutation of APP, presenilins and APOE ε4. Brain Imaging and Behavior. 11(3):818–828. doi:10.1007/s11682-016-9556-z.

Sun SW, Liang HF, Trinkaus K, Cross AH, Armstrong RC, Song SK. 2006. Noninvasive detection of cuprizone induced axonal damage and demyelination in the mouse corpus callosum. Magnetic Resonance in Medicine. 55(2):302–308. doi:10.1002/mrm.20774.

Swinnen SP. 2002. Intermanual coordination: From behavioural principles to neural-network interactions. Nature Reviews Neuroscience. 3(5):350–361. doi:10.1038/nrn807.

Swinnen SP, Dounskaia N, Duysens J. 2002. Patterns of Bimanual Interference Reveal Movement Encoding within a Radial Egocentric Reference Frame. Journal of Cognitive Neuroscience. 14(3):463–471. doi:doi.org/10.1162/089892902317361976.

Swinnen SP, Dounskaia N, Levin O, Duysens J. 2001. Constraints during bimanual coordination: the role of direction in relation to amplitude and force requirements. Behavioural Brain Research. 123(2):201–218. doi:doi.org/10.1016/S0166-4328(01)00210-8.

Swinnen SP, Gooijers J. 2015. Bimanual Coordination. Brain Mapping: An Encyclopedic Reference. 2:475–482. doi:10.1016/B978-0-12-397025-1.00030-0.

Swinnen SP, Jardin K, Verschueren S, Meulenbroek R, Franz L, Dounskaia N, Walter CB. 1998. Exploring interlimb constraints during bimanual graphic performance: effects of muscle grouping and direction. Behavioural Brain Research. 90:79–87. doi:doi.org/10.1016/S0166-4328(97)00083-1.

Swinnen SP, Wenderoth N. 2004. Two hands, one brain: Cognitive neuroscience of bimanual skill. Trends in Cognitive Sciences. 8(1):18–25. doi:10.1016/j.tics.2003.10.017.

Tang MX, Maestre G, Tsai WY, Liu XH, Lin Chung FY, Chun M, Schofield P, Stern Y, Tycko B, Mayeux R. 1996. Relative risk of Alzheimer disease and age-at-onset distributions, based on APOE genotypes among elderly African Americans, Caucasians, and Hispanics in New York City. American Journal of Human Genetics. 58(3):574–584.

Tankus A, Fried I. 2012. Visuomotor coordination and motor representation by human temporal lobe neurons. Journal of Cognitive Neuroscience. 24(3):600–610. doi:10.1162/jocn_a_00160.

Taylor JA, Krakauer JW, Ivry RB. 2014. Explicit and implicit contributions to learning in a sensorimotor adaptation task. Journal of Neuroscience. 34(8):3023–3032. doi:10.1523/JNEUROSCI.3619-13.2014.

Taylor W, Hsu E, Krishnanm K, MacFall J. 2003. Diffusion tensor imaging: background, potential, and utility in psychiatric research. Biological Psychiatry. 55(3):201–207. doi:10.1016/s0006-3223(03)00813-8.

Thal DR, Rüb U, Orantes M, Braak H. 2002. Phases of Aβ-deposition in the human brain and its relevance for the development of AD. Neurology. 58:1791–1800. doi:10.1212/WNL.58.12.1791.

Tippett WJ, Krajewski A, Sergio LE. 2007. Visuomotor integration is compromised in Alzheimer's disease patients reaching for remembered targets. European Neurology. 58(1):1–11. doi:10.1159/000102160.

Tippett WJ, Sergio LE. 2006. Visuomotor integration is impaired in early stage Alzheimer's disease. Brain Research. 1102(1):92–102. doi:10.1016/j.brainres.2006.04.049.

Tippett WJ, Sergio LE, Black SE. 2012. Compromised visually guided motor control in individuals with Alzheimer's disease: Can reliable distinctions be observed? Journal of Clinical Neuroscience. 19(5):655–660. doi:10.1016/j.jocn.2011.09.013.

Tiraboschi P, Hansen L, Masliah E, Alford M, Thal L, Corey-Bloom J. 2004. Impact of APOE genotype on neuropathologic and neurochemical markers of Alzheimer disease. Neurology. 62(11):1977–1983. doi:doi.org/10.1212/01.WNL.0000128091.92139.0F.

Tracy JI, Faro SS, Mohammed FB, Pinus AB, Madi SM, Laskas JW. 2001. Cerebellar mediation of the complexity of bimanual compared to unimanual movements. Neurology. 57(10):1862–1869. doi:doi.org/10.1212/WNL.57.10.1862.

Tuller B, Kelso JAS. 1989. Environmentally-specified patterns of movement coordination in normal and split-brain subjects. Experimental Brain Research. 75(2):306–316. doi:doi.org/10.1007/BF00247936.

Tzourio-Mazoyer N, Landeau B, Papathanassiou D, Crivello F, Etard O, Delcroix N, Mazoyer B, Joliot M. 2002. Automated anatomical labeling of activations in SPM using a macroscopic anatomical parcellation of the MNI MRI single-subject brain. NeuroImage. 15(1):273–289. doi:10.1006/nimg.2001.0978.

Uddin LQ, Kelly AMC, Biswal BB, Castellanos FX, Milham MP. 2009. Functional Connectivity of Default Mode Network Components: Correlation, Anticorrelation, and Causality. Human Brain Mapping. 30(2):625–637. doi:10.1002/hbm.20531.

Ullén F, Forssberg H, Ehrsson HH. 2003. Neural networks for the coordination of the hands in time. Journal of Neurophysiology. 89(2):1126–1135. doi:10.1152/jn.00775.2002.

Utevsky AV, Smith DV, Huettel SA. 2014. Precuneus is a functional core of the default-mode network. Journal of Neuroscience. 34(3):932–940. doi:10.1523/JNEUROSCI.4227-13.2014.

Vallee R. 1991. Mechanisms of fast and slow axonal transport. Annual Review of Neuroscience. 14(1):59–92. doi:10.1146/annurev.neuro.14.1.59.

Van Leemput K, Bakkour A, Benner T, Wiggins G, Wald LL, Augustinack J, Dickerson BC, Golland P, Fischl B. 2009. Automated segmentation of hippocampal subfields from

ultra-high resolution in vivo MRI. Hippocampus. 19(6):549–557. doi:10.1002/hipo.20615.

Vann SD, Aggleton JP, Maguire EA. 2009. What does the retrosplenial cortex do? Nature Reviews Neuroscience. 10(11):792–802. doi:10.1038/nrn2733.

Vaz M, Silvestre S. 2020. Alzheimer's disease: Recent treatment strategies. European Journal of Pharmacology. 887:173554. doi:10.1016/j.ejphar.2020.173554.

Vega-González A, Granat MH. 2005. Continuous monitoring of upper-limb activity in a free-living environment. Archives of Physical Medicine and Rehabilitation. 86(3):541–548. doi:10.1016/j.apmr.2004.04.049.

Veldsman M, Nobis L, Alfaro-Almagro F, Manohar S, Husain M. 2021. The human hippocampus and its subfield volumes across age, sex and APOE e4 status. Brain Communications. 3(1):fcaa219. doi:10.1093/braincomms/fcaa219.

Vemuri P, Jones D, Jack C. 2012. Resting state functional MRI in Alzheimer's Disease. Alzheimer's research & Therapy. 4(1):1–9. doi:https://doi.org/10.1186/alzrt100.

Villain N, Desgranges B, Viader F, De La Sayette V, Mézenge F, Landeau B, Baron JC, Eustache F, Chételat G. 2008. Relationships between hippocampal atrophy, white matter disruption, and gray matter hypometabolism in Alzheimer's disease. Journal of Neuroscience. 28(24):6174–6181. doi:10.1523/JNEUROSCI.1392-08.2008.

Villeneuve S, Reed BR, Wirth M, Haase CM, Madison CM, Ayakta N, Mack W, Mungas D, Chui HC, Decarli C, et al. 2014. Cortical thickness mediates the effect of β-amyloid on episodic memory. Neurology. 82(9):761–767. doi:10.1212/WNL.0000000000000170.

Virani SS, Alonso A, Aparicio HJ, Benjamin EJ, Bittencourt MS, Callaway CW, Carson AP, Chamberlain AM, Cheng S, Delling FN, et al. 2021. Heart Disease and Stroke Statistics - 2021 Update: A report from the American Heart Association. Circulation. 143(8):E254–E743. doi:10.1161/CIR.0000000000000950.

Voevodskaya O. 2014. The effects of intracranial volume adjustment approaches on multiple regional MRI volumes in healthy aging and Alzheimer's disease. Frontiers in Aging Neuroscience. 6:264. doi:10.3389/fnagi.2014.00264.

Von Der Heide RJ, Skipper LM, Klobusicky E, Olson IR. 2013. Dissecting the uncinate fasciculus: Disorders, controversies and a hypothesis. Brain. 136(6):1692–1707. doi:10.1093/brain/awt094.

Vos SB, Jones DK, Jeurissen B, Viergever MA, Leemans A. 2012. The influence of complex white matter architecture on the mean diffusivity in diffusion tensor MRI of the human brain. NeuroImage. 59(3):2208–2216. doi:10.1016/j.neuroimage.2011.09.086.

Wakana S, Caprihan A, Panzenboeck MM, Fallon JH, Perry M, Gollub RL, Hua K, Zhang J, Jiang H, Dubey P, et al. 2007. Reproducibility of quantitative tractography methods applied to cerebral white matter. NeuroImage. 36(3):630–644. doi:10.1016/j.neuroimage.2007.02.049.

Walker KA, Gross AL, Moghekar AR, Soldan A, Pettigrew C, Hou X, Lu H, Alfini AJ, Bilgel M, Miller MI, et al. 2020. Association of peripheral inflammatory markers with connectivity in large-scale functional brain networks of non-demented older adults. Brain, Behavior, and Immunity. 87:388–396. doi:10.1016/j.bbi.2020.01.006.

Waller R, Dotterer HL, Murray L, Maxwell AM, Hyde LW. 2017. White-matter tract abnormalities and antisocial behavior: A systematic review of diffusion tensor imaging studies across development. NeuroImage: Clinical. 14:201–215. doi:10.1016/j.nicl.2017.01.014.

Walsh RR, Small SL, Chen EE, Solodkin A. 2008. Network activation during bimanual movements in humans. NeuroImage. 43(3):540–553. doi:10.1016/j.neuroimage.2008.07.019.

Wang J, Zhang M, Cheng H, Lin X, Chen J, Wu H, Song Y, Chen S, Ge H, Yan Z, et al. 2022. An Activation Likelihood Estimation Meta-Analysis of Specific Functional Alterations in Dorsal Attention Network in Mild Cognitive Impairment. Front Neurosci. 16:876568. doi:10.3389/fnins.2022.876568.

Wang K, Liang M, Wang L, Tian L, Zhang X, Li K, Jiang T. 2007. Altered functional connectivity in early Alzheimer's disease: A resting-state fMRI study. Human Brain Mapping. 28(10):967–978. doi:10.1002/hbm.20324.

Wang L, Benzinger TL, Su Y, Christensen J, Friedrichsen K, Aldea P, McConathy J, Cairns NJ, Fagan AM, Morris JC, et al. 2016. Evaluation of Tau imaging in staging Alzheimer disease and revealing interactions between β-Amyloid and tauopathy. JAMA Neurology. 73(9):1070–1077. doi:10.1001/jamaneurol.2016.2078.

Wang L, Roe Catherine M., Snyder AZ, Brier MR, Thomas JB, Xiong C, Benzinger TL, Morris JC, Ances BM. 2012. Alzheimer disease family history impacts resting state functional connectivity. Annals of Neurology. 72(4):571–577. doi:10.1002/ana.23643.

Wang L, Roe Catherine M, Snyder AZ, Brier MR, Thomas JB, Xiong C, Benzinger TL, Morris JC, Ances BM. 2012. Alzheimer's disease family history impacts resting state functional connectivity. 72(4):571–577. doi:10.1002/ana.23643.Alzheimer.

Wang X, Wang J, He Yi, Li H, Yuan H, Evans A, Yu X, He Yong, Wang H. 2015. Apolipoprotein e ε4 Modulates Cognitive Profiles, Hippocampal Volume, and Resting-State Functional Connectivity in Alzheimer's Disease. Journal of Alzheimer's Disease. 45(3):781–795. doi:10.3233/JAD-142556.

Ward A, Crean S, Mercaldi CJ, Collins JM, Boyd D, Cook MN, Arrighi HM. 2012. Prevalence of Apolipoprotein E4 genotype and homozygotes (APOE e4/4) among patients diagnosed with alzheimer's disease: A systematic review and meta-analysis. Neuroepidemiology. 38(1):1–17. doi:10.1159/000334607.

Weiss E, Siedentopf CM, Hofer A, Deisenhammer EA, Hoptman MJ, Kremser C, Golaszewski S, Felber S, Fleischhacker WW, Delazer M. 2003. Sex differences in brain activation pattern during a visuospatial cognitive task: A functional magnetic resonance imaging study in healthy volunteers. Neuroscience Letters. 344(3):169–172. doi:10.1016/S0304-3940(03)00406-3.

Wenderoth N, Van Dooren M, Vandebroek A, De Vos J, Vangheluwe S, Stinear CM, Byblow WD, Swinnen SP. 2009. Conceptual binding: Integrated visual cues reduce processing costs in bimanual movements. Journal of Neurophysiology. 102(1):302–311. doi:10.1152/jn.91090.2008.

Westlye LT, Reinvang I, Rootwelt H, Espeseth T. 2012. Effects of APOE on brain white matter microstructure in healthy adults. Neurology. 79(19):1961–1969. doi:10.1212/WNL.0b013e3182735c9c.

Wheeler-Kingshott CAM, Cercignani M. 2009. About "axial" and "radial" diffusivities. Magn Reson Med. 61(5):1255–1260. doi:10.1002/mrm.21965.

Whitfield-Gabrieli S, Nieto-Castanon A. 2012. Conn: A Functional Connectivity Toolbox for Correlated and Anticorrelated Brain Networks. Brain Connectivity. 2(3):125–141. doi:10.1089/brain.2012.0073.

Whitlock JR. 2017. Posterior parietal cortex. Current Biology. 27(14):R691–R695. doi:doi.org/10.1016/j.cub.2017.06.007.

Wiestler T, Mcgonigle DJ, Diedrichsen J. 2011. Integration of sensory and motor representations of single fingers in the human cerebellum. J Neurophysiol. 105:3042–3053. doi:10.1152/jn.00106.2011.-The.

Wig GS. 2017. Segregated systems of human brain networks. Trends in Cognitive Sciences. 21(12):981–996. doi:10.1016/j.tics.2017.09.006.

Wig GS, Laumann TO, Petersen SE. 2014. An approach for parcellating human cortical areas using resting-state correlations. NeuroImage. 93:276–291. doi:10.1016/j.neuroimage.2013.07.035.

Wise SP, Boussaoud D, Johnson PB, Caminiti R. 1997. Premotor and parietal cortex: Corticocortical connectivity and combinatorial computations. Annual Review of Neuroscience. 20(1):25–42. doi:10.1146/annurev.neuro.20.1.25.

Wise SP, di Pellegrino G, Boussaoud D. 1996. The premotor cortex and nonstandard sensorimotor mapping. Canadian Journal of Physiology and Pharmacology. 74(4):469–482. doi:10.1139/cjpp-74-4-469.

Wisse LEM, Chételat G, Daugherty AM, de Flores R, la Joie R, Mueller SG, Stark CEL, Wang L, Yushkevich PA, Berron D, et al. 2021. Hippocampal subfield volumetry from structural isotropic 1 mm3 MRI scans: A note of caution. Human Brain Mapping. 42(2):539–550. doi:10.1002/hbm.25234.

Wolf A, Scheiderer R, Napolitan N, Belden C, Shaub L, Whitford M. 2014. Efficacy and task structure of bimanual training post stroke: A systematic review. Topics in Stroke Rehabilitation. 21(3):181–196. doi:10.1310/tsr2103-181.

Wolk DA, Dickerson BC. 2010. Apolipoprotein E (APOE) genotype has dissociable effects on memory and attentional-executive network function in Alzheimer's disease. Proceedings of the National Academy of Sciences of the United States of America. 107(22):10256–10261. doi:10.1073/pnas.1001412107.

Wooten GF, Currie LJ, Bovbjerg VE, Lee JK, Patrie J. 2004. Are men at greater risk for Parkinson's disease than women? Journal of Neurology, Neurosurgery and Psychiatry. 75(4):637–639. doi:10.1136/jnnp.2003.020982.

World Health Organization. 2015. First WHO Ministerial Conference on global action against dementia. Geneva, Switzerland.

World Health Organization. 2019. Risk reduction of cognitive decline and dementia: WHO guidelines.

Worsley KJ, Marrett S, Neelin P, Vandal AC, Friston KJ, Evans AC, Brain M. 1996. A unified statistical approach for determining significant signals in images of cerebral activation. Human Brain Mapping. 4(1):58–73. doi:doi.org/10.1002/(SICI)1097-0193(1996)4:1<58::AID-HBM4>3.0.CO;2-O.

Wu T, Wang L, Hallett M, Li K, Chan P. 2010. Neural correlates of bimanual anti-phase and in-phase movements in Parkinson's disease. Brain. 133(8):2394–2409. doi:10.1093/brain/awq151.

Wu X, Li Q, Yu X, Chen K, Fleisher AS, Guo X, Zhang J, Reiman EM, Yao L, Li R. 2016. A triple network connectivity study of large-scale brain systems in cognitively normal APOE4 carriers. Frontiers in Aging Neuroscience. 8:231. doi:10.3389/fnagi.2016.00231.

Wycoco V, Shroff M, Sudhakar S, Lee W. 2013. White Matter Anatomy. What the Radiologist Needs to Know. Neuroimaging Clinics of North America. 23(2):197–216. doi:10.1016/j.nic.2012.12.002.

Xie L, Wisse LEM, Das SR, Vergnet N, Dong M, Ittyerah R, de Flores R, Yushkevich PA, Wolk DA. 2020. Longitudinal atrophy in early Braak regions in preclinical Alzheimer's disease. Human Brain Mapping. 41(16):4704–4717. doi:10.1002/hbm.25151.

Xu W, Tan Lan, Wang HF, Jiang T, Tan MS, Tan Lin, Zhao QF, Li JQ, Wang J, Yu JT. 2015. Meta-analysis of modifiable risk factors for Alzheimer's disease. Journal of Neurology, Neurosurgery and Psychiatry. 86(12):1299–1306. doi:10.1136/jnnp-2015-310548.

Yeatman JD, Dougherty RF, Myall NJ, Wandell BA, Feldman HM. 2012. Tract profiles of white matter properties: Automating fiber-tract quantification. PLoS ONE. 7(11):49790. doi:10.1371/journal.pone.0049790.

Yeo BT, Krienen FM, Sepulcre J, Sabuncu MR, Lashkari D, Hollinshead M, Roffman JL, Smoller JW, Zöllei L, Polimeni JR, et al. 2011. The organization of the human cerebral cortex estimated by intrinsic functional connectivity. Journal of Neurophysiology. 106(3):1125–1165. doi:10.1152/jn.00338.2011.

Yonelinas AP, Hopfinger JB, Buonocore MH, Kroll NEA, Baynes K. 2001. Hippocampal, parahippocampal and occipital-temporal contributions to associative and item recognition memory: An fMRI study. NeuroReport. 12(2):359–363. doi:10.1097/00001756-200102120-00035.

Zeineh MM, Engel SA, Thompson PM, Bookheimer SY. 2003. Dynamics of the hippocampus during encoding and retrieval of face-name pairs. Science. 299(5606):577–580. doi:10.1126/science.1077775.

Zhang C, Cahill ND, Arbabshirani MR, White T, Baum SA, Michael AM. 2016. Sex and Age Effects of Functional Connectivity in Early Adulthood. Brain Connectivity. 6(9):700–713. doi:10.1089/brain.2016.0429.

Zhang C, Dougherty CC, Baum SA, White T, Michael AM. 2018. Functional connectivity predicts gender: Evidence for gender differences in resting brain connectivity. Human Brain Mapping. 39(4):1765–1776. doi:10.1002/hbm.23950.

Zhang W, Olivi A, Hertig SJ, van Zijl P, Mori S. 2008. Automated fiber tracking of human brain white matter using diffusion tensor imaging. NeuroImage. 42(2):771–777. doi:10.1016/j.neuroimage.2008.04.241.

Zhang Y, Du AT, Hayasaka S, Jahng G ho, Hlavin J, Zhan W, Weiner MW, Schuff N. 2010. Patterns of age-related water diffusion changes in human brain by concordance and discordance analysis. Neurobiology of Aging. 31(11):1991–2001. doi:10.1016/j.neurobiolaging.2008.10.009.

Zhang Z, Zheng H, Liang K, Wang H, Kong S, Hu J, Wu F, Sun G. 2015. Functional degeneration in dorsal and ventral attention systems in amnestic mild cognitive impairment and Alzheimer's disease: An fMRI study. Neuroscience Letters. 585:160–165. doi:10.1016/j.neulet.2014.11.050.

Zhu XC, Tan L, Wang HF, Jiang T, Cao L, Wang C, Wang J, Tan CC, Meng XF, Yu JT. 2015. Rate of early onset Alzheimer's disease: A systematic review and meta-analysis. Annals of Translational Medicine. 3(3):38. doi:10.3978/j.issn.2305-5839.2015.01.19.